Finite time deployment and collision avoidance for wheeled mobile robots

Matteo Guerra

N. d'ordre 284

ÉCOLE CENTRALE DE LILLE

THÉSE

Présentée en vue
d'obtenir le grade de

DOCTEUR

En

Automatique, Génie informatique, Traitement du Signal et des Images

Par

MATTEO GUERRA

DOCTORAT DELIVRÉ PAR L'ÉCOLE CENTRALE DE LILLE

Titre de la thése:

LE DÉPLOIEMENT ET L'ÉVITEMENT D'OBSTACLES EN TEMPS FINI POUR ROBOTS MOBILES À ROUES

Soutenue le 8 Decembre 2015 devant le jury d'examen:

Présidente: Mme Brigitte D'ANDRÉA NOVEL *Professeur* - CAOR Mines Paristech (Paris, FR)
Rapporteur: M. Philippe FRAISSE *Professeur* - Université Montpellier 2 (Montpellier, FR)
Rapporteur: M. Antonio LORIA *Directeur de Recherche CNRS* - Laboratoire de Signaux et Systèmes (Supélec, FR)
Membre: M. Arie LEVANT *Professeur* - Tel-Aviv University (Tel-Aviv, Israel)
Directeur de Thèse: M. Wilfrid PERRUQUETTI *Professeur* - École Centrale de Lille (Villeneuve-d'Ascq, FR)
Codirecteur de Thèse: M. Denis EFIMOV *Chargé de Recherche* INRIA - Équipe NON-A (Villeneuve-d'Ascq, FR)
Codirecteur de Thèse: M. Gang ZHENG *Chargé de recherche* INRIA - Équipe NON-A (Villeneuve-d'Ascq, FR)

Thèse preparé dans le laboratoire CRIStAL UMR 9189
École Doctorale SPI 072
PRES Université Lille Nord-de-France

...ai miei genitori
...alla mia sorellina
...ai miei nonni

È ricercando l'impossibile che l'uomo ha sempre realizzato il possibile. Coloro che si sono saggiamente limitati a ciò che appariva loro come possibile, non hanno mai avanzato di un solo passo. (Michail Alexandrovic Bakunin)

Preface

Abstract

This dissertation work addresses the obstacle avoidance for wheeled mobile robot. The considered scenarios vary from the control of a single robot avoiding obstacles to the formation control in a leader-follower configuration avoiding collision between the members of the formation and external obstacles. The literature regarding the subject is huge and finds its roots in the second half of the last century; nevertheless new technologies, sensors and the rapid increase of the use of robots in several fields (as defense, agricolture and every-day needs) makes the topic still interesting and open to further developments as the ones proposed.

Obstacle avoidance is a part of the the navigation problem in robotics, which is the union of several sub-tasks to obtain a smooth a rapid path to the destination: the robot has to sense the environment through the sensor, elaborate the information to build a map, extract a trajectory to follow and be able to act by consequence when some unexpected events occur, applying a smart and efficient control law, which has to be the result of a tailored solution based on the robot model.

Indeed, modelling the robot is a crucial part of the chain of decisions to make. The choice of a particular model influences the way each behaviour is represented and treated. In this work, due to the scenarios and the class of robot treated, the standard kinematic model is used with the addition of input disturbances, which help to characterize some neglected dynamics.

The supervisory control framework coupled with the output regulation technique allowed to solve the obstacle avoidance problem and to formally prove, as the first contribution of this dissertation, the existence of an effective solution: stabilization of two outputs for two objectives, reaching the goal and avoiding the obstacles. To have fast, reliable and robust results with respect to the introduced perturbation the designed control laws are *finite-time*, a particular class very appropriate to the purpose. The novelty of the approach lies in the easiness of the geometric approach to avoid the obstacle and on the formal proof provided under some assumptions. The solution has been thus extended to control a leader-follower formation which, sustained from the previous result, uses two outputs but three controls to nail the problem. The Leader role is redesigned to be the reference of the group and not just the most advanced agent, moreover it has a active role slowing down the formation in case of collision avoidance manoeuvre for some robots. The proposed method, formally proven, makes the group move together and allows each agent to avoid obstacles or collision in a decentralized way.

In addition, a further contribution of this dissertation, it is represented by a modification of the well known potential field method to avoid one of the common drawback

of the method: the appearance of local minima. Control theory tools help again to propose a solution that can be formally proven: the application of Input-to-State Stability (ISS) for decomposable sets allows to treat separate obstacles adding a perturbation which is able to move the trajectory away from a critic point.

The two collision avoidance strategies have been successfully implemented on a Turtlebot II robot, reference platform for the Robotic Operating System (ROS) while the formation control is under testing for final validation.

To conclude, the dissertation includes, in the appendix, two works in which finite-time and homogeneous techniques are applied to the extension link of a robotic arm to gather information about non-measurable data and to control it compensating a dead-zone of the control input.

List of Publications

Journals

I M. Guerra, D. Efimov, G. Zheng and W. Perruquetti, FINITE-TIME OBSTACLE AVOIDANCE FOR UNICYCLE-LIKE ROBOT SUBJECT TO ADDITIVE INPUT DISTURBANCES, *Autonomous Robots*.

II M. Guerra, C. Vazquez, D. Efimov, G. Zheng, L. Freidovich and W. Perruquetti, OUTPUT STABILIZATION OF A HYDRAULIC CRANE VIA ϵ-INVARIANT HOMOGENEOUS APPROACH WITH DEAD ZONE COMPENSATION, *(under review)*.

III M. Guerra, C. Vazquez, D. Efimov, G. Zheng, L. Freidovich and W. Perruquetti, ON-LINE DIFFERENTIATION: ERROR ESTIMATION USING INTERVAL OBSERVER, *(under review)*.

IV M. Guerra, D. Efimov, G. Zheng and W. Perruquetti, AVOIDING LOCAL MINIMA IN THE POTENTIAL FIELD METHOD USING INPUT-TO-STATE STABILITY, *(under review)*.

Proceedings of Peer-Reviewed International Conferences

I M. Guerra, C. Vazquez, D. Efimov, G. Zheng, L. Freidovich and W. Perruquetti, ϵ-INVARIANT OUTPUT STABILIZATION: HOMOGENEOUS APPROACH AND DEAD ZONE COMPENSATION, *to appear on the proceedings of the 54th IEEE Conference on Decision and Control (CDC), December 15-18, 2015, Osaka, Japan*.

II M. Guerra, D. Efimov, G. Zheng and W. Perruquetti, AN ISS BASED SOLUTION TO AVOID LOCAL MINIMA IN THE POTENTIAL FIELD METHOD, *14th European Control Conference (ECC), July 15-17, 2015, Linz, Austria*.

III M. Guerra, D. Efimov, G. Zheng and W. Perruquetti, ROBUST DECENTRALIZED SUPERVISORY CONTROL IN A LEADER- FOLLOWER CONFIGURATION WITH OBSTACLE AVOIDANCE, *1st IFAC Conference on Modelling, Identification and Control (MICNON), Jun 24-26, 2015, Saint-Petersburg, Russia*.

IV M. Guerra, D. Efimov, G. Zheng and W. Perruquetti, FINITE-TIME SUPERVISORY STABILIZATION FOR A CLASS OF NONHOLONOMIC MOBILE ROBOTS UNDER INPUT DISTURBANCES, *19th IFAC World Congress, Aug 2014, Cape Town, South Africa*.

V M. Guerra, M. Rhudy, Y. Gu, B. Seanor, and M. R. Napolitano. MOBILE GROUND CONTROL STATION DEVELOPMENT FOR FAULT TOLERANT UAV RESEARCH, *AIAA Guidance, Navigation, and Control Conference, p. 4544. Minneapolis, Minnesota (US) 2012*.

Contents

List of Figures

List of Tables

Chapter 1

Introduction

1.1 The origin of the word Robot

"The year was 1920 when old Rossum, a great philosopher [...] discovered a substance which behaved exactly like living matter although it was of a different chemical composition. [...] Old Rossum wrote among his chemical formulae : "Nature has found only one process by which to organize living matter. There is, however, another process, simpler, more moldable and faster, which nature has not hit upon at all. [...]
Imagine, he took it into his head to manufacture everything just as it is in the human body, right down to the last gland. The appendix, the tonsils, the belly button all the superfluities. It took him ten years. [...]"
And then young Rossum, an engineer, the son of the old man, came here. An ingenious mind. When he saw what a scene his old man was making he said : "This is nonsense! Ten years to produce a human being?! If you can't do it faster than nature then just pack it in." And he himself launched into anatomy.[...]
It was only young Rossum who had the idea to create living and intelligent labor machines from this mess.[...]
Young Rossum was of a new age. The age of production following the age of discovery. When he took a look at human anatomy he saw immediately that it was too complex and that a good engineer could simplify it. [...] A human being is something that feels joy, plays the violin, wants to go for a walk, and in general requires a lot of things which are, in effect, superfluous. [...] Manufacturing artificial workers is exactly like manufacturing gasoline engines. Production should be as simple as possible and the product the best for its function. What do you think? Practically speaking, what is the best kind of worker? [...] The cheapest. The one with the fewest needs. Young Rossum did invent a worker with the smallest number of needs, but to do so he had to simplify him. He chucked everything not directly related to work, and doing that he virtually rejected the human being and created the ***Robot****. Robots are not people. They are mechanically more perfect than we are, they have an astounding intellectual capacity, but they have no soul. The product of an engineer is technically more refined than the creation of nature."*

The passage above is from *R.U.R, Rosumovi Univerzální Roboti* (Rossum's Universal Robots), a 1920 science fiction play from the Czech author Karel Căpek which pre-

Figure 1.1: A photo from the play R.U.R. in the Billy Rose Theatre, New York 1922 as it appears in [59].

miered in 1921. The play was a success at the point that, at the end of 1923, it was already been translated in thirty languages. It describes a world in which robots, close to the today's idea of cyborgs or androids, were massively produced to help humans. The word robots has been introduced in English after this play and comes from the Czech word *robota* (slave), that is the word Căpek uses to call the workers Doctor Rossum creates. Although in the play the robot idea was different from the one we have, it introduced several concepts that characterise robotics nowadays: a robot must be as easy as possible to produce, must help with several tasks and more important it must be autonomous and smart.

1.2 Robotics today

The data from the International Federation of Robotics (IFR) [65] are quite clear: the world is facing an economic crisis but this crisis did not affect the industrial robotic market. In 2013, the number of industrial units sold is 178132, increasing of 12% the amount of the previous year. This growth is something that is increasing since 2008 with an average of the 9.5% per year, leading the amount of working robots sold since 1960 up to *one and a half million* (each one with and average life time of 15 years). For the period 2014-2017 the previsions foresee a further increase that could reach the 15% (averaged). The increase has been registered in general industry especially among the automotive parts suppliers that aim to the modernisation, keeping an eye on energy efficiency and new materials along with human machine collaboration.

Previous data refer to industrial robots, nonetheless the market of *service robots* is increasing too, 4% compared to the 2013 data. In 2012 the IFR released a document which provided four definitions that characterize service robots [66]:

- A *robot* is an actuated mechanism programmable in two or more axes with a degree of autonomy, moving within its environment, to perform intended tasks. Autonomy in this context means the ability to perform intended tasks based on current state and sensing, without human intervention.

- A *service robot* is a robot that performs useful tasks for humans or equipment excluding industrial automation application. [1]

- A *personal service robot* or a service robot for personal use is a service robot used for a non-commercial task, usually by lay persons. Examples are domestic servant robot, automated wheelchair, personal mobility assist robot, and pet exercising robot.

- A *professional service robot* or a service robot for professional use is a service robot used for a commercial task, usually operated by a properly trained operator. Examples are cleaning robot for public places, delivery robot in offices or hospitals, fire-fighting robot, rehabilitation robot and surgery robot in hospitals. In this context an operator is a person designated to start, monitor and stop the intended operation of a robot or a robot system.

Almost half of this market is represented by service robots utilised in defense applications, nevertheless a consistent increase of service robots sales cover a variety of application fields: not only milking robots, barn cleaners or automatic fencers, to mention the farming field, but also automated vehicles operating in manufacturing environments registered an increase of sales along with the medical field with robots employed in surgeries and therapies. A category more known to the general audience, that has to be treated in a stand-alone way is the one represented by the domestic robots: vacuum and floor cleaning, lawn mowing, entertainments and leisure robots but also handicap assistance robots[2]. The increase of sales for such a robots has been of 15% from 2012 to 2013 with a total of 2.7 million units sold. The projections for the period 2014-2017 foreseen a further increase robotic goods sales.

1.3 Mobile Robotics

This dissertation work focuses on motion for ground robots, and the first step when designing a ground robot is to decide the solution to adopt to realize the motion itself: which kind of actuators should the robot have?

Nowadays biological inspired solutions allow robots, especially in the research field, to realize any kind of motion, but practically the choice is often made among wheeled and legged robot. Both have advantages and shortcomings but wheeled robot has been proven to be more effective on flat grounds; they are indeed the most widespread robots in the market of service robotics with their adaptability to carry out a large variety of task in a stand alone or cooperative way. But how can a wheeled mobile robot sense the environment around it? How can it decide how to safely move in that environment? One of the easiest solution is teleoperation in which an operator is in charge to ”sense” (*i.e.* interpreting data from dedicated sensors) the environment and of the decision making process; the reader can think about the Fukushima nuclear plant accident in Japan, 2011 where a mobile robot designed by the Japan Atomic Energy Research Institute was used to monitor the overall situation inside de damaged buildings, in particular the amount of radiations, [64]. Even though very interesting teleoperation is not enough for researchers which aim to give robots the complete *autonomy*, equipping

[1] The classification of a robot into industrial robot or service robot is done according to its intended application.

[2] The handicap assistance robots is the category that registered the most impressive step up with an increase of 345%

them with sensors to give the capability to sense the environment and localize themselves. Nowadays, localization can be achieved with a huge variety of sensing devices depending on the situation: in outdoors mission positioning is often based on satellite systems [71], like the American GPS , the Russian GLONASS (or the upcoming European GALILEO) and related sensors, which give a precise localization. When these systems are not reliable (like in indoor missions) or for local detection, equipment like sonars, laser range finders, cameras or smart piece of equipment taking cue from animal kingdom are designed (like robotic whiskers [132]) to operate where other devices have serious difficulties. Once equipped with the right sensor, a robot must have the capability to localize itself and tackle the navigation problem which means recognize the environment properties, building a map and navigate in it avoiding obstacles. Bringing the problem to a higher level, once a robot is able to navigate, it could be asked to share its information with other robots and find a way to cooperate with them. It is easy for the reader to understand that *a robot* is indeed the integration of a variety of different systems assembled together to deliver the best behaviour as it is easy to infer that a lot of disciplines are involved. A roboticist has to deal with signal processing, because the robot has to gather data from a huge variety of sensors and transmit them in a proper way. A roboticist must be an expert in computer science and probability theory to take the most from the gathered data, reconstruct them and deliver the best localization and path planning result. A roboticist must be able to describe the kinematics and dynamics of the robot find out a model, deal with the incertitude in it, and use control theory to give appropriate commands to follow the path specified by the planner and react to unexpected events. A roboticist must be trained in mechanics and electronics to properly convert the commands obtained and transmit them to the motors that power the robot actuators. The chain of events, just described, that occur during a mobile robot activation is represented in Fig. 6.1.

The roboticist writing this dissertation, along with the people working with him, belongs to the kind which uses control theory trying to give his contribution in the field. The idea is to conceive algorithms to deploy one or more mobile robots toward a destination while avoiding obstacles. These solutions should be easy to implement in any circumstance and for any kind of mobile robot given the model. To do that the acquisition of knowledge in several fields was necessary.

Section 1.4 presents briefly the wheeled mobile robots *modelling*, or rather, how the mechanical design, under some working assumptions, affect the behaviour of the mobile robot and consequently the way to control it in case of a particular task and why in this work the use of a particular implementation of the kinematic model is preferred to others. Section 1.5 exposes the *navigation* problem and the most common solutions utilised in robotics to move the robot from a starting point to a destination in a (partially-)known environment avoiding obstacles in a smart way. Finally Section 1.6 gives a review of the strategies adopted to realize a formation of generic agents; every strategy can be, of course, adapted to be used in robotics to make mobile robots to cooperate performing various missions previously not doable or increasing the efficiency with respect to the same mission conducted by a single robot.

1.4 The modeling of Wheeled Mobile Robot

The modelling of wheeled mobile robots (WMRs) is a crucial aspect when dealing with the huge amount of tasks they have been devoted in the last thirty years. Knowing how the system reacts, and its properties, allows to design specific solutions to achieve

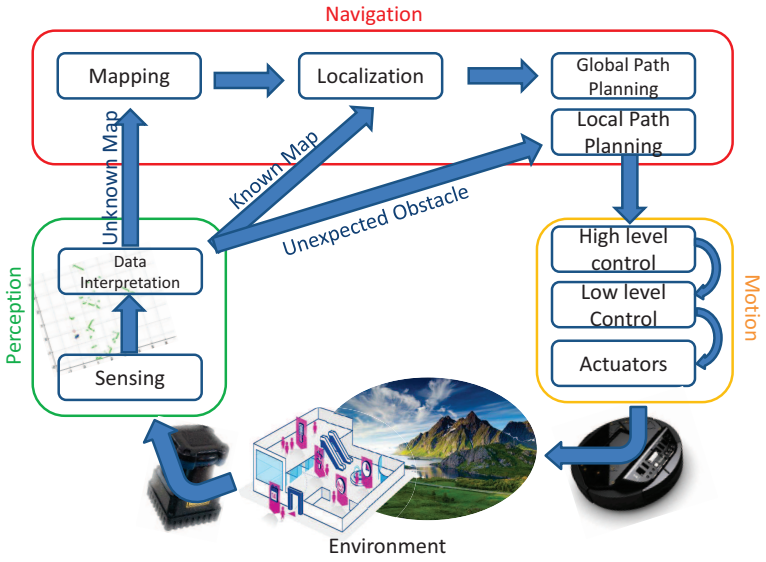

Figure 1.2: General control scheme for a mobile robot

the task is the best way. The diffusion of mobile robotics due to technical innovations and the interesting characteristics of this kind of robots encouraged a lot of researchers, from different fields, to give a formal formulation that could be used to represent these systems. Several works [19],[107],[128] came to different formulations that have resulted to be equivalents. Two are the models typology one can use when working with WMR, *dynamic* one and *kinematic* one: the first represents all the forces and torques that act on the robot, and takes into account the mass and the center of mass giving a precise description of the system, while the second one is simpler giving information just about the posture and the basic characteristics which describes the robot motion. Following the work presented by Campion *et al.* in [19], the WMRs kinematic representations will be exposed along with several concepts used to classify mobile robots. The WMRs will be classified introducing the concept of *degree of mobility* and *degree of steerribility*, combining these two characteristics all WMRs can be assigned to one of five classes. The five classes can be modelled with a state space representation emphasizing the kinematic or dynamic properties using the *posture* representation, useful to analyse the control properties of the system, or the *configuration* representation, which highlights movement constraints of the WMR. The usual hypothesis when one deals with wheeled robots is to assume the robot frame to be rigid and the wheels to be non deformable. Once defined a fixed global reference frame, the plane of motion, represented by the base $\mathcal{G} = \{I_1, I_2\}$, the easiest way to represent a mobile robot is to define its position with respect to $\mathcal{G}$. Consider the base $\mathcal{G}_\mathcal{R} = \{X_1, X_2\}$ attached to the robot frame, Fig. 1.3. Being $P = (q_x, q_y)$ the position of a chosen point of the robot frame (typically the center of mass) and q_θ the orientation of the $\mathcal{G}_\mathcal{R}$ frame with

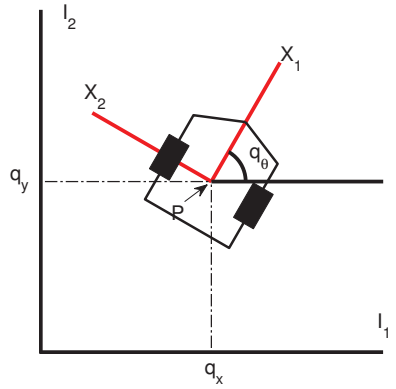

Figure 1.3: Visual representation of the WMR posture and working frames $\mathcal{G}_{\mathcal{R}}$, $\mathcal{G}$

respect to $\mathcal{G}$ one can define:

Definition 1. *[19] The* Posture *of a mobile robot is the vector:*

$$p \triangleq \begin{pmatrix} q_x \\ q_y \\ q_\theta \end{pmatrix} \tag{1.1}$$

1.4.1 The Wheels Typology

A lot of the properties of the mobile robot are in a strict relationship with the number of wheels, because as it is easy to guess, they define the characteristic of the robot itself. Making the assumption that during the motion each wheel spins around its horizontal axis staying in vertical position, with a single contact point with the soil, a classification of wheel types can be given. A first one divides them in *conventional* or *swedish* (*omnidirectional*). For conventional wheels it is supposed the rolling to happen without slipping or skidding, this hypothesis usually called *pure rolling condition* which implies that the velocity in the contact point between the wheel and the ground has zero value both in its orthogonal and parallel components with respect to the plane of the wheel itself. To summarize the pure rolling condition by points:

- the WMR must not slide in the orthogonal direction with respect to the wheel plane;
- it must not be skidding between the wheel and the ground;
- the WMR wheel is non-deformable (*i.e.* the radius r is constant);
- the ground is supposed to be flat.

The Swedish wheel differs from the conventional one because just one of the mentioned velocity components has zero value. In the following, the $R(q_\theta)$ matrix that appears is

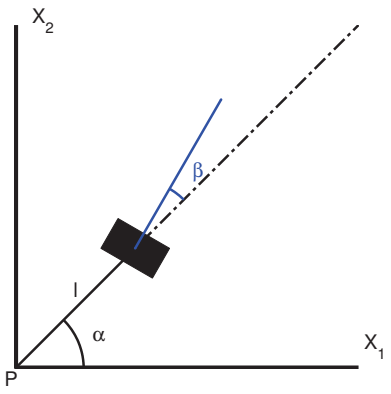

Figure 1.4: Visual representation of fixed conventional wheels and centered orientable wheels parameters

the classical rotation matrix

$$R(q_\theta) = \begin{pmatrix} \cos q_\theta & \sin q_\theta & 0 \\ -\sin q_\theta & \cos q_\theta & 0 \\ 0 & 0 & 1 \end{pmatrix}. \tag{1.2}$$

According to the assumption made, conventional wheels can be sorted in three subcategory and, for each of them, constraints regarding the velocities components can be derived explicitly:

- ***Fixed wheels***: firstly one can describe the position of the wheel with respect to the robot frame with an l distance and an α angle, then the orientation β of the wheel plane with respect of the position just defined; a visual explanation of the three parameters is shown in Fig. 1.4. The $\varphi(t)$ function represents the rotation angle of the wheel around is horizontal axle and r is the wheel radius. Once defined the four parameters $(\alpha, \beta, \varphi, r)$ and the function $\varphi(t)$ one can define the two constraints, along the wheel plane and on the orthogonal plane, respectively:

$$[-\sin(\alpha+\beta) \quad \cos(\alpha+\beta) \quad l\cos(\beta)]\, R(q_\theta)\dot{p} + r\dot{\varphi} = 0 \tag{1.3}$$

$$[\cos(\alpha+\beta) \quad \sin(\alpha+\beta) \quad l\sin(\beta)]\, R(q_\theta)\dot{p} = 0. \tag{1.4}$$

- ***Centered orientable wheels***: The main difference between the centered orientable wheel and the fixed one (Fig. 1.4) stays in the fact that the wheel plane orientation $\beta(t)$ is a time varing function; in the light of this difference the constraints have, finally, the same equations (in the following β is to be considered as $\beta(t)$, the dependence on time has been removed to keep the notation lighter):

$$[-\sin(\alpha+\beta) \quad \cos(\alpha+\beta) \quad l\cos(\beta)]\, R(q_\theta)\dot{p} + r\dot{\varphi} = 0 \tag{1.5}$$

$$[\cos(\alpha+\beta) \quad \sin(\alpha+\beta) \quad l\sin(\beta)]\, R(q_\theta)\dot{p} = 0. \tag{1.6}$$

- ***Off-centered orientable wheels*** (*castor* wheels): along with the possibility to move the wheel plane with respect to the frame, a castor wheel has the capability

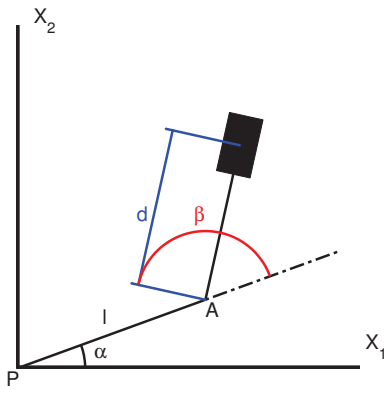

Figure 1.5: Visual representation of Off-centered orientable wheel parameters and variables

to change also its position; the rotation does not happen around the wheel plane though (see Fig. 1.5). To describe a castor wheel an additive parameter d is needed, giving the length of a rod which connects the robot frame (point A in Fig. 1.5) to the center of the wheel; the rod can rotate around the A point. The parameters which describe a castor wheel are (α, d, φ, r) with two time varying function $\varphi(t)$ and $\beta(t)$ generating the following constraints:

$$[-\sin(\alpha+\beta) \quad \cos(\alpha+\beta) \quad l\cos(\beta)]\, R(q_\theta)\dot{p} + r\dot{\varphi} = 0 \tag{1.7}$$

$$[\cos(\alpha+\beta) \quad \sin(\alpha+\beta) \quad d + l\sin(\beta)]\, R(q_\theta)\dot{p} + d\dot{\beta} = 0. \tag{1.8}$$

The Swedish wheel has a peculiarity, it is able to move in any direction in any time. It is required to add a parameter, the angle γ (Fig. 1.6), to derive the motion constraint:

$$[-\sin(\alpha+\beta+\gamma) \quad \cos(\alpha+\beta+\gamma) \quad l\cos(\beta+\gamma)]\, R(q_\theta)\dot{p} + r\cos\gamma\dot{\varphi} = 0. \tag{1.9}$$

It is worth to remark that for a Swedish wheel the value $\gamma = \pi/2$ corresponds to the zero value velocity on the orthogonal plane of the wheel, in such a condition this kind of wheel loose the advantage to be mounted on a mobile robot being subject to the same constraints of the conventional wheels in case the non slipping one.

1.4.2 Degree of mobility and degree of steeribility

The definition of the movement constraints for each wheel typology is the base to introduce further properties which will lead to the characterization of different classes of WMRs. First of all, one can consider a generic mobile robot with a generic number of wheels N; to differentiate them, four different subscripts will be used: f for conventional fixed, c for conventional centered, oc for conventional off-centered and sw for swedish wheels. Consequently the number N of wheels of the generic mobile robot will be the sum of each kind of wheel: $N = N_f + N_c + N_{oc} + N_{sw}$. To define the robot configuration one can use the posture p_θ, Definition 1, the angular coordinates depending on the wheels $\beta_c(t)$ or $\beta_{oc}(t)$ and the information about the rotation

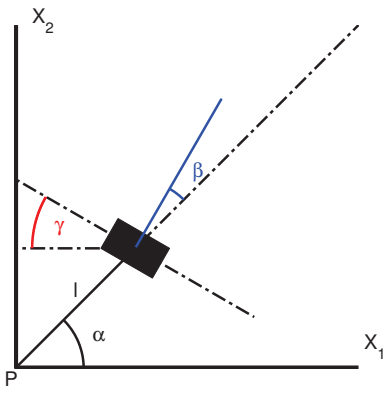

Figure 1.6: Visual representation of a sweedish wheel parameters and variables

coordinates $\varphi(t) = [\varphi_f(t), \varphi_c(t), \varphi_{oc}(t), \varphi_{sw}(t)]^T$. The set of posture, angular and rotation coordinates is called *configuration coordinates* set. Moreover one can express the motion constraints with:

$$J_1(\beta_c, \beta_{oc})R(q_\theta)\dot{p} + J_2\dot{\varphi} = 0 \tag{1.10}$$

$$C_1(\beta_c, \beta_{oc})R(q_\theta)\dot{p} + C_2\dot{\beta_{oc}} = 0. \tag{1.11}$$

where

$$J_1(\beta_c, \beta_{oc}) \triangleq \begin{pmatrix} J_{1f} \\ J_{1c}(\beta_c) \\ J_{1oc}(\beta_{oc}) \\ J_{1sw} \end{pmatrix} \tag{1.12}$$

includes the constraints (1.5), (1.3), (1.7), (1.9), J_2 is a diagonal matrix which has the radii on the main diagonal (for Swedish wheels the radii are multipied by $\cos\gamma$).

$$C_1(\beta_c, \beta_{oc}) \triangleq \begin{pmatrix} C_{1f} \\ C_{1c}(\beta_c) \\ C_{1oc}(\beta_{oc}) \end{pmatrix}, C_2 \triangleq \begin{pmatrix} 0 \\ 0 \\ C_{2oc} \end{pmatrix} \tag{1.13}$$

In C_1 one can find the constraints (1.4), (1.6) and (1.8), while the component C_{2oc} of C_2 is the diagonal matrix which contains the d values of the off centered wheels. Let us consider equation (1.11) in case of fixed and centered wheels ($N = N_f + N_c$):

$$C_{1f}R(q_\theta)\dot{p} = 0 \tag{1.14}$$

$$C_{1c}(\beta_c)R(q_\theta)\dot{p} = 0 \tag{1.15}$$

it is straightforward to state that the product $R(q_\theta)\dot{p}$ belongs to the null space of

$$C_1^*(\beta_c) \triangleq \begin{pmatrix} C_{1f} \\ C_{1c}(\beta_c) \end{pmatrix} \tag{1.16}$$

and that if the rank of such a matrix is full, then $R(q_\theta)\dot{p} = 0$ and no movement is possible. From (1.14) and (1.15) we can infer that at each instant the WMR moves around a point which is the intersection of all the straight lines passing from all the

Wheels	α	β	L	radius
Fixed (lower)	0	0	l	r_1
Fixed (upper)	π	0	l	r_1
Orientable	$\frac{3\pi}{2}$	$\beta(t)$	l	r_2

Table 1.1: Positiong parameter for the two wheels

wheels center and orthogonal to the wheel planes, this point is called Instantaneous Center of Rotation (ICR) and it is shown in Fig.1.8 for a two wheels robot while figure 1.9 shows three other scenarios, two degenerate robots in which the motion is not possible Fig. 1.9(b) and Fig. 1.9(c) and the ICR for a car-like robot Fig. 1.9(a). Of course the position of the ICR with respect to the frame can be time-varying depending on the wheel type and robot design.

Example 1. *Let us see how the matrices look like in the case of a WMR with three wheels: two conventional fixed ones and a conventional centered orientable wheel. The α, β, l, parameters and the radii for the three wheels are represented in Table 1.1.*

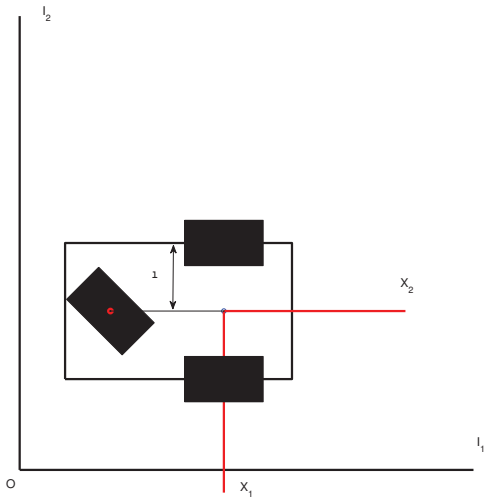

Figure 1.7: Visual representation of a 2 wheeled robot

First we derive the condition (1.3)*,* (1.4)*,* (1.5) *and* (1.6)*:*

- *for the first (lower in Fig. 1) conventional fixed wheel:*

$$\begin{bmatrix} 0 & 1 & l \end{bmatrix} R(q_\theta)\dot{p} + r_1\dot{\varphi} = 0$$
$$\begin{bmatrix} 1 & 0 & 0 \end{bmatrix} R(q_\theta)\dot{p} = 0;$$

- *for the second (upper in Fig. 1) conventional fixed wheel:*

$$\begin{bmatrix} 0 & -1 & l \end{bmatrix} R(q_\theta)\dot{p} + r_1\dot{\varphi} = 0$$
$$\begin{bmatrix} -1 & 0 & 0 \end{bmatrix} R(q_\theta)\dot{p} = 0;$$

- *for the conventional orientable centered wheel:*

$$\begin{bmatrix}\cos(\beta) & \sin(\beta) & l\cos(\beta)\end{bmatrix} R(q_\theta)\dot{p} = 0$$
$$\begin{bmatrix}\sin(\beta) & -\cos(\beta) & l\sin(\beta)\end{bmatrix} R(q_\theta)\dot{p} + r_2\dot{\varphi} = 0.$$

It follows that the matrices J_1, J_2, C_1 and C_2 are the following:

$$J_1(\beta_f, \beta_c) = \begin{pmatrix} 0 & 1 & l \\ 0 & -1 & l \\ \cos(\beta(t)) & \sin(\beta(t)) & l\cos(\beta(t)) \end{pmatrix}, \quad J_2 = diag(r_i) \tag{1.17}$$

$$C_1(\beta_f, \beta_c) = \begin{pmatrix} 1 & 0 & 0 \\ -1 & 0 & 0 \\ \sin(\beta(t)) & -\cos(\beta(t)) & l\sin(\beta(t)) \end{pmatrix}, C_2 = 0. \tag{1.18}$$

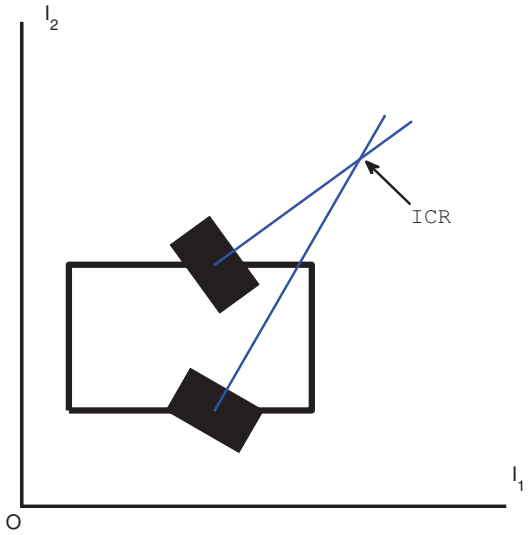

Figure 1.8: Visual representation of the Istantaneous Center of Rotation (ICR) for a 2 wheels WMR

One can easily understand that the rank of the $C_1^*(\beta_c)$ gives information about the mobility of the robot and the following definitions can be given:

Definition 2. *The* degree of mobility δ_m *of a WMR is defined as:*

$$\delta_m = \dim \mathcal{N}\left[C_1^*(\beta_c)\right] = 3 - \operatorname{rank}\left[C_1^*(\beta_c)\right]. \tag{1.19}$$

Definition 3. *A wheeled mobile robot is* non-degenerate *if:*

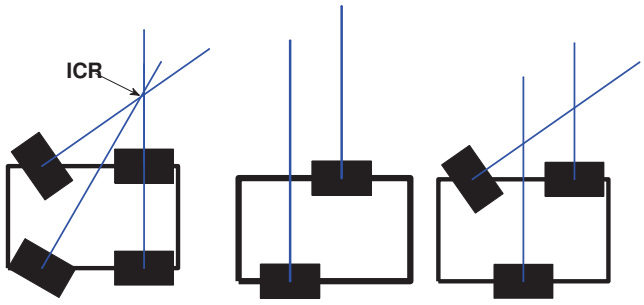

(a) ICR in case of car-like robot

(b) Degenerate robot: no ICR, no motion possible

(c) Degenerate robot: double ICRs, no motion possible

Figure 1.9: Exemples of different ICRs

- $\text{rank}\,[C_{1f}] \leq 1$;
- $\text{rank}\,[C_1^*(\beta_c)] \leq 2$.

The first condition in Definition 3 implies that if the robot has more than one fixed wheels, these must be on the same axle; moreover, following Definition 3 if the robot has fixed and center orientable wheels, the center of centered orientable wheels do not belong to the common axle of the fixed ones and that the rank of the matrix $C_{1c}(\beta_c)$ is the number of centered orientable wheels that can be oriented independently to steer the robot.

Definition 4. *The* degree of steeribility δ_s *of a WMR is defined as:*

$$\delta_s = \text{rank}\,[C_{1c}(\beta_c)]\,. \tag{1.20}$$

The number $\delta_s \leq 2$ of steering wheels is a design parameter but of course if it is higher than 2 the behavior of the wheels must be appropriate and must guarantee the existence of the ICR for any instant of time.

Example 2. *Looking at the Example 1, with the robot configuration showed in Fig. 1.7, we can try to evaluate the degree of mobility and steeribility in the presented case and to verify that it is not a degenerate robot. Having the robot one convetional fixed wheel and one convention cantered orientable wheel the matrix $C_1^*(\beta_c)$ results to be equal to the defined C_1 matrix and it follows that the degree of mobility results to be:*

$$\delta_m = \dim \mathcal{N}\,[C_1] = 3 - \text{rank}\,[C_1] = 3 - 2 = 1, \tag{1.21}$$

while the degree of steeribility:

$$\delta_s = \text{rank}\,[C_{1c}(\beta_c)] = 1, \tag{1.22}$$

having just 1 conventional centered orientable wheel. It is straightforward to verify the condition of Definition 3 and conclude that the presented example is not a degenerate robot.

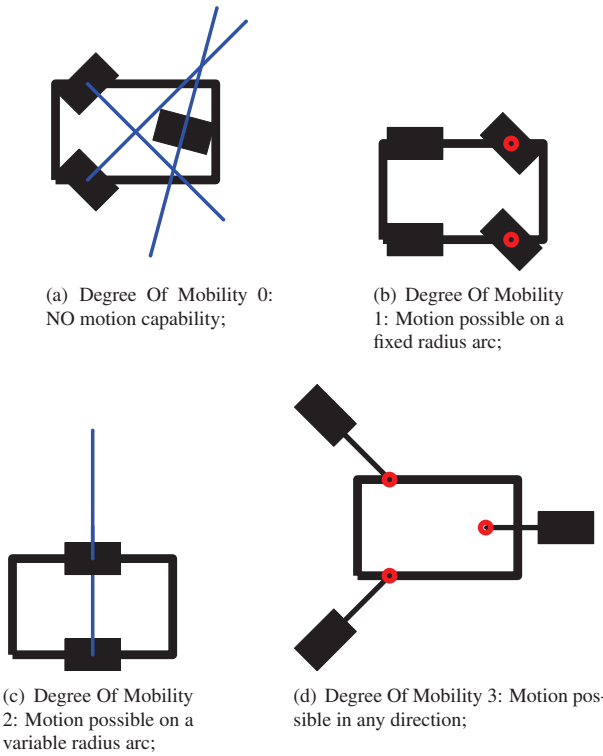

(a) Degree Of Mobility 0: NO motion capability;

(b) Degree Of Mobility 1: Motion possible on a fixed radius arc;

(c) Degree Of Mobility 2: Motion possible on a variable radius arc;

(d) Degree Of Mobility 3: Motion possible in any direction;

Figure 1.10: Different values of *degree of mobility*

From the definition of degree of mobility and degree of steeribility just *five* nonsingular classes of WMR can be defined (see Table 1.2).

Table 1.2: The *five* nonsingular types of WMR

δ_m	3	2	2	1	1
δ_s	0	0	1	1	2

The following inequality applies:

$$2 \leq \delta_s + \delta_m \leq 3. \tag{1.23}$$

The degree of mobility has a lower bound of 1 because the obvious choice it is to consider only robot that can actually move. Concerning the degree of steeribility the upper bound implies the absence of fixed wheels while the lower one can be achieved only without centered orientable wheels. Let us take a look at the five typologies and their properties:

- **Type (3,0)**[3], also called *omnidirectional* robots, they don't have fixed or centered

[3]For each typology the first term in the parenthesis represents the degree of mobility δ_m and the second one the degree of steeribility δ_s.

orientable wheels and can move in any direction in any instant of time.

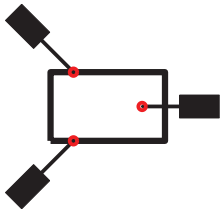

Type (3,0) WMR

- **Type (2,0)**, also known as *unicyle-like* robots, they do not have centered orientable wheels but one fixed wheel or several fixed wheels on the same axle (if not so the $\mathrm{rank}[C_{1f}]$ would be greater than 1); they have restricted mobility since characterized by velocity constraints that deny the possibility to orientate the velocity vector in any direction at any time.

Type (2,0) WMR

- **Type (2,1)**, also robots with restricted mobility, have no conventional fixed wheels and at least one centered orientable wheel.

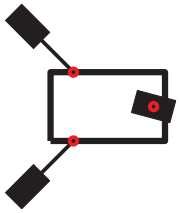

Type (2,1) WMR

- **Type (1,1)**, characterized by several conventional fixed wheels on the same axle and one or several centered orientable wheels that must not be on the same axle of the fixed ones. The centered orientable wheels must behave such that $\mathrm{rank}\, C_{1c}(\beta_c) = \delta_s = 1$. The velocity constraint on this restricted mobility robot is parametrized by the orientation of one of the orientable centered wheels. They are frequently called *car-like* WMR.

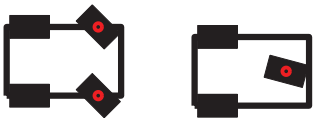

Type (2,0) WMR

- **Type (1,2)**, no fixed wheels for this type of WMR but at least two conventional centered orientable wheels. If more than two then the behavior must satisfy the condition $\mathrm{rank}\, C_{1c}(\beta_c) = \delta_s = 2$. The velocity constraint for these robots is parametrized using the orientation of two of the centered orientable wheels.

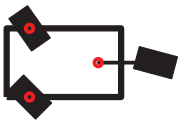

Type (1,2) WMR

1.4.3 The Posture Kinematic Model

In control theory, to analyse system properties, it is useful to give a state space representation. Starting from the definition given above, we will present such a representation and some properties for the *Type (2,0)* WMR since the works in the following chapters will focus on this model (or a modification of it). Each mobile robot has constraints because of which at any time the velocity belongs to the distribution Δ_c defined as

$$\dot{p}(t) \in \Delta_c \triangleq \operatorname{span}\{\operatorname{col} R^T(q_\theta)\Sigma(\beta_c)\} \qquad \forall t \tag{1.24}$$

where the columns of $\Sigma(\beta_c)$ form a basis of $\mathcal{N}[C_1^*(\beta_c)] = \operatorname{span}\{\operatorname{col}\Sigma(\beta_c)\}$, thus we can write that:

$$\dot{p} = R^T(q_\theta)\Sigma(\beta_c)\eta \tag{1.25}$$

where η is a vector that has the dimension of the degree of mobility δ_m and can be considered as a velocity input vector for the system. In case of absence of centered orientable wheels ($\delta_s = 0$) the matrix Σ is constant while in case of presence of such a wheels ($\delta_s \geq 1$) the β_c variables become state variables:

$$\dot{p} = R^T(q_\theta)\Sigma(\beta_c)\eta \tag{1.26}$$

$$\dot{\beta}_c = \zeta. \tag{1.27}$$

The representation obtained this way with (1.26) and (1.27) is called *posture kinematic model*. To simplify the notation let us define

$$q \triangleq \begin{pmatrix} p \\ \beta_c \end{pmatrix}, \quad G(q) \triangleq \begin{pmatrix} R^T(q_\theta)\Sigma(\beta_c) & 0 \\ 0 & I \end{pmatrix}, \quad u \triangleq \begin{pmatrix} \eta \\ \zeta \end{pmatrix} \tag{1.28}$$

and obtain:

$$\dot{q} = G(q)u. \tag{1.29}$$

For any non-degenerate WMR (see Definition 3), it is possible to prove that choosing a reference frame attached to the robot for which the kinematic model represents exactly the robot typology [19].

Example 3. *Willing to conclude the modelling of Example 1, for the mobile robot with the configuration showed in Fig 1.7, the null space of the matrix* $\Sigma(\beta_c)$ *assumes the value*

$$\Sigma(\beta_c) = \begin{pmatrix} 0 \\ l\sin(\beta) \\ \cos(\beta) \end{pmatrix}. \tag{1.30}$$

It follows from (1.26)*, that*

$$\dot{p} = R^T(q_\theta)\Sigma(\beta_c)\eta = \begin{pmatrix} -l\sin(\beta)\sin(q_\theta) \\ l\sin(\beta)\cos(q_\theta) \\ l\cos(\beta) \end{pmatrix}\eta \tag{1.31}$$

For such a robot with a centered orientable wheel the state need do be represented with more then the posture as depicted in (1.28) *so the final kinematic model for the Type (1,1) robot taken into account is, following* (1.29)*:*

$$\dot{q} = \begin{pmatrix} \dot{p} \\ \dot{\beta} \end{pmatrix} = \begin{pmatrix} -l\sin(\beta)\sin(q_\theta) & 0 \\ l\sin(\beta)\cos(q_\theta) & 0 \\ l\cos(\beta) & 0 \\ 0 & 1 \end{pmatrix}\begin{pmatrix} \eta \\ \zeta \end{pmatrix} \tag{1.32}$$

Example 4. *For instance for a type (2,0) robot, the unicycle like WMR, the origin of the robot reference frame is placed on the axle which connects the two driving wheels as shown in Fig. 1.3; this placement brings to a posture kinematic model in the form:*

$$\dot{q} = \begin{pmatrix} \dot{q_x} \\ \dot{q_y} \\ \dot{q_\theta} \end{pmatrix} = \begin{pmatrix} \cos(q_\theta) & 0 \\ \sin(q_\theta) & 0 \\ 0 & 1 \end{pmatrix} \begin{pmatrix} v \\ \omega \end{pmatrix} = \begin{pmatrix} \cos(q_\theta) \\ \sin(q_\theta) \\ 0 \end{pmatrix} v + \begin{pmatrix} 0 \\ 0 \\ 1 \end{pmatrix} \omega, \tag{1.33}$$

where the inputs vector $u = \eta = (v \quad \omega)^T$ *consists of the linear,* v*, and angular,* ω*, velocities of the WMR while the* $G(q)$ *matrix specified in* (1.29) *is:*

$$G(q) = [g_1(q) \quad g_2(q)] = \begin{pmatrix} \cos(q_\theta) & 0 \\ \sin(q_\theta) & 0 \\ 0 & 1 \end{pmatrix} \tag{1.34}$$

1.4.4 WMR constraints and controllability

The main characteristic of the system (1.29) in the form (1.33) is to be subject of motion constraints of *non-holonomic* type. A holonomic constraints can be expressed as a function of the position parameters (p, φ), while a non-holonomic one depends on the motion parameters, thus the derivatives $(\dot{p}, \dot{\varphi})$, furthermore, a non-holonomic constraints cannot be integrated. WMR with reduced mobility have non-holonomic constraints and that is due to the *pure rolling* hypothesis made while deducting the models (Section 1.4.1). Let us define $\mathcal{C} \in \mathbb{R}^n$ as the *configuration space* of all the possible configurations (*i.e.* postures) of the WMR, $q \in \mathcal{C}$. A non-holonomic constraint, can be written in the Pfaffian form [128]:

$$a(q, \dot{q}) = 0 \tag{1.35}$$

or in the matrix form

$$A^T(q)\dot{q} = 0. \tag{1.36}$$

Definition 5. *The* degree of freedom *is the difference between the number of generalized coordinates and the number of independent constraints.*

$$DOF = n - m. \tag{1.37}$$

Consider the system as in (1.29), with k Pfaffian constraints in the form (1.36), it follows that all the admissible velocities belong to the $n - k$ dimensional $\mathcal{N}\left[A^T(q)\right]$. Being $\{g_1(q), \ldots, g_{n-k}(q)\}$ a basis of $\mathcal{N}\left[A^T(q)\right]$ all the admissible trajectories are described by the solution of

$$\dot{q} = G(q) = \sum_{j=1}^{m} g_j(q) u_j, \qquad m = n - k \tag{1.38}$$

The holonomy or non-holonomy of the constraints are related to the controllabilty property of the model [73]:

1. If the system (1.38) is controllable, given two configurations q_i and q_j in the configuration space $\mathcal{C}$, one can find a control $u(t)$ that brings the WMR from q_i to q_j (*i.e.* it exist a trajectory which joins the two configurations satisfying the constraint (1.36)).

2. If the system (1.38) is not controllable the constraint (1.36) reduces the set of admissible configuration in $\mathcal{C}$ that implies that the constraints are totally or partially integrable depending on the dimension ν of the accessible space:
   - if $m < \nu < n$, the constraints are partially integrable but the system is still non-holonomic;
   - if $\nu = m$, the constraints are integrables and the system is holonomic.

The same conclusions could be deducted using the *accessibility rank condition*:

$$\dim \Delta_A(q) = n, \tag{1.39}$$

where $\Delta_A(q)$ is called accessibility distribution associated to system, namely the involutive closure of $\Delta = \{g_1(q), \ldots, g_m(q)\}$ (please refer to Appendix D for more details); it follows:

1. If (1.39) holds, the system (1.38) is controllable and the constraints are non-holonomic;
2. If (1.39) does not hold, the system (1.38) is not controllable and the constraints are partially or totally integrable, being $\dim \Delta_A(q) = \nu < n$:
   - if $m < \nu < n$, the constraints are partially integrable but the system is still non-holonomic;
   - if $\nu = m$, the constraints are integrable and the system is holonomic.

For the Unicycle-like WMR described as in (1.33), the pure rolling constraint can be written as:

$$\dot{q}_x \sin q_\theta - \dot{q}_y \cos q_\theta = [\sin q_\theta \quad \cos q_\theta]\dot{q} = 0, \tag{1.40}$$

note that, as in (1.33):

$$G(q) = \begin{pmatrix} \cos(q_\theta) & 0 \\ \sin(q_\theta) & 0 \\ 0 & 1 \end{pmatrix} \quad \text{with} \quad g_1(q) = \begin{pmatrix} \cos(q_\theta) \\ \sin(q_\theta) \\ 0 \end{pmatrix} \quad g_2(q) = \begin{pmatrix} 0 \\ 0 \\ 1 \end{pmatrix} \tag{1.41}$$

where $g_1(q)$ and $g_2(q)$ represent a basis of the null space of the Pfaffian constraint. Following the theory to verify the controllability for non linear systems [73], the Lie Brackets of the two input vector field is

$$[g_1, g_2](q) = \left(\frac{\partial g_2}{\partial q} g_1 - \frac{\partial g_1}{\partial q} g_2 \right) = \begin{bmatrix} -\cos(q_\theta) \\ \sin(q_\theta) \\ 0 \end{bmatrix}. \tag{1.42}$$

It follows that the matrix

$$(g_1(q), g_2(q), [g_1, g_2](q)) = \begin{pmatrix} \cos(q_\theta) & 0 & -\cos(q_\theta) \\ \sin(q_\theta) & 0 & \sin(q_\theta) \\ 0 & 1 & 0 \end{pmatrix} \tag{1.43}$$

has maximum rank, which implies that

$$\dim \Delta_A = \dim \operatorname{span}\{g_1(q), g_2(q), [g_1, g_2](q)\} = 3, \tag{1.44}$$

meaning that a WMR of type $(2, 0)$ modeled as (1.33) is controllable and has non-holonomy degree $k = 2$ and that the constraint (1.41) is non-holonomic. A result presented by Brockett in 1983 [18] established that a mobile robot, which has non-holonomic constraints, even though controllable, cannot be stabilized by a continuous state-feedback control law. Thus stabilizing WMRs has been seen as a challenging problem and drawn attention of the control community. The stabilization of a non-holonomic robots is presented in many papers and books [128],[129], [32], [25], using time-varying , hybrid [99], discontinuous [29], [4],[43], backstepping [110], and switched [35],[111] control laws.

1.4.5 More than the Kinematic Representation?

As it is obvious the kinematic model for WMR cannot fit all the needs and sometimes it is useful to adopt a model more tied to the dynamics of the robot in use: it is the case of outdoor application in which this model allows to handle the field properties and how the dynamics of the robots would react to uncertain conditions. The *dynamic* model represents all the forces and the masses and relates them via the accelerations involved [19]. It gives more information and allows the representation that cannot be represented by the use of velocities (Kinematic Modelling) but requires the accelerations; however these information come with a cost, using a dynamical model requires the knowledge of several parameters like masses, inertial constants and gravity center of the various systems forming the robot, and not always these values are available; the second drawback is, of course, that any strategy design and implementation becomes more complex to treat. The dynamic model of the WMR could be generalized ad follows:

$$J(q)\dot{u} + C(q, u)u = D(q)\tau + A^T(q)\lambda \tag{1.45}$$

where: $J(q)$ is an inertia matrix, $C(q, u)$ is the centripetal and coriolis matrix, $D(q)$ is the input matrix and τ is the input vector; $A(q)$ is the matrix associated with the kinematic constraints, and λ is a Lagrange multipliers vector.

As mentioned above the choice of the dynamic or kinematic model is based on the needs, and not just the property of the field in indoor or outdoor scenarios but also the desired performances for the specified task. A lot of factors must be taken into account, how the masses vary during the task and if these variations could endanger the robot itself, or the velocities one wants to reach during the mission and how to reach them, since this could cause the breaking of the assumption of Section 1.4. It has to be said that if the robot is not under-actuated (with respect to the mobility degree) it is possible to find a *feedback linearization* which allows to control the WMR with velocity commands, having, thus the same adavantages of the Kinematic model.

This work of thesis considers small mobile robots working in an indoor environment, the velocities reached and the manoeuvres realized along with the scenarios considered are not such to justify the increase of difficulties due to the employment of a dynamic model. Therefore, the kinematic model (1.33) can be modified to handle some perturbation of interest. A first example can be found in [26] and [85] in which perturbation are added to the model to allow the robot to break the pure-rolling and not-skidding constraints to test the robustness of some control algorithms. Other approaches consider the skidding property governed by linear velocity command sent to the wheel and product of wheel radius and angular velocity [86],[151]. The unicycle model (1.33) in the following will be considered perturbed too but the disturbances taken into account have as purpose to model different kinds of unmodeled dynamics

better treated in Section 2.1

1.5 Navigation Problem

The navigation problem in robotics has been thoroughly studied in the last forty years. The first attempt to propose a collision free path date back to the beginning of second half of the last century but it is in the 80's that the research increased and produced results which are used up to the present day [63, 135]. One of them describes obstacles as *polyhedral object* can be found in [95], and very early the robotic community realized that the navigation problem was indeed the union of two separate task [97]: the *motion planning* which starts from a complete or partial knowledge of the environment and allows the mobile robot to plan the movements to arrive to destination and the *reacting* part, which is in charge to identify changes in the a-priori knowledge and gives instructions to deal with them. In the following a brief review of the path planning algorithms and collision avoidance algorithms is carried out.

1.5.1 Path Planning Algorithms

Usually for path planning the WMR is considered to be holonomic or even a point in 2D dimension; this is due to the fact that one of the most widespread type of WMR is the differential type (Type (2,0)) robot, which can rotate in place if necessary. The path planning algorithms starts from a map that can be represented geometrically or be the results of a decomposition[4], and gives a suitable trajectory to get to the destination. The ways to analyse the map data and convert them to a path can be divided in two different kind strategies: *graph search* strategies, that build a connectivity graph and then perform, usually offline, algorithms to extract the motion plan, and *potential field* strategies based on rigorous mathematical functions whose gradient brings the WMR to the destination.

Building the graphs

When a representation of the working space is given, the first step to realize is the construction of a graph able to connect any free points of the environment. Of course there are several ways to define nodes and edges, one of them is to build a *visibility graph* [81] which tends to place nodes and edges to realize the shortest path in the free space: each edge connects two vertices that have a free path between them with a straight line (*i.e.* the shortest path). The easiness of implementation of the visibility graph is counterbalanced by the complexity it gets when the obstacles number increases and by the fact that, with such a graph, the solution obtained tends to prefer the path closest to the obstacles. A second approach which puts first the maintenance of the distance from the obstacle is based on the *Voronoi diagram* [5]. For each point in the space it is computed the distance to the nearest obstacle, points that are equidistant from two or more obstacles represent nodes and in case of polygonal obstacles the edges are either straight lines or quadratic functions. This approach is useful to find the optimal path with respect of the length of the path, but it has a drawback tied to the sensors used for the localization, since the better the sensor range the better the localization and thus the evaluation of the map due to the fact that the diagram is based on the maximization of obstacles distance. Another approach is called *exact cell decomposition*, it consists

[4] For the different kinds of map representations we refer the reader to [129], chapter 5

on a division of the working space based on the vertices of the obstacles, resulting in cells that are either free or occupied; the path to follow is, obviously, chosen to pass trough the free ones. Again, the complexity of this kind of graph increases as the density of the obstacles does so, for that reason a more common representation used in robotics is the *approximate cell decomposition* in which the size of the cell is fixed *a priori* and the representation said just if the cell is occupied or not and it is actually the most common map representation [105].

The algorithms

Given the graph that represents the environment it is necessary to find a nice algorithm to find the best path available to move in the working space. Of course the best path is the one that minimize/maximize the property that has more weight for the user and it depends thus on the optimization criteria. As it is possible to guess the solution is not unique and it depends on how the graph is read, for instance one could give weight or not to the edges giving to the graph complete different meanings.

Among the algorithms which do not consider weighted edged one can find the *breadth-fist search* and the *depth first search*. The first one [22] performs a node expansion (it visits all nodes to check for a free path) marking at each iteration the less number of edge to cover the path to the farther node to finally get to the final destination. With the hypothesis of equal cost for each edge it gives the optimal path. The depth-first search performs a different kind of visit which visits the graph up to the deepest level then going back to previously visited nodes to expand again in a new direction. The drawback of this method consists in the presence of redundant path due to the multiple visits of the same nodes, but this inconvenient can be avoided with a cautious implementation. Definitely more renowned are the algorithms which include some heuristics to find the more suitable path, like a weight for the edges to find out if the crossing could be convenient or not, or a distance to the final destination. *Dijkstra's* algorithm [31], is conceived to find the shortest path between two nodes of a weighted graph: similar to the breadth-first, it expands all the nodes but giving a *key* to each node, the key is the results of the expansion taking into account the *cost* to arrive in that node, once the node key is the minimum possible the node is marked and not visited again. In robotics Dijkstra algorithm is used backward starting from the goal position to have the best path for each starting position of the WMR.

Nowadays the A^* algorithm [60] is one of the most widespread, that is a consequence of the large use of the occupancy grip map representation. In fact the heuristic utilized in this algorithm assign to each grid cell a value that represents the distance from the goal point. The expansion is thus carried on following the path given by the neighbours of the nodes that have the smallest value till the goal. It has been proved that this representation improves a lot the performances compared with the Dijkstra algorithm. A modification of the A^* algorithm called *dynamic* A^*, D^* [78], [94], is able to evaluate in real time the changes that could happen in the map and starting from the solution given from a previous A^* execution re-evaluate the (sub-)optimal solution.

Within the algorithms able to deal with high complex environment in which the Dijkstra algorithm or the A^* / D^* would provide a slow solution it is useful to use methods that visiting the graph in a random way, could give better results. In this case the *Rapidly exploring Random Trees* (RRTs) algorithms [83, 82] build a graph start-

ing from the obstacle map representation while visiting the environment; following the robot model, at each iteration a new couple node-edge is added to a graph (that at the beginning could be empty) in a collision free point of the space, until a pre-defined condition is verified. The method may speed up proceeding at the same time from the starting and ending point building partial trees and merging them at the end.

Changing completely the approach, *Potential Field* (PF) relies on a formal mathematical definition of the working space and on a function, *i.e.* the field, whose gradient is used as a reference to bring the WMR to the destination point. The method has been firstly developed for robotic manipulator by Khatib [76] and then has found a lot of users among the mobile robotic community. The goal point, the minimum of the function, attracts the robots while each obstacle acts as a repulsive force on the WMR to keep it away from the obstacle itself. The main advantage of this technique is represented by the easiness with which the gradient trajectories can be used as a reference for a control law to apply to the WMR. It has been shown that this solution, even though mathematically elegant and quite effective practically, has some drawbacks when special events occur [79]. The main inconvenient with the method is the appearance of local minima which block the robot due to particular obstacle configurations. Koditschek et al. in [121] proposed a modification of the PF based on navigation functions: in an n-dimensional spherical space the adopted field had no other local minima than the target specified, supposing though the complete environment to be known a priori. Other solutions use a harmonic potential field proposed in [24, 126], and more recently in [98], in which the method computes solutions to Laplace's Equation in arbitrary n-dimensional domains to have local minima free field, and results in a weak form of [121]. In [150], a different field formulation and obstacle representation is considered: the potential field includes two super-quadratic functions, one for the obstacle avoidance and one for the approaching resulting in a elliptic isopotential contour of the obstacles to model a large variety of shapes. Last flaw of the method is the possibility to miss the target in case of an obstacle too close to it. This problem called Goals Non-Reachable with Obstacles Nearby (GNRON), treated in [48], deals with the case in which the repulsive force generated by an obstacle close to the target generate a force higher than the attractive one, preventing the robot to accomplish the task. There are also methods which do not eliminate unwanted equilibriums but generate local forces, Virtual Hill, to escape the disturbing minimum as in [113].

1.5.2 Obstacle Avoidance

After the planners detected the suitable path (optimal or not as it has been stated above) the WMR can start its mission, it can happen though that some changes happened in the map after the planning of the motion. It is in these moments that local planners become active relying on the most recent sensors information and eventually on the previous knowledge of the map and a set of previous informations.

The Bug Algorithms

The first approaches used in robotics are the *Bug* algorithms [96], which basically were based to react *just* using the most recent sensor data. It is the simplest method that one can think: basically it just follows the contour of the encountered obstacle; in the very early version the robot would complete a tour around the obstacle also if a free path to the goal would be possible, that is why the *Bug 2* removed this flaw interrupting

the contour following when a free path to the destination would be detected. A modification, called *Tangent bug* presented in 1996 by Kamon *et al.* [70] implements a local representation of the environment which forces the robot to move on a *local tangent graph* to avoid obstacles to go back to the global path when the avoidance is achieved.

Vector Field Histogram, (VFH)

Within the local planners directly derived from the PF approach, as mentioned above, the VFH method firstly presented in [15] (see also its more recent modifications [145, 144]) represents also a widely used solution to real-time obstacle avoidance. The first experiments ran on WMRs showed the shortcomings of the bug algorithms and the ones inherited after the PF approach: the possibility for the WMR to get stuck in traps, usually represented by non convex obstacle which corresponds to local minima in the field. Thus, hybrid modifications like VFH+ or VFH*, were proposed: at each iteration a new grid map is created locally for a subset of active cells, then it is filled with recent data from the equipped sensors. The method first evaluates the PF for the updated cells, builds an obstacle histogram and reduces it to a polar form. This polar form gives information about the most suitable direction to take to continue the motion avoiding obstacles; this information is thus coupled with the previous desired direction in a cost function which takes into account (if possible) also the robot type. In particular the WMR type and kinematic constraints (refer to Sec.1.4.4) are taken into account in the VFH+ variant of the algorithm.

Dynamic Windows Approach

The Dynamic Windows Approach (DWA), presented by Fox *et al.* in [45], relies on the kinematic model of the WMR (Sec. 1.4.3) and it defines a *velocity space* of the linear v and angular ω velocities. Based on the sample period and on the current speed of the robot, the method makes an estimation of all the possible positions the robot can assume with the admissible velocity commands within the next sampling period. At a later stage it keeps just the couple (v, ω) that guarantee a safe stop before any obstacle is hit, the set of the couples kept is the set of the admissible velocities; once the set is defined the DWA method chooses the couple evaluating a cost function to minimize a function of the heading to the goal, the linear velocity and the distance from the destination. The highest priority is given to the heading which keeps the robot farther from any obstacle while trying to head to the goal anyway. The DWA has also a global variant presented by Brock and Khatib [17], what it does, it is to add in the cost function mentioned above a term which takes into account the results of a breadth-fist search algorithm (Sec. 1.5.1) evaluated on a local map around the actual WMR position. The peculiarity is that the dimension of the local map is not fixed but it may vary (augment) if due to the robot constraints no solution is found.

Curvature Velocity Approach (CVA)

This approach, presented by Simmons in [130], also takes into account the vehicle kinematics constraints, like the DWA it defines a velocity space considering the possible velocities one can apply to the robot and making the hypothesis the WMR moves on curves $c = v/\omega$ where v is the linear velocity and ω is the angular one. The difference with the DWA is that the CVA consider the obstacle in a Cartesian space with respect to the WMR and totally contained in a circle and removes all the curves that

Table 1.3: Comparison of Obstacle Avoidance Methods

	Obstacle Avoidance Methods				
	Obstacle shape	Kinematics	Dynamics	Map	Remarks
T-BUG	point			local graph	robust, not always efficient
VFH+	circle	basic	generic	histogram grid	suffer local minima, fast exectution
VFH*	circle	basic	generic	histogram grid	suffer local minima, slow execution
CV	circle	exact	basic	histogram grid	suffer local minima, slow exectution
DWA	circle	exact	basic	obstacle line field	suffer local minima, ductile

would made the WMR collide with it. At the end the choice will be made in a set of curves from which the velocities command can be gathered. This very local approach to avoid the obstacle could lead to local minima which could make the robot to stuck in traps.

1.5.3 Contrasting the methods

A real comparison for the presented obstacle avoidance methods it is not easy to carry out because the techniques have essential differences. What it can be done is to compare them depending on the needs and the applications. As specified in Section 1.4.5, depending on the task, the scenario and the way the environment is represented, one has to choose an appropriate model; the choice forces the user toward a collision avoidance method or another. Using a dynamic model one should opt for a strategy able to handle such a model as the DWA [45] and its modifications since among the presented methods it is the one which uses at least a basic dynamic representation to achieve the avoidance. If the application is (as in the case of this dissertation) oriented to indoor small differential drive WMR, the kinematic model is the usual choice so DWA must be compared with the other methods. One can consider the complexity and the robustness, then the choice could be the tangent bug, but as highlighted above the method it is not the most efficient one using just points to represent obstacles; therefore, it is better to deal with PF based methods and, again, the DWA, both of them suffer from local minima problems, being local strategies, but just the DWA takes into account the non-holonomic constraints of the vehicle. It could seem that DWA easily outperforms the other strategies but the potential field methods as VFH+ or VFH* result less complex to implement and (usually) demand less computational power when it is possible to reduce the kinematic model at the basic level: that is the case of slow velocity application in which a point can be used to define the trajectory and a control law is in charge to follow that trajectory in a reliable way. A visual comparison of the characteristics of the different algorithms is given in Table 1.3

1.6 Formation Control

Being mobile robotics a very thoroughly investigated field, the community has begun to look for more stimulating approaches that could bring to achieve tasks in a more efficient and rapid solution [91]. The idea is simple, implementing multi-agent systems, one can seek to optimized solutions, like in exploring application, where using multiple robots which share data can improve the overall results and cut the operation time. Moreover multiple agents increase the reliability solving the problem of failures due to single agent utilization. In addition several robots could cooperate to achieve what it is impossible for a single one, like manipulating the environment. Therefore, one can think about designing several WMRs, each one specialized in one task, rather than realizing a single one, more complex and difficult to manage. When more than one agent takes part in a mission it must have directives to follow to work with others without interfering and obviously colliding; that is the difficult part form the engineering point of view: to coordinate all the aspects guaranteeing a satisfactory result. To coordinate a group of WMR two approaches became very popular, the first one is based on self organization in which each agent has a set of instructions to react to different situation and they are often inspired by natural behaviours, the second type is based on a geometric approach and each WMR has not a fully autonomous behaviour but is more tied to directives that force it to stay in a formation with strict rules. It follows a brief overview of the different kinds of approaches used in robotic to control a group of WMR.

1.6.1 Behavior Based Formation

Usually in this approach each agent follows predefined rules for each basic behaviour as obstacle avoidance, formation keeping and goal seeking while the final action is defined giving a weight to each rule and averaging the result [8]; in [33] they define the *social potential fields*: simple artificial force laws between the robots of the group. The force laws are inverse-power force laws, incorporating both attraction and repulsion, the result of the forces applied give the overall behaviour of the formation. Other solutions rely on behaviour inspired by physics as in [9], where agents follow the way molecular covalent bonding is realized in crystals[5]. In this approach each robot has particular spots in the zone around itself that can be taken by other robots creating a bond that characterize the final formation since the created link will influence the agents future actions. One can consider in this category also flocking and consensus based formation strategy. Indeed, one of the first work in the field can be retrieved in [119] in which a model to simulate consensus is derived starting from the behaviour of a herd of animals in which each agent tries to avoid collision with neighbours and to assume the same "velocity profile"; a model derived from [119] is used in [149] to realize a efficient graphic simulation for elements called *boids*. A deep analysis of flocking strategy has been carried out by Tanner *et al.* in [137, 138] in which the authors investigates the stability properties of a system of multiple mobile agents with double integrator dynamics first in the case of fixed topology, then in the case of dynamic one.

[5]Covalent bonding occurs when pairs of electrons are shared by atoms. Atoms will covalently bond with other atoms in order to gain more stability, which is gained by forming a full electron shell. By sharing their outer most (valence) electrons, atoms can fill up their outer electron shell and gain stability.

1.6.2 The Leader-Follower

As suggested by the name, the *leader-follower* techniques are based on a leader whether physical [30],[47],[80],[49] or virtual [20],[87]; in these structures, the leader agent leads the formation while all the others follow it, according to a predefined rule. These rules may vary and follow a more classical scheme, [30] in which a follower has to respect distances and angles ($l - l$ scheme in case of two distances, $l - \varphi$ in case of a distance and an angle) or like in [87] the strategy may be hybrid and utilise an artificial potential field to define interaction control forces between neighbouring vehicles and to enforce a desired inter-vehicle spacing; the leader (in the cited work virtual) acts as moving reference point that influences vehicles close to it. Furthermore, the paper [140] introduces the concept of *leader-to-formation stability* based on input-to-state stability [133] and its invariance properties [67] under cascading; it describes the relation between the errors of the formation leader and the interconnection errors observed inside the formation characterizing how leader inputs and disturbances affect the stability of the group.

1.6.3 Virtual Structures

In this kind of formation, introduced by Lewis and Tan in 1997 [92] strict rules about the shape of the formation are given and each agent has to respect its role during the motion. Following Lewis the definition of *virtual structure* is the following: a virtual structure is a collection of elements (robots) which maintain a (semi-) rigid geometric relationship to each other and to a frame of reference. In particular each agent has a reference that could be a point of the structure or, similarly to the virtual leader in the leader-follower approach, a virtual point. The virtual structure approach for a WMR group has the advantage of employing relatively uncomplicated behaviour coordination. The main flaw of this approach is that it treats all the WMR as a unique rigid structure that can result in a common point of failure for the whole system. The implementation can be realized in several ways, giving distance and angle with respect to a virtual point obtaining a trajectory to follow and tracking it with a appropriate control laws [101] or modelling each robot as an electric charge [120], and due to repulsive forces between the identical charges, regular polygon formations can be achieved. This approach has been also popular in the control of spacecraft, or satellite formation [10, 118]

1.7 Contribution

In Fig. 1.11 the reader can recognize Fig. 6.1 in which the highlighted parts represent where this dissertation intents to place its contribution: the blocks *Local Path Planning* and *High Level Control*. In light of what has been considered in Section 1.4.5 and Section 1.5.3, the following chapters present obstacle avoidance strategies (*Local path planning*) for WMRs represented by a kinematic model, modified to consider a class of perturbation additive on the input, realized by the use of finite time control laws (*High Level Control*)

Firstly (Chapter 2), starting from the results in [35] a novel solution to local obstacle avoidance problem is proposed for unicycle-like wheeled mobile robots using a simple geometric approach. Moreover a particular formulation of the kinematic model

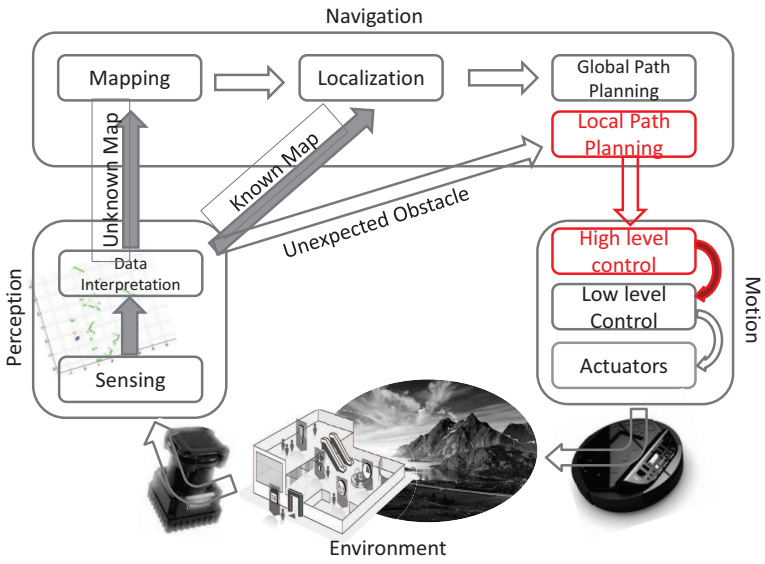

Figure 1.11: Fields of Contribution of this Dissertation Work

is adopted aiming to compensate for the neglected dynamics of the robot; the idea of having disturbances additive on the robot inputs relies on the intuition that, commanding the velocities, when the robot is not moving no disturbances can perturb it. The obstacle avoidance is achieved in two steps: the definition of a goal position and the avoidance itself combined thanks to the supervisory control framework. Each step is regulated via robust finite time controllers formally proven with Lyapunov based proofs. The contribution is thus twofold, a novel technique to avoid obstacles in a easy en effective way and the proven robustness with respect to the considered disturbances for the kinematic model of a unicycle-like robot. The analysis demonstrated a nice behaviour in a real environment when tested on an actual mobile platform and when compared with the well known DWA algorithm (Section 1.5.2).

Secondly, (Chapter 3), a modification of the standard Potential Field method has been designed. The PF is widely used in many research areas, in particular in robotics for both path planning and obstacle avoidance purposes. It suffers of a main flaws though: the mathematical elegance of the method is counterbalanced by the appearance of local minima that cause the robot to stuck. Supported by a novel field definition and recent control theory results [2], a new method to avoid local minima is proposed. Starting from a double variable integrator, a complete proof of the theoretical precision of the method is provided: the system has an attracting equilibrium at the target point, repelling equilibriums in the obstacles centers and saddle points on the borders. Those unstable equilibriums are avoided capitalizing on the established Input-to-State Stability (ISS) property of this multistable system: the ISS property is not lost for small

perturbation and properly designing a small disturbance the global attractivity of the target point is proven and the avoidance achieved. Simulation for the double variables integrator are provided showing the failure of the standard method and the exactness of the proposed one. The trajectories of the two variables integrator are thus used to guide an Unicycle-like mobile robot to the destination point avoiding obstacles; to do that two different controls are designed and formally proven convergent. The first is a classical solution which is not able to control the orientation, the second and most relevant one is a finite time control realization which drives the robot to the goal. The two methods are thus compared in simulation with the standard one and discussed. A real implementation of the method is also provided to show the capabilities in a real scenario.

Lastly, (Chapter 4), summarizing the experience obtained, a solution to the leader-follower formation problem is proposed combining finite-time identification and control techniques and the supervisory control framework. The goal is to direct a group of autonomous robots to a destination point following a leader and maintaining a predefined distance to it. During the mission, it is assumed the robots to know each other position and orientation. As for the other works of this dissertation the model is perturbed so the solution must be robust with respect to the additive disturbance considered on the input. The supervisory control algorithm that solves the problem take the most of finite-time differentiators used to estimate the leader velocities, then it orchestrates three control algorithms responsible for the following, rendezvous and collision avoidance manoeuvres. Respectively the controllers must regroup the robots (rendevous), make them move together following the leader (following) and in case of collision threat avoid it (collision avoidance) and go back to the more suitable of the two previous modes. Everything is realized in a decentralized way: each robot takes its own decision depending on two distances, the one from the leader that define the following or rendezvous status, and the one from agents or obstacles around, which define if the collision avoidance controller must be activated. It is shown that all controls ensure a finite-time regulation for the robots orientation and a finite-time fulfilment of the required performance constraints and everything is then sustained by numerical experiments.

To conclude, let the author mention two works (reported in Appendix C and B) that due to the faced topics are not in line with the dissertation but which represent a part of the path which brought to the end of this academic itinerary. In the first one the problem of gathering information which are not available with the equipped sensor measurements is tackled for a robotic crane used in forestry. An interval observer is proposed for on-line estimation of differentiation errors in some class of high-order differentiators (like a high-gain differentiator from [146], or homogeneous nonlinear differentiator from [115], or super-twisting differentiator [89]). The results are verified and validated on the telescopic link of a robotic arm mentioned above in which is common to measure the extension with encoder sensors and the mentioned approaches are used to estimate the extension velocity while the interval observer gives bounds to this estimation.

The second one addresses another problem for the same platform, that is the stabilization of dynamical systems in presence of uncertain bounded perturbations using ϵ-invariance theory. Under some assumptions, the problem is reduced to the stabilization of a chain of integrators subject to a perturbation and is treated in two steps. The evaluation of the disturbance and its compensation. Homogeneous observer and control

[13],[115] are the tools utilized to achieve a global asymptotic stability and robustness. The result is formally proven and, to validate the theory, it is applied to the control the same link of the robotic crane and compared with standard techniques.

Chapter 2

Finite Time Supervisory Control: Collision Avoidance with Disturbance Rejection

As previously mentioned in Chapter 1.3, nonholonomic mechanical systems are characterized by kinematic non-integrable constrains and a well-known result by [18] states that it is not possible to stabilize such systems via a smooth time-invariant static state feedback. Several strategies have been proposed in the literature, like continuous time-varying feedback control, discontinuous feedback control laws, hybrid/switched control laws and optimal control laws to tackle the stabilization problem ([25], [110], [1], [29], [153]) while one of the first work on the stabilization using a finite-time technique can be found in [54].
The collision avoidance problem has been largely treated in the previous chapter, in which well known algorithms are presented and compared; nonetheless a variety of switching control strategies has been proposed addressing the stabilization and the collision avoidance for WMR by [35], [125], [139] also taking into account external disturbances (for instance in submarine applications [111]). In addition, to deal with model inaccuracies in literature various types of perturbations are considered; in [142], for instance, a constant input additive disturbance is studied and compensated with an adaptive approach. In [27] a most rigorous study is carried out where slipping and skidding behaviours are characterized and a study on the controllability is illustrated; [123] uses the formulation of [27] and compensates the effects of matched and unmatched perturbations with an integral sliding mode approach. In the present work, perturbations are added to the classic kinematic model to compensate neglected dynamics. These perturbations are additive to the inputs, that comes from the intuition that if no command is given to the WMR, then the robot will not move and, thus, no perturbations have to be considered independently of the control. Such a kind of disturbances could come from the settling time of the PID controller, that translates the velocity commands in current inputs and sends them to the motors.

In this chapter the obstacle avoidance is realized using a supervisory switching control technique to regulate two outputs in order to guarantee a robust result. The capability to switch between two different non-linear systems allows us to tackle the two tasks

separately. The first objective is the stabilization of the system by regulating the first output, the second objective, and thus the second output to regulate, is related to the proximity of eventual obstacles while trying to complete the main task. A supervisor has been designed to oversee the switches between the two components of the control deriving from [35] and relaxing it without the need of dwell time and adding input disturbances. The result is presented taking into account the notions of stability for switched system ([93]) and the definition of input-to-output stability ([134], [61]).

2.1 Problem Formulation

Let us consider a non-holonomic system, a unicycle-like WMR as presented in ((1.33)), in which the input is affected by the kind of additive input disturbances depicted above:

$$\begin{aligned} \dot{q}_x &= (1+d_1)v\cos(q_\theta), \\ \dot{q}_y &= (1+d_1)v\sin(q_\theta), \\ \dot{q}_\theta &= (1+d_2)\omega, \end{aligned} \tag{2.1}$$

where $q = [q_x\ q_y\ q_\theta]^T$ is the state space vector and $(q_x, q_y) \in \mathbb{R}^2$, define the Cartesian position of the robot, and $q_\theta \in [0, 2\pi)$ is the orientation of the robot with respect of the world reference frame, v and ω are the control inputs, the linear velocity and the angular velocity respectively. The additive disturbances on the inputs are unknown, but supposed to be bounded, $-1 < d_{min} \leq d_i \leq d_{max}$, $i = 1, 2$. The lower bound, $d_{min} > -1$, ensures that the disturbance does not induce a change of control sign (a constraint satisfied in practice). To achieve the tasks the robot has to be driven to the origin avoiding obstacles that it could, eventually, encounter during the path. As a solution, two independent controllers can be designed to reach the goals (i.e. stabilization in the origin and collision avoidance) with their posterior uniting ([35]). These controls can be designed in order to regulate two different outputs:

$$z_1(q_x, q_y) = \sqrt{q_x^2 + q_y^2}, \tag{2.2}$$

$$z_2(q_x, q_y) = \min\left[Y, \max_{1\leq i\leq N}\left(\sqrt{(q_x - x_{o_i})^2 + (q_y - y_{o_i})^2}\right)^{-1}\right] \tag{2.3}$$

where z_1 is the distance from the origin and z_2 is the inverse of the distance from the closest obstacle represented by its Cartesian position $(x_{o_i}, y_{o_i})_{i,\dots,N}$, with N is a finite number of obstacles, $Y > 0$ is a parameter ensuring global boundedness of z_2 and related with dimensions of the obstacles. Clearly, driving z_2 to a sufficiently small value means to move away from an obstacle avoiding it. Under the assumption that between the obstacles there were enough space we can consider one obstacle each time without loosing generality. We will also assume that $z_2(0, 0) > Y$, i.e.the origin is not occupied by an obstacle.
Therefore, the problem we want to solve is to stabilize the system (2.1) regulating the output z_1 to reach the desired position, and z_2 to realize the collision avoidance. In addition, we want to cancel the effects of the disturbances acting on the control inputs. In the following section a supervisory control solution is proposed.

2.2 Theoretical Formulation

Consider the following system (a non-holonomic WMR model):

$$\dot{x} = f(x, u, d),\ z_1 = h_1(x),\ z_2 = h_2(x), \tag{2.4}$$

where $x \in \mathbb{R}^n$ is the state, $u \in \mathbb{R}^m$ is the control input and $d \in \mathbb{R}^m$ is a disturbance, with $d \in \Omega = \{d \in \mathcal{L}_m^\infty : ||d|| \leq D\}$ for some $D \in \mathbb{R}_+$.
We want to regulate the outputs $z_1 \in \mathbb{R}^{p_1}$ and $z_2 \in \mathbb{R}^{p_2}$ assuming that the functions f, h_1 and h_2 are continuous and locally Lipschitz. It is needed to design a control $u : \mathbb{R}^n \to \mathbb{R}^m$ that will provide the *uOS*[1] property with respect to the output z_1, and will keep the second output z_2 in a predefined limit. In other words, to achieve the desired tasks it is needed that for all initial conditions $x_0 \in \mathbb{R}^n$, $d \in \Omega$ and $t \geq t_0 \geq 0$:

$$|z_1(t, x_0, d)| \leq \beta(|h_1(x_0)|, t - t_0), \tag{2.5}$$

$$|z_2(t, x_0, d)| \leq \sigma(\max(\Delta, |h_2(x_0)|)), \tag{2.6}$$

the value of Δ is given, β is a $\mathcal{KL}$[2] function whereas σ is a function from class $\mathcal{K}$. It can be noted that (2.5) is exactly the definition of the *uOS* property. The second output must be smaller than $\sigma(\Delta)$. In the case $|h_2(x_0)| > \Delta$ the trajectory should converge to a subset where $|h_2(x)| \leq \sigma(\Delta)$. In addition, to solve the problem we need that the intersection between the sets $h_1(x) = 0$ and $|h_2(x)| \leq \sigma(\Delta)$ would be not empty, thus we assume the existence of a function ρ of class $\mathcal{K}$ and a scalar $0 < \rho_0 < \sigma(\Delta)$ such that:

$$|h_2(x)| \leq \rho(|h_1(x)|) + \rho_0. \tag{2.7}$$

2.2.1 Description of independent controls

Thus the problem consists in an output uniform stabilization under constraints imposed on another output. Following [35], assume that two right-continuous controls $u_i : \mathbb{R}^n \to \mathbb{R}^m$, $i \in \{1, 2\}$ are given guaranteeing an independent stabilization for the corresponding output z_i, i.e. the system

$$\dot{x} = f(x, u_i(x), d),\ z_i = h_i(x),$$

is forward complete and has continuous solutions $x(t, x_0, d)$, in addition the system is *uOS* with respect the output z_i and disturbance $d \in \Omega$. We also assume that during an activation of u_2 for all $t \geq 0$

$$|z_1(t, x_0, d)| \leq |h_1(x_0)|.$$

Next subsection is devoted to uniting of these controls in order to solve the posed problem.

[1] A *forward complete* system $\dot{x} = f(x, u, d), y = h(x)$ is called uniformly Output-Stable (uOS) with respect to output y and input d, if for all $x_0 \in \mathbb{R}^n$ and $d \in \Omega$ there exists a function $\beta \in \mathcal{KL}$ such that $|y(t, x_0, d)| \leq \beta(|h(x_0)|, t - t_0)$ for all $t \geq t_0$.

[2] A continuous function $g : \mathbb{R}_+ \to \mathbb{R}_+$ belongs to class $\mathcal{K}$ if it is strictly increasing and $g(0) = 0$; a continuous function $h : \mathbb{R}_+ \times \mathbb{R}_+ \to \mathbb{R}_+$ belongs to class $\mathcal{KL}$, if $h(\cdot, t) \in \mathcal{K}$ for any $t \in \mathbb{R}_+$, and $h(s, \cdot)$ is strictly decreasing to zero for any $s \in \mathbb{R}_+$ for $t \to \infty$.

2.2.2 Supervisory control

Under the assumption of having two controls which solve the output regulation for z_1 and z_2 independently, a *supervisor* is proposed to oversee the activation of the controls to achieve both required condition (2.5) and (2.6) simultaneously. The idea is that the controller u_2 is activated when $|z_2(x)|$ reaches a threshold Δ and remains active until the constraint $|z_2(x)| \leq \delta$ is satisfied, where $0 < \delta < \Delta$ is a given parameter. For this reason we define two sets

$$\begin{aligned}
&\mathbf{X}_1 = \{x \in \mathbb{R}^n : |h_2(x)| \leq \delta\} \\
&\mathbf{X}_2 = \{x \in \mathbb{R}^n : |h_2(x)| \leq \Delta\} \\
&\mathbf{X}_1 \subset \mathbf{X}_2.
\end{aligned}$$

Then the control

$$U(t) = u_{i(t)}(x(t)),\ i : \mathbb{R}_+ \to \{1, 2\} \tag{2.8}$$

is ruled by

$$t_0 = 0,\ i(t_0) = \begin{cases} 1 & \text{if } x(t_0) \in \mathbf{X}_2, \\ 2 & \text{otherwise,} \end{cases}$$

while $i(t) = i(t_j)$ for $t \in [t_j\ t_{j+1})$, and

$$i(t_{j+1}) = \begin{cases} 1 & \text{if } x(t_{j+1}) \in \mathbf{X}_1 \\ 2 & \text{if } x(t_{j+1}) \notin \mathbf{X}_2 \end{cases}, \tag{2.9}$$

where t_j is the generic switching instant defined as follows:

$$t_j = \begin{cases} \underset{t \geq t_j}{\arg\inf}\ x(t) \notin \mathbf{X}_2 & \text{if } i(t_j) = 1 \\ \underset{t \geq t_j}{\arg\inf}\ x(t) \in \mathbf{X}_1 & \text{if } i(t_j) = 2 \end{cases}.$$

A similar supervisor has been presented in [35], but in the present work a dwell time condition is not imposed. The control U has the u_1 part active if $|z_2| < \Delta$, which means that we are stabilizing the output z_1 according to condition (2.5). If $|z_2|$ becomes greater or equal than Δ, then u_2 will be activated driving z_2 to a value less than δ according to condition (2.6). Inside the set $H = \mathbf{X}_2 \backslash \mathbf{X}_1$ the control will not be switched, this set acts as a hysteresis zone being helpful to avoid a chattering phenomena of switching between u_1 and u_2.

Assumption 1. $\sup_{x \in H, d \in \Omega, i \in \{1,2\}} |f(x, u_i(x), d)| = F < +\infty$.

This assumption states that the system velocity on the set H is finite, which holds for example if f is $\mathcal{C}^0$ and u_i is piecewise continuous because of the compactness of $\Omega \times H$ then since $F < +\infty$ and $d \in \Omega$ there exists a dwell-time delay $\tau_D > 0$ between any two switches, i.e. $t_{j+1} - t_j \geq \tau_D$ for all $j \geq 0$. The conditions for solution of the posed problem using the supervisory control algorithm (2.8), (2.9) are described in the following theorem.

Theorem 1. *Let Assumption 1 be satisfied and $\beta_1(s, \tau_D) = \lambda s$ for all $s \in \mathbb{R}_+$ and some $0 \leq \lambda < 1$. Then the system (2.4) with supervisor (2.9) and control (2.8) is forward complete and for all initial conditions $x_0 \in \mathbb{R}^n$, $d \in \Omega$ and $t \geq 0$:*

$$
\begin{gathered}
|z_1(t, x_0, d)| \leq \beta_1(|h_1(x_0)|, 0), \\
|z_2(t, x_0, d)| \leq \sigma(\max\{\Delta, |h_2(x_0)|\}), \\
\lim_{t \to +\infty} |z_1(t, x_0, d)| = 0,
\end{gathered}
$$

where $\sigma(s) = \beta_2(s, 0)$.

Proof. The existence of dwell-time $\tau_D > 0$ implies right-continuity of the switching signal $i(t)$, the same property for the right-hand side of the system (2.4), (2.8), (2.9) (due to composition limit rule) and continuity of the system solutions with the absence of chattering. Since for both u_i, $i \in \{1, 2\}$ the solutions of the system are well defined for all $t \geq 0$, then a finite-time escape phenomenon is impossible and solutions of the switched system (2.4), (2.8), (2.9) are well defined for all $t \geq 0$.
By definition of a function from class $\mathcal{KL}$, there exists $0 < T_2 < +\infty$ such that $\delta = \beta_2(\Delta, T_2)$. For both controls the following inequalities are satisfied for the outputs:

$$
\begin{cases}
i(t) = 1 \quad \forall t \in [t_j, t_{j+1}), \\
|z_1(t, x(t_j), d)| \leq \beta_1(|h_1(x(t_j))|, t - t_j), \\
|h_2(t, x(t_j), d)| \leq \rho \circ \beta_1(|h_1(x(t_j))|, t - t_j) + \rho_0,
\end{cases} \tag{2.10}
$$

$$
\begin{cases}
i(t) = 2 \quad \forall t \in [t_j, t_{j+1}), \\
|z_2(t, x(t_j), d)| \leq \beta_2(|h_2(x(t_j))|, t - t_j), \\
|z_1(t, x(t_j), d)| \leq |h_1(x(t_j))|.
\end{cases} \tag{2.11}
$$

Therefore, the following scenarios are possible. *First*, $x(0) \in \Xi = \{x \in \mathbb{R}^n : \rho \circ \beta_1(|h_1(x)|, 0) + \rho_0 \leq \Delta\}$, then $x(0) \in \mathbf{X_2}$, $i(0) = 1$ and, according to (2.10), $i(t) = 1$ with $|z_2(t, x(0), d)| \leq \Delta$ for all $t \geq 0$. *Second*, $x(0) \in \mathbf{X}_2 \setminus \Xi$ and there exists $0 < t_1 < +\infty$ such that (2.10) is satisfied for $t \in [t_0, t_1)$ and

$$
\begin{aligned}
|h_2(x(t_1))| &= \Delta, \\
|z_1(t_1)| &\leq \beta_1(|h_1(x(t_0))|, t_1 - t_0) \\
&\leq \beta_1(|h_1(x(t_0))|, \tau_D) \\
&= \lambda |h_1(x(t_0))| < |h_1(x(t_0))|.
\end{aligned}
$$

Note that if $t_1 = +\infty$, then this case is identical to the first scenario. Thus according to (2.11)

$$
\begin{gathered}
|z_2(t, x(t_1), d)| \leq \beta_2(\Delta, t - t_1) \quad \forall t \in [t_1, t_2), \\
|z_2(t_2, x(t_1), d)| = \delta, \\
|z_1(t, x(t_1), d)| \leq |z_1(t_1)| \leq \lambda |h_1(x(t_0))| \quad \forall t \in [t_1, t_2),
\end{gathered}
$$

where $t_1 < t_2 \leq t_1 + T_2$. Summarizing these estimates we get

$$
\begin{gathered}
|z_1(t, x(t_0), d)| \leq \beta_1(|h_1(x(t_0))|, 0) \quad \forall t \in [t_0, t_2), \\
|z_2(t, x(t_0), d)| \leq \beta_2(\Delta, 0) \quad \forall t \in [t_0, t_2), \\
|z_1(t_2, x(t_0), d)| \leq \lambda |h_1(x(t_0))|.
\end{gathered}
$$

Next, there exists a sequence of time instants t_{2k}, $0 \leq k \leq K \leq +\infty$ with $i(t) = 1$ for all $t \in [t_{2k}, t_{2k+1})$ and $i(t) = 2$ for all $t \in [t_{2k+1}, t_{2k+2})$. Repeating the arguments above we obtain

$$\begin{gathered} |z_1(t, x(t_0), d)| \leq \beta_1(|h_1(x(t_0))|, 0) \quad \forall t \in [t_0, t_{2k+2}), \\ |z_2(t, x(t_0), d)| \leq \beta_2(\Delta, 0) \quad \forall t \in [t_0, t_{2k+2}), \\ |z_1(t_{2k+2}, x(t_0), d)| \leq \lambda^k |h_1(x(t_0))| \end{gathered} \tag{2.12}$$

for any $0 \leq k \leq K$. Assume that $K < +\infty$, then it means that $i(t) = 1$ for all $t \geq t_{2K}$ (the control u_2 can be active on a finite interval only by its definition) and from (2.10)

$$\begin{gathered} |z_1(t, x(t_0), d)| \leq \beta_1(|h_1(x(t_{2K}))|, 0) \\ \leq \beta_1(|h_1(x(t_0))|, 0) \quad \forall t \geq t_{2K}, \\ |z_2(t, x(t_0), d)| \leq \Delta \leq \beta_2(\Delta, 0) \quad \forall t \geq t_{2K}, \\ \lim_{t \to +\infty} |z_1(t, x(t_0), d)| = 0, \end{gathered}$$

i.e. it is a situation similar to the first scenario. If $K = +\infty$, then from (2.12) with $k \to +\infty$ we have the same properties, consequently

$$\begin{gathered} |z_1(t, x(t_0), d)| \leq \beta_1(|h_1(x(t_0))|, 0) \quad \forall t \geq t_0, \\ |z_2(t, x(t_0), d)| \leq \beta_2(\Delta, 0) \quad \forall t \geq t_0, \\ \lim_{t \to +\infty} |z_1(t, x(t_0), d)| = 0. \end{gathered} \tag{2.13}$$

Third, $x(0) \notin \mathbf{X}_2$ and in this case there is a time instant $t_1 > t_0$ such that the estimates (2.11) are satisfied for all $t \in [t_0, t_1)$

$$\begin{aligned} |z_2(t, x(t_0), d)| &\leq \beta_2(|h_2(x(t_0))|, t - t_0), \\ |z_1(t, x(t_0), d)| &\leq |h_1(x(t_0))| \end{aligned}$$

and $|z_2(t_1, x(t_0), d)| = \delta$. Since $x(t_1) \in \mathbf{X}_2$ the following system behavior is similar to the second scenario and from (2.13) we obtain

$$\begin{gathered} |z_1(t, x(t_0), d)| \leq \beta_1(|h_1(x(t_0))|, 0) \quad \forall t \geq t_0, \\ |z_2(t, x(t_0), d)| \leq \beta_2(\max\{\Delta, |h_2(x(t_0))|\}, 0) \quad \forall t \geq t_0, \\ \lim_{t \to +\infty} |z_1(t, x(t_0), d)| = 0. \end{gathered}$$

Therefore, these estimates are satisfied in all three possible scenarios for all $t \geq 0$. □

2.3 Control Tasks

In this section two finite-time controllers (u_i, $i \in \{1, 2\}$) are designed for (2.1); the former one is designed to regulate the output z_1 in (2.2), for the stabilization part, and the second one is to regulate the output z_2 in (2.3), providing the collision avoidance. The main feature of these controls is that all control tasks are solved not asymptotically, but in a finite time.

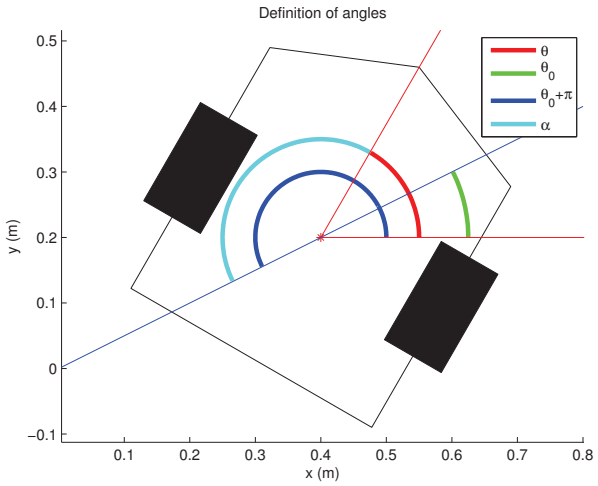

Figure 2.1: Definition of the angles for the Stabilization Control Law

2.3.1 Stabilization

As mentioned above, the first control u_1 is designed in order to drive the robot to the desired point (the origin in this formulation without loss of generality, thus stabilize z_1). Following control theory, let us consider the following Lyapunov function: $V_1 = 0.5z_1^2$. Its derivative has the form

$$\dot{V}_1 = \dot{z_1} z_1 \tag{2.14}$$

$$= \sqrt{q_x^2 + q_y^2} \frac{q_x \dot{q_x} + q_y \dot{q_y}}{\sqrt{q_x^2 + q_y^2}} \tag{2.15}$$

$$= q_x \dot{q_x} + q_y \dot{q_y}; \tag{2.16}$$

following easy trigonometric rules, one can rewrite $q_x = z_1 \cos\theta_0$ and $q_y = z_1 \sin\theta_0$, it follows that

$$\dot{V}_1 = v(1+d_1)z_1 \left(\cos q_\theta \cos\theta_0 + \sin q_\theta \sin\theta_0\right) \tag{2.17}$$

$$= \cos(\theta_0 - q_\theta) v(1+d_1) z_1, \tag{2.18}$$

where $\theta_0 = \arctan(q_y/q_x)$. Define $\alpha = q_\theta - \theta_0 - \pi$, $\alpha \in [-\pi, \pi)$, which implies the deviation from the robot's current orientation q_θ to its desired final orientation $\theta_0 + \pi$, then we have

$$\dot{V}_1 = -\cos(\alpha) v(1+d_1) z_1.$$

In order to ensure the negative definiteness (or semi-definiteness) of $\dot{V}_1$, the following control is proposed:

$$v = \begin{cases} k_1 z_1 & \text{if } |\alpha| \leq k\pi \\ 0 & \text{otherwise} \end{cases},$$

with k_1 positive and $0 < k \leq 0.5$, with which the semi-definiteness of $\dot{V}_1$ can be

ensured (Fig. 2.1 shows a visual description of the WMR and of the listed angles), since

$$\begin{cases} \dot{V}_1 \leq -\cos(\alpha)(1-d_{min})k_1 z_1^2 & \text{if } |\alpha| \leq k\pi \\ \dot{V}_1 = 0 & \text{otherwise} \end{cases}.$$

then we have

$$\dot{V}_1 \leq -2c_1 V_1 \;\; for\; |\alpha| \leq k\pi,$$

where $c_1 = k_1 \cos(k\pi)(1-d_{min})$.
Then let us consider the regulation of the robot's orientation to its desired one, i.e. stabilization of α to 0. Following the definition of α, its dynamics can be expressed as follows:

$$\dot{\alpha} = \omega(1+d_2) + \sin(\alpha) z_1^{-1}(1+d_1)v.$$

By choosing the following Lyapunov function $V_2 = 0.5\alpha^2$, we obtain its derivative as:

$$\dot{V}_2 = \omega\alpha(1+d_2) + \alpha\sin(\alpha)v(1+d_1)z_1^{-1}$$

which can be separated into two cases, depending on v when it is equal to zero (most of the time) or not (for $|\alpha| \leq k\pi$). Thus it can written as:

$$\dot{V}_2 = \begin{cases} \omega\alpha(1+d_2) + k_1\alpha\sin(\alpha)(1+d_1) & \text{if } |\alpha| \leq k\pi \\ \omega\alpha(1+d_2) & \text{otherwise} \end{cases}.$$

In order to guarantee the negative definiteness of $\dot{V}_2$, we propose the control ω in the following form:

$$\begin{aligned} \omega = -k_2\zeta(\alpha)\text{sign}(\alpha),\; k_2 \geq \frac{(1+d_{max})k_1 + 2^{-3/4}\eta_1}{1-d_{min}}, \\ \zeta(\alpha) = \max\{|\alpha|^{0.5}, |\alpha|\},\; \eta_1 > 0, \end{aligned} \tag{2.19}$$

which yields

$$\dot{V}_2 \leq \begin{cases} -k_2|\alpha|\zeta(\alpha)(1-d_{min}) & \\ +k_1\alpha^2(1+d_{max}) & \text{if } |\alpha| \leq k\pi \\ -k_2|\alpha|\zeta(\alpha)(1-d_{min}) & \text{otherwise.} \end{cases}$$

Since $|\alpha|\zeta(\alpha) \geq \alpha^2$, we always have:

$$\dot{V}_2 \leq -\eta_1 \max\{V_2, V_2^{3/4}\},$$

Let us remark that the term k_2 allows us to compensate the disturbances. Based on the above inequality, we can conclude that the $\alpha(t)$ admits the following upper estimate:

$$\begin{aligned} |\alpha(t)| \leq \begin{cases} |\alpha_0| e^{-0.5\eta_1(t-t_0)} & \text{if } t \in [t_0, t_1], \\ \sqrt{2}[\min\{1, 2^{-1/4}\sqrt{|\alpha_0|}\} & \\ -2^{-2}\eta_1(t-t_1)]^2 & \text{if } t \in (t_1, t_2], \\ 0 & \text{if } t > t_2, \end{cases} \\ t_1 = t_0 + \max\{0, \eta_1^{-1}\ln(0.5\alpha_0^2)\}, \\ t_2 = t_1 + 2^{-2}\eta_1^{-1}\min\{1, 2^{-1/4}\sqrt{|\alpha_0|}\}, \end{aligned} \tag{2.20}$$

where $t_0 \geq 0$ is the instant when this control has been activated and $\alpha_0 = \alpha(t_0) \in [-\pi, \pi)$ is the initial condition. Therefore there exists $0 \leq T_1(\alpha_0) < \infty$ for all $\alpha_0 \in [-\pi, \pi)$ such that $|\alpha(t)| < k\pi$ for all $t \geq t_0 + T_1(\alpha_0)$. For simplicity, we can use the dynamics of α with $v = 0$ to compute $T(\alpha_0)$, which is as follows:

$$T_1(\alpha_0) \leq \begin{cases} \max\left\{0, \frac{2}{\eta_1} \ln\left(\frac{|\alpha_0|}{k\pi}\right)\right\} & \text{if } k\pi \geq 1, \\ t_1 + 4\eta_1^{-1}[\min\{1, 2^{-1/4}\sqrt{|\alpha_0|}\} & \\ -2^{-1/4}\sqrt{k\pi}] & \text{otherwise.} \end{cases}$$

Since $|\alpha_0| \leq \pi$ we finally obtain

$$T_1(\pi) = \eta_1^{-1} \begin{cases} -2\ln(k) & \text{if } k\pi \geq 1, \\ \ln(0.5\pi^2) + 4(1 - 2^{-1/4}\sqrt{k\pi}) & \text{otherwise.} \end{cases}$$

Thus it follows that

$$z_1(t) \leq z_1(t_0) \min\{1, e^{-c_1(t - T_1(\pi) - t_0)}\} \; \forall t \geq t_0, \tag{2.21}$$

which implies that the first output z_1 is exponentially stabilized by using the designed controls v and ω. Thus the first control u_1 can be summarized as follows:

$$u_1 = \begin{cases} v = \begin{cases} k_1 z_1 & \text{if } |\alpha| \leq k\pi \\ 0 & \text{otherwise} \end{cases} \\ \omega = -k_2 \zeta(\alpha) \text{sign}(\alpha). \end{cases}, \tag{2.22}$$

The above arguments are equivalent to the following lemma.

Lemma 1. *In the system (1.33) with control (2.22) the estimates (2.21) and (2.20) are satisfied (a uniform exponential stabilization for z_1 and a uniform finite-time stabilization for α).*

Remark: It deserves to be precised that despite the fact that the convergence of the z_1 output is exponential, a zone around the origin can be always reached in a finite time.

2.3.2 Collision Avoidance

The first controller u_1 can drive the robot to the desired position, if no obstacle will be encountered during the navigation. This is however not the real case in practice. In order to take into account the obstacle, we need to construct another controller, named u_2, which needs to achieve the following two tasks:

- driving the robot away from the encountered obstacle (i.e. collision avoidance);
- keeping the distance z_1 between the robot and the desired final position not increasing (i.e. still approaching to the desired final position).

In order to design such a controller, we consider each obstacle as a point in the plane and then define an associated safe distance to be maintained. Each obstacle is an element of the set $O = \{(x_{o_i}, y_{o_i}, \rho_{i,min})\}_{i=1,\ldots,N}$, with N number of possible obstacles, $Y = 1/\min_{1 \leq i \leq N}\{\rho_{i,min}\}$. It is assumed in this work that each obstacle is entirely

contained in the circle of radius $\rho_{i,min}$ which is a designed distance considering the radius of the obstacle itself and a distance equal to the radius of the circle in which the robot can be inscribed. Moreover, in order to augment the safety, the collision avoidance controller u_2 will be activated when the robot reaches a distance $\rho_i > \rho_{i,min}$, which adds an additional safety level to the collision avoidance manoeuvre. Then, the goal of the control u_2 is to ensure the avoidance by augmenting the distance from ρ_i to a predefined $R_i > \rho_i$. In terms of the output z_2, it is equivalent to decrease z_2 from $\Delta_i = \rho_i^{-1}$ to $\delta_i = R_i^{-1}$. Moreover, during this manoeuvre, it is required that the control u_2 will not make the output z_1 increasing.
Before stating collision avoidance controller u_2, for the sake of simplicity, let us make the following assumptions:

Assumption 2. *Assume that* $\max_{1\leq i\leq N} 1/\sqrt{x_{o_i}^2 + y_{o_i}^2} < \min_{1\leq i\leq N} \delta_i$*, i.e. the origin is well separated from an obstacle.*

Assumption 3. *Assume that* $\Upsilon_i \cap \Upsilon_j = \emptyset$ *for any* $i \neq j \in \{1, \ldots, N\}$*, where* $\Upsilon_i = \{(q_x, q_y) \in \mathbb{R}^2 : (q_x - x_{o_i})^2 + (q_y - y_{o_i})^2 \leq R_i^2\} = \{(q_x, q_y) \in \mathbb{R}^2 : z_2(q_x, q_y) \geq \delta_i\}$ (i.e. *any two obstacles are separated and the collision avoidance problem can be addressed for an isolated obstacle).*

In order to design the control u_2, we need to plan a strategy to move the robot from the distance Δ_i to δ_i. For this, when the robot reaches a distance $\rho_i > \rho_{i,min}$, we define an intermediate point $B = (x_B, y_B)$, and the goal of u_2 is to control the robot moving from current position to this new point B such that $z_1(x_B, y_B) \leq z_1(q_x(t_{ca}), q_y(t_{ca}))$ and $z_2(x_B, y_B) \leq \delta_i$, where t_{ca} is the instant of time in which the control u_2 is switched on, i.e. $z_2(q_x(t_{ca}), q_y(t_{ca})) = \Delta_i$. The following details the algorithm for the choice of the point B.

Choice of point B

Let us firstly define a preliminary point B^- as an intersection point of the circle centered in (x_{o_i}, y_{o_i}) of radius R_i and the tangent line to the circle centered at (x_{o_i}, y_{o_i}) of radius Δ_i (see the red one in Fig. 2.2). Using this approach, the coordinate of the point B^- can be calculated as follows:

$$\begin{aligned}
x_{B^-} =& \frac{1}{m}\left(mx - y + y_B\right), \\
y_{B^-} =& \frac{y + mx_{o_i} - mx + m^2 y_{o_i} \pm C_1}{m^2 + 1}, \\
C_{1,1} =& m(R_i m + R_i - mx_{o_i} + 2mxx_{o_i} - mx + 2mx_{o_i}y_{o_i} \\
& - 2mx_{o_i}y - 2mxy_{o_i} + 2mxy - y_{o_i} + 2y_{o_i}y - y), \\
m =& -\left[\tan(\theta_i)\right]^{-1}, \quad \theta_i = \tan^{-1}\left(\frac{y - y_{o_i}}{x - x_{o_i}}\right).
\end{aligned}$$

Although this approach is very efficient, under a special situation it cannot provide the second requirement of the control, i.e. $\dot{z}_1(t) \leq 0$, that is the case when the obstacle center, the robot and the origin are on the same straight line (see Fig. 2.3). In this case, the preliminary B^- point will be in the intersection of two circles: the first centered in (x_{o_i}, y_{o_i}) of radius R_i (the green one in Fig. 2.3) and the second circle centered at the origin of radius $|z_1(t_{ca})|$ (the blue one in Fig.2.3). Following this approach, we can obtain the following coordinate for B^-:

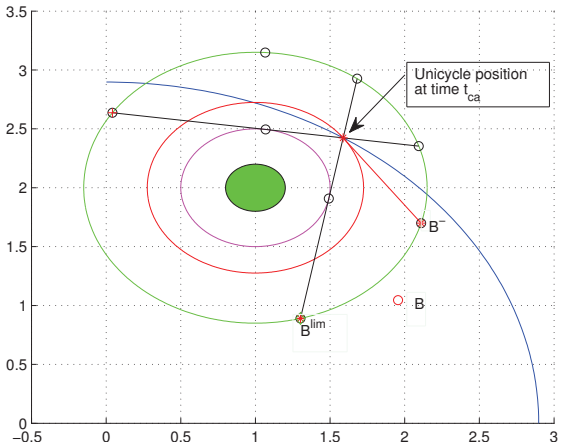

Figure 2.2: Circles used in the definition of the B^-, B^{lim} and then the B points with the "tangent" approach

$$
\begin{aligned}
x_{B^-} =& \frac{x_{o_i}^2 - R_i^2 + y_1 + y_{o_i} - 2y_{o_i}d_{o_i}^2}{2x_{o_i}}, \\
y_{B^-} =& \frac{x_{o_i}^2 y_{o_i} - R_i^2 y_{o_i} + y_1 y_{o_i} + y_{o_i}^3 \pm C_{1,2}}{2d_{o_i}^2}, \\
C_{1,2} =& x_{o_i}[(-R_i + 2R_i y_1 + x_{o_i} - y_1 + y_{o_i}) \\
& (R_i + 2R_i y_1 - x_{o_i} + y_1 - y_{o_i})], \\
d_{o_i} =& \sqrt{x_{o_i}^2 + y_{o_i}^2}.
\end{aligned}
$$

In order to determine the final coordinates of B for both cases, let us define the distance $\rho_{i,min}$ as a limit not to be crossed, represented in Fig. 2.2 and Fig. 2.3 by the purple circle. Then we can determine the point B^{lim}, which is an intersection of a straight line initiated at the robot position and tangent to the circle centered at (x_{o_i}, y_{o_i}) with radius $\rho_{i,min}$. Thus we can freely choose a point B' on the circle of radius R_i between the points B^{lim} and B^- taking a safe distance from them proportional to d_{max} (in order to avoid the risk of being steered backward due to a disturbance). Finally, the point $B = (x_B, y_B)$ can be selected on the line passing the current robot position and the point B' with the condition that $z_2(x_B, y_B) < \delta$ (outside the set Υ_i, green circle in both Fig. 2.2and 2.3). With such a selection of the point B, it is possible to achieve the avoidance and to keep, in addition, the condition $\dot{z}_1(t) \leq 0$. Once the point B is defined, we can then design a control u_2, which should drive the robot from current position to this point, which will be detailled in the next section.

Collision avoidance controller

The collision avoidance problem can be solved by using a similar approach as the stabilization problem in the previous section, which needs only to replace the origin

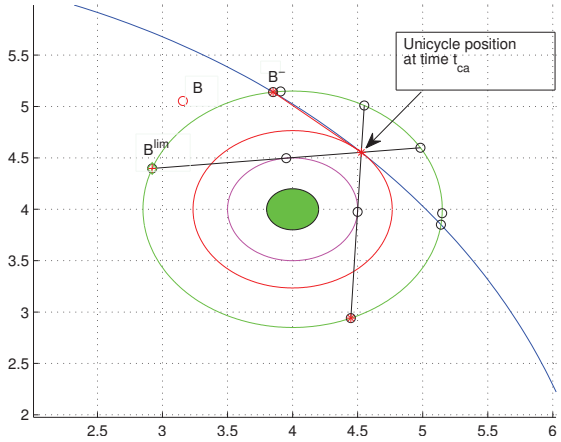

Figure 2.3: Circles used in the definition of the B^{-}, B^{lim} and then the B points with the "circles" approach

in the stabilization problem by the chosen point B. For this, let us define the robot distance to the point B as

$$D_B(x,y) = \sqrt{(q_x - x_B)^2 + (q_y - y_B)^2},$$

in such a formulation the imposed restriction $z_2(x_B, y_B) < \delta$ becomes crucial and the point B will not be reached during the collision avoidance manoeuvre. It is important, since in a stabilized point the robot loses controllability (in our case this corresponds to division on the distance D_B in the equation (2.25) below). Focusing on the function $D_B(x,y)$, after differentiation:

$$\dot{D}_B = \frac{(q_x - x_B)\dot{q}_x + (q_y - y_B)\dot{q}_y}{D_B} \tag{2.23}$$

$$= \frac{(q_x - x_B)\cos q_\theta v(1+d_1) + (q_y - y_B)\sin q_\theta v(1+d_1)}{D_B}, \tag{2.24}$$

Following the same argument used in the stabilization section, let us define the angle of desired orientation of the robot towards the point B as $\theta_g = \tan^{-1}\left(\frac{q_y - y_B}{q_x - x_B}\right)$, and define the deviance from the desired angle for the collision avoidance control as $\gamma = \theta_g - q_\theta$. Using basic trigonometry rules we obtain that:

$$\begin{array}{l}(x_B - q_x) = D_B\cos\theta_g \\ (y_B - q_y) = D_B\sin\theta_g\end{array},$$

it follows that

$$\dot{D}_B = -\left[\cos\theta_g\cos q_\theta + \sin\theta_g\sin q_\theta\right] v(1+d_1)$$

thus, being $\cos\theta_g\cos q_\theta + \sin\theta_g\sin q_\theta = \cos(\theta_g - q_\theta)$, it follows:

$$\dot{D}_B = -\cos(\gamma)v(1+d_1).$$

Define $\vartheta = \inf_{(q_x,q_y)\in\Upsilon_i} D_B(q_x,q_y)$ the distance from the point B to the set Υ_i. In order to stabilize D_B, we propose the following controller for v:

$$v = \begin{cases} k_3 D_B & \text{if } \cos(\alpha) \geq 0 \text{ and } |\gamma| \leq \epsilon\pi \\ 0 & \text{otherwise} \end{cases},$$

where $k_3 > 0$ and $0 < \epsilon < 0.5$. Since this control has to be applied into the set Υ_i only, then $v \geq k_3\vartheta$. For the designed control v, a Lyapunov function $W_1(D_B) = 0.5D_B^2$ has the following derivative:

$$\dot{W}_1 \leq \begin{cases} -2c_2 W_1 & \text{if } \cos(\alpha) \geq 0 \text{ and } |\gamma| \leq \epsilon\pi \\ 0 & \text{otherwise} \end{cases},$$

where $c_2 = k_3\cos(\epsilon\pi)(1-d_{min})$, and it can be seen that the designed v can exponentially stabilize D_B.
Then γ has the following dynamics:

$$\dot{\gamma} = -\omega(1+d_2) + \frac{\sin\gamma}{y_B}v(1+d_1). \tag{2.25}$$

Using the Lyapunov function $W_2 = 0.5\gamma^2$, we obtain:

$$\dot{W}_2 = -\omega\gamma(1+d_2) + \gamma\frac{\sin\gamma}{D_B}v(1+d_1)$$

Setting $\zeta(\gamma) = \max\{|\gamma|^{0.5}, |\gamma|\}$, the proposed expression for the control ω has the form:

$$\begin{aligned} \omega &= k_d\dot{\gamma} + \frac{\sin\gamma}{D_B}v + k_{ca}\zeta(\gamma)\text{sign}(\gamma),\ k_d > 0, \\ k_{ca} &\geq k_3\frac{\sqrt{\pi}(d_{max}-d_{min})[1+k_d(1+d_{max})]}{(1-d_{min})[1+k_d(1-d_{min})]} \\ &+2^{-3/4}\eta_2\frac{1+k_d(1+d_{max})}{1-d_{min}},\ \eta_2 > 0. \end{aligned} \tag{2.26}$$

A straightforward calculation shows that $\dot{W}_2 \leq -\eta_2\max\{W_2, W_2^{3/4}\}$, then

$$|\gamma(t)| \leq \begin{cases} |\gamma_0|e^{-0.5\eta_2(t-t_{ca})} & \text{if } t\in[t_{ca},t_3], \\ \sqrt{2}[\min\{1, 2^{-1/4}\sqrt{|\gamma_0|}\}] & \\ -2^{-2}\eta_2(t-t_3)]^2 & \text{if } t\in(t_3,t_4], \\ 0 & \text{if } t > t_4, \end{cases} \tag{2.27}$$

$$\begin{aligned} t_3 &= t_{ca} + \max\{0, \eta_2^{-1}\ln(0.5\gamma_0^2)\}, \\ t_4 &= t_3 + 2^{-2}\eta_2^{-1}\min\{1, 2^{-1/4}\sqrt{|\gamma_0|}\}, \end{aligned}$$

where $t_{ca} \geq 0$ is an instant of activation of the control u_2 and $\gamma_0 = \gamma(t_{ca})$. Thus the proposed control steers the robot in a finite time to the desired orientation, indeed there exists $0 < T_2 < \infty$ such that $\gamma(t_{ca}+T_2) < \epsilon\pi$ for all $\gamma\in[-\pi,\pi)$:

$$T_2 = \eta_1^{-1}\begin{cases} -2\ln(\epsilon) & \text{if } \epsilon\pi \geq 1, \\ \ln(0.5\pi^2) + 4(1-2^{-1/4}\sqrt{\epsilon\pi}) & \text{otherwise.} \end{cases}$$

As we can note, the controls (2.19) and (2.26) used for regulation of α and γ respectively are rather similar and have analogous stability properties, so a kind of control (2.26) can be used for stabilization of α, and *vice versa*.
Following the geometric construction of the point B, the inequality $\cos(\alpha)|_{\gamma=0} > 0$ is verified, then there is a time instant $t_{ca} \leq \bar{t} \leq T_2$ such that the conditions $\cos(\alpha(t)) \geq 0$ and $|\gamma(t)| \leq \epsilon\pi$ (involved in the control v activation) are satisfied for $t \geq \bar{t}$. Starting from the instant $\bar{t}$ the robot starts to move without an interruption since $v \geq k_3\vartheta$. Therefore, with the decreasing properties of γ, the distance y_B is decreasing and admits an estimate:

$$D_B(t) \leq D_B(t_0)e^{-c_2(t-T_2-t_{ca})} \; \forall t \geq t_{ca}.$$

Since the point B is located outside the set Υ_i, then there exists a finite time $T_{ca} > t_{ca}$ such that $z_2(T_{ca}) = \delta$, hence the collision avoiding is accomplished. It is worth to stress that it is possible to have a local increment of the regulated output z_2 due to the geometric construction of the point B. On the other hand, after a certain amount of time the output z_2 decreases with the controller v. In addition, as it has been shown above, it is not possible to steer the robot toward the obstacle, and the robot itself will not enter the circle of radius $\rho_{i,min}$. The output z_1 does not increase during the collision avoiding manoeuvre since the constraint $\cos(\alpha) \geq 0$ has been introduced in the control v (and v is positive).
The controller u_2 for the two control inputs v and ω pushes the robot in a finite time toward a point far from the obstacle, while keeping the distance z_1, and it can be summarized as follows:

$$u_2 = \begin{cases} v = \begin{cases} k_3 D_B & \text{if } \cos(\alpha) \geq 0 \text{ and } |\gamma| \leq \epsilon\pi \\ 0 & \text{otherwise} \end{cases} \\ \omega = k_d\dot{\gamma} + \frac{\sin\gamma}{D_B}v + k_{ca}\zeta(\gamma)\text{sign}(\gamma). \end{cases}, \tag{2.28}$$

The following properties have been substantiated.

Lemma 2. *The system (1.33) with control (2.28) has the properties for $t_{ca} \geq 0$:*
1. *Uniform finite-time stability with respect to the variable $\gamma(t)$ (the estimate (2.27)).*
2. *There exists $T_{ca} > t_{ca}$ such that $\delta_i \leq z_2(t) < \rho_{i,min}^{-1}$ for all $t \in [t_{ca}, T_{ca}]$ and $y_2(T_{ca}) = \delta$.*
3. *$\dot{V}_1(t) \leq 0$ for all $t \in [t_{ca}, T_{ca}]$.*

Following the presented strategy for the choice of point B when encountering an obstacle, the item 1 of the above lemma implies that the control u_2 can orient the robot in the direction of the chosen point B in finite time. The second and the third item of the above lemma state that this control u_2 can drive the robot away from the obstacle, at the same time it will not increase the distance between the robot and the desired final point.

2.3.3 Supervision

As presented in the previous section, the proposed control u_1 can drive the robot directly to the desired final position if it will not encounter any obstacle. If it does encounter one, when approaching to the obstacle at a certain distance, the robot will intelligently choose an intermediate point B, and switch to the second control u_2. This second control will navigate the robot away from the obstacle to this point, by keeping the distance z_1 between the robot and the desired final point decreasing. When the

robot feels safe, i.e. far enough away the obstacle, it will then switch back to u_1 to continuously approach the desired final point. This intelligent strategy on the commutation between the controls (2.22) and (2.28) can be formulated by the following supervisor:

$$U(t) = u_{i(t)}[q_x(t), q_y(t), q_\theta(t)],\ i : \mathbb{R}_+ \to \{1, 2\} \tag{2.29}$$

$$t_0 = 0,\ i(t_0) = \begin{cases} 1 & \text{if } (q_x(t_0), q_y(t_0)) \in \mathbf{X_2}, \\ 2 & \text{otherwise}, \end{cases}$$
$$i(t) = i(t_j) \quad \forall t \in [t_j\ t_{j+1}),$$

$$i(t_{j+1}) = \begin{cases} 1 & \text{if } q(t_{j+1}) \in \mathbf{X_1} \\ 2 & \text{if } q(t_{j+1}) \notin \mathbf{X_2} \end{cases}, \tag{2.30}$$

$$t_j = \begin{cases} \underset{t \geq t_j}{\arg\inf}\ q(t) \notin \mathbf{X_2} & \text{if } i(t_j) = 1 \\ \underset{t \geq t_j}{\arg\inf}\ q(t) \in \mathbf{X_1} & \text{if } i(t_j) = 2 \end{cases},$$

where:

$$\mathbf{X_1} : \left\{(q_x, q_y) \in \mathbb{R}^2 : \mathbb{R}^2 \setminus \cup_{j=1}^{N} \Upsilon_j\right\},$$
$$\mathbf{X_2} : \left\{(q_x, q_y) \in \mathbb{R}^2 : \mathbb{R}^2 \setminus \cup_{j=1}^{N} \Xi_j\right\},$$
$$\Xi_j = \{(x, y) \in \mathbb{R}^2 : (q_x - x_{o_j})^2 + (q_y - y_{o_j})^2 \leq \rho_i^2\}.$$

Thus the control u_1 is applied if $z_2 < \delta_j$ and the control u_2 has to be activated if $z_2 = \Delta_j$ for some $j \in \{1, \ldots, N\}$. The stability properties of the WMR (2.1) with the control (2.29) and the supervisor (2.30) can be then achieved.

2.3.4 Application to unicycle

We will now provide the main result for the unicycle considering the supervisory control described in this section.

Corollary 1. *Consider the system (2.1) with the supervisor (2.30) and control (2.29), then:*

$$z_1(t) \leq z_1(0) \quad \forall t \geq 0,$$
$$\lim_{t \to \infty} z_1(t) = 0,$$
$$z_2(t) \leq \sigma(\max\{\Delta, z_2(0)\}) \quad \forall t \geq 0,$$

where $\Delta = \max_{1 \leq i \leq N} \Delta_i$ *and* $\sigma(s) = s/(\Delta Y)$.

Proof. According to definitions of z_1 and z_2, define

$$\rho_0 = z_2(0, 0) = \max_{1 \leq i \leq N} 1/\sqrt{x_{o_i}^2 + y_{o_i}^2},$$

by assumptions $\rho_0 < \delta$. Since N and Y are finite, then there exists a function $\rho \in \mathcal{K}$ such that $|h_2(q)| \leq \rho(|h_1(q)|) + \rho_0$ for all $x \in \mathbb{R}^n$. Assumption 1 is satisfied since

the controls (2.22), (2.28) are right-continuous functions of time (only one switch is possible for an activation due to uniform finite-time stability of α and γ achieved in lemmas 1 and 7). From Lemma 1, $\beta_1(s,r) = e^{c_1 T_1(\pi)} s e^{-c_1 r} \in \mathcal{KL}$, but additionally $z_1(t) \leq z_1(t_0)$ for all $t \geq t_0$, therefore the estimates (2.10) are satisfied. In addition, z_1 preserves its value during steering, and while moving the distance z_1 is always decreasing, therefore the condition $\beta_1(s,\tau_D) = \lambda s$ is valid for some $\lambda \in [0,1)$. From Lemma 7 the estimates (2.11) are satisfied. Therefore, all conditions of Theorem 1 have been verified. The estimates stated in the corollary can also be checked by a straightforward calculations. □

2.4 Simulation Results

For simulations purpose, the number of obstacles is $N = 3$, the sample time used is $t_s = 0.1$, this value is a further proof of the robustness of the proposed control law since the lower the sampling time, the fewer are the information received to evaluate the control action. The disturbances have form $d_i = \chi \sin(t) + 0.1 * rand$ where $rand$ is a pseudo-random values drawn from the standard uniform distribution on the open interval $(0,1)$ with $i \in \{1,2\}$ and $|\chi| \leq 0.5$. For the collision avoidance part the distances were defined as follows: let r be the generic obstacle radius, $\rho_{i,min} = r + 0.3$, $\rho_i = \rho_{i,min} + 0.3$ $R_i = \rho_i + 0.35$. The ϵ and k values are equal to $1/30$.

The values of control gains are listed in tables 2.1 and 2.2. They were carefully tuned to avoid any saturation in the control input signal for the real robot utilised in Section 4.1.2.

Table 2.1: Stabilization Controller Gains

Gain	Value
k_1	0.5
η	0.5

Table 2.2: Collision Avoidance Controller Gains

Gain	Value
k_3	0.5
η_2	0.5
k_d	0.05
k_{ca}	1.015

As it can be seen in Fig. 2.4, each time the robot enters the zone where $z_2 \geq \Delta$, it starts the maneuver to reach the point B making collision avoidance. Once it enters the zone $z_2 \leq \delta$ it continues to move toward the origin. The center of the robot, red star in Fig. 2.4, never enters the circle of radius $\rho_{i,min}$ preventing the robot to collide. This explains us better why in Section 2.3 the radius of the robot has been considered as a design parameter $\rho_{i,min}$; indeed the two figures showed in 2.3.2 (Fig. 2.2 and Fig. 2.3) display the behavior of the algorithm to choose the B point in the two activations of the controller. In Fig. 2.5 and 2.6 the vertical black lines represent the switching instants and it is shown that all controlled variables behave as wanted. In particular in Fig. 2.5 it is shown how the variables α and γ are stabilized both in finite time by

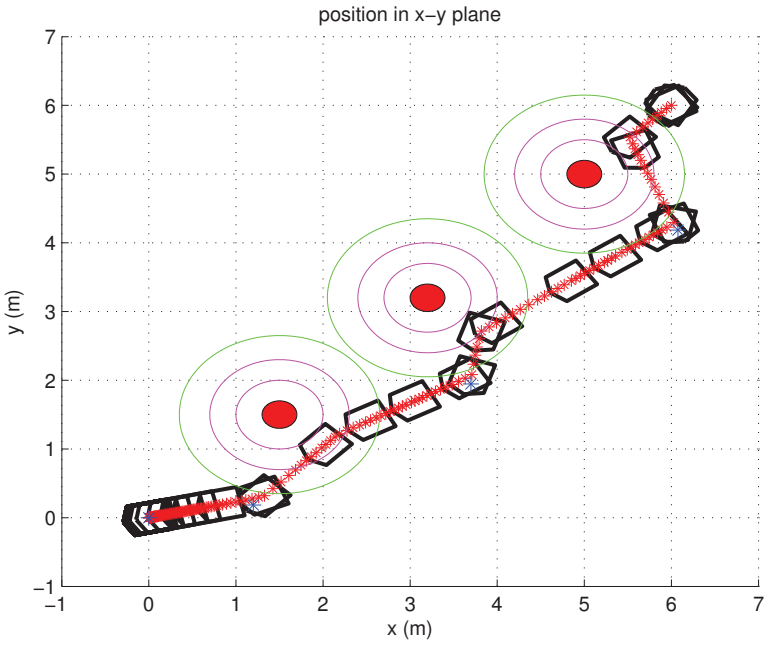

Figure 2.4: Stabilization of the unicycle with three obstacles

the controllers to steer the robot facing the desired point. The angle γ appears in the plot only when the controller u_2 is active. In the same plot the value of $\cos\alpha$ is shown (in order to demonstrate that the condition for the v part of the controller under the collision avoidance maneuver is always kept).

It is also shown the behavior of the two outputs, z_2 indeed increases the value during the collision avoidance maneuver in all the activations, but before the successive switch the value is always less than the starting one. We would like to remark that z_1 never increases.

2.5 Experimental Results

The presented strategy has been implemented on a Turtlebot2 (`http://www.turtlebot.com/`) mobile robot. The WMR was equipped with a Hokuyo® (`http://www.hokuyo-aut.jp`) UTM-30LX LIDAR device. The necessary libraries to communicate with the WMR were found on Robotic Operating System (ROS), "Groovy" release (www.ros.org). An easy LIDAR based obstacle detection algorithm has been implemented to get obstacle(s)' positions (x_{o_i}, y_{o_i}) and radius r_i used to define also the values of $\rho_{i,min} = r_i + 0.3$, $\rho_i = \rho_{i,min} + 0.3$ and $R_i = \rho_i + 0.35$. The values of ϵ and k are equal to $1/30$, the control gains are $k_1 = \eta = 0.5$ for the stabilization controller and $k_3 = k_p = 1.5$, $k_{ca} = 0.1$, $k_d = 0.05$ for the collision avoidance one. Several scenarios have been tested for the presented Finite Time Obstacle Avoidance (FTOA) technique, in addition the performances have been compared with the well know DWA [45] which is included in the ROS.

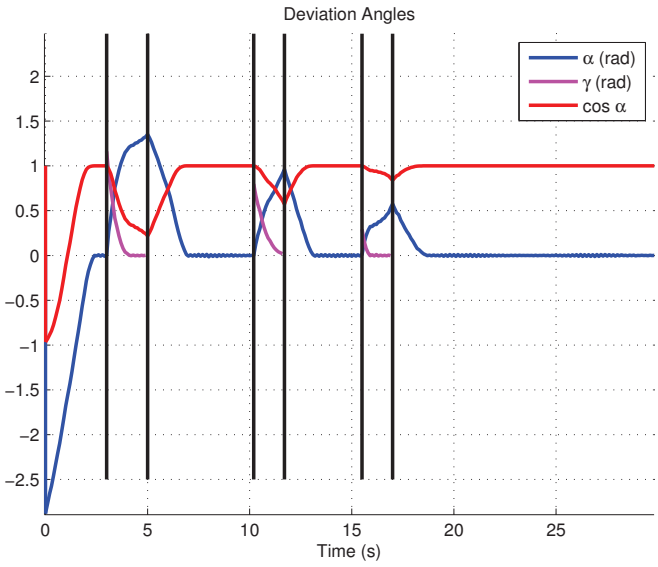

Figure 2.5: Evolution of angles α and γ

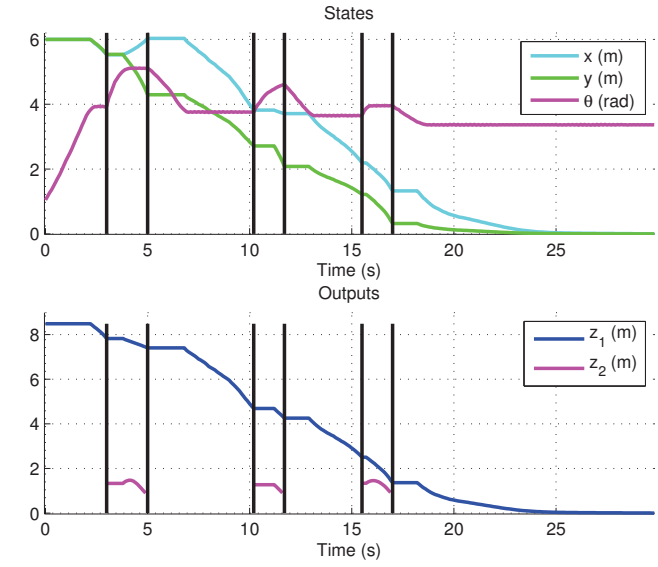

Figure 2.6: a) State evolution b) Outputs

The implementation of the algorithm can be divided in two main parts. Firstly, Algorithm 1 translates in pseudo-code the supervisor (2.30) which regulates the switching between the two controls. The *if* statement determines the activation of the collision avoidance control and it can be noticed that such controller is kept active until the condition in the *elseif* statement is verified, that is when the WMR exits the circle of radius R_i. The function *getbp(state,*z_2*)* follows the instructions presented in Section 2.3.2 to determine the B point, while the variable *Flag* assures that the controller is not switched when the WMR is in the zone between Δ_i and δ_i. Secondly, Algorithm 2 represents the complete proposed algorithm where firstly the laser scans are used to localize the robot in a map (*getpos(laser_scan)*) then to evaluate the presence of an eventual obstacle (*getz_2(laser_scan)*). As can be seen by analyzing the two algorithms the FTOA method is also very simple to implement requiring very few steps and, as a result, very low computational power.

Algorithm 1 Supervisor

Flag = **Supervisor**(z_2,Flag) {
  if $z_2 \geq \Delta$ && Flag == 1
    B = getbp(state, z_2);#section 2.3.2
    Flag = 2;
  elseif $z_2 \leq \delta$
    Flag = 1;
  end
}

Algorithm 2 Main Code

Flag = 1;
(x, y) = getpos(laser_scan);
z_2 = getz_2(laser_scan);
while$||(x, y)|| \leq \epsilon_1$
    #Not arrived at the origin
  Flag = Supervisor(z_2, Flag);
  if Flag ==2
    (v, ω) = U_2(state,B);#eq.(2.28)
  else
    (v, ω) = U_1(state); #eq.(2.22)
  end
state_update(v, ω);
(x, y) = getpos(laser_scan);
z_2 = getz_2(laser_scan);
end

2.5.1 Experimental Behaviour

Fig. 2.7 and Fig. 2.8 show the different trajectories followed by the WMR using two different methods on different soil's condition. The decision to run tests on two different soils has been taken for two main reasons: firstly, to justify the choice of the

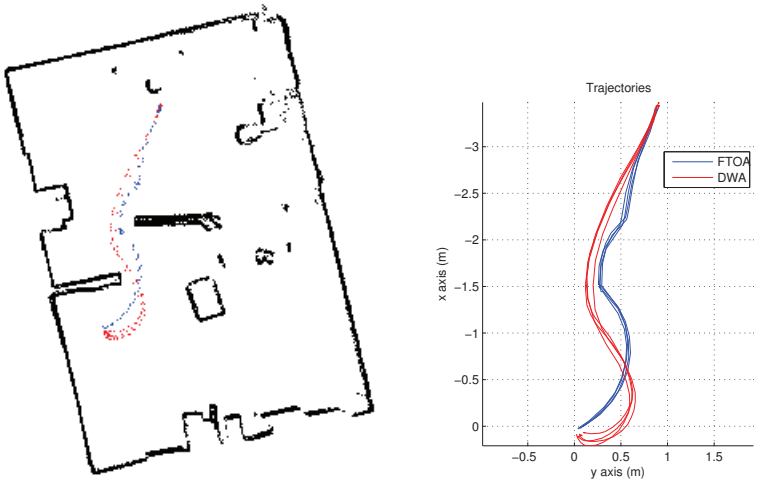

Figure 2.7: Left: Real scenario with coarse soil (moquette). Right: Zoom on trajectories

perturbed model (2.1), then to show the robustness of the controller designed in section 2.1 with respect to this change. Without adapting the PID gains which translates the velocities commands in current inputs, the soil properties represent a real perturbation for the system, because for the same velocity input the WMR reacts differently following different trajectories. It can be seen how the proposed method handles these perturbations in a better way than traditional strategies producing repeatable trajectories. In Fig. 2.7, for a coarse soil (moquette), it can be noticed that all the trajectories generated by the FTOA are close to each other and that they change (even if not much) for the DWA. Repeating the experiment on a smooth soil (linoleum), Fig. 2.8, the changes in the trajectories are more clear, that it is given by the reduced friction between the wheels and the soil that caused grip issues for the WMR. Again, the FTOA method gives better results (repeatability, time spent, distance traveled) than the DWA.

The comparison between FTOA and DWA for the scenarios showed in Fig. 2.7 and Fig. 2.8, with equal maximal linear and angular velocities, based on 10 trials, showed that the FTOA can achieve the avoiding in a faster (*wrt* time) and shorter (*wrt* distance) way; detailed results are presented in Tables 2.3 and 2.4.

In addition, Fig. 2.9 shows how the outputs behave in a typical stabilization execution from a point to the origin; the vertical black lines represent the switching instants. The data comes from an execution for the scenario shown in Fig. 2.7. The z_2 output (2.3) decreases between two successive switches and it is worth to remark that z_1 output (2.2) never increases, not even during the collision avoidance maneuver; that is exactly how the controllers (2.22) and (2.28) overseen by the supervisor (2.30) should work.

2.5.2 Discussion

Trying not to increase the distance from the target point (in this work the origin with any loss of generality) over the complete maneuver causes the robot having trajectories less smooth than other methods but, as it has been proven, this behavior does

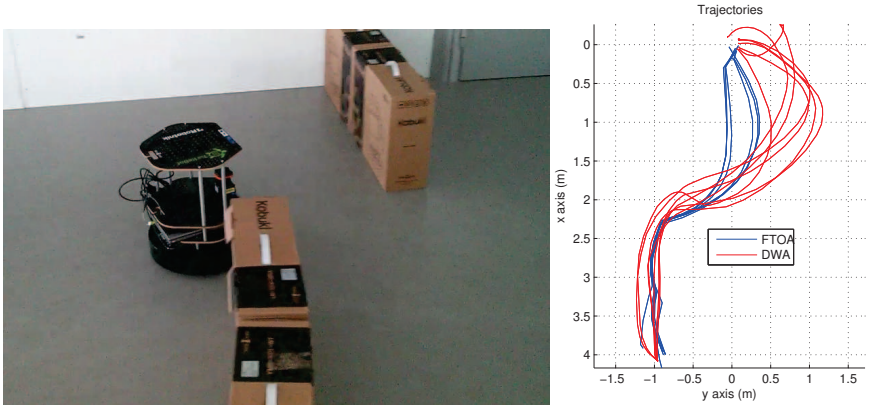

Figure 2.8: Left: Real scenario with smooth soil (linoleum). Right: Zoom on trajectories

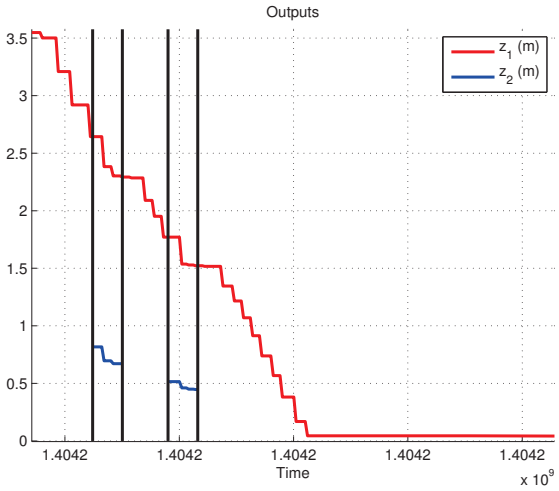

Figure 2.9: Outputs evolution

	DWA			FTOA		
Time (s)	min	max	average	min	max	average
	22.43s	26.30s	24.41s	14.2s	19.2s	**16.47s**
Distance (m)	min	max	average	min	max	average
	4.23m	4.39m	4.32m	3.83m	3.92m	**3.86m**

Table 2.3: Comparison between FTOA method and DWA on coarse soil

	DWA			FTOA		
Time (s)	min	max	average	min	max	average
	25.36s	42.95s	32.00s	16.2s	19.1s	**18.4s**
Distance (m)	min	max	average	min	max	average
	5.42m	6.10m	5.79m	4.36m	4.86m	**4.59m**

Table 2.4: Comparison between FTOA method and DWA on smooth soil

not worsen the overall performances. The smoothness of the trajectories can be adjusted augmenting the parameters k for (2.22) and ϵ for (2.28) that will cause a decay in the performances wrt time spent and distance traveled as it is obvious. Moreover, under the assumption to deal with the single obstacle, the proposed method has no issues related to small non-convex obstacles because of the way the collision avoidance is realized and the obstacle described, nevertheless, being a reactive (local) method, there is a high probability that it fails if the WMR is trapped in a U-shaped trap, like others local approaches. Other inconvenient could appear if the obstacle has a very long shape (a wall), that could cause an unwanted oscillatory behavior. All the issues listed above could be solved integrating the algorithm in a global planner which gives suitable points as targets to stabilize progressively.

2.6 Conclusion

This chapter presented a switching based solution to stabilize a unicycle-like WMR, locally avoiding obstacles and rejecting disturbances due to neglected dynamics. A supervisor orchestrates two different controls to regulate two respective outputs. It has been shown how the cooperation of the two controls leads to a practically finite-time robot deployment, while the collision avoidance is always achieved in a finite time. In addition, the results of this work have been proven and tested on a real platform to show the effectiveness of the method also comparing it with a well-known method as the DWA. The presented solution treats the case of static obstacles but several experiments have been run with slow moving obstacles with preliminary results; it is in the intention of the authors to extend the results for moving obstacles. Future work will also involve the integration of the proposed strategy in a global planner as specified in Section 2.5.2 to overcome the limitations of the method and to relax the hypothesis of circular shaped obstacles.

Chapter 3

Input-to-State Stability to improve the classical Potential Field Method

It is in the spirit of the research to find out new way to solve problems and trying to ameliorate the existing ones. In Section 1.5, the Potential Field method has been presented along with its advantages and drawbacks; the appearance of local minima, which causes the WMR to stop and not accomplish the task, is one of these drawbacks.

In this chapter, a recent control theory result [2], is used to presents a new approach to avoid local minima in the Potential Field (PF) method to realize 2D real time obstacles avoidance (a summary of the results present in [2] can be found in Appendix A). Starting from the hypothesis of disjoints obstacles, very common in literature for the method [75], a new potential field is designed and the gradient of such a field is used as input for a two variables integrator. Under proper assumptions, the system is shown to be Input-to-State-Stable (ISS) with respect to decomposable invariants sets [2]. The Input-to-State Stability (ISS) property is the key of the proposed modification. It allows to deal with local minima in an effective way, suggesting thus a novel solution to the problem which is easy and elegant and that guarantees, thanks to some manipulations, the collision avoidance for the WMR without the risk to remain blocked in a local minimum.

The new formulation of the PF and its properties are used to avoid local minima is thus applied to drive a unicycle like Wheeled Mobile Robot (WMR) subject to additive input disturbances to a target (i.e. the origin). It is necessary to take into account the non-holonomic constraints whose the robot is subject which preclude certain movements. The aim is to have the WMR to track the movement of the 2D particle. The tracking problem for non-holonomic WMR has been previously treated in literature [75, 124, 111, 55], often in obstacles free scenario. This chapter will present 2 approaches: the former one applies an output linearization technique [128, 110] and it is indeed the simplest. The controls obtained for the particle case may be applied, with a simple change of coordinates, to the mobile robot; this approach does not allow the control of the orientation of the robot though. A second one is, thus, designed to control both linear velocity and orientation of the WMR. This controller assigns for the linear velocity the norm of the field gradient while the angular velocity command is regulated with a finite-time control similar to the one used in [55]. It is formally shown that the finite time control robustly guarantees the convergence of the robot orientation to the gradient lines direction and simulations have been carried to show the very sat-

isfying result. The experimental part sees a Turtlebot 2 WMR avoiding obstacles in an office-like environment. Usually, obstacle avoidance methods (as the PF one) relied on ultrasonic sensor [148] or infrared ones [114] while the actual trend is to use camera devices or laser range finders; in this work we use a LIDAR device to localize the WMR in a map and to realize the avoidance.

3.1 Potential field method with static obstacles

First, let us consider a simplified model of a mobile agent represented by doubled integrator dynamics:

$$\begin{aligned} \dot{x} &= u_x, \\ \dot{y} &= u_y, \end{aligned} \tag{3.1}$$

where $x \in \mathbb{R}$ and $y \in \mathbb{R}$ are the coordinates of the agent in the plane, $z = [x\ y]^T$, $u_x \in \mathbb{R}$ and $u_y \in \mathbb{R}$ are the corresponding controls. It is necessary to design the controls u_x, u_y providing the agent regulation to the origin under avoidance of collisions with isolated point-wise obstacles, which are defined by their coordinates $\zeta_i = (x_i, y_i)$ and safe distances d_i around them for $i = 1, \dots, N$, where $N > 0$ is a finite number of obstacles. We will assume that $|\zeta_i - \zeta_j| > \max\{d_i, d_j\}$ and $|\zeta_i| > d_i$ for all $1 \leq i \neq j \leq N$, *i.e.* the obstacles are separated and the origin is not occupied by an obstacle.

The problem will be solved using the potential field method, whose idea consists in defining a repulsion potential U_r with respect to the obstacles and attraction potential U_a with respect to the origin, next the controls can be designed proportional to the "forces" generated by the total potential U [128, 121]. The main drawback of that approach consists in appearance of local conditional extrema, which theoretically do not allow a global problem solution to be guaranteed by the method. In this work we will use the results presented in the previous section to design the agent dynamics that is C^1 and ISS with respect to the set $\mathcal{W}$ composed by equilibriums, among them the equilibrium at the origin is attractive, the equilibriums related to the obstacles are repulsing, while ones corresponding to the local extrema are saddle. Next, applying specially designed small perturbations to that ISS system we will avoid the unstable equilibriums.

To design the attraction potential U_a we would like to impose the followin constraints:

- it should be twice continuously differentiable with respect to x and y;
- its gradient should be globally bounded (the velocity of movement out the origin in the collision-free case should be approximately constant in a robotic application).

The following potential yields these constraints:

$$U_a(z) = \begin{cases} |z|^2 & \text{if } |z| \leq \upsilon, \\ |z| & \text{if } |z| \geq \Upsilon, \\ \lambda(|z|)|z|^2 + [1 - \lambda(|z|)]|z| & \text{otherwise}, \end{cases}$$

$$\lambda(s) = \left(\frac{2s^3 - 3(\upsilon + \Upsilon)s^2 + 6\Upsilon\upsilon s + \Upsilon^2(\Upsilon - 3\upsilon)}{\Upsilon^2(\Upsilon - 3\upsilon) + \upsilon^2(3\Upsilon - \upsilon)} \right)^2,$$

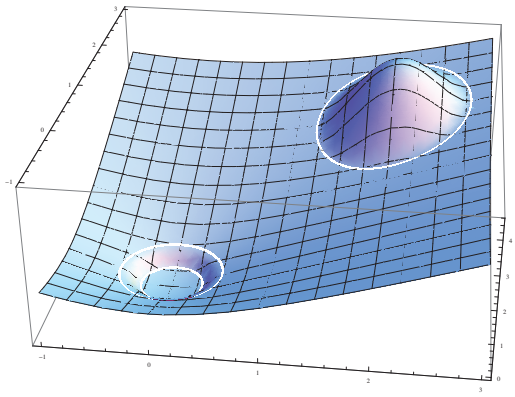

Figure 3.1: The continuous field in the case of a single obstacle with $\nu = 0.3$, $\Psi = 0.5$, $\zeta_1 = (2, 2)$, $d_1 = 0.8$ and $\alpha = 4$

where $0 < \upsilon < \Upsilon < +\infty$ are the design parameters. Thus, the potential U_a is quadratic in z close to the origin, it has a linear growth rate far enough and the function λ ensures a smooth transition between these zones.

The repulsion potential U_r should be also twice continuously differentiable with respect to x and y, and it should be active only on a small zone around the obstacle (the agent can detect the obstacle presence only locally in an uncertain environment in a robotic application, for example):

$$U_r(z) = \alpha \sum_{i=1}^{N} \max\{0, d_i^2 - |z - \zeta_i|^2\}^2,$$

where $\alpha > 0$ is a tuning parameter.

The total potential U, Fig.3.1, has the form:

$$U(z) = U_a(z) + U_r(z), \tag{3.2}$$

with the gradient

$$\nabla_z U(z) = \nabla_z U_a(z) + \nabla_z U_r(z),$$

$$\nabla_z U_a(z) = \begin{cases} 2z & \text{if } |z| \le \upsilon, \\ z|z|^{-1} & \text{if } |z| \ge \Upsilon, \\ \varphi(z) & \text{otherwise,} \end{cases}$$

$$\nabla_z U_r(z) = -4\alpha \sum_{i=1}^{N} (z - \zeta_i) \max\{0, d_i^2 - |z - \zeta_i|^2\},$$

where $\varphi(z) = \nabla_z \left(\lambda(|z|)|z|^2 + [1 - \lambda(|z|)]|z|\right)$ is the corresponding C^1 function ensuring a continuous transition between $2z$ and $z|z|^{-1}$. Note that by construction $\nabla_z U(z)$ is a C^1 function of z. As usual in the potential field method we assign:

$$\begin{bmatrix} u_x \\ u_y \end{bmatrix} = -\nabla_z U(z) + v, \tag{3.3}$$

where $v \in \mathbb{R}^2$ is an auxiliary bounded input to be designed later, then the closed-loop system (3.1), (3.3) takes the gradient form:

$$\dot{z} = -\nabla_z U(z) + v. \tag{3.4}$$

Next, we are going to show that for $v = 0$ this system has an attracting equilibrium at the origin, repulsing equilibriums in a vicinity of ζ_i for each $i = 1, \ldots, N$ and a saddle equilibrium in the border of the repulsion zone around ζ_i for each $i = 1, \ldots, N$. Therefore, a compact invariant set $\mathcal{W}$ containing all α- and ω-limit sets[1] of (3.4) for $v = 0$ is decomposable (in the sense of Definition 12 appendix A), and that Theorem 7 in Appendix A can be applied to establish ISS with respect to the set $\mathcal{W}$ for the input v.

3.1.1 Equilibrium at the origin

Under the restrictions $|\zeta_i| > d_i$ for all $1 \leq i \leq N$, the system (3.4) is reduced to

$$\dot{z} = -2z$$

for $|z| \leq \tilde{v}$ for some $0 < \tilde{v} \leq v$, which is obviously locally attractive. For simplicity of presentation below we will assume that the constants v and Υ are selected in a way to provide $|\zeta_i| \geq \Upsilon + d_i$ for all $1 \leq i \leq N$.

3.1.2 Equilibriums around the obstacles

Since the obstacles are separated from one another and from the origin, around each obstacle the system (3.4) takes a reduction ($|z| \geq \Upsilon$):

$$\dot{z} = -z|z|^{-1} + 4\alpha(z - \zeta_i)\max\{0, d_i^2 - |z - \zeta_i|^2\} + v$$

for some $1 \leq i \leq N$. Clearly, if $d_i < |z - \zeta_i|$ then $\dot{z} = -z|z|^{-1}$ and there is no equilibrium, thus we may restrict attention to the case $|z - \zeta_i| \leq d_i$ and

$$\dot{z} = -z|z|^{-1} + 4\alpha(z - \zeta_i)(d_i^2 - |z - \zeta_i|^2) + v.$$

On this set the equilibriums of (3.4) satisfy the vector equation

$$z = 4\alpha(z - \zeta_i)(d_i^2 - |z - \zeta_i|^2)|z|$$

or the corresponding scalar equation

$$\begin{aligned} &|z|^2 - 8\alpha(d_i^2 - |z - \zeta_i|^2)|z|\, z^T(z - \zeta_i) \\ &+16\alpha^2|z - \zeta_i|^2(d_i^2 - |z - \zeta_i|^2)^2|z|^2 = 0. \end{aligned}$$

Introducing parametrization $z = \kappa\zeta_i + \eta$, where $\kappa \in \mathbb{R}$ and $\eta \in \mathbb{R}^2$, and substituting it in the last equation it is tedious but straightforward to obtain that for any $|\eta| \neq 0$ the equality is not satisfied. Therefore setting $\eta = 0$, then under substitution $z = \kappa\zeta_i$ we have:

[1] For the definition of α- and ω-limit sets refer to Appendix A

$\kappa^2|\zeta_i|^2 - 8\alpha[d_i^2 - (\kappa-1)^2|\zeta_i|^2]\kappa|\zeta_i|\kappa(\kappa-1)|\zeta_i|^2 + 16\alpha^2\kappa^2(\kappa-1)^2|\zeta_i|^2[d_i^2 - (\kappa-1)^2|\zeta_i|^2]^2|\zeta_i|^2 =$

$\kappa^2|\zeta_i|^2\{1-8\alpha[d_i^2-(\kappa-1)^2|\zeta_i|^2]|\zeta_i|(\kappa-1)+16\alpha^2(\kappa-1)^2[d_i^2-(\kappa-1)^2|\zeta_i|^2]^2|\zeta_i|^2\} =$

$\kappa^2|\zeta_i|^2\{1-8\alpha[d_i^2-(\kappa-1)^2|\zeta_i|^2]|\zeta_i|(\kappa-1)+16\alpha^2(\kappa-1)^2[d_i^2-(\kappa-1)^2|\zeta_i|^2]^2|\zeta_i|^2\} =$

$\kappa^2|\zeta_i|^2\{1 - 4\alpha[d_i^2 - (\kappa-1)^2|\zeta_i|^2]|\zeta_i|(\kappa-1)\}^2 = 0,$

the equation for equilibriums is reduced to

$$1 - 4\alpha[d_i^2 - s^2|\zeta_i|^2]|\zeta_i|s = 0$$

for $s = \kappa - 1$, or

$$s^2 - \frac{d_i^2}{|\zeta_i|^2}s + \frac{1}{4\alpha|\zeta_i|^3} = 0$$

that is a depressed cubic equation, which by the Cardano's method has only real roots if

$$\alpha d_i^3 > \frac{3\sqrt{3}}{8}. \tag{3.5}$$

Next, by the Routh–Hurwitz stability criterion the equation has 2 roots with positive real parts. Therefore, for $|z - \zeta_i| \leq d_i$ the system (3.4) has two equilibriums $z_0^{i,1}$ and $z_0^{i,2}$ under the condition (3.5). The Cardano's method also provides the expressions of exact solutions and, hence, the coordinates of the equilibriums $z_0^{i,1}$, $z_0^{i,2}$ (both equilibriums are located farther from the origin than the obstacle ζ_i on the line connecting the origin and the point (x_i, y_i)). Finally, the system (3.4) is continuously differentiable, then the linearization shows that the equilibrium $z_0^{i,1}$ (closer to ζ_i) is purely repulsing, and another one $z_0^{i,2}$ is saddle (the corresponding local minimum).

To evaluate the zone of repulsion around ζ_i a Lyapunov function for linearization around $z_0^{i,1}$ can be used, or let us consider a Lyapunov function $V(e) = |e|^2$ for $e = z - \zeta_i$ and $v = 0$:

$$\begin{aligned} \dot{V} &= 2e^T[-z|z|^{-1} + 4\alpha e(d_i^2 - |e|^2)] \\ &= -2e^T z|z|^{-1} + 8\alpha V(d_i^2 - V) \\ &\geq -2|e| + 8\alpha V(d_i^2 - V). \end{aligned}$$

Note that $|e| = \sqrt{V}$ then

$$\dot{V} \geq [4\alpha\sqrt{V}(d_i^2 - V) - 1]2\sqrt{V}.$$

The Cardano's method can be used to find the solutions of the equation $4\alpha\sqrt{V}(d_i^2 - V) = 1$, which determines the sign definiteness of $\dot{V}$. The expression in the square brackets $4\alpha\sqrt{V}(d_i^2 - V) - 1$ reaches its maximum $\frac{2}{\sqrt{3}}\left(\frac{8}{3\sqrt{3}}\alpha d_i^3 - 1\right)d_i$ for $V = \frac{1}{3}d_i^2$, which is positive if the condition (3.5) is fulfilled (note that since the value of d_i is constrained by the physical dimensions of the agent, then (3.5) is a condition for α to satisfy). Thus the repulsion zone around the obstacle exists and it can be easily estimated.

3.1.3 Robustness with respect to v

The conditions on existence of the equilibriums, established above, are as follows:

Assumption 4. *Let the condition (3.5) be satisfied,* $|\zeta_i - \zeta_j| > \max\{d_i, d_j\}$ *and* $|\zeta_i| \geq \Upsilon + d_i$ *for all* $1 \leq i \neq j \leq N$.

Now we would like to show that the set

$$\mathcal{W} = \{\{0\}, z_0^{1,1}, z_0^{1,2}, \ldots, z_0^{i,1}, z_0^{i,2}, \ldots, z_0^{N,1}, z_0^{N,2}\},$$

which is composed by the equilibrium at the origin and N pairs of equilibriums $z_0^{i,1}, z_0^{i,2}$ associated with each obstacle, contains all α- and ω-limit sets of (3.4) for $v = 0$ and it is decomposable in the sense of Definition 12 in Appendix A. The system (3.4) has a Lyapunov function $U(z)$, by construction $\alpha_1(|z|) \leq U(z) \leq \alpha_2(|z|)$ for all $z \in \mathbb{R}^2$ and some $\alpha_1, \alpha_2 \in \mathcal{K}_\infty$, whose derivative has the form:

$$\begin{aligned} \dot{U} &= -|\nabla_z U(z)|^2 + \nabla_z^T U(z) v \\ &\leq -0.5|\nabla_z U(z)|^2 + 0.5|v|^2 \end{aligned} \tag{3.6}$$

and the total potential stops to decrease for $v = 0$ only on the set where $\nabla_z U(z) = 0$, but by consideration above it is $\mathcal{W}$: *i.e.* there exist $\gamma_1, \gamma_2 \in \mathcal{K}_\infty$ such that $\gamma_1(|z|_\mathcal{W}) \leq |\nabla_z U(z)| \leq \gamma_2(|z|_\mathcal{W})$ for all $z \in \mathbb{R}^2$. There is no cycle in the decomposition of $\mathcal{W}$ due to the same property $\dot{U} \leq 0$ for $v = 0$ (indeed the obstacles are separated and to pass from one saddle equilibrium around the obstacle ζ_i to another one around ζ_j it is necessary to cross the zone where $\nabla_z U(z) = \nabla_z U_a(z)$ and $\dot{U} < 0$, therefore a trajectory cannot return back). Thus, $\mathcal{W}$ is decomposable and contains all α- and ω-limit sets of (3.4) for $v = 0$. Further,

$$\dot{U} \leq -0.5\gamma_1^2(|z|_\mathcal{W}) + 0.5|v|^2,$$

and by compactness of $\mathcal{W}$ and since $0 \in \mathcal{W}$

$$|z|_\mathcal{W} \leq |z| \leq |z|_\mathcal{W} + R$$

for all $z \in \mathbb{R}^2$ and some $R > 0$ (diameter of the set $\mathcal{W}$). Next, by the properties of functions from the class $\mathcal{K}_\infty$

$$\gamma_1^2(0.5|z|_\mathcal{W} + 0.5R) \leq \gamma_1^2(|z|_\mathcal{W}) + \gamma_1^2(R)$$

then:

$$\begin{aligned} \dot{U} &\leq -0.5\gamma_1^2(0.5[|z|_\mathcal{W} + R]) + 0.5\gamma_1^2(R) + 0.5|v|^2 \\ &\leq -0.5\gamma_1^2(0.5|z|) + 0.5\gamma_1^2(R) + 0.5|v|^2 \\ &\leq -0.5\gamma_1^2[0.5\alpha_2^{-1}(U)] + 0.5\gamma_1^2(R) + 0.5|v|^2 \end{aligned}$$

then U is an ISS Lyapunov function and by Theorem 7 Appendix A, the following result has been proven.

Lemma 3. *Under Assumption 4 the system (3.4) is ISS with respect to the set* $\mathcal{W}$ *for the input* v.

3.1.4 Design of the input v to escape local minima

The advantage of the ISS property is that appearance of any bounded disturbance v does not lead to the system instability. In our case the total potential function U is also an ISS Lyapunov function for the system (3.4). If $v = 0$ and the agent in (3.4) is approaching an unstable equilibrium, then according to the expression of $\dot{U}$ the velocity of the agent is decreasing proportionally to $|\nabla_z U(z)|$. Thus, if $|\nabla_z U(z)| \leq \epsilon$ for some predefined $\epsilon > 0$ and we are far from the origin, it can be a signal of closeness to a saddle equilibrium, then an input $v \neq 0$ can be generated to shift the movement direction.

The input v can be selected bounded and pushing the system in an arbitrary direction with a uniform distribution, by ISS property the solutions asymptotically will stay close to $\mathcal{W}$ and it is possible to show that the origin will be globally attractive. However, using the Lyapunov function U the input v always can be designed in order to additionally guarantee a decreasing of U. From (3.6)

$$v = \begin{cases} \rho \begin{bmatrix} \nabla_y U(z) \\ -\nabla_x U(z) \end{bmatrix} & \text{if } |\nabla_z U(z)| \leq \epsilon \text{ and } |z| > \upsilon, \\ 0 & \text{otherwise,} \end{cases} \tag{3.7}$$

$$\rho = \text{sgn}\left(y - \frac{y_i}{x_i}x\right),\ i = \arg\inf_{1 \leq j \leq N} |z - \zeta_j|,$$

$$\text{sgn}(s) = \begin{cases} 1 & \text{if } s \geq 0, \\ -1 & \text{otherwise} \end{cases}$$

ensures that $\dot{U} \leq 0$ for all $t \geq 0$ ($\dot{U} = -|\nabla_z U(z)|^2$ while $v \neq 0$) and for $U = 0$ as well, and for the case of agent velocity dangerous decreasing ($|\nabla_z U(z)| \leq \epsilon$) far from the origin ($|z| > \upsilon$) the proposed input v generates an orthogonal disturbance to the current direction of movement. The variable ρ defines the orientation of this orthogonal perturbation, in (3.7) it points out from the line connecting the origin and the point (x_i, y_i) (that is the coordinate of the closest obstacle) and where we have the unstable equilibriums.

Theorem 2. *Under Assumption 4 the system (3.4) with the avoidance control (3.7) has the origin attractive from all initial conditions $z(0) \notin \mathcal{W} \setminus \{0\}$.*

Usually, for a robotic application, it is assumed that the robot starts in the collision-free conditions, *i.e.* $z(0) \notin \mathcal{D} = \cup_{i=1}^{N} \mathcal{D}_i$ where $\mathcal{D}_i = \{z \in \mathbb{R}^2 : |z - \zeta_i| \leq d_i\}$. Therefore, in this case definitely $z(0) \notin \mathcal{W} \setminus \{0\}$ since $\mathcal{W} \setminus \{0\} \subset \mathcal{D}$.

Proof. Considering the ISS Lyapunov function U for the system (3.4) with the avoidance control (3.7) we obtain:

$$\dot{U} = -|\nabla_z U(z)|^2$$

since $\nabla_z^T U(z) v = 0$ always. In addition, by construction v shifts the system trajectories out from the line $y = \frac{y_i}{x_i}x$ that contains the unwanted equilibriums $z_0^{i,1}, z_0^{i,2}$, then the only point to stop is the origin. □

Formally the control (3.7) does not use ISS property of the set $\mathcal{W}$, it is designed from a pure Lyapunov approach. We may modify (3.7) as follows in order to make the

attractiveness of the origin global:

$$v = \begin{cases} \rho \frac{\varepsilon}{|z|} \begin{bmatrix} y \\ -x \end{bmatrix} & \text{if } |\nabla_z U(z)| \leq \epsilon \text{ and } |z| > \upsilon, \\ 0 & \text{otherwise,} \end{cases} \tag{3.8}$$

$$\rho = \text{sgn}\left(y - \frac{y_i}{x_i}x\right),\ i = \arg \inf_{1 \leq j \leq N} |z - \zeta_j|,$$

$$\text{sgn}(s) = \begin{cases} 1 & \text{if } s \geq 0, \\ -1 & \text{otherwise} \end{cases}$$

where $\varepsilon > 0$ is a design parameter. It is easy to check that $v^T z = 0$ for all $z \in \mathbb{R}^2$ and $|v| = \varepsilon$ if $|\nabla_z U(z)| \leq \epsilon$ and $|z| > \upsilon$ in (3.8).

Theorem 3. *Under Assumption 4 the system (3.4) with the avoidance control (3.8) has the origin globally attractive provided that $\varepsilon > 2\epsilon$ and $\epsilon > 0$ is selected sufficiently small.*

Proof. From Lemma 3 the system (3.4) is ISS with respect to the set $\mathcal{W}$ for the input v. By Theorem 7 in Appendix A, we known that in this case all solutions in the system remain bounded since $|v| \leq \varepsilon$, and due to the asymptotic gain property (Appendix A) we have

$$\limsup_{t \to +\infty} |z(t)|_{\mathcal{W}} \leq \eta(\varepsilon)$$

for some $\eta \in \mathcal{K}$. If the value of ϵ has been selected sufficiently small, then the set $\mathcal{A} = \{z \in \mathbb{R}^2 : |z|_{\mathcal{W}} \leq \eta(\varepsilon)\}$ is a union of separated sets $\mathcal{A}_i^1$ and $\mathcal{A}_i^2$ contained only one equilibrium point $z_0^{i,1}$ and $z_0^{i,2}$ respectively, and a neighborhood $\mathcal{A}_0$ of the origin, *i.e.* $\mathcal{A} = \mathcal{A}_0 \cup \bigcup_{i=1}^N (\mathcal{A}_i^1 \cup \mathcal{A}_i^2)$. In $\mathcal{A}_0$ the system is converging to the origin. Assume that $|z(t)|_{\mathcal{W}} \in \mathcal{A}_i^1$ or $|z(t)|_{\mathcal{W}} \in \mathcal{A}_i^2$ for some $1 \leq i \leq N$, then for $|\nabla_z U(z)| \leq \epsilon$ and $|z| > \upsilon$ the input v is always acting from $z_0^{i,1}, z_0^{i,2}$ by construction, then U is strictly decreasing. Indeed, for all cases $\nabla_z U_a(z)$ is proportional to z, then $v^T \nabla_z U_a(z) = 0$ for all $z \in \mathbb{R}^2$. Next,

$$\nabla_z U_r(z) = 4\alpha(z - \zeta_i)(d_i^2 - |z - \zeta_i|^2) \text{for } z \in \mathcal{D}_i,$$

then $v^T \nabla_z U_r(z) = -4\alpha(d_i^2 - |z - \zeta_i|^2) v^T \zeta_i$ where $4\alpha(d_i^2 - |z - \zeta_i|^2) \geq 0$ for $z \in \mathcal{D}_i$. Due to selection of ρ we have $v^T \zeta_i > 0$, then

$$\dot{U} = -|\nabla_z U(z)|^2 + v^T \nabla_z U(z)$$

with $v^T \nabla_z U(z) \leq 0$ for all $|\nabla_z U(z)| \leq \epsilon$ and $z \in \mathcal{D}_i$. Therefore, U is not increasing. Note that $v^T \nabla_z U(z) = 0$ only if $d_i^2 = |z - \zeta_i|^2$, *i.e.* z belongs to the border of $\mathcal{D}_i$. By selection ϵ (and ε) sufficiently small it is possible to ensure that intersections of $\mathcal{A}_i^1$ and $\mathcal{A}_i^2$ with the set where $|\nabla_z U(z)| \leq \epsilon$ belongs to the interior of $\mathcal{D}_i$, then $v^T \nabla_z U(z) < 0$ always for all $|\nabla_z U(z)| \leq \epsilon$ and $|z| > \upsilon$, thus U is strictly decreasing to zero. In addition, from (3.4):

$$|\dot{z}|^2 = (v - \nabla_z U(z))^T (v - \nabla_z U(z)) = |\nabla_z U(z)|^2 - 2v^T \nabla_z U(z) + |v|^2$$

and for $|\nabla_z U(z)| \leq \epsilon$ and $|z| > \upsilon$ we have

$$|\dot{z}|^2 \geq -2\varepsilon\epsilon + \varepsilon^2 > 0,$$

then there is no new equilibrium point induced by v (as can be seen also in Fig. 3.2). □

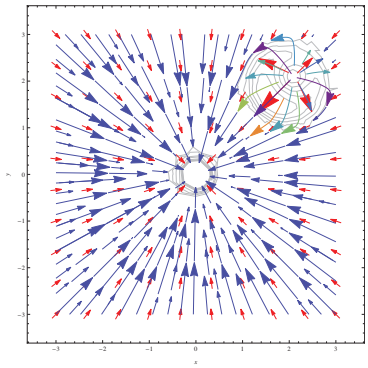

Figure 3.2: Gradient Lines in the case of a single obstacle with $\nu = 0.3$, $\Psi = 0.5$, $\zeta_1 = (2, 2)$, $d_1 = 0.8$,$\alpha = 4$ and $\epsilon = 0.1$

3.1.5 More complex situations

Of course in reality the assumption about separation between obstacles may be not satisfied, but even for this case the approach can be easily extended. Application of perturbation v with the amplitude ε do not destroy boundedness of the system trajectories by ISS property. If ε has been selected sufficiently small, then asymptotically $z(t)$ enters $\mathcal{A}$, as it has been defined above, whose separated subsets contain a single isolated extreme point of U. The function $|\nabla_z U(z)|$ is C^1 by construction, then $\nabla_z |\nabla_z U(z)|$ can be calculated and locally v can be selected proportional to $\nabla_z |\nabla_z U(z)|$ in order to maximize $|\nabla_z U(z)|$, which is equivalent of the extreme point avoidance. In the simple case presented above the calculation of $\nabla_z |\nabla_z U(z)|$ may be avoided.

3.1.6 Results of simulation

For $v = 0.1$, $\Upsilon = 0.5$, $\alpha = 2$, $N = 1$ and $(x_1, y_1) = (2, 2)$ with $d_1 = 1$, the results of the system (3.4) simulation for different initial conditions with $v = 0$ are shown in Fig. 3.3a. The results of the system (3.4) simulation with (3.7) and (3.8) are shown in Fig 3.3b (the difference between the controls (3.7) and (3.8) is not visible in this scale). As we can conclude, for $v = 0$ the potential field method sticks in the local extreme for some initial conditions, while with the proposed modifications (3.7) or (3.8) the origin is attractive under provided restrictions.

3.2 WMR obstacle avoidance

Consider a wheeled mobile robot whose kinematic model is perturbed like in 2.1, following the same considerations about such a kind of perturbations:

$$\begin{aligned} \dot{q}_x &= \cos(q_\theta) u(1 + \delta_1), \\ \dot{q}_y &= \sin(\theta) u(1 + \delta_1), \\ \dot{q}_\theta &= \omega(1 + \delta_2), \end{aligned} \tag{3.9}$$

where $(q_x, q_y) \in \mathcal{M}$ is the robot position and $\mathcal{M} \subset \mathbb{R}^2$ is a compact set containing the origin, $q_\theta \in (-\pi, \pi]$ is the robot orientation, $|u| \leq u_{\max}$ and $|\omega| \leq \omega_{\max}$ are linear

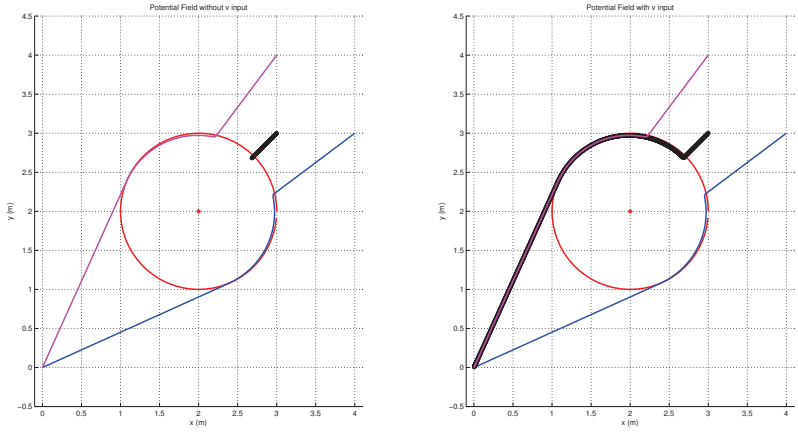

Figure 3.3: The results of the system (3.4) simulation

and angular velocities of the robot respectively ($u_{\max}$ and $\omega_{\max}$ are given bounds), $\delta_k \in [\delta_{\min}, \delta_{\max}]$, $k = 1, 2$ are exogenous bounded disturbances [53], $-1 < \delta_{\min} < \delta_{\max} < +\infty$.

The easiest way to apply the strategy to an unicycle-like WMR would be to linearize the system [128] considering the dynamics of a point Ψ on the x axis of the robot reference frame (Fig. 3.4) and apply the control (3.3) to it. In particular the point $\Psi = (\Psi_x, \Psi_y)^T = (q_x + \psi \cos q_\theta \, , \, q_y + \psi \sin q_\theta)^T$, with ψ the distance between the robot center and Ψ, has the following dynamics:

$$\begin{bmatrix} \dot{\Psi}_x \\ \dot{\Psi}_y \end{bmatrix} = R \begin{bmatrix} u(1+\delta_1) \\ \omega(1+\delta_2) \end{bmatrix} \, , \; R = \begin{bmatrix} \cos q_\theta & -\psi sin q_\theta \\ \sin q_\theta & \psi \cos q_\theta \end{bmatrix}. \tag{3.10}$$

The expression (3.10) can be rewritten as

$$\begin{bmatrix} \dot{\Psi}_x \\ \dot{\Psi}_y \end{bmatrix} = R \begin{bmatrix} u \\ \omega \end{bmatrix} + R \begin{bmatrix} u\delta_1 \\ \omega\delta_2 \end{bmatrix}. \tag{3.11}$$

Let us consider $R \begin{bmatrix} u \\ \omega \end{bmatrix} = \begin{bmatrix} u_x \\ u_y \end{bmatrix}$ of (3.3) and (3.8), the following theorem will apply:

Theorem 4. *Let Assumption 1 to be satisfied. The system (3.11) with control (3.3) and (3.8), where $\varepsilon > 2$, $\epsilon > 0$ sufficiently small, has the origin globally attractive, provided that $||\delta|| < \max\left\{\psi, \psi^{-1}\right\}$.*

Proof. Let us consider that $\left| R \begin{bmatrix} u\delta_1 \\ \omega\delta_2 \end{bmatrix} \right| \leq |d| \, |R| \left| \begin{bmatrix} u \\ \omega \end{bmatrix} \right|$. Being $\begin{bmatrix} u_x \\ u_y \end{bmatrix} = -\nabla_\Psi U(\Psi) +$ $v = R \begin{bmatrix} u \\ \omega \end{bmatrix}$, and considering $V = U(\Psi)$ as a Lyapunov function, with $U(\Psi)$ defined as (3.2), then:

$$\begin{aligned} \dot{V} &= \nabla_\Psi U(\Psi) \left(-\nabla_\Psi U(\Psi) + v + R \begin{bmatrix} u\delta_1 \\ \omega\delta_2 \end{bmatrix} \right) \\ &\leq -|\nabla_\Psi U(\Psi)|^2 + |\nabla_\Psi U(\Psi)| \, v + |R| \left|R^{-1}\right| |d| \, |\nabla_\Psi U(\Psi)|^2 \\ &\leq \left(|R| \left|R^{-1}\right| |d| - 1 \right) |\nabla_\Psi U(\Psi)|^2 + |\nabla_\Psi U(\Psi)| \, v \end{aligned}$$

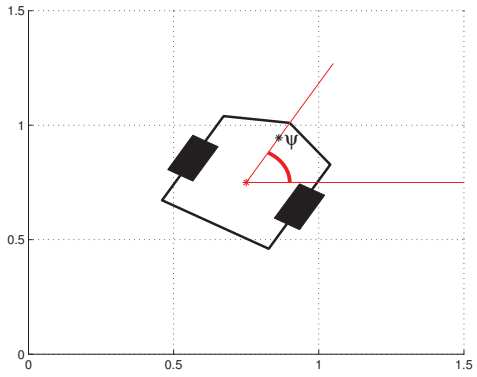

Figure 3.4: Position of the Ψ point.

it follows that if $|R|\left|R^{-1}\right||\delta| < 1$ the stability is proven using the results of Lemma 3 and Theorem 3. □

The value $|R|\left|R^{-1}\right||\delta|$ can be rewritten as $\max\left(\psi, \psi^{-1}\right)|\delta|$, it means that selecting ψ carefully the condition is always verified.

Such a technique is easy and effective as can be seen in Fig. 3.5 (blue path), but it doesn't allow the direct control on the WMR orientation and on the positivity of the linear velocity, resulting for instance in backward maneuvers (this happens when the initial conditions are not ideal, like the WMR non facing the target point). We would like to avoid this kind of movements for practical reasons.

For this purpose, to control both linear velocity and orientation of the WMR the trajectory generated by (3.4), (3.8) (or with (3.7)) can be used as a reference for (3.9), defining $\theta_d = \text{arctan2}\left(\nabla_y U(z), \nabla_x U(z)\right)$ and $\gamma = \theta_d - q$:

$$\begin{aligned} u &= \frac{u_{\max}}{1+\varepsilon}\sqrt{u_x^2 + u_y^2}, \\ \omega &= \left(\omega_{\max}\sqrt{|\gamma|} + \overline{k}\right)\text{sign}(\gamma). \end{aligned} \tag{3.12}$$

Theorem 5. *Let Assumption 4 hold. The control (3.12) stabilizes the $\gamma(t)$ variable in finite-time orienting the robot as the gradient $\nabla_z U(z)$ of the field , it follows that the system (3.9) with control (3.12) has the origin globally attractive.*

Proof. Let us consider the variable $\gamma(t)$, and consider the Lyapunov function $V = \frac{1}{2}\gamma^2$, then:

$$\dot{V} = \gamma\left[\dot{\gamma} - \omega\left(1 + \delta_2\right)\right].$$

As specified in section 3.1, the $U(z)$ field is a C^1 function therefore the derivative of $\gamma(t)$ exists, is continuous and bounded because of the construction of the field $U(z)$. Such a derivative is bounded, then it is possible to find a

$$\overline{k} \geq \left(\frac{d}{dt}\left(\text{arctan2}\left(\nabla_y U(z), \nabla_x U(z)\right)\right)\right) / \left(1 - \delta_{min}\right)$$

to have $\dot{V} \leq 0$. Since, of consequence, $\exists\ T \geq t_0$ time in which the robot orientation is aligned with one of the gradient lines, under Assumption 4 and Theorems 2 and 3, the controller u in (3.12) asymptotically stabilizes the WMR. □

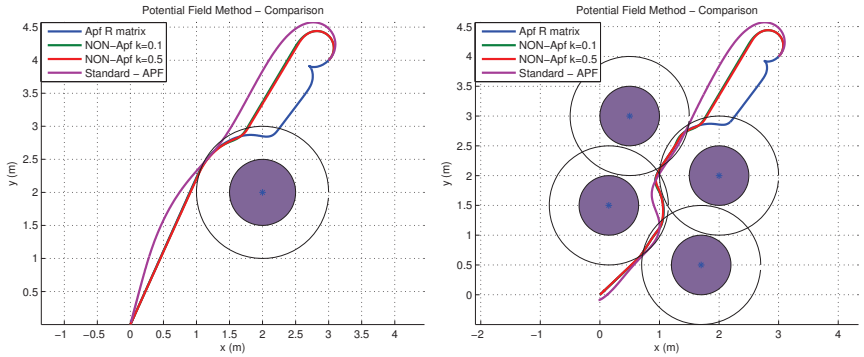

(a) Single obstacle (b) Several obstacles

Figure 3.5: The result of simulations for the three different modifications of the PF method.

3.2.1 Simulations

The results of simulation for the system (3.11) with control (3.3) and (3.8) and for the system (3.9), (3.12) are shown in Fig. 3.5. The bounds for the inputs are $u_{\max} = 1$ and $\omega_{\max} = 3$. Two cases are presented: single obstacle (Fig.3.5(a)) and multiple obstacles (Fig. 3.5(b)). In both parts of Fig. 3.5 the obstacle is the zone filled in violet, while the distance of influence is the black circle around the obstacle itself. The proposed methods are called *Apf-R matrix* and *NON-Apf*, the latter to emphasize the *non* asymptotic (finite time) behavior of the controller acting on the orientation of the WMR. Moreover the proposed modifications have been compared with the standard APF [121].

In both figures of Fig. 3.5 the comparison with the standard APF has been made for 2 values of $\bar{k}$, when using the *NON-Apf* control, to show how it affects the control inputs and the overall performances.

The unwanted behavior of the controller *Apf-R* matrix method discussed in the previous section is visible both in Fig. 3.5 and Fig. 3.7; the path followed by the WMR (Fig. 3.5) using this method clearly shows a backward maneuver, as it is confirmed from Fig. 3.7, where it is shown the negative linear velocity input.

Fig. 3.6 shows the orientation of the robot q_θ with respect to the direction of the field θ_d, the desired angle, as the $\bar{k}$ gain changes (not controlling the orientation of the WMR the *Apf-R matrix* method has been omitted from the plot). The second column of Fig. 3.6 shows how the controlled variable γ evolves. As it can be gathered from the plots, as the value of $\bar{k}$ increases the WMR reacts faster to the change of direction of the field due to the obstacles presence, decreasing also the instantaneous value of the γ error variable. Nevertheless, these improvements come with a drawback, increasing $\bar{k}$ (see $\bar{k} = 0.5$, Fig. 3.6 and Fig.3.7) could cause a bit of chattering around the stabilization point due to the increased control effort as it can be noticed also in Fig. 3.7.

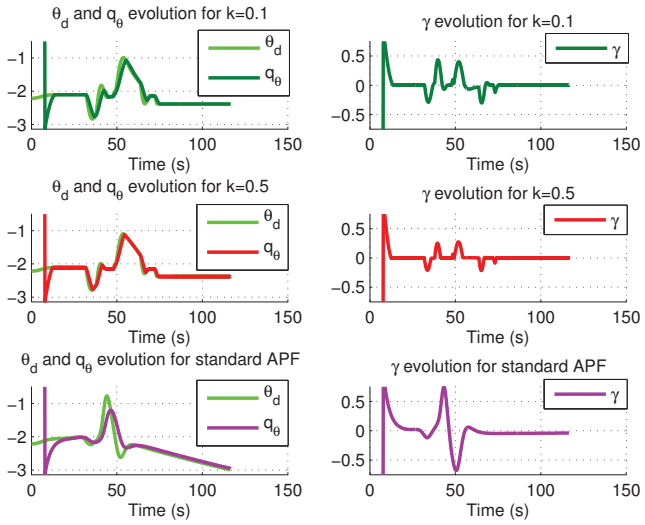

Figure 3.6: Evolution of the WMR orientation q_θ and desired angle θ_d and respective error variable dynamic γ

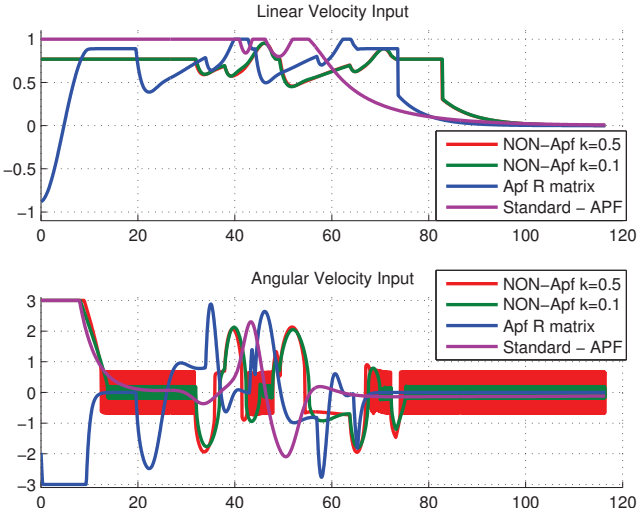

Figure 3.7: Input Signals for the different methods

3.2.2 More complex scenarios

Several simulations were run also for more complex scenarios, in which the features of the equipped sensor for the implementation are taken into account. In the case the real WMR has a LIDAR laser ranger finder. In Fig. 3.8(b) is shown the path followed by the WMR using the proposed modification of the potential field, while in Fig. 3.8(a) the strategy to decide which is the "point" to use as reference for the obstacle. Basically, the chosen point ζ, green star in Fig. 3.8(a), is the averaging on the x and y coordinates of the LIDAR sensed points in a predefined range; the radius is the distance among ζ itself and the farthest sensed point of the scan, which leads to the definition of the influence distance d that is the radius augmented of the diameter of the robot.

3.2.3 Implementation

The presented strategy has been implemented on a Turtlebot2 (http://www.turtlebot.com/) mobile robot. The WMR was equipped with a Hokuyo® (http://www.hokuyo-aut.jp) UTM-30LX LIDAR device. The necessary libraries to communicate with the WMR were found on Robotic Operating System (ROS), "Groovy" release (www.ros.org). The same strategy used in Section 3.2.2 to simulate the LIDAR based obstacle detection algorithm has been implemented to get obstacles positions $\zeta_i = (x_i, y_i)$ in real time. The WMR showed an excellent behavior avoiding obstacles without any previous knowledge of the environment, nevertheless some oscillations have been noticed while moving in narrow corridors. The trajectories followed in an office-kind environment are shown in Fig.3.9(a), the WMR objective is to reach the origin of the global frame in the lower-right corner, a plot of the trajectories in the Cartesian plane is given in Fig. 3.9(b) while Fig. 3.10 shows the evolution of the q_x and q_y through the origin. As it can be seen the robot avoids the obstacles and passes trought a narrow passage ($80cm$) to finally arrive to its destination (it is useful to remark that the robot has no knowledge of the obstacles a priori).

3.3 Conclusions

This chapter presented a novel formulation of the PF method in which the field is continuous everywhere and the ISS property of the system guarantees the global attractiveness of the origin avoiding local minima. It has been formally shown how the introduction of a small perturbation v as input does not introduce new equilibriums for the system; the goal remains the only attractive point.

To make a unicycle-like WMR to follow the reference created by the two variable integrator two strategies have been proposed: the first strategy linearises the output to directly apply the results synthesized for the particle case, without having the capability to control the orientation of the robot. A second strategy is, thus, presented which uses the particle case results as a base to design a control. The control steers the robot in the direction of the field lines in finite time to achieve the task. Both formulations are presented in simulations for a unicycle-like WMR, showing nice behaviours avoiding standing alone and multiple obstacles and in complex environments. Real experiments with a Turtlebot II platform in an office environment gave nice results, with some issues noticed in presence of narrow passages and target excessively close to an obstacle which did not prevent to reach the goal.

In the next future the intention is to improve the method to cancel any oscillations,

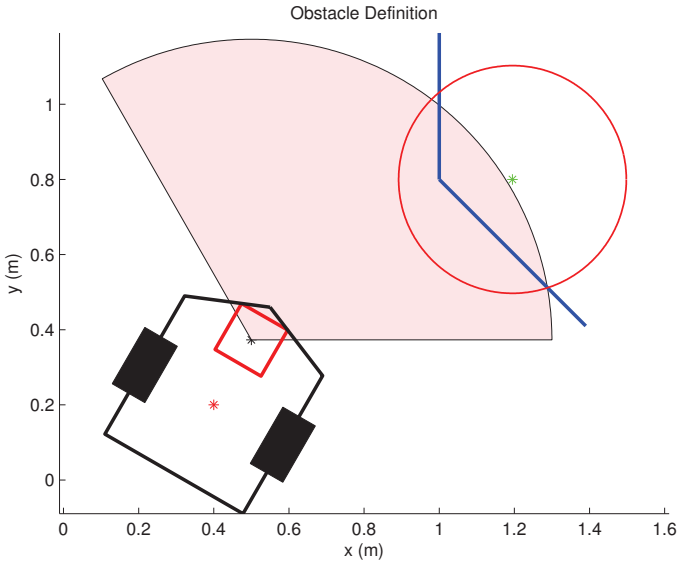

(a) WMR equipped with a LIDAR laser range finder: obstacle definition

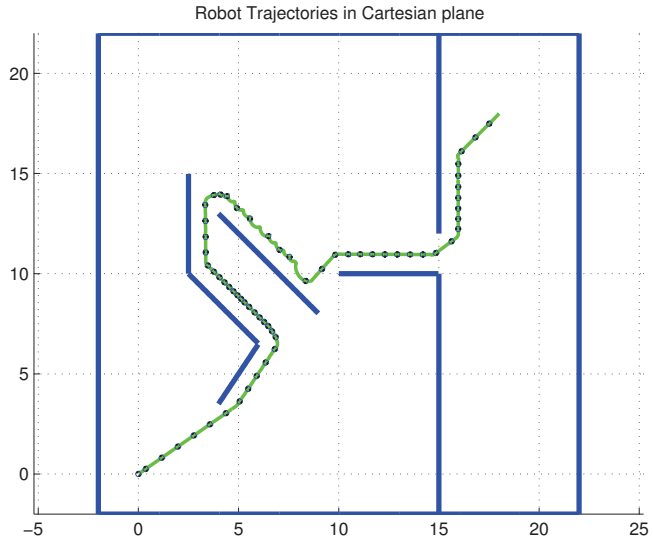

(b) The path followed by the WMR in a complex scenario

Figure 3.8: Results on complex environment

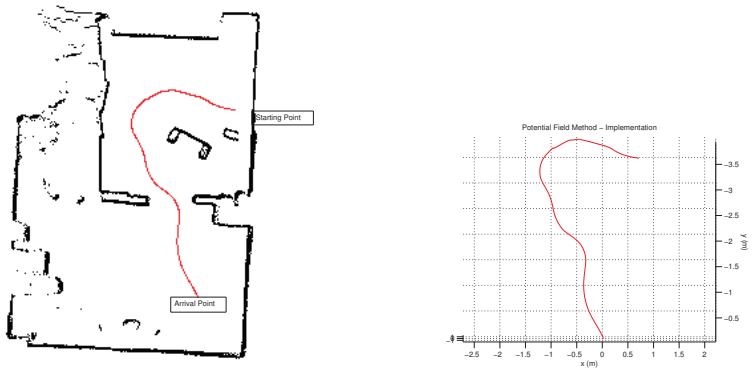

(a) Trajectories in the map

(b) Trajectories in Cartesian plane

Figure 3.9: The trajectories followed by the WMR in a real environment

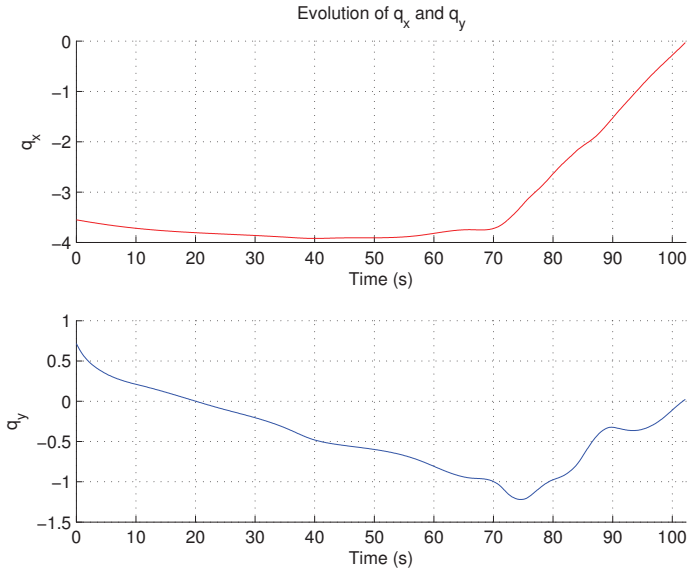

Figure 3.10: Evolution of the q_x and q_y variables.

to augment the dimension to the 3D case and to extend it to be used in the case of multi-agent systems.

Chapter 4

Leader-Follower Formation using Supervisory Control

Chapter 1, along with the modelling and the navigation problem, treated the most common formation strategies for mobile robots since multi-agent systems have been deeply treated in the last decade with different approaches [91]. This chapter deals with the Leader-Follower formation problem, where the leader, either physical or virtual [30],[47], [49], [80], is the most advanced agent in the formation and it has the role to lead the formation and acts as reference for all other robots which follow it according to a predefined rule.

The aim of this chapter is to present an original leader-follower approach for a group of wheeled mobile robots (WMRs). The goal is to move the leader and the followers to a destination point without sharing the leader velocity, and being able to avoid collision between the agents and external obstacles. Despite the classical $l-l$ and $l-\phi$ schemes ([49]), where an angle and one or more distances were given to the agents to achieve the formation and avoid collisions, in the proposed solution just a desired distance to the leader is given to each agent, which means that the leader does not represent the most advanced robot of the formation but more a reference to follow.

To reach such a goal the solution makes use of the output stabilization and the supervisory control frameworks taking into account the notions of stability for switched systems [93] and output-to-state stability property definition [134]: each agent, except for the leader, switches between three controllers which regulate *two* different outputs proportional to the distance to the leader and the distance between robots/obstacles respectively; a specifically designed supervisor similar to the one proposed in Chapter 2 (in its turn, inspired by [35]) orchestrates the switches.

The first controller is in charge of achieving the *rendezvous*[1] with the leader, *i.e.* the agent has to approach the leader. The second one, called the *following* control, assures the follower to maintain the heading and the velocity of the leader (which, as it has been specified, is not shared on the network but it is obtained using a homogeneous differentiator [115]). The third controller regulates a second output designed to *avoid collisions* between agents and obstacles.

As for the previous chapters the synthesis of the controllers is carried out to be robust with respect to additive input disturbances. The supervisor oversees the switches

[1] From the French expresison *rendez-vous*, that means appointment

between the three controls.

In the following two approaches are presented: in the former one, the leader acts just as a reference to follow, it is completely autonomous and it is not aware of the status of the other members of the formation. This approach is showed to be efficient via simulation and some conjectures. The latter sees the leader participating to the manoeuvre actively, waiting in case one or more agents to be involved in the collision avoidance manoeuvre; this modification to the problem allowed a formal verification of the method via the control theory tools.

4.1 Leader Follower - Autonomous Leader

Let us consider a group of $N \in \mathbb{R}_+$ unicycle WMRs, in which the input is affected by additive disturbances (each robot has the same model presented in the two previous chapters):

$$\begin{aligned} \dot{q}_{x,i} &= \cos(q_{\theta,i})(1+d_{1,i})v_i\,, \\ \dot{q}_{y,i} &= \sin(q_{\theta,i})(1+d_{1,i})v_i\,, \\ \dot{q}_{\theta,i} &= (1+d_{2,i})\omega_i\,, \end{aligned} \tag{4.1}$$

where $(q_{x,i}, q_{y,i}) \in \mathbb{R}^2$ define the Cartesian position of each robot, and $q_{\theta,i} \in [0, 2\pi)$ is the orientation of the robots with respect to the world reference frame, v_i and ω_i are the control inputs (the linear velocity and the angular velocity respectively). The additive disturbances on the inputs are unknown, but supposed to be bounded as: $-1 < d_{min} \leq d_{k,i} \leq d_{max}$, $k = 1, 2$, $i = 1, \ldots, N$. The aim is to design control laws providing the rendezvous and leader-following (the robots must create a formation around the leader) with collision/obstacle avoidance capability for the specified group of unicycle WMRs. The proposed solution uses a supervisor which articulates the activation of three controls (designed below) depending on the needs. To achieve all the tasks just information about the leader state and other follower positions are used, this forces the use of a derivative estimator to retrieve the information about leader linear and angular velocity. The communication topology considered is fixed, it means it does not change during the mission. In order to define rendezvous, leader-following and obstacle avoidance goals, two outputs to regulate are defined using the accessible information:

$$z_{1i} = \sqrt{(q_{x,L} - q_{x,i})^2 + (q_{y,L} - q_{y,i})^2}, \tag{4.2}$$

$$z_{2i} = \max\left\{0, \frac{1+\Lambda_i}{1+d_{ci}} - 1\right\},\ \Lambda_i > 0, \tag{4.3}$$

where z_{1i} being the distance from the leader (i.e. $(q_{x,L}, q_{y,L})$ is the leader Cartesian position), and z_{2i} is an output function of the distance $d_{ci} = \sqrt{(x_c - q_{x,i})^2 + (y_c - q_{y,i})^2}$ from a point with the coordinates (x_c, y_c) (defined in Section 4.2.1, and dependent on other robot positions). The first output z_{1i} is used to manage the switch between the rendezvous and following controllers, while the second output z_{2i} is the one designed to tackle the collision/obstacle avoidance part and design the dedicated controller. To proceed, several assumptions must be introduced. Firstly the maximum leader velocity must be smaller than the maximum followers velocities, i.e. $\omega_{L,max} \leq \omega_{i,max}$ and $v_{L,max} \leq v_{i,max}$, where the suffix *max* defines the maximum velocity. Then each follower enters the *following* mode when it reaches a distance δ_i from the leader, which

can be different for different robots and bounded: $\delta_{min} < \delta_i < \delta_{max}$, where δ_{min} is tied to the collision avoidance minimum distance and δ_{max} is proportional to the number N of robots. There is a safe distance around each robot λ_i, which ensures absence of collisions. We will also assume that the linear velocity of the leader v_L is nonnegative (i.e. it is moving forward).

Theoretical Problem Formulation

The problem can be generalized as follows. Consider $N \in \mathbb{R}_+$ dynamical systems

$$\dot{q_i} = f(q_i, u_i, d_i),\ z_{1i} = h_1(q_i),\ z_{2i} = h_{2i}(q_i), \tag{4.4}$$

where $q_i \in \mathbb{R}^n$ is the state, $q = [q_1^T, \ldots, q_N^T]^T$, $u_i \in \mathbb{R}^m$ is the control input and $d_i \in \mathbb{R}^m$ is a disturbance, with $d_i \in \Omega = \{d_i \in \mathcal{L}_m^\infty : ||d_i|| \leq D\}$ for some $D \in \mathbb{R}_+$ ($\mathcal{L}_m^\infty$ denotes the set of essentially bounded functions $d_i : \mathbb{R}_+ \to \mathbb{R}^m$). We want to regulate the outputs $z_{1i} \in \mathbb{R}^{p_1}$ and $z_{2i} \in \mathbb{R}^{p_2}$ assuming that the functions f, h_1 and h_{2i} are continuous and locally Lipschitz. It is needed to design the controls $u_i : \mathbb{R}^n \to \mathbb{R}^m$ guaranteeing that both outputs z_{1i} and z_{2i} will be kept under certain thresholds: i.e. for all $1 \leq i \leq N$ and all initial conditions $q_{i0} \in \mathbb{R}^n$, $q_0 = [q_{10}^T, \ldots, q_{N0}^T]^T$, all $d_i \in \Omega$ and $t \geq t_0 \geq 0$:

$$|z_{1i}(t, q_0, d_i)| \leq \sigma_{1i}(\max(\Delta_i, |h_1(q_{0i})|)), \tag{4.5}$$

$$|z_{2i}(t, q_0, d_i)| \leq \sigma_{2i}(\max(\Upsilon_i, |h_{2i}(q_0)|)), \tag{4.6}$$

where the values of Δ_i and Υ_i are given (they are related with δ_i and λ_i), whereas σ_{ji}, $j = 1, 2$, are functions from the class $\mathcal{K}$ (continuous strictly increasing functions, $\sigma(0) = 0$). The first output, (4.5), must be smaller than $\sigma_{1i}(\Delta_i)$, in the case $|h_1(q_{0i})| > \Delta_i$ the trajectory should converge to a subset where $|h_1(q_i)| \leq \sigma_{1i}(\Delta_i)$. In the same way (4.6) must be smaller than $\sigma_{2i}(\Upsilon_i)$. In the case $|h_{2i}(q_0)| > \Upsilon_i$ the trajectory should converge to a subset where $|h_{2i}(q)| \leq \sigma_{2i}(\Upsilon_i)$. For the designed outputs, the restriction (4.5) implies that all robots should find their positions sufficiently close to the leader (on the distance $\sigma_{1i}(\Delta_i)$), and a safe distance should be preserved between the robots and obstacles ($\sigma_{2i}(\Upsilon_i)$).

4.1.1 The Supervisory Control

In this section , firstly, the *Supervisor* scheme is presented, then it is shown how to derive the controllers and how to prove their stability properties.

The Supervisor

To proceed the following sets have to be defined:

$$X_{\delta_i} = \{q_i \in \mathbb{R}^n : |h_1(q_i)| \leq \delta_i\},$$
$$X_{\Delta_i} = \{q_i \in \mathbb{R}^n : |h_1(q_i)| \leq \Delta_i\}$$

$$X_{\lambda_i} = \left\{j \in \{1, \ldots, N\} \setminus \{i\} : \sqrt{(q_{x,j} - q_{x,i})^2 + (q_{y,j} - q_{y,i})^2} \leq \lambda_i\right\} \cup$$
$$\left\{j \in \{1, \ldots, N_o\} : \sqrt{(q_{x,jo} - q_{x,i})^2 + (q_{y,jo} - q_{y,i})^2} \leq \lambda_i\right\}$$
$$X_{\Lambda i} = \left\{j \in \{1, \ldots, N\} \setminus \{i\} : \sqrt{(q_{x,j} - q_{x,i})^2 + (q_{y,j} - q_{y,i})^2} \leq \Lambda_i\right\} \cup$$
$$\left\{j \in \{1, \ldots, N_o\} : \sqrt{(q_{x,jo} - q_{x,i})^2 + (q_{y,jo} - q_{y,i})^2} \leq \Lambda_i\right\}$$

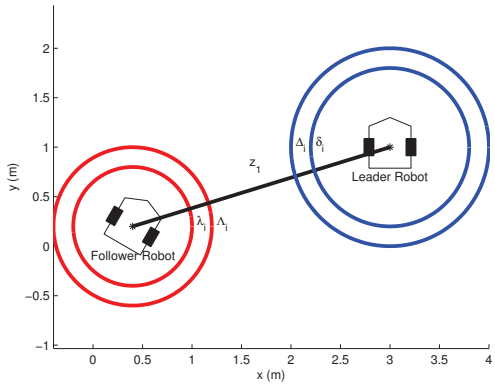

Figure 4.1: Graphical explanation of the presented sets

where N_o is the number of (static) obstacles with the coordinates $(q_{x,jo}, q_{y,jo})$ (the number N_o could be considered finite), $\{\lambda_i, \Lambda_i, \delta_i, \Delta_i\} \in \mathbb{R}^4_+$ are given values of parameter ($\lambda_i < \Lambda_i$ and $\delta_i < \Delta_i$), whose meaning will be explained below. Once defined those sets, one can describe the switching sequence: the controller U_{1i} (following) is activated when $q_i \notin X_{\lambda_i}$ and the distance from the leader is less than the threshold δ_i and it is kept active while the output $h_{1i}(q_i)$ remains less than Δ_i (this is a safety measure to avoid continuous switching between U_{1i} and U_{2i} controllers); the controller U_{2i} (rendezvousing) is active when $q_i \notin X_{\lambda_i}$ and the output $h_{1i}(q_i)$ is greater than δ_i. The third controller U_{3i} (collision/obstacle avoiding) becomes active as soon as $q_i \in X_{\lambda_i}$ and it is kept active until $q_i \notin X_{\Lambda_i}$; also in this case a hysteresis is added to avoid continuous switching, or chattering, between the controllers [93]. Therefore, the supervisory control law u_i for all $i = 1, \dots N$ can be summarized as follows

$$u_i(t) = U_{p_i(t)i}(q(t)),\ p_i : \mathbb{R}_+ \to \{1, 2, 3\} \tag{4.7}$$

with the initial conditions

$$t_0 = 0,\ p_i(t_0) = \begin{cases} 1 & \text{if } q_i(t_0) \in X_{\delta_i} \text{and } q(t_0) \notin X_{\lambda_i}, \\ 2 & \text{if } q_i(t_0) \notin X_{\delta_i} \text{and } q(t_0) \notin X_{\lambda_i}, \\ 3 & \text{if } q_i(t_0) \in X_{\lambda_i}, \end{cases}$$

and $p_i(t) = p_i(t_j)$ for $t \in [t_j\ t_{j+1})$, where

$$p_i(t_{j+1}) = \begin{cases} 1 & \text{if } q_i(t_{j+1}) \in X_{\delta_i} \text{and } q(t_{j+1}) \notin X_{\lambda_i} \\ 2 & \text{if } q_i(t_{j+1}) \notin X_{\delta_i} \text{and } q(t_{j+1}) \notin X_{\lambda_i} \\ 3 & \text{if } q_i(t_{j+1}) \in X_{\lambda_i} \end{cases}, \tag{4.8}$$

with t_j is the generic switching instant defined as follows:

$$t_{j+1} = \arg\ \inf_{t \geq t_j} \begin{cases} q(t) \in X_{\lambda_i} & \text{if } p_i(t_j) \in \{1, 2\}, \\ q(t) \notin X_{\Lambda_i} \text{ and } q_i(t) \in X_{\delta_i} & \text{if } p_i(t_j) \in \{2, 3\}, \\ q(t) \notin X_{\Lambda_i} \text{ and } q_i(t) \notin X_{\delta_i} & \text{if } p_i(t_j) \in \{3\}, \\ q(t) \notin X_{\Lambda_i} \text{ and } q_i(t) \notin X_{\Delta_i} & \text{if } p_i(t_j) \in \{1\}. \end{cases}$$

Now let us define the estimators and all U_{ki}, $k = 1, 2, 3$.

The Homogeneous Estimator

As specified in the introductive paragraph each follower can access just the position and the orientation of the leader robot; to gather information about the leader velocities v_L and ω_L, linear and angular, an observer is necessary. We will assume that the leader has the following dynamics:

$$\begin{aligned}\dot{q}_{x,L} &= \cos(q_{\theta,L})v_L\,,\\ \dot{q}_{y,L} &= \sin(q_{\theta,L})v_L\,,\\ \dot{q}_{\theta,L} &= \omega_L\,,\end{aligned}$$

where the terms v_L and ω_L may contain perturbations with respect to some reference controls, but for the cooperation objective we need to estimate not the reference controls applied to the leader, but its real inputs v_L and ω_L. If $\dot{q}_{x,L}$, $\dot{q}_{y,L}$ and $\dot{q}_{\theta,L}$ would be available for all followers, then

$$v_L = \sqrt{\dot{q}_{x,L}^2 + \dot{q}_{y,L}^2},\ \omega_L = \dot{q}_{\theta,L}.$$

Thus since $q_{x,L}$, $q_{y,L}$ and $q_{\theta,L}$ are only available, then the estimates of the derivatives of these variables have to be calculated. To estimate the derivatives the following homogeneous finite-time differentiator [115] has been adopted:

$$\begin{aligned}\dot{\xi}_1 &= -\alpha|e|^{0.75}\text{sign}(e) + \xi_2,\\ \dot{\xi}_2 &= -\beta|e|^{0.5}\text{sign}(e),\ \hat{f} = \xi_2,\\ e &= \xi_1 - f,\end{aligned}$$

where ξ_1, ξ_2 are the states of the differentiator, f is the measured signal to be differentiated (i.e $q_{x,L}$, $q_{y,L}$ or $q_{\theta,L}$), $\hat{\dot{f}} = \xi_2$ is the estimate of derivative we are looking for (i.e. $\hat{\dot{q}}_{x,L}$, $\hat{\dot{q}}_{y,L}$ and $\hat{\dot{q}}_{\theta,L}$). The use of this kind of observer helps also to filter the disturbances and to have a better estimation of both velocities. It has been proven in [115] that $\max\{|\eta_v|, |\eta_\omega|\} \leq \bar{\eta}$ where $\eta_v = v_L - \hat{v}_L$, $\eta_\omega = \omega_L - \hat{\omega}_L$ are the estimation errors and

$$\hat{v}_L = \sqrt{\hat{\dot{q}}_{x,L}^2 + \hat{\dot{q}}_{y,L}^2},\ \hat{\omega}_L = \hat{\dot{q}}_{\theta,L}.$$

Therefore, in all calculations below the estimates $\hat{v}_L$, $\hat{\omega}_L$ can be used assuming presence of bounded errors η_v and η_ω.

Following

The *Following* control U_{1i}= (v_i, ω_i) should be activated when a follower reaches the circle of radius δ_i around the leader, it forces the orientation of the *i*th robot to track the leader's one. Defining a deviation angle $\epsilon_f = q_{\theta,L} - q_{\theta,i}$, the dynamics of this error can be easily derived from the WMR model (4.1):

$$\dot{\epsilon}_f = \dot{q}_{\theta,L} - \dot{q}_{\theta,i} = \hat{\omega}_L + \eta_\omega - \omega_i(1 + d_{2i}). \tag{4.9}$$

Select a Lyapunov function $V_f = \frac{1}{2}\epsilon_f^2$ with

$$\dot{V}_f = \epsilon_f[\hat{\omega}_L + \eta_\omega - \omega_i(1 + d_{2i})],$$

then the following control can be proposed:

$$\omega_i = \frac{\hat{\omega}_L + [K_f|\epsilon_f| + \rho_f + \rho_0]\text{sign}(\epsilon_f)}{1 - d_{min}}, \tag{4.10}$$

where K_f and ρ_f are the design parameters,

$$\rho_0 = |\hat{\omega}_L|\frac{d_{max} - d_{min}}{1 - d_{min}} + \bar{\eta}.$$

Then:

$$\dot{V}_f \leq -2K_f V_f - \rho_f\sqrt{2V_f},$$

which yields the following upper estimate for ϵ_f:

$$|\epsilon_f(t)| \leq \begin{cases} \left(|\epsilon_0| + \frac{\rho_f}{K_f}\right) e^{K_f(t_0 - t)} - \frac{\rho_f}{K_f} & \text{if } t < t_0 + \bar{T}^f_{\epsilon_0}, \\ 0 & \text{if } t \geq t_0 + \bar{T}^f_{\epsilon_0}, \end{cases} \tag{4.11}$$

where t_0 is the instant in which the control is switched on and $\epsilon_0 = \epsilon_f(t_0)$ is the value of the angle error at t_0 with $\epsilon_0 \in [-\pi, \pi]$,

$$\bar{T}^f_{\epsilon_0} = -K_f^{-1} \ln \frac{\rho_f}{K_f|\epsilon_0| + \rho_f}.$$

Thus the control (4.10) stabilizes the orientation of the robot in a finite time, and this time has the upper bound

$$\bar{T}_f = \sup_{\epsilon_0 \in [-\pi, \pi]} \bar{T}^f_{\epsilon_0} = K_f^{-1} \ln \left[1 + \frac{K_f \pi}{\rho_f}\right].$$

The velocity part v_i of the *Following* control U_{1i} cannot be a simple estimation of the leader velocity $\hat{v}_L$ because of the disturbance d_{1i} acting on the follower. To explain the idea of the control used in this case, consider the Lyapunov function $W_f = z_{1i}$ with

$$\dot{W}_f = -(1 + d_{1i})v_i \cos(\alpha_i - q_{\theta,i}) + (\hat{v}_L + \eta_v)\cos(\alpha_i - q_{\theta,L}),$$

where $\alpha_i = \text{atan}\left(\frac{q_{y,L} - q_{y,i}}{q_{x,L} - q_{x,i}}\right)$ is the angle between the leader and the follower robots. For the sake of simplicity hereafter, denote $C_\alpha = \cos(\alpha_i - q_{\theta,L})$ and $S_\alpha = \sin(\alpha_i - q_{\theta,L})$, then:

$$\dot{W}_f = -(1 + d_{1i})v_i \left[C_\alpha \cos(\epsilon_f) - S_\alpha \sin(\epsilon_f)\right] + (\hat{v}_L + \eta_v)C_\alpha.$$

From (4.11) $\epsilon_f(t) = 0$ for all $t \geq t_0 + \bar{T}_f$, then

$$\dot{W}_f = -C_\alpha(1 + d_{1i})v_i + C_\alpha(\hat{v}_L + \eta_v)$$

that leads to the chosen linear velocity control:

$$v_i = \begin{cases} \zeta_i(z_{1i})\text{sign}\,(C_\alpha)\,\frac{\bar{\eta} + d_{max}\hat{v}_L}{1 - d_{min}} + \hat{v}_L & \text{if } \epsilon_f = 0, \\ 0 & \text{otherwise,} \end{cases}$$

where

$$\zeta_i(z_1) = \begin{cases} 0 & z_1 \leq \underline{\delta}_i \\ 1 & z_1 \geq \bar{\delta}_i \\ \frac{z_1 - \underline{\delta}_i}{\bar{\delta}_i - \underline{\delta}_i} & \underline{\delta}_i < z_1 < \bar{\delta}_i \end{cases}$$

with design parameters $\underline{\delta}_i, \overline{\delta}_i$ such that $\underline{\delta}_i < \delta_i \leq \overline{\delta}_i \leq \Delta_i$. Substitution of this control gives:

$$\dot{W}_f < 0 \quad \forall z_{1i} \geq \overline{\delta}_i$$

if $\epsilon_f = 0$. While the error ϵ_f goes to zero in the finite time $\bar{T}_f$, then the distance z_{1i} may increase/decrease its value by $v_{max}\bar{T}_f$. Therefore, since $z_{1i}(t_0) \leq \delta_i$, then the control assures the follower to stay in the zone

$$z_{1i}(t) \leq \delta_i + v_{max}\bar{T}_f \tag{4.12}$$

for all $t \geq t_0$. To prevent unnecessary switching to the rendezvousing control U_{2i} it is necessary to assume that $\delta_i + v_{max}\bar{T}_f \leq \Delta_i$. From another side, in order to avoid a collision with the leader we have to impose that $\delta_i - v_{max}\bar{T}_f > \lambda_i$.

The *Following* control can be summarized as follows:

$$U_{1i} = \begin{cases} v_i = \begin{cases} \zeta_i(z_{1i})\text{sign}\,(C_\alpha)\,\frac{\bar{\eta}+d_{max}\hat{v}_L}{1-d_{min}} + \hat{v}_L & \text{if } \epsilon_f = 0, \\ 0 & \text{otherwise,} \end{cases} \\ \omega_i = \frac{\hat{\omega}_L + [K_f|\epsilon_f| + \rho_f + \rho_0]\text{sign}(\epsilon_f)}{1-d_{min}}. \end{cases} \tag{4.13}$$

We have proven the following result.

Lemma 4. *The control (4.13) for the system (4.1) provides an uniform finite-time stabilization for the variable $\epsilon_f = \theta_L - \theta_i$ (with an upper estimate (4.10)) and boundedness of the output z_{1i} (4.12).*

In other words the control (4.13) ensures the resolution of the leader following problem in the absence of collisions with other robots and obstacles.

Rendezvous

The *Rendezvous* control, $U_{2i} = (v_i, \omega_i)$, assures the robot to approach the leader. Define a desired orientation angle as $\epsilon_{rdv} = \theta_i - \alpha_i$, where $\alpha_i = \text{atan}\left(\frac{q_{y,L}-q_{y,i}}{q_{x,L}-q_{x,i}}\right)$. Consider a Lyapunov function $W_{rdv} = z_{1i}$, whose derivative admits the estimate:

$$\dot{W}_{rdv} = C_\alpha(\hat{v}_L + \eta_v) - \cos(\epsilon_{rdv})v_i(1 + d_{1i}).$$

To preserve the semi-definitiveness of the function $\dot{W}_{rdv}$ the proposed control v_i has the form:

$$v_i = \begin{cases} \frac{\cos(\epsilon_{rdv})[C_\alpha(\hat{v}_L+\eta_v)+\rho_{rdv}]}{1-d_{min}} & \text{if } |\epsilon_{rdv}| \leq \kappa\frac{\pi}{2}, \\ 0 & \text{otherwise,} \end{cases} \tag{4.14}$$

where $0 < \kappa < 1$, $\rho_{rdv} > \frac{\hat{v}_L+\bar{\eta}}{\cos^2(\kappa\frac{\pi}{2})} + \rho_1$ and $\rho_1 > 0$ are design parameters. Substitution of (4.14) gives

$$\begin{aligned} \dot{W}_{rdv} &\leq (\hat{v}_L + \bar{\eta}) - \cos^2(\epsilon_{rdv})\rho_1\frac{1+d_{1i}}{1-d_{min}} \\ &\leq -\rho_1 \end{aligned}$$

for $|\epsilon_{rdv}| \leq \kappa\frac{\pi}{2}$. Then we define the Lyapunov function $V_{rdv} = \frac{1}{2}\epsilon_{rdv}^2$ and evaluate its derivative:

$$\dot{V}_{rdv} = \epsilon_{rdv}\left\{\omega_i + \frac{S_\alpha(\hat{v}_L + \eta_v) + \sin(\epsilon_{rdv})v_i[1 + d_{1i}]}{z_{1i}}\right\},$$

which leads to the following expression for ω_i:

$$\begin{aligned}\omega_i &= -\frac{S_\alpha \hat{v}_L + |S_\alpha|\bar{\eta} + \sin(\epsilon_{rdv})[1+d_{max}]v_i}{z_{1i}} \\ &\quad -\rho_{rdv}\text{sign}(\epsilon_{rdv}) - \left(K_{rdv} + \frac{[d_{max}-d_{min}]|v_i|}{z_{1i}}\right)\epsilon_{rdv},\end{aligned} \tag{4.15}$$

where $K_{rdv} > 0$ and $\rho_{rdv} \geq 0$ are design parameters. Applying this control, the Lyapunov function derivative $\dot{V}_{rdv}$ can be rewritten as follows:

$$\dot{V}_{rdv} \leq -2K_{rdv}V_{rdv} - \rho_{rdv}\sqrt{2V_{rdv}}.$$

Therefore, the proposed control stabilizes the variable ϵ_{rdv} heading the robot toward the leader in a finite time, and as for the previous controller the time of orientation can be evaluated referring to the ϵ_{rdv} variable dynamics. The estimation for ϵ_{rdv} is

$$|\epsilon_{rdv}(t)| \leq \begin{cases} \left(|\epsilon_0| + \frac{\rho_{rdv}}{K_{rdv}}\right)e^{K_{rdv}(t_0-t)} - \frac{\rho_{rdv}}{K_{rdv}} & \text{if } t < t_0 + \bar{T}^{rdv}_{\epsilon_0}, \\ 0 & \text{if } t \geq t_0 + \bar{T}^{rdv}_{\epsilon_0}, \end{cases} \tag{4.16}$$

where t_0 is the instant in which the control is switched on and $\epsilon_0 = \epsilon_{rdv}(t_0)$ is the value of the angle error at t_0 with $\epsilon_0 \in [-\pi, \pi]$,

$$\bar{T}^{rdv}_{\epsilon_0} = -K^{-1}_{rdv}\ln\frac{\rho_{rdv}}{K_{rdv}|\epsilon_0| + \rho_{rdv}}.$$

Thus the the upper bound of the orientation time is

$$\bar{T}_{rdv} = \sup_{\epsilon_0 \in [-\pi,\pi]} \bar{T}^{rdv}_{\epsilon_0} = K^{-1}_{rdv}\ln\left[1 + \frac{K_{rdv}\pi}{\rho_{rdv}}\right].$$

Then for any $0 < \kappa < 1$ and any initial orientation ϵ_0, the time of reaching the zone where $|\epsilon_{rdv}| \leq \kappa\frac{\pi}{2}$ is less than $\bar{T}_{rdv}$.

The controller can be resumed as:

$$U_{2i} = \begin{cases} v_i = \begin{cases} \frac{\cos(\epsilon_{rdv})[C_\alpha(\hat{v}_L+\eta_v)+\rho_{rdv}]}{1-d_{min}} & \text{if } |\epsilon_{rdv}| \leq \kappa\frac{\pi}{2}, \\ 0 & \text{otherwise,} \end{cases} \\ \omega_i = -\frac{S_\alpha\hat{v}_L + |S_\alpha|\bar{\eta} + \sin(\epsilon_{rdv})[1+d_{max}]v_i}{z_{1i}} \\ -\rho_{rdv}\text{sign}(\epsilon_{rdv}) - \left(K_{rdv} + \frac{[d_{max}-d_{min}]|v_i|}{z_{1i}}\right)\epsilon_{rdv}, \end{cases} \tag{4.17}$$

From the inequality $\dot{W}_{rdv} \leq -\rho_1$ obtained above for the case $|\epsilon_{rdv}| \leq \kappa\frac{\pi}{2}$ it follows that for $t \geq t_0 + \bar{T}_{rdv}$ the distance z_{1i} is uniformly decreasing to zero in a finite time. The distance z_{1i} may increase on the value $v_{max}\bar{T}_{rdv}$ during the orientation phase, and $z_{1i}(t_1) \leq z_{1i}(t_0) + v_{max}\bar{T}_{rdv}$ where the instant $t_1 \in [t_0, t_0 + \bar{T}_{rdv}]$ such that $|\epsilon_{rdv}(t_1)| \leq \kappa\frac{\pi}{2}$ for the first time, then:

$$z_{1i}(t) \leq \begin{cases} z_{1i}(t_0) + v_{max}\bar{T}_{rdv} & \text{if } t_0 \leq t \leq t_1, \\ z_{1i}(t_1) - \rho_1(t-t_1) & \text{if } t_1 \leq t \leq t_1 + T_1, \\ 0 & \text{if } t \geq t_1 + T_1, \end{cases} \tag{4.18}$$

$$T_1 = \frac{z_{1i}(t_1)}{\rho_1} \leq \frac{z_{1i}(t_0) + v_{max}\bar{T}_{rdv}}{\rho_1}.$$

In the rendezvous task the robot has to reach the distance δ_i from the leader. The necessary time to travel till this distance is

$$\bar{t}_{rdv} = \frac{z_{1i}(t_1) - \delta_i}{\rho_1} \leq \frac{z_{1i}(t_0) + v_{max}\bar{T}_{rdv} - \delta_i}{\rho_1}.$$

Considering the worst case scenario the time in which the control (4.17) will achieve his task would be $T_{rdv} = \bar{t}_{rdv} + \bar{T}_{rdv}$. Thus the following claim has been proven.

Lemma 5. *The control (4.17) provides for the system (4.1):*

1. *Uniform finite-time stability with respect to the variable ϵ_{rdv} (see (4.16));*

2. *Uniform boundedness and finite-time convergence with respect to the variable z_{1i} (see (4.18));*

3. *$\exists T_{rdv} = T_{rdv}(z_{1i}(t_0)) \in \mathbb{R}_+$ such that $z_{1i}(T_{rdv}) \leq \delta_i$.*

Thus the control (4.17) guarantees a solution of the rendezvous problem in the finite-time T_{rdv} in the absence of collisions/obstacles.

Collision/Obstacle Avoidance

The *Collision/Obstacle Avoidance* control becomes active when either the leader or other robots of the group (or an external obstacle, or all of them) enter the safety zone around a robot, which is specified by the circle of radius λ_i. This control is kept active until all the robots exit a bigger circle of radius Λ_i; the annulus delimited the two radii can be considered as a hysteresis to avoid Zeno/chattering phenomena. To achieve the task, an effective strategy has been designed. Firstly, each robot who finds itself in a collision avoidance condition, evaluates a point (x_c, y_c) as follows:

$$x_c = \frac{1}{M}\sum_{j=1}^{M} q_{x,j},\ y_c = \frac{1}{M}\sum_{j=1}^{M} q_{y,j},$$

where $(x_c, y_c) \in X_{\lambda_i}$ is the medium point among all robots/obstacles participating in the collision avoidance maneuver, with X_{λ_i}defined as in Section 4.1.1, $0 < M \leq N + N_o$ is the number of robots and obstacles. The point (x_c, y_c) represents the point from which the robot has to go away to exit the collision avoidance conditions. In order to maximize the distance d_{ci} from the point (x_c, y_c) for all participating robots, the following Lyapunov function is introduced

$$W_{ca}(x) = z_2 = \max\left\{0, \frac{1+\Lambda_i}{1+d_{ci}} - 1\right\}.$$

Let $\bar{\gamma}_i = \text{atan}\left(\frac{y_c - q_{y,i}}{x_c - q_{x,i}}\right)$ be the angle between the robot and the point (x_c, y_c). The derivative $\dot{W}_{ca} = 0$ if $d_{ci} > \Lambda_i$ (the avoiding is performed), and for $d_{ci} \leq \Lambda_i$ it has the form:

$$\dot{W}_{ca} = \frac{v_i \cos(q_{\theta,i} - \bar{\gamma}_i)\{1 + d_{1i}\} - \frac{1}{M}\sum_{j=1}^{M} v_j \cos(q_{\theta,j} - \bar{\gamma}_i)\{1 + d_{1j}\}}{(\Lambda + 1)^{-1}(1 + d_{ci})^2}. \tag{4.19}$$

Let us introduce the desired orientation that the robot has to reach to go away from the point (x_c, y_c). It is given by the angle $\gamma_i = q_{\theta,i} - (\bar{\gamma}_i + \pi)$, where π is the natural choice to get away from that point. Evaluating the derivative of the Lyapunov function $V_{ca} = \frac{1}{2}\gamma_i^2$:

$$\begin{aligned}\dot{V}_{ca} = \gamma_i\omega_i(1 + d_{2i}) - \tfrac{\gamma_i}{d_c} v_i(1 + d_{1i})\sin\gamma_i \\ -\tfrac{\gamma_i}{d_c M}\sum_{j=1}^{M} v_j \sin(q_{\theta,j} - \bar{\gamma}_i)(1 + d_{1j})\end{aligned}. \tag{4.20}$$

The proposed controller has the form:

$$U_{3i} = \begin{cases} v_i = \begin{cases} v_{max} & \text{if } |\gamma_i| \le k\pi, \\ 0 & \text{otherwise,} \end{cases} \\ \omega_i = \frac{-[\rho_{ca}+\rho_2]\text{sign}(\gamma_i)}{1-d_{min}} \end{cases}, \tag{4.21}$$

where $\rho_{ca} \ge \frac{v_{max}(1+d_{max})}{d_{ci}}$ and $\rho_2 > 0$. Substituting the control (4.21) in the equation (4.20) we obtain:

$$\dot{V}_{ca} \le -\rho_2\sqrt{2V_{ca}},$$

which gives us a finite time convergence on the variable $\gamma_i(t)$. This time can be evaluated from the estimation of $\gamma_i(t)$:

$$|\gamma_i(t)| \le |\gamma_0| - \rho_2(t - t_0), \tag{4.22}$$

where $\gamma_0 \in [-\pi, \pi]$ is the initial value of γ_i at the instant t_0 when the collision avoidance control has been switched on. Thus the time, when the condition $|\gamma_i| \le k\pi$ can be verified, is

$$t_{ca}^{\gamma_0} = \frac{\max\{0, |\gamma_0| - k\pi\}}{\rho_2},$$

and for the worst case scenario

$$t_{ca} = \sup_{\gamma_0 \in [-\pi,\pi]} t_{ca}^{\gamma_0} = \frac{(1-k)\pi}{\rho_2}.$$

Following this result and (4.21), the value of λ_i has to satisfy $\lambda_i > t_{ca}v_{max}$ (the maximal movement velocity for the point (x_c, y_c) is v_{max}). Denote $C_{k\pi} = \cos(k\pi)$, then (4.19) with the control (4.21) satisfies the estimate:

$$\dot{W}_{ca} \le v_{max}\frac{\Lambda+1}{(1+d_{ci})^2}[-\frac{M-1}{M}C_{k\pi}\{1-d_{min}\} + \frac{M-2}{M}\{1+d_{max}\}],$$

where the upper bound $M-2$ on the number of terms in the sum appears since one term leaves for $j = i$ and at least one (in the worst case) has a negative value of $\cos(q_{\theta,j} - \bar{\gamma}_i)$. If we can assure that the quantity in the square brackets is negative, then we can assure decreasing W_{ca}. It can be shown that there exist sufficiently small values d_{min}, d_{max} and k close to 1 such that this term is negative (it is easy to see that it is true for $d_{min} = d_{max} = 0$ and $C_{k\pi} > \frac{M-2}{M-1}$, next it will be true by continuity for sufficiently small values of d_{min}, d_{max} and some k). To conclude, z_{2i} may increase during the orientation phase t_{ca} (due to constraint $\lambda_i > t_{ca}v_{max}$ a collision is not possible), but next is decreasing to zero, thus this distance is bounded and there is a finite time $T_{ca} > 0$ such that $z_{2i}(t)$ becomes sufficiently small for $t \ge t_0 + T_{ca}$ and $q(t_0 + T_{ca}) \notin X_{\Lambda_i}$, thus the collision avoiding is finished.

Lemma 6. *The system (4.1) with the control (4.21) admits the properties:*
1. *Uniform finite-time stability with respect to the variable γ_i (see the estimate (4.22));*
2. *$\exists d_{min}, d_{max}$ and k such that the variable z_{2i} is bounded and there exists $T_{ca} > 0$ such that $q(t_0 + T_{ca}) \notin X_{\Lambda_i}$.*

A static obstacle is considered as a robot, which has zero linear and angular velocities.

Supervisory control

Summarizing the results obtained so far and using the results of [35, 53], the following statement can be obtained.

Conjecture 1. *The system (4.4) with the supervisor (4.8) and controls (4.28) is forward complete and for all* $q_0 \in \mathbb{R}^n$, $d \in \Omega$

$$|z_{1i}(t, q_{0i}, d_i)| \leq \max(\Delta_i, |h_1(q_{0i})|),$$
$$|z_{2i}(t, q_{0i}, d_i)| \leq \max(\Upsilon_i, |h_{2i}(q_{0i})|)$$

for $t \geq 0$, $\Upsilon_i = \frac{1+\Lambda_i}{1+\lambda_i - t_{ca} v_{max}} - 1$.

4.1.2 Simulations

In the simulations the number of WMRs is $N = 4$, with sampling time $t_s = 0.01$ $[sec]$; the maximum velocity for the leader is set to $v_{L,max} = 0.5$ while the maximum velocity for the followers is $v_{i,max} = 2$. The disturbances have form $d_i = \chi \sin(t) + 0.1 * rand$ where $rand$ is a pseudo-random values drawn from the standard uniform distribution on the open interval $(0, 1)$ with $i \in \{1, 2\}$ and $|\chi| \leq 0.5$. The *Following* controller has $\delta_i \in \{x \in \mathbb{R} : 0.7 < x < 0.9 + 0.1N\}$, $K_f = 5$ and $\rho_f = 0.01$; for the *rendezvous* control the values are: $\rho_1 = 2$, $\rho_{rdv} = 0.1$. For the *obstacle avoidance* $\rho_2 = 0.1$. Fig. 4.2 and Fig. 4.3 represent how the agents behave when the presented strategy is implemented. The leader follows a predefined path, while the followers are placed randomly with random orientation at $t = 0$. Indeed, each agent reaches the *Following* controller and the formation movement is accomplished. The distance of each robot from the leader is shown in Fig. 4.3 and the straight horizontal lines of the same colors represent the corresponding values of Δ_i while the black line represents the limit distance beyond which the collision/obstacle avoidance is activated. When the collision avoidance control is not active, the followers reach the *Following* mode and remain in it if no external perturbation are applied (as an obstacle could be). If necessary, at the end of the *collision avoidance* maneuver, they switch back to the *rendezvous* control to reach again the minimum distance, which is necessary to switch back in the *Following* mode. Thoroughly analyzing Fig. 4.3 though, it can be noticed that the activation of the collision avoidance controller not always forces the WMR to switch back to the *rendez-vouz* one once the maneuver is accomplished switching back directly to the *Following* one.

4.2 Leader-Follower: Active Leader

In this modification of the solution the leader as specified at the beginning of the chapter takes an active role to assure the maintenance of the formation. The group of $N \in \mathbb{R}_+$ unicycle WMRs, has the same model (4.1):

$$\dot{q}_{x,i} = \cos(q_{\theta,i})(1 + d_{1,i})v_i\,,$$
$$\dot{q}_{y,i} = \sin(q_{\theta,i})(1 + d_{1,i})v_i\,,$$
$$\dot{q}_{\theta,i} = (1 + d_{2,i})\omega_i\,,$$

Denote the state vector $X_i = [x_i, y_i, \theta_i]^T$ for a robot and the corresponding control vector $u_i = [v_i, \omega_i]$, then $X = [X_1^T, \ldots, X_N^T]^T$ is the state of the robot formation.

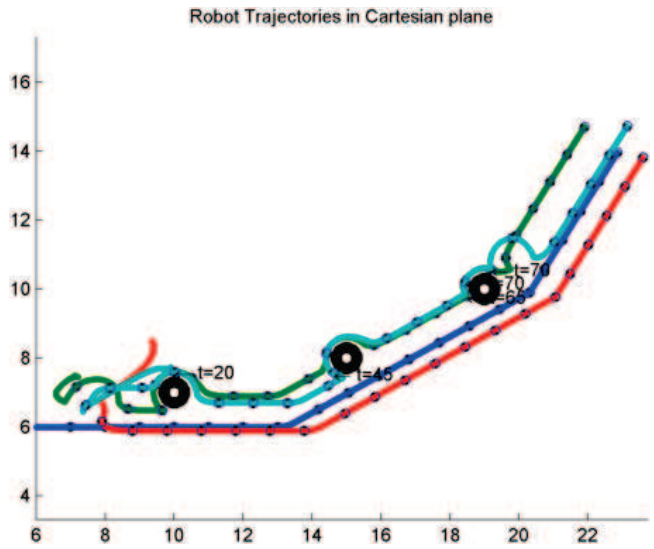

Figure 4.2: The path followed in an environment with obstacles, where the blue one is the leader WMR

Assuming the leader to have the following dynamics:

$$\begin{aligned} \dot{q}_{x,0} &= \cos(q_{\theta,0})v_0\,, \\ \dot{q}_{y,0} &= \sin(q_{\theta,0})v_0\,, \\ \dot{q}_{\theta,0} &= \omega_0\,, \end{aligned} \tag{4.23}$$

where the terms v_0 and ω_0 may contain perturbations with respect to some "reference" controls (like $d_{k,i}$, $k = 1, 2$ in (4.1)), but for this particular cooperative control we need to know the leader real inputs v_0 and ω_0 only. Denote $X_0 = [q_{x,0}, q_{y,0}, q_{\theta,0}]^T$ and $u_0 = [v_0, \omega_0]$.

Let N_o be the number of (static) obstacles with the coordinates $X_k^o = (x_{ko}, y_{ko})$ for $k = 1, 2, \ldots, N_o$. The number N_o could be considered finite. In addition, if we assume that all obstacles are sufficiently isolated, then the choice $N_o = 1$ is reasonable and simplifies the consideration without any loose of generality, denote $X^o = [(X_1^o)^T, \ldots, (X_N^o)^T]^T$.

As for the previous problem, it is wanted to realise a supervisor able to articulate the activation three different controls depending on the needs. The hypothesis of not knowing the leader velocities is maintained, of consequence just information about the leader state X_0 and other follower positions X_i are used, the coordinates X^o are also assumed available when necessary. Thus, it is not possible to access the robot controls u_i and u_0, which forces the use the homogeneous estimator [115] to retrieve the information about linear and angular velocities.

In this formulation of the problem the two outputs to regulate are redefined as

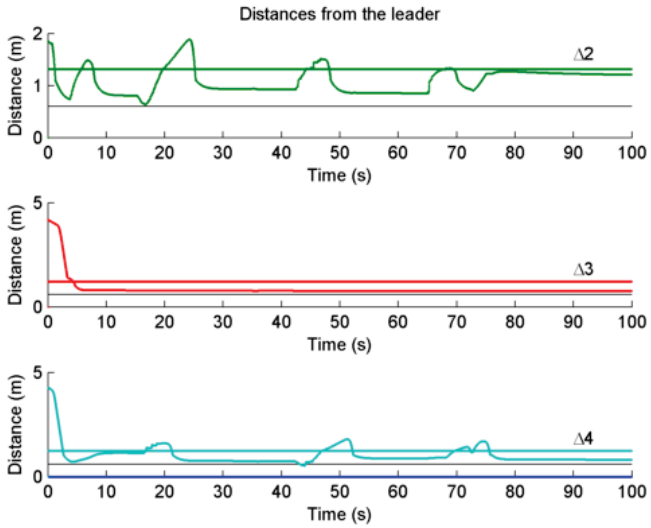

Figure 4.3: Distances of each agent from the leader and relative Δ_i values

follows using the accessible information:

$$z_{1i} = h_1(X_0, X_i) = \sqrt{(q_{x,0} - q_{x,i})^2 + (q_{y,0} - q_{y,i})^2}, \tag{4.24}$$

$$z_{2i} = h_{2i}(X_0, X, X^o) = \min\{\mathbb{D}_{ci}, \max\{z_{1i}^{-1}, \max_{1\leq j\neq i\leq N} \frac{1}{\sqrt{(q_{x,j} - q_{x,i})^2 + (q_{y,j} - q_{y,i})^2}}, \max_{1\leq k\leq N_o} \frac{1}{\sqrt{(x_{ko} - q_{x,i})^2 + (y_{ko} - q_{y,i})^2}}\}\}, \tag{4.25}$$

where z_{1i} being the distance from the leader, and z_{2i} is a function of the distances to other robots $(q_{x,j}, q_{y,j})$ and obstacles (x_{ko}, y_{ko}), $\mathbb{D}_{ci} > 0$ is a constant ensuring finiteness of z_{2i}. Again, the first output z_{1i} gives information about the collective motion manoeuvre, *i.e.* how to switch between the rendezvous and following controllers, while the second output z_{2i} is designed to tackle the collision/obstacle avoidance part and design the dedicated controller.

To proceed, several assumptions must be introduced dealing with technical restrictions. Firstly, as in the previous formulation the maximum leader velocity must be smaller than the maximum followers velocities, *i.e.* $\omega_{0,max} \leq \omega_{i,max} = \omega_{max}$ and $v_{0,max} \leq v_{i,max} = v_{max}$, where the suffix *max* define the maximum velocity. Secondly, we will assume the the linear velocity of the leader v_0 is non-negative (*i.e.* it is moving in forward direction only).

Theoretical Formulation

It is needed to design the controls $u_i : \mathbb{R}^n \to \mathbb{R}^m$ guaranteeing that both outputs z_{1i} and z_{2i} will be kept under certain thresholds: for all $1 \leq i \leq N$ and all initial conditions $X_{i0} \in \mathcal{X} = \mathbb{R}^2 \times [0, 2\pi)$ (denote $\mathbb{X}_0 = [X_{10}^T, \ldots, X_{N0}^T]^T$), all $d_i \in \Omega$ and

$t \geq 0$:

$$z_{1i}(t) \leq \max\{\Psi_i, \sigma_{1i} \circ h_1(X_{00}, X_{i0})\}, \tag{4.26}$$
$$z_{2i}(t) \leq \max\{\Upsilon_i, \sigma_{2i} \circ h_{2i}(X_{00}, \mathbb{X}_0, X^o)\}, \tag{4.27}$$

where the values of Ψ_i and Υ_i are given, whereas σ_{ji}, $j = 1, 2$, are functions from the class $\mathcal{K}$ (continuous strictly increasing functions, $\sigma(0) = 0$). The first output, (4.26), must be smaller than Ψ_i, in the case $\sigma_{1i}(h_1(X_{00}, X_{i0})) > \Psi_i$ the trajectory should converge to a subset where $h_1(X_0, X_i) \leq \Psi_i$. In the same way (4.27) must be smaller than Υ_i. In the case $\sigma_{2i}(h_{2i}(X_{00}, \mathbb{X}_0, X^o)) > \Upsilon_i$ the trajectory should converge to a subset where $h_{2i}(X_0, X, X^o) \leq \Upsilon_i$. The restriction (4.26) implies that all robots should find their positions sufficiently close to the leader (on the distance Ψ_i), while (4.27) means that a safe distance, characterizes by Υ_i, should be preserved between the robots and obstacles in X^o.

4.2.1 The Supervisory Control

In this section the three control algorithms U_{1i}, U_{2i}, U_{3i} will be presented again and, if necessary, the design will be proposed to achieve the control goal (4.26), (4.27), *i.e.* leader following U_{1i}, rendezvousing U_{2i} and collision avoiding U_{3i}.

The Supervisor

Considering the given values $\{\lambda_i, \Lambda_i, \delta_i, \Delta_i\} \in \mathbb{R}^4_+$ (Fig. 4.3) with $\lambda_i < \Lambda_i$ and $\delta_i < \Delta_i$, we can describe the switching sequence: the controller U_{1i} (leader following) becomes active when $z_{2i} < \lambda_i^{-1}$ and the distance from the leader $z_{1i} \leq \delta_i$ and it is kept active while $z_{1i} \leq \Delta_i$ (the same safety measure to avoid continuous switching between U_{1i} and U_{2i} controllers specified for the first supervisor definition); the controller U_{2i} (rendezvousing) is active while $z_{2i} < \lambda_i^{-1}$ and $z_{1i} > \delta_i$. The third controller U_{3i} (collision/obstacle avoiding) becomes active as soon as $z_{2i} \geq \lambda_i^{-1}$ and it is kept active until $z_{2i} < \Lambda_i^{-1}$ (also in this case a hysteresis is added to avoid continuous switching, or chattering, between the controllers [93]). We will also ask a right orientation of the robot after avoidance manoeuvre with heading on the leader, *i.e.* it should be $q_{\theta,i} = \alpha_i$, where $\alpha_i = \text{atan}\left(\frac{q_{y,0} - q_{y,i}}{q_{x,0} - qx,i}\right)$. Therefore, the supervisory control law u_i for all $i = 1, \ldots N$ can be summarized as follows

$$u_i(t) = U_{p_i(t)i}(X_0(t), X(t), X^o),\ p_i : \mathbb{R}_+ \to \{1, 2, 3\} \tag{4.28}$$

with the initial conditions

$$t_0 = 0,\ p_i(t_0) = \mathcal{F}_i(\mathbb{X}_0, X_{00}, X^o),$$
$$\mathcal{F}_i(X, X_0, X^o) = \begin{cases} 1 & \text{if } h_1(X_0, X_i) \leq \delta_i \text{ and } h_{2i}(X_0, X, X^o) < \lambda_i^{-1}, \\ 2 & \text{if } h_1(X_0, X_i) > \delta_i \text{ and } h_{2i}(X_0, X, X^o) < \lambda_i^{-1}, \\ 3 & \text{if } h_{2i}(X_0, X, X^o) \geq \lambda_i^{-1} \end{cases}$$

and $p_i(t) = p_i(t_j)$ for $t \in [t_j\ t_{j+1})$, where

$$p_i(t_{j+1}) = \mathcal{F}_i(X(t_{j+1}), X_0(t_{j+1}), X^o), \tag{4.29}$$

with t_j is the generic switching instant defined as follows:

$$t_{j+1} = \arg\ \inf_{t \geq t_j} \begin{cases} h_{2i}(X_0(t), X(t), X^o) \geq \lambda_i^{-1} & \text{if } p_i(t_j) \in \{1,2\}, \\ h_{2i}(X_0(t), X(t), X^o) \leq \Lambda_i^{-1} & \text{if } p_i(t_j) \in \{3\}, \\ \text{and } \theta_i(t) = \alpha_i(t) & \\ h_1(X_0, X_i(t)) \leq \delta_i & \text{if } p_i(t_j) \in \{2\}. \end{cases}$$

Now let us define the estimators and all U_{ki}, $k = 1, 2, 3$.

The Following

For the *Following* controller the same used in Sec. 4.1.1, with analogues results, can be used:

$$U_{1i} = \begin{cases} v_i = \begin{cases} \zeta_i(z_{1i}) \text{sign}\,(C_\alpha)\, \frac{\bar{\eta} + d_{max}\hat{v}_0}{1 - d_{min}} + \hat{v}_0 & \text{if } \epsilon_f = 0, \\ 0 & \text{otherwise,} \end{cases} \\ \omega_i = \frac{\hat{\omega}_0 + [K_f|\epsilon_f| + \rho_f + \rho_0]\text{sign}(\epsilon_f)}{1 - d_{min}}. \end{cases} \tag{4.30}$$

The Rendez-vous Control

As for the *Following*, the *rendez-vous* controller is the same used in Sec. 4.1.1

$$U_{2i} = \begin{cases} v_i = \begin{cases} \frac{\cos(\epsilon_{rdv})[C_\alpha(\hat{v}_0 + \eta_v) + \rho_{rdv}]}{1 - d_{min}} & \text{if } |\epsilon_{rdv}| \leq \kappa\frac{\pi}{2}, \\ 0 & \text{otherwise,} \end{cases} \\ \omega_i = -\frac{S_\alpha \hat{v}_0 + |S_\alpha|\bar{\eta} + \sin(\epsilon_{rdv})[1 + d_{max}]v_i}{z_{1i}} \\ -\rho_{rdv}\text{sign}(\epsilon_{rdv}) - \left(K_{rdv} + \frac{[d_{max} - d_{min}]|v_i|}{z_{1i}}\right)\epsilon_{rdv}, \end{cases} \tag{4.31}$$

Collision/Obstacle Avoidance

The *Collision/Obstacle Avoidance* control becomes active when either the leader or other robots of the group (or an external obstacle, or all of them) enter the safety zone around a robot, which is specified by the circle of radius λ_i. This control is kept active until all robots exit a bigger circle of radius Λ_i. The annulus delimited the two radius can be considered as a hysteresis to avoid chattering phenomena.

Solving the avoidance problem it is desirable to ensure simultaneously the absence of collisions and decreasing the distances z_{1i} for each robot after the avoidance maneuvers.

Assume that the leader is not in the collision conditions and it is not moving during the avoidance maneuver ($v_0(t) = 0$). The case, when the goal point (the leader position) is fixed and there is only one obstacle and one moving robot that performs the avoidance maneuver, has been considered in Chapter 2. The idea of the collision avoidance consists in selection of a point $B = (x_B, y_B)$ moving to that the robot avoids the obstacle and ensure that $z_{1i}(t) \leq z_{1i}(t_0)$ during all the maneuver (the coordinates (x_B, y_B) should be selected such that $z_{2i} < \Lambda_i^{-1}$, then the avoidance maneuver has to be finished before the point B is reached). The following control is a mild modification

of one given in 2.3.2:

$$
\begin{aligned}
U_{3i} &= [v_i\ \omega_i]^T, \qquad (4.32)\\
v_i &= \begin{cases} k_{ca} d_B & \text{if } |\gamma_i| < \kappa\pi \\ & \text{and } z_{2i} < \lambda_o^{-1}\ ,\ \kappa \in (0, 0.5), \\ 0 & \text{otherwise} \end{cases}\\
\omega_i &= k_d \dot{\gamma}_i + \sin(\gamma_i)\frac{v_i}{d_B}\\
&\quad +\rho_{ca}\max\{|\gamma_i|^{0.5}, |\gamma_i|\}\text{sign}(|\gamma_i|),\\
d_B &= \sqrt{(x_i - x_B)^2 + (y_i - y_B)^2},\ k_{ca} > 0,\\
\rho_{ca} &\geq k_{ca}\frac{\sqrt{\pi}(d_{max} - d_{min})[1 + k_d(1 + d_{max})]}{(1 - d_{min})[1 + k_d(1 - d_{min})]}\\
&\quad +2^{-3/4}\rho_2\frac{1 + k_d(1 + d_{max})}{1 - d_{min}},\ \rho_2 > 0,\ k_d > 0
\end{aligned}
$$

and $\gamma_i = \bar{\gamma}_i - q_{\theta,i}$ where $\bar{\gamma}_i = \text{atan}\left(\frac{y_B - q_{y,i}}{x_B - q_{x,i}}\right)$ is the angle between the robot and the point B. The value of λ_o is introduced in the following result that has been proven in 2.3.2:

Proposition 1. *Let $v_0(t) = 0$ for all $t \geq t_0 \geq 0$ and $N = N_o = 1$. Then there is a point $B = (x_B, y_B)$ such that for (1.33), (4.32):*
1. *The system is uniformly finite-time stable with respect to the variable γ_i and there is $t_{ca} > 0$ such that $|\gamma_i(t)| \leq \kappa\pi$ for all $t \geq t_0 + t_{ca}$ for any $\gamma_i(t_0) \in (-\pi, \pi]$.*
2. *There are $0 < \lambda_o \leq \lambda_i$ and $T_{ca} > 0$ such that $\Lambda_i^{-1} \leq z_{2i}(t) < \lambda_o^{-1}$ for all $t \in [t_0, t_0 + T_{ca})$ and $z_{2i}(t_0 + T_{ca}) < \Lambda_i^{-1}$.*
3. *$z_{1i}(t) \leq z_{1i}(t_0)$ for all $t \in [t_0, t_0 + T_{ca}]$.*

A detailed explanation, how the point B can be selected, is given in 2.3.2. Following Proposition 1 we can assign $\mathbb{D}_{ci} > \lambda_o^{-1}$. As in [53] we will assume that $\mathcal{O} > 2\Lambda_{max}$ where $\Lambda_{max} = \max_{1 \leq i \leq N'} \Lambda_i$ and

$$\mathcal{O} = \min_{1 \leq k \neq r \leq N_o} \sqrt{(x_{ko} - x_{ro})^2 + (y_{ko} - y_{ro})^2}$$

is the minimum distance between the obstacles. Under such a restriction the obstacles are sufficiently isolated and the consideration given for one obstacle with the control (4.32) in Proposition 1 is essential.

Now, let us return to the general case, then remarks have to be done about the rules of inclusion/exclusion of robots from the group performing the avoidance. To simplify notation in this section we will denote $1 \leq N' \leq N+1$ and $0 \leq N'_o \leq N_o$ the numbers of robots and obstacles participating in the manoeuvre respectively, and

$$2 \leq M = N' + N'_o \leq N + N_o + 1$$

is the total number of participants. Without loosing generality assume that the first $N'(N'_o)$ robots (obstacles) are in the collision conditions. If there exist three distinct indexes $1 \leq i_1 < i_2 < i_3 \leq N'$, such that the distances between robots i_1, i_2 and i_2, i_3 are less than λ_{i_2} while the distance between i_1, i_3 is bigger than $\max\{\lambda_1, \lambda_3\}$, then anyway all of them form the same group for the avoidance. If during fulfilment

of the manoeuvre a robot arrives to the collision conditions, then the procedure of collision/obstacle avoidance has to be re-initiated following the algorithm (if a robot exits the safety zone then there is no re-initialization for the rests according to (4.8)):

Collision avoidance:
Let $\mathcal{N} = \{1 \leq i \leq N'\}$ and $\mathcal{I} = \{i \in \mathcal{N} : z_{1i}(t_0) \leq \lambda_i\}$,

$$\mathcal{N} = \mathcal{N} \setminus \mathcal{I}.$$

1. The closest robot to the leader is found with the index $i' = \arg\min_{i \in \mathcal{N}} z_{1i}(t_0)$. If i' is not unique, then an auxiliary sorting can be performed,

$$\mathcal{N} = \mathcal{N} \setminus \{i'\}.$$

2. Assign $v_i(t) = 0$ for all $\mathcal{N} \cup \mathcal{I}$ and let the robot i' to perform the collision avoidance maneuver using the control (4.32) while $\Lambda_i^{-1} \leq z_{2i'}(t) < \lambda_o^{-1}$.
3. If $\Lambda_i^{-1} \leq z_{2i'}(t)$, then apply the rendezvous orientation control (4.15) until $\theta_i = \alpha_i$.
4. The procedure is repeated for the robots in $\mathcal{N}$ starting from the Step 1 while $\mathcal{N} \neq \emptyset$.

The algorithm is accompanied by an assumption that the leader is not moving during the avoidance maneuver if $\mathcal{I} = \emptyset$ (this condition can be easily realized in practice):

Assumption 5. *Let $v_0(t) = 0$ if there is a group of robots in the collision conditions with the indexes in the set $\mathcal{J} \subset \{1, \ldots, N\}$ such that $z_{1j}(t_0) > \lambda_j$ and $p_j(t) = 3$ for all $j \in \mathcal{J}$.*

Roughly speaking this assumption means that the leader waits while some of robots in the group are in the collision conditions if they are far enough. And it can move only if all robots in collision form a unique group which is close to the leader. In fact, the geometrical construction presented in Proposition 1 and in 2.3.2 can be performed for a moving leader (in its frame) but with increased complexity of presentation, which we would like to avoid here.

In the step 3 the rendezvous orientation is performed for the robots, the role of this orientation will be explained in the next section considering the supervisory control and switching among $U_{k,i}$.

If $z_{1i}(t_0) > \lambda_i$ for all $1 \leq i \leq N'$ and the set $\mathcal{I}$ is empty, then the leader is not moving as assumed. Since $\mathcal{O} > 2\Lambda_{max}$ and the closest to the leader robot starts to move, then i' is always in the conditions of Proposition 1 (an "obstacle" there can be presented by an obstacle (x_{ko}, y_{ko}) or a not moving robot with the index $j \in \{1, \ldots, N'\} \setminus \{i'\}$ with $z_{1i'} \leq z_{1j}$ and it is not on the way for i'). Therefore, for each i' there is a time instant $T_{ca}^{i'}$ such that $z_{2i'}(t_0 + T_{ca}^{i'}) < \Lambda_{i'}^{-1}$ and the robot exits the collision conditions. Obviously after $t \geq t_0 + \sum_{i=1}^{N'} T_{ca}^{i}$ all robots will finish the avoidance maneuver. The following result has been proven.

Lemma 7. *Let Assumption 5 be satisfied, $\mathcal{O} > 2\Lambda_{max}$, $z_{1i}(t_0) > \lambda_i$ for all $1 \leq i \leq N'$, and $\dot{M}(t) \leq 0$ for almost all $t \geq t_0$ (there is no other robot joining the avoidance maneuver), then the system (4.1) with the presented algorithm admits the properties:*
1. *Uniform finite-time stability with respect to the variables γ_i, $1 \leq i \leq N'$;*
2. *There exists $\overline{T}_{ca} > 0$ such that $\Lambda_i^{-1} \leq z_{2i}(t) < \lambda_o^{-1}$ for all $t \in [t_0, t_0 + \overline{T}_{ca}]$ and $z_{2i}(t_0 + \overline{T}_{ca}) < \Lambda_{i'}^{-1}$, $\theta_i(t_0 + \overline{T}_{ca}) = \alpha_i(t_0 + \overline{T}_{ca})$ for all $1 \leq i \leq N'$;*
3. *$z_{1i}(t) \leq z_{1i}(t_0)$ for all $t \in [t_0, t_0 + \overline{T}_{ca}]$ and all $1 \leq i \leq N'$.*

If the set $\mathcal{I}$ is not empty, then those robots in $\mathcal{I}$ are not moving, for the rest robots in $\mathcal{N}$ application of the avoidance strategy from 2.3.2 and the control (4.32) may lead to a fail, in this case for an index i' the condition $z_{2i'}(t') = \lambda_o^{-1}$ is satisfied and the robot stops (the collision avoidance maneuver is finished in this way). Anyway in such a group the maximum distance to the leader would be bounded as

$$z_{1i} \leq \sum_{i=1}^{N'} \lambda_i$$

and it is independent in the number of obstacles since if there is a robot with an index j which has distance to other robots more than λ_j but they all are close to a common obstacle, then the robot j forms an independent group of collision avoidance. The leader will be able to move if all robots are in the collision around it and it will stop as soon as it exits from the collision conditions with any robot in that group, thus even in this case the distance to the leader stay bounded as

$$z_{1i} \leq \sum_{i=1}^{N'} \lambda_i + \Lambda_{max}.$$

Lemma 8. *Let Assumption 5 be satisfied, $\mathcal{O} > 2\Lambda_{max}$, $z_{1i}(t_0) \leq \lambda_i$ for some $i \in \{1, \ldots, N'\}$, and $\dot{M}(t) \leq 0$ for almost all $t \geq t_0$, then the system (1.33) with the proposed algorithm admits the properties:*

1. *Uniform finite-time stability with respect to the variables γ_i, $1 \leq i \leq N'$;*
2. *$z_{2i}(t) \leq \lambda_o^{-1}$ for all $t \geq t_0$ and all $1 \leq i \leq N'$;*
3. *$z_{1i}(t) \leq \max\{z_{1i}(t_0), \sum_{i=1}^{N'} \lambda_i + \Lambda_{max}\}$ for all $t \geq t_0$ and all $1 \leq i \leq N'$.*

Supervisory control

Summarize the restrictions obtained so far as follows:

Assumption 6. *Let $\delta_i + v_{max}\bar{T}_f \leq \Delta_i$, $\delta_i - v_{max}\bar{T}_f > \lambda_i$, $\lambda_i < \Lambda_i < \delta_i$ and $\mathcal{O} > 2\Lambda_{max}$ for all $i = 1, \ldots, N$.*

Following the results in Chapter 2, [53] and [35]:

Theorem 6. *Let assumptions 5 and C.3 be satisfied for $N \geq 1$ and $N_o \geq 1$. For all $d \in \Omega$ and all $\mathbb{X}_0 \in \mathcal{X}^N$, $X_{00} \in \mathcal{X}$ such that $h_1(X_{00}, X_{i0}) \geq \delta_i, h_{2i}(X_{00}, \mathbb{X}_0, X^o) \geq \lambda_i$, $i = 1, \ldots, N$ in the robot group (4.1), (4.23) under the supervisor (4.29) and the control (4.28), the estimates*

$$|z_{1i}(t)| \leq \max(\Psi_i, |h_1(X_{00}, X_{1i0})|),$$
$$|z_{2i}(t)| \leq \max(\Upsilon_i, |h_{2i}(X_{00}, \mathbb{X}_0, X^o)|)$$

hold for all $t \geq 0$, where $\Psi_i = \max\{\Delta_i, \sum_{i=1}^{N} \lambda_i + \Lambda_{max}\}$ and $\Upsilon_i = \lambda_o^{-1}$.

Proof. Two different initial scenarios are possible: $p_i(0) = 1$ or $p_i(0) = 2$ for all $i = 1, \ldots, N$ (the case $p_i(0) = 3$ is excluded by the condition $h_{2i}(X_{00}, \mathbb{X}_0, X^o) \geq \lambda_i$). First, let $p_i(0) = 2$, then from Lemma 5 the variable z_{1i} is bounded and converging, and there is a time instant $T_{rdv} = T_{rdv}(z_{1i}(t_0))$ such that $z_{1i}(T_{rdv}) \leq \delta_i$ and $p_i(T_{rdv}) = 1$ provided that there is no collision. If there is a collision and $p_i(t') = 3$ for some $t' > 0$, then the robot is either in the conditions of Lemma 7 or Lemma 8. In the

former ones, always there is an instant that the avoidance maneuver is accomplished, $z_{2i} < \Lambda_i^{-1}$ and $\theta_i = \alpha_i$, while the leader was not moving during all the maneuver. Then returning to $p_i = 2$ is performed under the conditions that $\epsilon_{rdv} = 0$ and from Lemma 5 the distance z_{1i} is not increasing. In the conditions of Lemma 8 the distance to the leader is bounded ($z_{1i}(t) \leq \max\{z_{1i}(t'), \sum_{i=1}^{N} \lambda_i + \Lambda_{max}\}$) and $z_{2i} \leq \lambda_o^{-1}$. Note that if $z_{1i}(t') > \sum_{i=1}^{N} \lambda_i + \Lambda_{max}$, then it should be that case of Lemma 7 (the robot is sufficiently far from the leader), thus $z_{1i}(t) \leq \sum_{i=1}^{N} \lambda_i + \Lambda_{max}$ in this case. Next, the consideration is similar to the second initial scenario with $p_i(0) = 1$, then according to Lemma 4 $z_{1i} \leq \Delta_i$ in a finite time provided that there is no collision. If there is a risk of collision and $p_i(t') = 3$ for some $t' > 0$, then according to lemmas 7, 8 the variable z_{2i} is bounded (in the worst case $z_{2i} \leq \Upsilon_i$) and

$$z_{1i}(t) \leq \max\{z_{1i}(t'), \sum_{i=1}^{N} \lambda_i + \Lambda_{max}\}.$$

However, in this case $z_{1i}(t') \leq \Delta_i$, then

$$z_{1i}(t) \leq \max\{\Delta_i, \sum_{i=1}^{N} \lambda_i + \Lambda_{max}\}.$$

□

Therefore, the developed supervisory control solves the posed problem of collective motion coordination with collision avoidance under rather mild assumptions.

4.2.2 Conclusion

This chapter presented two switching-based solutions to the leader-follower formation problem for a group of WMR in the presence of additive input disturbances with obstacle/collision avoidance. Both solutions rely on a supervisor able to regulate two different outputs orchestrating three different controls: one to regroup the robots (*rendezvous* controller), a second one to make them follow the leader (*Following* controller) and the latter in charge of the collisions/obstacles avoidance when necessary during the motion.

It is worth to remark that in both cases no assumption have been made about *a priori* knowledge of the positions of obstacles or leader velocities. In the first case the leader does not participate the manoeuvre and the follower agents are the responsible to the formation maintenance. In the second approach the leader has an active role in the formation participating in the collision avoidance manoeuvre slowing down the formation to allow the agents to accomplish that and move again right after. The main advantage of the second approach is that with the proposed modification we were able to formally prove the stability of the formation regulated by the three controllers and the supervisor.

Anyway, in both cases it has been formally shown that each control robustly achieves the task it is designed for and, in addition, the robots orientations are provided in a finite-time. Simulations are performed for a group of 4 WMRs to prove the effectiveness of the strategy in the first case while a formal proof is given in the second case.

Chapter 5

Conclusions and Perspectives

In this dissertation we have addressed the problem of the obstacle avoidance for wheeled mobile robots both in the case of a lonely robot or in the case of a formation deployment. Different solutions have been proposed that cover different scenarios. The vehicles control always took advantage of the finite time control framework; the intent is to have reliable results and disturbance rejection for the perturber kinematic model. The perturbations are introduced to deal with some unmodeled dynamics. The author, along with the people who participated in this dissertation work, aimed to proposed efficient solutions, characterised by an easy implementation, that could be adapted to different kinematic model and, of consequence, WMRs; that is indeed something that represents one of the future directions for the three different approaches presented. The main results and contributions of the study presented in this dissertation may be summarized as follows.

5.1 Contributions

The first contribution of this dissertation is a simple but effective obstacle avoidance reactive algorithm for WMRs which relies on a geometric approach to find a suitable point to avoid eventual obstacles when these are encountered. The algorithm, in addition, uses a control law able to reject disturbances added to describe unmodeled dynamics. The framework which allows a satisfactory result to be presented is the supervisory control one: two outputs regulated by just as many controls. The first control is in charge of the goal seeking (*i.e.* stabilization, in the proposed solution), the second one able to avoid obstacles. The solution is formally proven using the control theory tools and sustained by simulations and extensive experiments in which the method is compared with the well known and widespread DWA approach.

Then, a modification of the standard Potential Field method has been presented. Again control theory and its evolution came in help to propose a novel field definition along with a new method to avoid local minima, which are the most annoying drawbacks of the PF method. A complete theoretical treatise has been carried out to expose how the control theory tools are applied to get the result. Under some, not too restrictive assumptions, capitalizing on the Input-to-State Stability (ISS) property for multi-stable systems, the global attractivity of the target point is proven and the avoidance is achieved. The result is thus utilised to generate the trajectory that is tracked by a wheeled mobile robot, a Unicycle-like WMR in the case. Both, a classic approach

and a specifically designed one are firstly treated theoretically, and proved convergent using control theory tools, then simulated and compared to the standard PF method. The most efficient of the two, based on a finite-time control for the orientation, which provides finite-time completion of the task is thus implemented on a Turtlebot II WMR to test the method in a real environment and verify the theoretical result obtained.

The last part of the dissertation presented a leader-follower formation algorithm which is an evolution of the first part of this work of thesis. The framework is again the supervisory one; in this application two outputs are regulated via three controls to regroup the robots (*rendezvous*), to make them move together following the leader (*following*) and to avoide eventual obstacle or collision between agents (*collision avoidance*). The novelty lies in the formation definition, the leader acts as a reference and it is not the most advanced agent of the formation but more a reference to follow. The realization is completely decentralized: each robot takes its own decision depending on two distances, the one from the leader that define the following or rendezvous status, and the one from agents or obstacles around, which define if the collision avoidance controller must be activated. Two modifications have been presented, the first in which the leader act just as a reference and it is completely autonomous not participating in the manoeuvre and the second one in which it is actually active and slows down the formation in case of one or more agents have to avoid obstacles or collisions. The second approach presented allowed to formally prove the stability of the formation.

5.2 Future Directions

The three contributions presented could be enhanced, each one in its own way.

The finite time collision avoidance presented in Chapter 2 must be incorporated in a complete navigation system to make it cooperate with a global planner; that should avoid the appearance of situation that could make the approach to fail. That is the usual step that one has to make when dealing with local planners. With the aim to make the algorithm more suitable for complex applications the case in which the obstacles are not stationary should be considered along with the generalization for other classes of WMRs. It has to be said that preliminary experiments have been run with this purpose and gave promising results.

The eventual extensions of the new formulation of the PF are at least two one can easily see: the first is to extend the application on a three dimensional level (for instance for flying or underwater robots), since the presented experiments where basically carried out in 2D; that is possible since the theory which motivated the work is presented in a n dimensional space. The second extension concern the use of the presenter modification in a formation scenario since as mentioned in Chapter 1, the potential field method is often a base to realize robots formation.

Lastly, the leader-follower approach presented has as major flaw the fact of not to have been implemented in real platform to test the effectiveness in a real scenario, some tests have been carried to propose a final implementation. The evolution of the method could see a hierarchical organization of several formations coordinated by several leaders to achieve tasks of increasing complexity.

Chapter 6

Resumé en Français

Le mot robot a été utilisé pour la première fois dans la langue anglais dans les années vingts après avoir été utilisé dans une comédie théâtrale intitulée Rosumovi Univerzální Roboti. Le mot vient du tchèque esclave, parce que dans la pièce de théâtre les robots, proche de ce qu'on appelle androïdes, sont dénués de sensibilité et doués d'une intelligence très développée, en plus ils doivent être faciles à produire et autonomes, pour remplacer les ouvriers humains.

Dans le même esprit, les modernes robots mobiles doivent avoir les mêmes caractéristiques pour être classés dans une de typologie indiquées par la Fédération International de la Robotique. Elle définit le robot de service comment une machine capable de exécuter de tâches de façon autonome en utilisant le données disponibles sans l'aide d'un opérateur extérieur. On peut retrouver deux différentes typologies de robots de service: service à la personne et service aux professionnels. Les premiers aident les gens dans les besoins quotidiens, comment pour exemple les futailles roulants ou plus simplement les robots aspirateurs. Les deuxièmes sont les robots qui ont des applications professionnels ou commerciaux, comment les robots utilisés dans la chirurgie et la rééducation, ou pour des opérations de secours en cas de catastrophes naturelles. Les données rendues publique par la Fédération International de la Robotique décrivent un marché de la robotique qui n'arrête pas croissance avec une augmentation des ventes du 15 en 2014 et une prévision de croissance positive aussi sur le période 2014-2017.

Ce travail de thèse traite de la commande pour de robots mobile à roues en particulier. Ces robots trouvent plein d'applications dans plusieurs domaines, mais les problématiques de base qui doivent affronter sont les mêmes pour chaque tâche: comment arriver à la destination en évitant les obstacles qui puissent eux s'opposer de la façon la plus intelligent possible selon des paramètres décidés à priori. Pour faire ça, la chaine d'évènements qui se produit est la suivent: il faut équiper le robot avec un capteur apte à la localisation, comme une antenne GPS pour de mission à l'extérieur où une caméra, un sonar où un capteur LIDAR (laser) pour les missions à l'intérieur, où le GPS ne marche pas; une fois que le capteur est choisi, un algorithme dois lui permettre de se localiser dans une carte (si disponible où de la créer), se deplacer dans l'espace et éviter les obstacles et si nécessaire partager des informations avec des autres robots pour accomplir la tâche. En particulier dans ce travail on va présenter des lois de commande qui vont permettre au robot mobile à roues d'éviter des obstacles; on va présenter une amélioration d'une stratégie existante, celle des champs de potentiels, et une nouvelle stratégie conçue en utilisant la technique du Supervisory Control. On

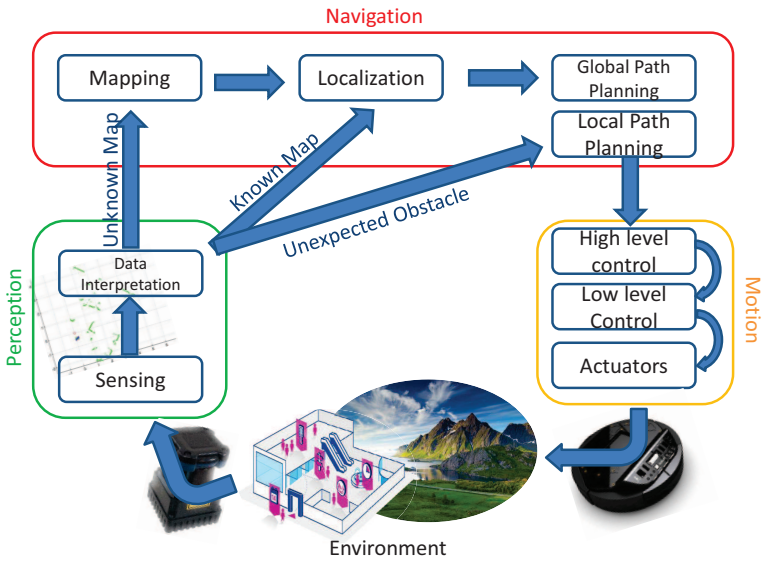

Figure 6.1: Scheme general pour un robot mobile a roues

va après comparer les deux avec les stratégies plus diffusées pour montrer l'efficacité de les solutions proposées. La deuxième technique et aussi étendue pour traiter les cas d'un groupe de robots mobiles qui se déplace selon le schème Leader-Follower. Dans toutes les solutions presentées, pour être le plus proche possible à la réalité, sans vouloir rendre les problèmes trop compliqué du point de vue du modèle, la choix plus logique a été l'utilisation du modèle cinématique à la place de celui dynamique, en ajoutant pourtant de perturbations aptes à modeler les dynamiques négligées.

6.1 Évitement d'obstacle en temps finit

La première contribution de ce travail de thèse est représentée par la synthèse d'une méthode d'évitement d'obstacle pour un robot mobile à rues de type unicycle. La particularité de ce type de modèle est l'appartenance à la classe des systèmes non-holonomes qui imposent des contraintes par rapport à la stabilisation. Dans la littérature plusieurs technique ont étés utilisées: de la commande par rétroaction qui varie dans le temps, discontinue, hybride/switch ou optimal pour aborder le problème de la stabilisation. En effet, dans la solution proposée, le problème d'évitement d'obstacle est divisé en deux sous-tâches, qui vont résoudre deux différentes problèmes de stabilisation avec la technique du Supervisory Control et de lois de commande en temps finit. Pendant l'exécution, la tâche du robot mobile est toujours d'arriver dans point de destination en évitant les obstacles. Deux différentes sorties sont définies: la première sortie donne la distance de la destination alors que la deuxième donne des informations par rapport à la distance de un éventuel obstacle trop proche du robot mobile et, donc, à

éviter. Le superviseur a la tâche de tenir sous contrôle la deuxième sortie et commuter entre les deux systèmes: si aucun obstacle n'est plus proche d'une distance de sécurité, définie à priori, une première commande s'occupe de régulation de la première sortie pour arriver à destination. Dans le cas que la distance entre le robot mobile et un obstacle soit inférieure à la limite imposée, un nouveau point de destination temporaire est défini alors que le superviseur commande le switch pour permettre la régulation de la deuxième sortie en utilisant une commande en temps finit appropriée. Le problème est traité d'ailleurs de façon théorique pour un système non-holonome générique et après mis en pratique pour un robot mobile à roues. Le modèle considéré pour le robot mobile à roues de types unicycle est le suivant :

$$\begin{aligned} \dot{q}_x &= (1+d_1)v\cos(q_\theta), \\ \dot{q}_y &= (1+d_1)v\sin(q_\theta), \\ \dot{q}_\theta &= (1+d_2)\omega. \end{aligned} \tag{6.1}$$

Les entrés pour commander le robot mobile sont, respectivement v, vitesse linéaire, et ω, vitesse angulaire. Les deux sorties dont on a besoin pour les deux tâches sont :

$$z_1(q_x, q_y) = \sqrt{q_x^2 + q_y^2}, \tag{6.2}$$

$$z_2(q_x, q_y) = \min\left[Y, \max_{1\le i\le N}\left(\sqrt{(q_x - x_{o_i})^2 + (q_y - y_{o_i})^2}\right)^{-1}\right] \tag{6.3}$$

où z_1 est la distance de l'origine et z_2 est l'inverse de la distance de l'obstacle le plus proche, défini avec ses cordonnées Cartésiennes (x_{o_i}, y_{o_i}). Avec l'hypothèse d'avoir assez d'espace entre deux obstacles séparés on peut considérer un obstacle à la fois. Pour le deux différentes tâches on considère deux différentes commandes : u_1 pour la stabilisation de la première sortie qui amène le robot mobile à sa destination et u_2 pour l'évitement d'obstacle et donc pour la deuxième sortie.

$$u_1 = \begin{cases} v = \begin{cases} k_1 z_1 & \text{if } |\alpha| \le k\pi \\ 0 & \text{otherwise} \end{cases} \\ \omega = -k_2\zeta(\alpha)\text{sign}(\alpha). \end{cases}, \tag{6.4}$$

Le régulateur u_2 pour l'évitement d'obstacle guide le robot mobile en temps finit vers un point à une distance de sécurité de l'obstacle sans faire augmenter la distance de l'origine :

$$u_2 = \begin{cases} v = \begin{cases} k_3 D_B & \text{if } \cos(\alpha) \ge 0 \text{ and } |\gamma| \le \epsilon\pi \\ 0 & \text{otherwise} \end{cases} \\ \omega = k_d\dot{\gamma} + \frac{\sin\gamma}{D_B}v + k_{ca}\zeta(\gamma)\text{sign}(\gamma). \end{cases}, \tag{6.5}$$

Le superviseur peut être formulée de la façon suivante :

$$U(t) = u_{i(t)}[q_x(t), q_y(t), q_\theta(t)],\ i : \mathbb{R}_+ \to \{1, 2\} \tag{6.6}$$

$$\begin{aligned} t_0 = 0,\ i(t_0) &= \begin{cases} 1 & \text{if } (q_x(t_0), q_y(t_0)) \in \mathbf{X_2}, \\ 2 & \text{otherwise}, \end{cases} \\ i(t) &= i(t_j) \quad \forall t \in [t_j\ t_{j+1}), \end{aligned}$$

$$i(t_{j+1}) = \begin{cases} 1 & \text{if } q(t_{j+1}) \in \mathbf{X_1} \\ 2 & \text{if } q(t_{j+1}) \notin \mathbf{X_2} \end{cases}, \tag{6.7}$$

$$t_j = \begin{cases} \underset{t \geq t_j}{\arg\inf}\ q(t) \notin \mathbf{X_2} & \text{if } i(t_j) = 1 \\ \underset{t \geq t_j}{\arg\inf}\ q(t) \in \mathbf{X_1} & \text{if } i(t_j) = 2 \end{cases}$$

Le superviseur gère deux différents régulateurs pour stabiliser deux sorties. La coopération de les deux régulateurs permit de conduire le robot mobile en temps fini vers sa destination; en plus, l'évitement de les obstacles est toujours atteint dans un temps fini. Les performances de ce travail ont été démontrées et testées sur un banc d'essai pour montrer l'efficacité de la méthode. La stratégie a été aussi comparé avec une méthode bien connue comme le Dynamic Windows Approach.

6.2 Méthode de champs de potentiels : modification avec la propriété de stabilité éntre-état

La méthode des champs potentiels, très utilisées pour la navigation et l'évidement d'obstacle en robotique a été présenté dans le Chapitre 1, avec ses avantages et ses inconvénients. Parmi les inconvénients, il y a l'apparition de minima locaux, qui causent l'arrêt du robot mobile et donc il lui ne permettent pas d'accomplir sa tâche. On va présenter une modification de l'approche, inspirée par de nouveau résultats sur la stabilité entré-état [2], pour éviter les minima locaux (dans le cas de deux dimensions). On fait l'hypothèse des obstacles disjoints, très fréquent dans la littérature, et on propose un nouveau champ de potentiel; le gradient du champ est utilisé comme entrée pour un système de deux intégrateurs. Avec des hypothèses appropriées, le système possède la propriété de stabilité entré-état (ISS) à l'égard des ensembles invariants et décomposables [2]. La propriété de stabilité entré-état (ISS) est la clé de la modification proposée. Elle nous permet de traiter les minima locaux d'une manière efficace, suggérant ainsi une nouvelle solution simple et élégante et qui garantit l'évitement des obstacles pour un robot mobile à roues, sans risque de rester bloqué dans un minimum local. Le robot mobile à roues considéré est de type unicycle et on ajoute de perturbations sur les entrées. Le but est de faire suivre au robot le mouvement de la particule 2D décrite par les deux intégrateurs. On va présenter deux approches, d'abord une technique de linéarisation plus simple: la commande obtenue pour le système d'intégrateurs peut être appliquée, avec un changement de coordonnées, au robot mobile; le problème est que cette approche ne permet pas de contrôler l'orientation du robot. Une seconde approche est, donc, conçu pour contrôler soit la vitesse linéaire soit l'orientation du robot mobile à roues. Le régulateur assigne pour le vitesse linéaire la norme du gradient du champ de potentiel, alors que la commande de vitesse angulaire est réalisée avec une commande en temps fini similaire à celle utilisée dans [55]. Il est formellement éprouvé que la commande en temps fini est robuste par rapport aux perturbations considérées et elle garantit la convergence de l'orientation du robot, en plus des simulations ont été réalisées et ont montré des résultats très satisfaisant. La partie expérimentale voit la méthode développée mise en pratique sur un robot mobile à roues de type unicycle (Turtlebot 2) qui se déplace dans un environnement en évitant des obstacles (dont il ne connessait pas la présence à priori) et aussi la comparaison avec la méthode classique. Quelques problèmes a été relevés en présence des passages

étroits et en cas de point de destination trop près d'un obstacle, mais ça n'a pas empêché d'atteindre l'objectif.

6.3 Contrôle d'une Formation avec la méthode Leader-Follower

La mise en œuvre des systèmes multi-agents permit de chercher des solutions optimisées, comme par exemple dans des applications d'exploration des endroits inconnues, où l'aide des plusieurs robots qui partagent des données peut améliorer la fiabilité et donc les résultats et réduire le temps pour atteindre la tâche. Plusieurs robots pourraient, aussi, coopérer pour réaliser des tâches impossibles pour un seul robot, comme la manipulation de l'environnement. On peut, aussi, penser au concept de l'utilisation de plusieurs robots mobiles, chacun spécialisé dans une tâche, plutôt que d'en utiliser que un, plus complexe et difficile à gérer. Lorsque plus d'un agent prend part à une mission, il doit avoir des directives à suivre pour travailler avec d'autres sans interférer et, évidemment, en évitant les collisions; celle la est la partie la plus difficile à gérer dans le point de vue de l'ingénierie: coordonner tous les aspects garantissant un résultat satisfaisant. Deux typologies d'approches sont devenues très populaire pour cordonner un groupe de robots mobiles: la première est basé sur l'auto-organisation, chaque agent a un ensemble d'instructions pour réagir à de différents situations. Ces approches sont souvent inspirés par des comportements naturels. La deuxième typologie est basée sur une approche géométrique où chaque robot mobile n'a pas un comportement totalement autonome, mais ses réactions sont liées à des directives qui les obligent à rester dans une formation avec des règles prédéfinies.

On va traiter le problème de la formation leader-follower, où le leader, soit physique (donc un vrai robot) ou virtuel, est l'agent le plus avancé de la formation et il agit comme référence pour tous les autres robots qui lui suivent. Le but est de présenter une approche leader-follower original pour un groupe de robots mobiles à roues. On veut déplacer le leader et les autres agents vers un point de destination sans que le leader soit obligé à partager sa vitesse; en plus on veut être capable d'éviter les collisions entre les agents et les obstacles externes. La solution proposée donne à chaque agent une distance souhaitée du leader, ce signifie que le leader ne représente pas le robot le plus avancé de la formation, mais plutôt une référence à suivre.

Pour atteindre un tel objectif on utilise la technique de la régulation de sortie, où plusieurs sorties sont gérés par un superviseur, tous en tenant compte de la notion de stabilité pour les systèmes switch et la définition de la propriété de stabilité sortie-état: chaque agent, à l'exception du leader, commute entre trois lois de commande qui vont régler deux sorties différentes. Une sortie proportionnelle à la distance du leader et une deuxième proportionelle à la distance entre l'agent et les autres robots ou obstacles; un superviseur, spécifiquement conçu, similaire à celui proposée pour la méthode d'évitement d'obstacle simple orchestre les activations de les différentes lois de commande.

Dans les trois lois de commande, le premier régulateur prend en charge la réalisation du *rendez-vous*, c'est-à-dire comment l'agent doit approcher le leader. Le deuxième, assure que les agents qui suivent maintenaient le même cap et vitesse du leader (qui ne partagé pas ces vitesses sur le réseau, elles sont obtenue en utilisant un dérivateur homogène [115]). La troisième lois de commande, agisse sur la deuxième sortie, destinée à éviter les collisions entre les agents et/ou les obstacles. Le modèle utilisé pour chaque

robot mobile à roues est, encore une fois, le modèle cinématique de l'unicycle avec de perturbations sur les entrées. Le superviseur surveille les commutations entre les trois lois de commande qui sont robustes par rapport aux perturbations considerées. En gardant la même idée de solution, deux approches différentes sont présentées: en premier, le leader est une référence à suivre, il est totalement autonome et il n'a pas connaissance de l'état des autres membres de la formation. Ensuite, le leader participe à la manœuvre activement, attendant dans le cas d'un ou plusieurs agents impliqués dans une manœuvre d'évitement de collision ou obstacle; cette modification au problème a permis une épreuve formelle de la méthode avec les outils de la théorie du contrôle.

Appendices

Appendix A

Input-to-State Stability with respect to decomposable invariant sets

For an n-dimensional $\mathcal{C}^2$ connected and orientable Riemannian manifold M without boundary ($0 \in M$), let the map $f : M \times \mathbb{R}^m \to T_xM$ be of class $\mathcal{C}^1$ (T_xM is the tangent space), and consider a nonlinear system of the following form:

$$\dot{x}(t) = f(x(t), d(t)) \tag{A.1}$$

where the state $x \in M$ and $d(t) \in \mathbb{R}^m$ (the input $d(\cdot)$ is a locally essentially bounded and measurable signal) for $t \geq 0$. We denote by $X(t, x; d(\cdot))$ the uniquely defined solution of (A.1) at time t fulfilling $X(0, x; d(\cdot)) = x$. Together with (A.1) we will analyze its unperturbed version:

$$\dot{x}(t) = f(x(t), 0). \tag{A.2}$$

A set $S \subset M$ is invariant for the unperturbed system (A.2) if $X(t, x; 0) \in S$ for all $t \in \mathbb{R}$ and for all $x \in S$. For a set $S \subset M$ define the distance to the set $|x|_S = \min_{a \in S} \delta(x, a)$ from a point $x \in M$, where the symbol $\delta(x_1, x_2)$ denotes the Riemannian distance between x_1 and x_2 in M, $|x| = |x|_{\{0\}}$ for $x \in M$ or a usual euclidean norm of a vector $x \in \mathbb{R}^n$. For a signal $d : \mathbb{R} \to \mathbb{R}^m$ the essential supremum norm is defined as $\|d\|_\infty = \operatorname{ess\,sup}_{t \geq 0} |d(t)|$.

Definition 6. *The point $\bar{x}$ is called an* omega limit point *of the solution of* (A.2) $x(t, x_0)$ *if there exists a sequence of time instants $t_1, \ldots, t_l, \ldots$ such that $t_k \to \infty$ as $k \to \infty$, for which the following holds:*

$$x(t_k, x_0) \to \bar{x}, \qquad k \to 0 \tag{A.3}$$

The set of all such point of $x(t_k, x_0)$ is called ω-limit set of $x(t_k, x_0)$ (or orbit $\gamma(x_0)$) and denoted $\omega(x_0)$.

Definition 7. *The point $\underline{x}$ is called an* alpha limit point *of the solution of* (A.2) $x(t, x_0)$ *if there exists a sequence of time instants $t_1, \ldots, t_l, \ldots$ such that $t_k \to -\infty$ as $k \to \infty$, for which the following holds:*

$$x(t_k, x_0) \to \underline{x}, \qquad k \to 0 \tag{A.4}$$

The set of all such point of $x(t_k, x_0)$ is called α-limit set of $x(t_k, x_0)$ and denoted $\alpha(x_0)$.

Definition 8. *A* heteroclinic orbit *γ_1 between two equilibria ζ_1 and ζ_2 of a continuous dynamical system as* (A.2)*, is a trajectory $x(t, x_0)$ that is backward asymptotic to ζ_1 and forward asymptotic to ζ_1.*

Definition 9. *A* heteroclinic cycle *is an invariant topological circle X consisting of the union of a set of equilibria $\zeta_1, \ldots, \zeta_k$ and orbits $\gamma_1, \ldots, \gamma_k$, where γ_i is a heteroclinic orbit between ζ_1 and ζ_{i+1}; and $\zeta_{k+1}\zeta_1$. If $k = 1$ then the single equilibrium and connecting orbit form a* homoclinic cycle*.*

A.1 Decomposable sets

Let $\Lambda \subset M$ be a compact invariant set for (A.2).

Definition 10. *[109] A decomposition of Λ is a finite and disjoint family of compact invariant sets $\Lambda_1, \ldots, \Lambda_k$ such that*

$$\Lambda = \bigcup_{i=1}^{k} \Lambda_i.$$

For an invariant set Λ, its attracting and repulsing subsets are defined as follows:

$$W^s(\Lambda) = \{x \in M : |X(t, x, 0)|_\Lambda \to 0 \text{ as } t \to +\infty\},$$
$$W^u(\Lambda) = \{x \in M : |X(t, x, 0)|_\Lambda \to 0 \text{ as } t \to -\infty\}.$$

Define a relation on $\mathcal{W} \subset M$ and $\mathcal{D} \subset M$ by $\mathcal{W} \prec \mathcal{D}$ if $W^s(\mathcal{W}) \cap W^u(\mathcal{D}) \neq \emptyset$.

Definition 11. *[109] Let $\Lambda_1, \ldots, \Lambda_k$ be a decomposition of Λ, then*

1. *An r-cycle ($r \geq 2$) is an ordered r-tuple of distinct indices $i_1, \ldots, i_r$ such that $\Lambda_{i_1} \prec \ldots \prec \Lambda_{i_r} \prec \Lambda_{i_1}$.*
2. *A 1-cycle is an index i such that $[W^u(\Lambda_i) \cap W^s(\Lambda_i)] - \Lambda_i \neq \emptyset$.*
3. *A filtration ordering is a numbering of the Λ_i so that $\Lambda_i \prec \Lambda_j \Rightarrow i \leq j$.*

As we can conclude from Definition 11, existence of an r-cycle with $r \geq 2$ is equivalent to existence of a heteroclinic cycle for (A.2) [52]. And existence of a 1-cycle implies existence of a homoclinic cycle for (A.2) [52].

Definition 12. *The set $\mathcal{W}$ is called decomposable if it admits a finite decomposition without cycles, $\mathcal{W} = \bigcup_{i=1}^{k} \mathcal{W}_i$, for some non-empty disjoint compact sets $\mathcal{W}_i$, which form a filtration ordering of $\mathcal{W}$, as detailed in definitions 10 and 11.*

Let a compact set $\mathcal{W} \subset M$ be containing all α- and ω-limit sets of (A.2) [14].

A.2 Robustness notions

The following robustness notions for systems in (A.1) have been introduced in [2].

Definition 13. *We say that the system (A.1) has the practical asymptotic gain (pAG) property if there exist $\eta \in \mathcal{K}_\infty$ [1]and a non-negative real q such that for all $x \in M$ and all measurable essentially bounded inputs $d(\cdot)$ the solutions are defined for all $t \geq 0$ and the following holds:*

$$\limsup_{t \to +\infty} |X(t, x; d)|_{\mathcal{W}} \leq \eta(\|d\|_\infty) + q. \tag{A.5}$$

If $q = 0$, then we say that the asymptotic gain (AG) property holds.

Definition 14. *We say that the system (A.1) has the limit property (LIM) with respect to $\mathcal{W}$ if there exists $\mu \in \mathcal{K}_\infty$ such that for all $x \in M$ and all measurable essentially bounded inputs $d(\cdot)$ the solutions are defined for all $t \geq 0$ and the following holds:*

$$\inf_{t \geq 0} |X(t, x; d)|_{\mathcal{W}} \leq \mu(\|d\|_\infty).$$

Definition 15. *We say that the system (A.1) has the practical global stability (pGS) property with respect to $\mathcal{W}$ if there exist $\beta \in \mathcal{K}_\infty$ and $q \geq 0$ such that for all $x \in M$ and all measurable essentially bounded inputs $d(\cdot)$ the following holds for all $t \geq 0$:*

$$|X(t, x; d)|_{\mathcal{W}} \leq q + \beta(\max\{|x|_{\mathcal{W}}, \|d\|_\infty\}).$$

It has been shown in [2] that to characterize (A.5) in terms of Lyapunov functions the following notion is appropriate:

Definition 16. *A $\mathcal{C}^1$ function $V : M \to \mathbb{R}$ is a practical ISS-Lyapunov function for (A.1) if there exists $\mathcal{K}_\infty$ functions $\alpha_1, \alpha_2, \alpha$ and γ, and scalar $q \geq 0$ and $c \geq 0$ such that*

$$\alpha_1(|x|_{\mathcal{W}}) \leq V(x) \leq \alpha_2(|x|_{\mathcal{W}} + c),$$

the function V is constant on each $\mathcal{W}_i$ and the following dissipative property holds:

$$DV(x) f(x, d) \leq -\alpha(|x|_{\mathcal{W}}) + \gamma(|d|) + q.$$

If the latter inequality holds for $q = 0$, then V is said to be an ISS-Lyapunov function.

Notice that the existence of α_2 and c follows (without any additional assumptions) by standard continuity arguments.

The main result of [2] connecting these robust stability properties is stated below:

Theorem 7. *Consider a nonlinear system as in (A.1) and let a compact invariant set containing all α and ω limit sets of (A.2) $\mathcal{W}$ be decomposable (in the sense of Definition 12). Then the following facts are equivalent.*

1. *The system admits an ISS Lyapunov function;*
2. *The system enjoys the AG property;*
3. *The system admits a practical ISS Lyapunov function;*
4. *The system enjoys the pAG property;*
5. *The system enjoys the LIM property and the pGS.*

A system in (A.1), for which this list of equivalent properties is satisfied, is called ISS with respect to the set $\mathcal{W}$ [2].

[1] A continuous function $h : [0, a) \to [0, \infty)$ belongs to class $\mathcal{K}$ if it is strictly increasing and $h(0) = 0$; it is said to belong to class $\mathcal{K}_\infty$ if $a = \infty$ and $h(r) \to \infty$ as $r \to \infty$ [73].

Appendix B

Output Stabilization of a Hydraulic Crane via ε-Invariant Homogeneous Approach with Dead Zone Compensation

B.1 Introduction

The problem of uniform stabilization of dynamical systems in the presence of uncertain bounded inputs has a rather long history [143]. By uniformity in this context we understand invariance (exact or approximate) of the closed-loop system with respect to disturbing inputs (disturbance rejection or cancellation are another names of that problem). Initiated by a French engineer Jean-Victor Poncelet [116], these ideas received a large attention in Soviet Union following the theory developed by Georgy Vladimirovich Shipanov [127], which is called the theory of ε-invariance (it was supposed to provide invariance up to $\varepsilon > 0$ deviations caused by disturbances of a given class). Next, many different solutions for ε-invariant stabilization have been proposed: time delay control [155], active disturbance rejection [57], universal integral controls [72, 46], various sliding-mode control algorithms [90, 41] converging in a finite time, model-free control [42] (just to mention a few, there are also many other adaptive/fuzzy/neural control solutions).

The statement of ε-invariant control design problem can be given following a recent development [42] (model-free control). Consider a SISO uncertain nonlinear system, whose model is given in the implicit form (it is not resolved with respect to the highest derivative):

$$f[y(t), \dot{y}(t), \ldots, y^{(n)}(t), u(t), d(t)] = 0, \ t \geq 0,$$

where $y(t) \in \mathbb{R}$ is the measured output, $u(t) \in \mathbb{R}$ is the control input, $d(t) \in \mathbb{R}^m$ is the vector of uncertain parameters/signals, $n \geq 1$ is the system dimension, which may be unknown, $f : \mathbb{R}^{n+m+1} \to \mathbb{R}$ is an unknown nonlinear function ensuring existence of the system solutions at least locally. Fixing $k \geq 1$, a local model can be extracted:

$$y^{(k)}(t) = u(t) + F(t),$$

where $F(t) \in \mathbb{R}$ is a new unknown input including $y, y^{(1)}, \dots, y^{(n)}$, u and d. If f is unknown such model can be obtained under mild assumption from the implicit function theorem. This model may have sense only locally, but under assumption that the dynamics of $y^{(k+1)}, \dots, y^{(n)}$ are stable (*i.e.* the system is minimum phase with relative degree k [72, 42]) the original stabilization problem for uncertain nonlinear system can be reduced to uniform (ε-invariant) stabilization of a chain of k integrators subjected by unknown matched input F. Frequently, some assumptions that F is bounded and it has a bounded derivative (at least locally) are additionally imposed.

There are many solutions to this problem, which are based on the idea that if it is possible to estimate $y^{(k)}(t)$ then $F(t) = y^{(k)}(t) - u(t)$ can be evaluated and compensated by the control. The difference is mainly in the tools used for estimation of $y^{(k)}(t)$ (high-gain observers in [72, 46], sliding-mode differentiators in [90, 41] or algebraic ones in [42]). Time delay is frequently introduced to break the algebraic loop [155, 7, 56, 62], which appears when using the estimate $y^{(k)}(t) - u(t)$ in the control $u(t)$ itself.

Another difference between [41, 42, 46, 72, 90] consists in the type of feedback used for the system stabilization. Theoretically sliding-mode controls provide a finite-time exact cancellation of matched disturbances [90, 41], which is better than ε-invariance provided by linear feedbacks from [42, 46, 72, 155]. But in practice the sliding-mode controls suffer from chattering that returns them back to ε-invariance setting. A related difference is robustness with respect to different nonlinearities of $y, y^{(1)}, \dots, y^{(n)}$ hidden in F (for example, linear feedback treats only Lipschitz or linear perturbations). In order to improve robustness and to avoid chattering, an intermediate solution should be proposed between linear and sliding modes.

Homogeneous high-gain controls [13] and observers [115] are nice candidates for such an improvement. Due to homogeneity, local asymptotic stability of this systems implies global one, and robustness with respect to disturbances is inherited next [11]. Adjusting nonlinear gains in control and estimation algorithms from [13, 115] it is possible to get a needed degree of robustness with respect to F.

A development of ε-invariant output control based on [13, 115] is presented in this work and it can be considered in the family of model free controls. This kind of control is widely used in several fields, from industrial processes [152] to robotics in which is applied for many applications, from motion control [136] to tracking problems for robotic arms [21, 84, 69]. Several works propose to increase the level of automation for hydraulic platforms [112, 154]; the approach developed is thus applied to control a specific link of an actuated industrial crane used in forestry. The aim is to achieve precision and smooth extension and retraction in a way that standard PID controller cannot guarantee [58] as it is shown in the experiments presented. In the treated example the telescopic link of the crane must track a reference trajectory using the proposed approach to compensate incertitudes due to a dead zone of the control input modeled as in [141] along with other perturbations.

B.2 Preliminaries

The following notations is used:

- $\mathbb{R}_+ = \{x \in \mathbb{R} : x \geq 0\}$, where $\mathbb{R}$ is the set of real number.
- $|\cdot|$ denotes the absolute value in $\mathbb{R}$, $\|\cdot\|$ denotes the Euclidean norm on $\mathbb{R}^n$.
- For a (Lebesgue) measurable function $d : \mathbb{R}_+ \to \mathbb{R}^m$ define the norm $||d||_{[t_0,t_1)} = \operatorname{ess\,sup}_{t\in[t_0,t_1)} \|d(t)\|$, then $||d||_\infty = ||d||_{[0,+\infty)}$ and the set of $d(t)$ with the

property $||d||_\infty < +\infty$ we further denote as $\mathcal{L}_\infty$ (the set of essentially bounded measurable functions).

- A continuous function $\alpha : \mathbb{R}_+ \to \mathbb{R}_+$ belongs to the class $\mathcal{K}$ if $\alpha(0) = 0$ and the function is strictly increasing. The function $\alpha : \mathbb{R}_+ \to \mathbb{R}_+$ belongs to the class $\mathcal{K}_\infty$ if $\alpha \in \mathcal{K}$ and it is unbounded. A continuous function $\beta : \mathbb{R}_+ \times \mathbb{R}_+ \to \mathbb{R}_+$ belongs to the class $\mathcal{KL}$ if $\beta(\cdot, t) \in \mathcal{K}_\infty$ for each fixed $t \in \mathbb{R}_+$ and $\lim_{t\to+\infty} \beta(s, t) = 0$ for each fixed $s \in \mathbb{R}_+$.
- $\lceil\cdot\rfloor^\alpha$ denotes the following operation $|\cdot|^\alpha \text{sign}(\cdot)$.
- The notation $DV(x)f(x)$ stands for the directional derivative of a continuously differentiable function V with respect to the vector field f evaluated at point x.

Following [28], consider a nonlinear system

$$\dot{x}(t) = f[x(t), d(t)], \tag{B.1}$$

where $x(t) \in \mathbb{R}^n$ is the state, $d(t) \in \mathbb{R}^m$ is the external input, $d \in \mathcal{L}_\infty$, and $f : \mathbb{R}^{n+m} \to \mathbb{R}^n$ is a locally Lipschitz (or Hölder) continuous function, $f(0, 0) = 0$. For an initial condition $x_0 \in \mathbb{R}^n$ and input $d \in \mathcal{L}_\infty$, define the corresponding solutions by $x(t, x_0, d)$ for any $t \geq 0$ for which the solution exists.

Definition 17. *The system (B.1) is called* input-to-state practically stable (ISpS)*, if for any input $d \in \mathcal{L}_\infty$ and any $x_0 \in \mathbb{R}^n$ there are some functions $\beta \in \mathcal{KL}$, $\gamma \in \mathcal{K}$ and $c \geq 0$ such that*

$$\|x(t, x_0, d)\| \leq \beta(\|x_0\|, t) + \gamma(||d||_{[0,t)}) + c \quad \forall t \geq 0.$$

The function γ is called nonlinear asymptotic gain*. The system is called* ISS *if $c = 0$.*

Definition 18. *A smooth function $V : \mathbb{R}^n \to \mathbb{R}_+$ is called* ISpS Lyapunov function *for the system (B.1) if for all $x \in \mathbb{R}^n$, $d \in \mathbb{R}^m$ and some $r \geq 0$, $\alpha_1, \alpha_2, \alpha_3 \in \mathcal{K}_\infty$ and $\theta \in \mathcal{K}$:*

$$\alpha_1(\|x\|) \leq V(x) \leq \alpha_2(\|x\|),$$
$$DV(x)f(x, d) \leq r + \theta(\|d\|) - \alpha_3(\|x\|).$$

Such a function V is called ISS Lyapunov function *if $r = 0$.*

Note that an ISS Lyapunov function can also satisfy the following equivalent condition for some $\chi \in \mathcal{K}$:

$$\|x\| > \chi(\|d\|) \Rightarrow DV(x)f(x, d) \leq -\alpha_3(\|x\|).$$

Theorem 8. *[28] The system (B.1) is ISS (ISpS) iff it admits an ISS (ISpS) Lyapunov function.*

B.2.1 Weighted homogeneity

Following [6], for fixed strictly positive numbers r_i, $i = 1, \ldots, n$ called weights and $\lambda > 0$, one can define:

- the *vector of weights* $\mathbf{r} = (r_1, \ldots, r_n)^T$, $r_{\max} = \max_{1\leq j\leq n} r_j$ and $r_{\min} = \min_{1\leq j\leq n} r_j$;

- the *dilation matrix* function $\Lambda_r(\lambda) = diag\{\lambda^{r_i}\}_{i=1}^n$, note that $\forall x \in \mathbb{R}^n$ and $\forall \lambda > 0$ we have $\Lambda_r(\lambda)x = (\lambda^{r_1}x_1, \dots, \lambda^{r_i}x_i, \dots, \lambda^{r_n}x_n)^T$.

Definition 19. *A function $g : \mathbb{R}^n \to \mathbb{R}$ is* **r**–homogeneous with degree $\mu \in \mathbb{R}$ *if $\forall x \in \mathbb{R}^n$ and $\forall \lambda > 0$ we have:*

$$\lambda^{-\mu} g(\Lambda_r(\lambda)x) = g(x).$$

A vector field $f : \mathbb{R}^n \to \mathbb{R}^n$ is **r**–homogeneous with degree $\nu \in \mathbb{R}$, *with $\nu \geq -r_{\min}$ if $\forall x \in \mathbb{R}^n$ and $\forall \lambda > 0$ we have:*

$$\lambda^{-\nu} \Lambda_r^{-1}(\lambda) f(\Lambda_r(\lambda)x) = f(x),$$

which is equivalent for i-th component of f being a **r**–*homogeneous function of degree $r_i + \nu$.*

The system (B.1) with $d = 0$ is **r**–*homogeneous of degree ν if the vector field f is* **r**–*homogeneous of degree ν.*

Theorem 9. *[122] For the system (B.1) with $d = 0$ and* **r**–*homogeneous and continuous function f the following properties are equivalent:*

- *the system (*B.1*) is (locally) asymptotically stable*;
- *there exists a continuously differentiable* **r**–*homogeneous Lyapunov function $V : \mathbb{R}^n \to \mathbb{R}_+$ such that*

$$\alpha_1(\|x\|) \leq V(x) \leq \alpha_2(\|x\|),\ DV(x)f(x,0) \leq -\alpha(\|x\|),$$
$$\lambda^{-\mu} V(\Lambda_r(\lambda)x) = V(x),\ \mu > r_{\max},$$

$\forall x \in \mathbb{R}^n$ and $\forall \lambda > 0$, for some $\alpha_1, \alpha_2 \in \mathcal{K}_\infty$ and $\alpha \in \mathcal{K}$.

Define

$$\tilde{f}(x,d) = [f(x,d)^T\ 0_m]^T \in \mathbb{R}^{n+m},$$

it is an extended auxiliary vector field for the system (B.1), where 0_m is the zero vector of dimension m.

Theorem 10. *[11] Let the vector field $\tilde{f}$ be homogeneous with the weights $\mathbf{r} = [r_1, \dots, r_n] > 0$, $\tilde{\mathbf{r}} = [\tilde{r}_1, \dots, \tilde{r}_m] > 0$ with a degree $\nu \geq -r_{\min}$, i.e. $f(\Lambda_r(\lambda)x, \Lambda_{\tilde{r}}(\lambda)d) = \lambda^\nu \Lambda_r(\lambda) f(x,d)$ for all $x \in \mathbb{R}^n$, $d \in \mathbb{R}^m$ and all $\lambda > 0$. Assume that the system (B.1) is globally asymptotically stable for $d = 0$, then the system (B.1) is ISS.*

Therefore, for homogeneous system (B.1) its ISS property follows asymptotic stability for $d = 0$ (as for linear systems [28]). The nonlinear asymptotic gain function has been also estimated in [11].

B.2.2 Homogeneous stabilizing control

Consider a nonlinear system

$$\begin{aligned} \dot{\xi}_i &= \xi_{i+1},\ i = 1, \dots, n-1, \\ \dot{\xi}_n &= -\sum_{i=1}^{n} a_i \lceil \xi_i \rfloor^{\alpha_i}, \end{aligned} \tag{B.2}$$

where $\xi = [\xi_1, \dots, \xi_n] \in \mathbb{R}^n$ is the state vector, α_i and a_i are real parameters. For $r_i = 1 + (i-1)\nu$ and $\alpha_i = \frac{1+n\nu}{1+(i-1)\nu}$, $i = 1, \dots, n$, where $\nu > -\frac{1}{n-1}$, the system (B.2) is **r**–homogeneous of degree ν.

Theorem 11. *[13] Let $a_1, \ldots, a_n$ form a Hurwitz polynomial, then there exists $0 < \varrho < \frac{1}{n-1}$ such that for any $\nu \in (-\frac{1}{n-1} + \varrho, 0)$ the system (B.2) with $\alpha_i = \frac{1+n\nu}{1+(i-1)\nu}$, $i = 1, \ldots, n$ is globally finite-time stable.*

Definition of finite-time stability can be found in [13, 106], roughly speaking it is a usual global asymptotic stability with convergence to the origin in a finite time dependent on initial conditions.

B.2.3 Homogeneous observer

Consider a nonlinear system

$$\begin{aligned} \dot{\xi}_i &= \xi_{i+1} - \lambda_i \lceil \xi_1 \rfloor^{\beta_i}, \ i = 1, \ldots, n-1, \\ \dot{\xi}_n &= -\lambda_n \lceil \xi_1 \rfloor^{\beta_n}, \end{aligned} \tag{B.3}$$

where $\xi = [\xi_1, \ldots, \xi_n] \in \mathbb{R}^n$ is the state vector, λ_i and β_i are real parameters. For $r_i = 1 + (i-1)\mu$ and $\beta_i = 1 + i\mu$ for all $i = 1, \ldots, n$, where $\mu > -\frac{1}{n}$, the system (B.3) is **r**–homogeneous of degree μ.

Theorem 12. *[115] Let $\lambda_1, \ldots, \lambda_n$ form a Hurwitz polynomial, then there exists $0 < \varrho < \frac{1}{n}$ such that for any $\mu \in (-\frac{1}{n} + \varrho, 0)$ the system (B.3) with $\beta_i = 1 + i\mu$, $i = 1, \ldots, n$ is globally finite-time stable.*

B.3 Problem statement

The following state-space representation will be considered in this work:

$$\begin{aligned} \dot{x}_i(t) &= x_{i+1}(t), \ i = 1, \ldots, k-1, \\ \dot{x}_k(t) &= u(t) + F(t), \ y(t) = x_1(t), \end{aligned} \tag{B.4}$$

where $x(t) = [x_1(t), \ldots, x_k(t)]^T \in \mathbb{R}^k$ is the state space vector of the system (B.4) at time instant $t \geq 0$; $u(t) \in \mathbb{R}$ and $F(t) \in \mathbb{R}$ are the control and disturbance inputs, respectively; $y(t) \in \mathbb{R}$ is the measured output. Since (B.4) is linear, then the measurement noise can be transferred to the input and included in F. The following restrictions are introduced for (B.4). Let $F \in \mathcal{L}_\infty$ and $\dot{F} \in \mathcal{L}_\infty$, in addition a constant $f > 0$ is given such that

$$||F||_\infty \leq f, \ ||\dot{F}||_\infty \leq f.$$

It is required to design a dynamical output feedback u such that for the given $\varepsilon > 0$ and all initial conditions $x_0 \in \mathbb{R}^k$,

$$\lim_{t \to +\infty} \|x(t)\| \leq \varepsilon$$

for all F satisfying Assumption C.3. The conditions of that assumption can also be relaxed supposing that F is a nonlinear function of x and asking for a semi-global ε-invariance.

B.4 Control design

First, the vector x has to be estimated. Due to the system structure this problem is equivalent to the estimation of the derivatives $y^{(1)}(t), \dots, y^{(k-1)}(t)$ for the output $y(t)$, for this purpose the following linear filter can be designed

$$\begin{aligned} \dot{z}_i &= z_{i+1} + l_i(y - z_1),\ i = 1, \dots, k-1, \\ \dot{z}_k &= l_k(y - z_1) + u, \end{aligned} \tag{B.5}$$

where $z = [z_1, \dots, z_k]^T \in \mathbb{R}^k$ and high-gain tuning parameters $l_i > 0$ for $i = 1, \dots, k$ form a Hurwitz polynomial (more precise restrictions on l_i will be given later). Denote $\hat{y}^{(i)}$ as an estimate of $y^{(i)} = x_{i+1}$, then we can select $\hat{y}^{(i)} = z_{i+1}$ for $i = 0, \dots, k-1$ and the filter estimation error $e = x - z$ has dynamics:

$$\begin{aligned} \dot{e}_i &= e_{i+1} - l_i e_1,\ i = 1, \dots, k-1, \\ \dot{e}_k &= -l_k e_1 + F. \end{aligned}$$

From the last equation the following estimate

$$\hat{F} = \hat{\dot{e}}_k + l_k e_1$$

of F can be calculated, where $\hat{\dot{e}}_k$ is an estimate of $\dot{e}_k$. In order to calculate $\hat{\dot{e}}_k$ a second filter/differentiator should be designed that has to converge faster than exponentially (the rate of decay in the linear one (B.5)). For this purpose a homogeneous high-gain differentiator can be used:

$$\begin{aligned} \dot{\zeta}_i &= \zeta_{i+1} - l_i e_1 + \lambda_i \lceil e_1 - \zeta_1 \rfloor^{\beta_i},\ i = 1, \dots, k, \\ \dot{\zeta}_{k+1} &= \lambda_{k+1} \lceil e_1 - \zeta_1 \rfloor^{\beta_{k+1}} + l_k l_1, \end{aligned} \tag{B.6}$$

where $\zeta = [\zeta_1, \dots, \zeta_k]^T \in \mathbb{R}^{k+1}$ and the tuning parameters $\beta_i > 0$ and $\lambda_i > 0$ for $i = 1, \dots, k+1$ will be derived later. Denote $\bar{e} = [e^T\ e_{k+1}]^T$, where

$$\begin{aligned} e_{k+1} &= -l_k e_1 + F, \\ \dot{e}_{k+1} &= -l_k \dot{e}_1 + \dot{F} = -l_k(e_2 - l_1 e_1) + \dot{F}, \end{aligned}$$

then we can select $\hat{\dot{e}}_k = \zeta_{k+1}$ and the estimation error $\epsilon = \bar{e} - \zeta$ has dynamics:

$$\begin{aligned} \dot{\epsilon}_i &= \epsilon_{i+1} - \lambda_i \lceil \epsilon_1 \rfloor^{\beta_i},\ i = 1, \dots, k, \\ \dot{\epsilon}_{k+1} &= -\lambda_{k+1} \lceil \epsilon_1 \rfloor^{\beta_{k+1}} - l_k e_2 + \dot{F}, \end{aligned}$$

which is **r**–homogeneous of order $\mu > -\frac{1}{k+1}$ for $r_i = 1 + (i-1)\mu$ and $\beta_i = 1 + i\mu$ for all $i = 1, \dots, k+1$ (if $\mu = -\frac{1}{k+1}$ then $\beta_{k+1} = 0$ and (B.6) reduces to a high-order sliding mode observer, while for all $\mu > -\frac{1}{k+1}$ the filter (B.6) stays continuous), i.e. a perturbed version of (B.3). Therefore,

$$\hat{F} = \zeta_{k+1} + l_k e_1. \tag{B.7}$$

Second, the control u can be introduced

$$u = -\sum_{i=0}^{k-1} a_{i+1} \left\lceil \hat{y}^{(i)} \right\rfloor^{\alpha_{i+1}} - \hat{F} = -\sum_{i=1}^{k} a_i \lceil z_i \rfloor^{\alpha_i} - \hat{F}, \tag{B.8}$$

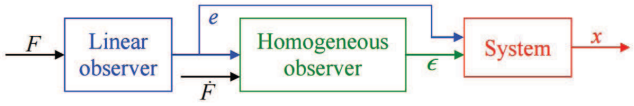

Figure B.1: Series cascade of e-subsystem, ϵ-subsystem and x-subsystem

where the coefficients a_i, $i = 1, \ldots, k$ form a Hurwitz polynomial and $\alpha_i > 0$, $i = 1, \ldots, k$ will be defined in the next section.

To conclude, the proposed model-free invariance control algorithm includes two filters (B.5) and (B.6) (one for differentiation and another for decoupling the control u and the estimate of F appearing into the same equation), the unknown input F estimate (B.7) and the stabilizing control (B.8).

B.5 Stability analysis

The dynamics of system (B.4) in closed loop with (B.5), (B.6), (B.7) and (B.8) can be analyzed in the coordinates $(x, e, \epsilon) \in \mathbb{R}^{3k+1}$:

$$\begin{aligned}
\dot{x}_i &= x_{i+1},\ i = 1, \ldots, k-1,\\
\dot{x}_k &= -\sum_{i=1}^{k} a_i \lceil x_i - e_i \rfloor^{\alpha_i} + F - \hat{F}\\
&= -\sum_{i=1}^{k} a_i \lceil x_i - e_i \rfloor^{\alpha_i} + F - \zeta_{k+1} - l_k e_1\\
&= -\sum_{i=1}^{k} a_i \lceil x_i - e_i \rfloor^{\alpha_i} + \epsilon_{k+1};
\end{aligned}$$

$$\begin{aligned}
\dot{\epsilon}_i &= \epsilon_{i+1} - \lambda_i \lceil \epsilon_1 \rfloor^{\beta_i},\ i = 1, \ldots, k,\\
\dot{\epsilon}_{k+1} &= -\lambda_{k+1} \lceil \epsilon_1 \rfloor^{\beta_{k+1}} - l_k e_2 + \dot{F};
\end{aligned}$$

$$\begin{aligned}
\dot{e}_i &= e_{i+1} - l_i e_1,\ i = 1, \ldots, k-1,\\
\dot{e}_k &= -l_k e_1 + F.
\end{aligned}$$

Note that, for $e = 0$ and $\epsilon_{k+1} = 0$, x-subsystem is $\mathbf{r}$–homogeneous of degree $\nu > -\frac{1}{k-1}$ for $r_i = 1 + (i-1)\nu$ and $\alpha_i = \frac{1+k\nu}{1+(i-1)\nu}$, $i = 1, \ldots, k$, *i.e.* a version of (B.2). Therefore, considering $(F, \dot{F})$ as an extended input, we have above a series cascade of e-subsystem, ϵ-subsystem and x-subsystem (Fig. B.1).

Denote

$$l = [l_1, \ldots, l_k]^T,\ A_k = \begin{bmatrix} 0 & 1 & 0 \ldots 0 & 0\\ \vdots & \vdots & \ddots & \vdots\\ 0 & 0 & 0 \ldots 0 & 1\\ 0 & 0 & 0 \ldots 0 & 0 \end{bmatrix} \in \mathbb{R}^{k \times k},$$

$$c_k = [1\ 0\ \ldots\ 0] \in \mathbb{R}^k,\ b_k = [0\ 0\ \ldots\ 1]^T \in \mathbb{R}^k,$$

if there exist $l \in \mathbb{R}^k$ and a matrix $P_l = P_l^T > 0$ satisfying the inequality

$$(A_k - lc_k)^T P_l + P_l(A_k - lc_k) + \gamma_l^{-1} P_l b_k b_k^T P_l + I_k < 0$$

for some $\gamma_l > 0$ with identity matrix $I_k \in \mathbb{R}^{k\times k}$, then e-subsystem is asymptotically stable and has L_∞ gain of the transfer $F \to e$ less than γ_l (the system is ISS with the asymptotic gain $\gamma(s) = \gamma_l s$).

Similarly, denote

$$\lambda = [\lambda_1, \dots, \lambda_{k+1}]^T \mathbb{R}^{k+1},\ a = [a_1, \dots, a_k]^T \in \mathbb{R}^k,$$

let λ and a are selected in such a way that the inequalities

$$\begin{gathered}(A_{k+1} - \lambda c_{k+1})^T P_\lambda + P_\lambda(A_{k+1} - \lambda c_{k+1}) \\ +\gamma_\lambda^{-1} P_\lambda b_{k+1} b_{k+1}^T P_\lambda + I_{k+1} < 0, \\ (A_k - ac_k)^T P_a + P_a(A_k - ac_k) + \gamma_a^{-1} P_a b_k b_k^T P_a + I_k < 0\end{gathered}$$

are satisfied for $P_\lambda = P_\lambda^T > 0$, $P_a = P_a^T > 0$ and some $\gamma_\lambda > 0$, $\gamma_a > 0$. The ϵ-subsystem subsystem for $e_2 = 0$ and $\dot{F} = 0$ has the form of (B.3), thus there exists a choice of $\mu > -\frac{1}{k+1}$ and β_i following the recommendations of Theorem 12 such that it is globally finite-time (asymptotically) stable. Next, it is easy to check applying Theorem 10 that it is also ISS with respect to e_2 and $\dot{F}$. Decreasing the value of γ_λ and recalculating λ it is possible to adjust the asymptotic gain of ϵ-subsystem.

For x-subsystem, since for $e = 0$ and $\epsilon_{k+1} = 0$ it has the form of (B.2), applying Theorem 11 we can conclude that there exists a selection of $\nu > -\frac{1}{k-1}$ and α_i such that this subsystem is globally finite-time (asymptotically) stable for $e = 0$ and $\epsilon_{k+1} = 0$. Then similarly from Theorem 10 we can substantiate ISS property with respect to inputs e and ϵ_{k+1}. Adjusting γ_a and a it is possible to decrease the asymptotic gain of x-subsystem. Finally, the global stability and ISS follows due to the serial structure of interconnection of these subsystems [28], see Fig. B.1.

Therefore, the following result has been proven.

Theorem 13. *Let Assumption C.3 be satisfied. Then for any given $\epsilon > 0$ there exist $l \in \mathbb{R}^k$, $\lambda \in \mathbb{R}^{k+1}$, $a \in \mathbb{R}^k$, $\mu \in (-\frac{1}{k+1}, 0)$, $\nu \in (-\frac{1}{k-1}, 0)$, $\beta_i = 1 + i\mu$ for $i = 1, \dots, k+1$, $\alpha_i = \frac{1+k\nu}{1+(i-1)\nu}$ for $i = 1, \dots, k$, such that in the system (B.4) with the output regulator (B.5)–(B.8) for all initial conditions*

$$\lim_{t\to+\infty} \|x(t)\| \le \varepsilon,$$

and $x \in \mathcal{L}_\infty^k$, $z \in \mathcal{L}_\infty^k$, $\zeta \in \mathcal{L}_\infty^{k+1}$. Moreover, the system (B.4), (B.5)–(B.8) is ISS with respect to the input $(F, \dot{F})$.

Since dynamics of all variables, $x(t)$, $\epsilon(t)$ and $e(t)$, are homogeneous, their asymptotic gains can be evaluated as it is proposed in [3] and using the parameters γ_l, γ_λ and γ_a. Finally, for given f the value of $\varepsilon(t)$ can be estimated. Since (B.6) and (B.8) contain nonlinear gains, then the asymptotic gain of (B.4), (B.5)–(B.8) (see [11] for an algorithm of its estimation) close to the origin is better than in a pure linear system (*i.e.* replacing (B.6) and (B.8) by linear filter and feedback, respectively).

B.6 Dead zone compensation

We are going to present the compensation of an input nonlinearity, known as a dead zone, which is depicted in Fig. B.2. This dead zone model is a static representation of diverse physical phenomena with negligible fast dynamics, see [141]. One well-known example is the model of an industrial electro-hydraulic valve in which the spool occludes the orifice with some overlap. In this case, system (B.4) should be rewritten as below:

$$\begin{aligned} \dot{x}_i(t) &= x_{i+1}(t),\ i = 1, \ldots, k-1, \\ \dot{x}_k(t) &= D(u(t)) + F(t),\ y(t) = x_1(t), \end{aligned} \tag{B.9}$$

where the dead zone input is represented by $D(u(t))$ and it has the following structure:

$$D(u(t)) = \begin{cases} m_r(u - b_r) & \text{if} \quad u \geq b_r, \\ 0 & \text{if} \quad -b_l \leq u \leq b_r, \\ m_l(u - b_l) & \text{if} \quad u \leq -b_l. \end{cases} \tag{B.10}$$

where $m_i = m_0 + \Delta m_i$ and $b_i = b_0 + \Delta b_i$, with $i = l, r$; the subscript l stands for "left" and r for "right", m_0 and b_0 are the nominal values while Δm_i and Δb_i are uncertain terms.

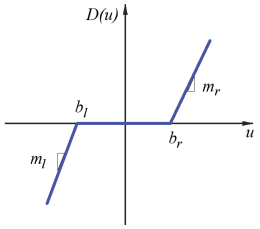

Figure B.2: Dead zone input nonlinearity.

Let $u_0(t)$ be the control signal from a model-free invariance control design. Then, our approach is based on the design of a nominal dead zone inverse, $DI(u_0(t))$, where the remaining uncertain terms Δm_i and Δb_i will be canceled by the invariance control algorithm. For this aim the nominal parameters m_0 and b_0 are assumed to be known and they are used for the construction of a static nominal dead zone inverse:

$$u(t) = DI(u_0(t)) = m_0^{-1}\left(u_0(t) + m_0\, b_0\ \text{sign}(u_0)\right). \tag{B.11}$$

Substituting (B.11) in (B.9) we obtain the following dynamics:

$$\begin{aligned} \dot{x}_i(t) &= x_{i+1}(t),\ i = 1, \ldots, k-1, \\ \dot{x}_k(t) &= u_0(t) + F_0(t),\ y(t) = x_1(t), \end{aligned} \tag{B.12}$$

where $u_0(t)$ is the final control input and $F_0(t)$ represents a perturbation containing new terms related with the uncertain parameters of a dead zone. Note that the inverse of a dead zone is a relay-type discontinuity that can be canceled if the inverse is exact, see [141]. Besides, with a nominal dead zone inverse the structure of system (B.4) is recovered and the uncertain terms are to be compensated by a model free invariance controller.

B.7 Hydraulic Actuator Case Study

The experimental setup is the telescopic link of a laboratory prototype of a typical industrial hydraulic forestry crane. Such industrial equipment is widely used in forestry and is a subject of many researches aimed at automation of these systems, see [112].

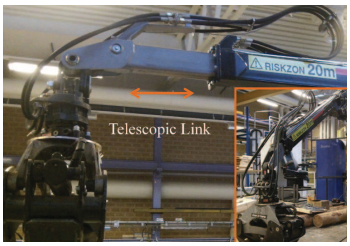

Figure B.3: Industrial hydraulic forestry crane.

Some physical parameters of the link are given in Table B.1.

Table B.1: Physical parameters of the link

A_a, m^2	A_b, m^2	V_{a0}, m^3	V_{b0}, m^3
$1.26 \cdot 10^{-3}$	$0.76 \cdot 10^{-3}$	$0.012 \cdot 10^{-3}$	$1.19 \cdot 10^{-3}$
p_t, Pa	p_s, Pa	$\bar{q}$, l/min	β, Pa
$5 \cdot 10^5$	$180 \cdot 10^5$	90	$17 \cdot 10^8$
m, kg	$\bar{f}_h$, N	$\bar{x}_p$, m	$\bar{x}_v$, m/s
200	8000	1.55	0.94

The telescopic link of the crane, see Fig. B.3, consists of a double-acting single-side hydraulic cylinder and a solid load, which is attached to a piston of the cylinder. Position of the link, x, varies from 0 to 1.55m; positive velocity $\dot{x}$ corresponds to extraction of the cylinder. This link can be described as a restricted 1-DOF mechanical system actuated by a hydraulic force, and the equation of motion is

$$m\ddot{x} = f_h - f_{grav} - f_{fric}, \tag{B.13}$$

where m is the mass, f_h is the force generated by the hydraulics, f_{grav} is the gravity and f_{fric} is the friction force. The force generated by the hydraulics is controlled via a current signal to the valve of the cylinder and it is given by

$$f_h = \begin{cases} p_a\, A_a - p_b\, A_b, & \text{if variables are in } R, \\ f_{uncertain}, & \text{otherwise,} \end{cases} \tag{B.14}$$

where the validity region

$$R = \{x \in (0, \bar{x}_p), \quad |\dot{x}| < \bar{x}_v, \quad p_a, p_b \in (p_t, p_s)\}, \tag{B.15}$$

is defined by certain constant bounds, see Table B.1; p_s is the pump pressure, and p_t is the return (exit) pressure; the piston areas A_a and A_b are known geometric parameters; p_a and p_b are the measured pressures in chambers A and B of the cylinder.

The friction and gravity terms are considered as unknown perturbations.

Note that the position of the link, x, is limited by geometrical constrains, the velocity is limited by the maximum achievable flow from a pump, pressures are limited through a set of service anti-cavitation and pressure-relief valves, which, in particular, ensure $p_t \leq p_i \leq p_s$, $i = a, b$. These devices play a fault-preventing role and do not influence a normal operation. Moreover, the initial conditions are within the region R and $f_{uncertain}$ prevent from leaving the region.

The dynamics of the pressures can be modeled, see [102, Sec. 3.8], by:

$$\begin{array}{ll} \dot{p}_a = \frac{\beta}{V_a(x)}\,(-\dot{x}\,A_a + q_a)\,, & \text{if variables are in } R, \\ \dot{p}_b = \frac{\beta}{V_b(x)}\,(\dot{x}\,A_b - q_b)\,, & \text{if variables are in } R, \\ \dot{p}_i = p_{uncertain},\ \ i = a, b & \text{otherwise,} \end{array} \tag{B.16}$$

and initial conditions $p_{a,b}(0) \in (p_t, p_s)$; $V_a(x) = V_{a0} + x\,A_a$ and $V_b(x) = V_{b0} - x\,A_b$ are volumes of the chambers A and B at the given piston position x, V_{a0} and V_{b0} are known geometric constants, β is a known bulk modulus, q_a and q_b are flows to the chamber A and from the chamber B. The flow q_a is positive when the oil goes into chamber A, and the flow q_b is positive when the oil goes out of chamber B.

Following [102, 108], the nonlinear equations describing the fluid flow distribution in the valve can be written, in their simplest forms, as: $q_a = c_a\,S_a(x_s)\,\sqrt{p_s - p_a}$ and $q_b = c_b\,S_b(x_s)\,\sqrt{p_b - p_t}$ for $x_s \geq 0$; $q_a = -c_a\,S_a(x_s)\,\sqrt{p_a - p_t}$ and $q_b = -c_b\,S_b(x_s)\,\sqrt{p_s - p_b}$ for $x_s < 0$. Here c_a and c_b are constant coefficients which depend on physical values (fluid density, discharge coefficient and other), $S_a(x_s)$ and $S_b(x_s)$ are (non-negative) areas of orifices for the ports A and B, x_s is a displacement of a spool inside a valve, this spool is actuated by an electromagnetic actuator where an input (current) signal u is applied, $u \in [-u^-, u^+]$. Assuming that the valve is symmetric, i.e. $\forall x_s : S_a(x_s) = S_b(x_s)$, we introduce the signed area function $S(x_s)$ given by $S(x_s) = S_a(x_s)\,\mathrm{sign}(x_s) = S_b(x_s)\,\mathrm{sign}(x_s)$. The absolute value of this function is equal to the area of the orifices and the sign indicates directions of the flows. Then, the flow equations can be rewritten as: $q_a = c_a\varphi_a S(x_s)$ and $q_b = c_b\varphi_b S(x_s)$, with: $\varphi_a = \sqrt{p_s - p_a}\frac{(\mathrm{sign}(x_s)+1)}{2} - \sqrt{p_a - p_t}\frac{(\mathrm{sign}(x_s)-1)}{2}$ and $\varphi_b = \sqrt{p_b - p_t}\frac{(\mathrm{sign}(x_s)+1)}{2} - \sqrt{p_s - p_b}\frac{(\mathrm{sign}(x_s)-1)}{2}$. Note that in industrial hydraulic systems a nonzero pressure difference through the valve is ensured by a set of service valves, *i.e.* $\varphi_a \geq 0$ and $\varphi_b \geq 0$. Taking into account a high-response servo valve and assuming that the spool displacement is proportional to the input signal, the signed area can be modeled as defined by the input signal u through a nonlinear static relation $S(x_s) = D(u)$. The shape of the function D strongly depends on a type of the valve; for industrial heavy-duty systems a dead-zone due to a leakage-preventing closed-center spool and a saturation due to limiting screws are common, see [3] and references therein. Taking the derivative of (B.14) and substituting (B.16), one obtains:

$$\dot{f}_h = -\varphi_0\dot{x} + \varphi_1 D(u), \tag{B.17}$$

where $\varphi_0 = \beta(\frac{A_a^2}{V_a(x)} + \frac{A_b^2}{V_b(x)})$ and $\varphi_1 = \beta(\frac{c_a A_a \varphi_a}{V_a(x)} + \frac{c_b A_b \varphi_b}{V_b(x)})$ with $0 < \underline{\varphi_i} \leq \varphi_i \leq \overline{\varphi_i}$ for $i = 0, 1$. Besides, the nonlinear function $D(u)$ can be represented by (B.10). Since $\dot{f}_h$ is bounded, sytem (B.17) can be rewritten as:

$$\dot{x} = \varphi D(u) - \varphi_0^{-1}\dot{f}_h, \tag{B.18}$$

where $\varphi = \frac{\varphi_1}{\varphi_0}$ and $\varphi = \bar{\varphi} + \Delta\bar{\varphi}$. Given an appropriate desired trajectory for (B.15), x_{ref}, with Lipschitz continuous second derivative, $\ddot{x}_{ref}$, the objective of this section is to design a control law for u to achieve the tracking of the cylinder position x.

B.7.1 Control Design for a First Order System

Let us consider a first order case, $k = 1$, together with the inverse dead zone compensation (B.11), $u = D^{-1}(u_0)$. Let x_d be the desired trajectory, defining the tracking error $e_d = x - x_d$:

$$\dot{e}_d = \bar{\varphi}u_0 + F_1 - \dot{x}_d.$$

Now consider the control input $u = \bar{\varphi}^{-1}(v + \dot{x}_d)$, where v is to be designed. Then, the estimation of e_d is given by a high-gain observer:

$$\dot{z} = le + v,$$

where $e = e_d - z$ and $\dot{e} = -le + F_1$. Setting $e_1 = e$ and $e_2 = \dot{e}$, we obtain $\dot{e}_2 = -le_2 + \dot{F}_1$. In order to estimate $\dot{e}$, the next homogeneous high gain differentiator is proposed:

$$\dot{\zeta}_1 = \zeta_2 - \lambda_1 \lceil \epsilon_1 \rfloor^{\beta_1} - l_1\epsilon_1,$$
$$\dot{\zeta}_2 = -\lambda_2 \lceil \epsilon_1 \rfloor^{\beta_2} - l_2\epsilon_2,$$

where $\epsilon_1 = e_1 - \zeta_1$and $\epsilon_2 = e_2 - \zeta_2$, obtaining the following error dynamics:

$$\dot{\epsilon}_1 = \epsilon_2 - \lambda_1 \lceil \epsilon_1 \rfloor^{\beta_2} - l_1\epsilon_1,$$
$$\dot{\epsilon}_2 = -\lambda_2 \lceil \epsilon_1 \rfloor^{\beta_2} - l_2\epsilon_2 - le_2 + \dot{F}_1.$$

Finally the estimate $\hat{F}_1$ is obtained: $\hat{F}_1 = \zeta_2 + le_1$, and the control law for the first order system is constructed as follows:

$$v = -a_1 \lceil z \rfloor^{\alpha_1} - \hat{F}_1. \tag{B.19}$$

B.7.2 Experiments

In this subsection the performances of the proposed approach will be implemented on the robotic crane presented above.

The experiments are carried out using a real-time platform dSpace 1401 with sample time of 1ms using forward Euler integration method. The position of the telescopic link is measured with a wire-actuated encoder which provides 2381 counts for the range from 0 to 1.55m with a quantization interval of $Q = 0.651\text{mm}$. The desired trajectory is selected as a sinusoidal signal: $x_d = 0.8 + 0.4\sin(\omega t)$. In the experiments the values used for the dead zone compensation (B.11) are $m_0 = 1$ and $b_0 = 0.3$; being such values the nominal ones, the controller should be able to compensate the gap between nominal and real values, namely compensate the remaining uncertain terms Δm_i and Δb_i along with other perturbations. Firstly (Fig. B.4), after tuning the a_1, λ_1 and l coefficients, let us examine the performances of the controller varying the parameter α_1 which determines the non-linearity of the controller and evaluating the effect of the $\hat{F}_0$ estimate. It can be seen how the error in the tracking is smaller decreasing α_1

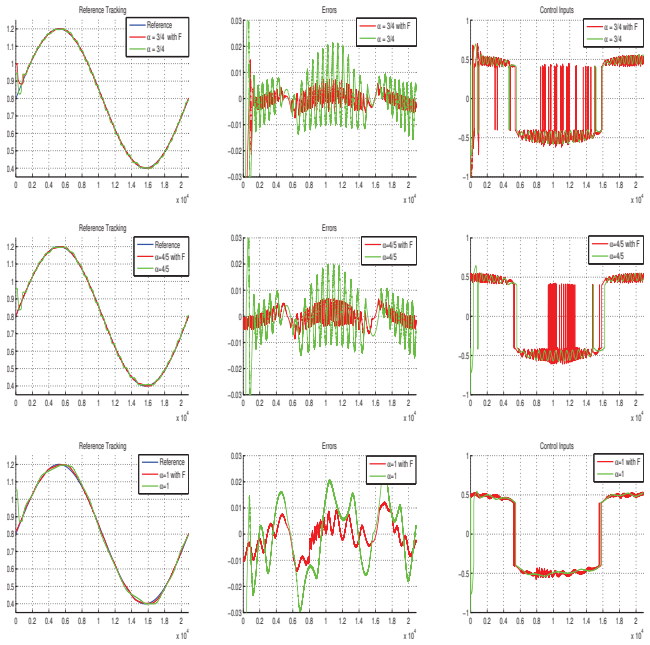

Figure B.4: Experimental results on the telescopic link with controller (B.19) with sample time $ts = 1ms$, $a_1 = 2$, $\lambda = 45$, $l = 80$, $\omega = 0.3$ varying α_1. (x-axis in samples, y-axis in meter)

and even smaller adding the $\hat{F}_0$ compensation, which proves clearly the efficiency of the method; it is worth to remark thought that a high frequency oscillatory behavior present in the error (and control input) for $\alpha_1 < 1$ which is not desirable in the application considered. An α_1 equal or close to one had to be chosen to avoid it. The closest α_1 to 1 the faster the oscillations, which are not propagated from the control input to the telescopic link guaranteeing a smooth extension or retraction. To lay stress on the good performances of the method, Fig. B.5 shows the behavior of the controller (B.19) in comparison with a standard PI approach often used to regulate such a system. It can be seen that although the integral action applied, the link could not follow the reference as well as the homogeneous control which does not have what appears to be a static error with respect to the reference; that it could be caused by the nominal values used for the dead zone compensation. As stated above the homogeneous controller is able to handle the error between nominal and real values, that's not achieved with the PI control despite the tuning to have the best behavior possible.

B.8 Conclusion

This paper presented the synthesis of a control method for system which can be described as in (B.4). A linear filter allows the decoupling of the control variables and the disturbances, which are afterward estimated starting from the estimation error using a homogeneous high gain observer. The estimation of perturbations is then included in the controller to compensate them. The approach is fully proven theoreti-

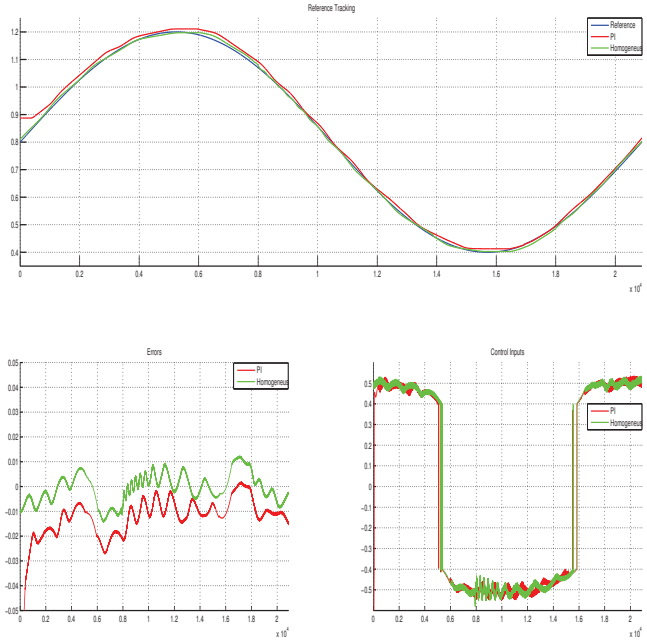

Figure B.5: Comparison between the Homogeneous controller and the PI approach. (x-axis in samples, y-axis in meter)

cally then applied on the telescopic link of a hydraulic actuated robotic crane used in forestry. To deal with such a platform an easy but effective dead zone compensation technique has been implemented; such a compensation relies just on nominal parameters. The proposed controller behaves as expected, compensating perturbations and dead zone incertitudes, and outperforming the standard PI control as it is shown with experiments.

Appendix C

On-line Differentiation: Error Estimation using Interval Observer

C.1 Introduction

State estimation is an important problem in many areas of the control engineering science dealing with plant regulation, synchronization or fault detection [12, 103, 44]. In many cases, if the model of the system is highly uncertain, then a design of conventional Luenberger-like observers is not possible and various model-free estimation techniques can be used [42]. Many of them are based on estimation of derivatives since a large class of systems can be transformed in output canonical forms where the state is represented as the output and its derivatives. That is why many differentiation algorithms are proposed in the literature [51], some of them have a form of nonlinear (Luenberger-like) observer [89, 115, 146]. One of the main characteristics of differentiators is their sensitivity or robustness with respect to measurement noise, for almost all existing differentiation techniques there exist estimates providing qualitative [89, 115], and sometimes quantitative [146], estimates of errors caused by a non-differentiable noise presence. Even existent, these estimates are a kind of "worst-case asymptotic" bounds, and more accurate derivations are appreciated in applications.

Interval observers, proposed in [50] and developed for instance in [39, 23, 36, 38, 100, 104], follow the ideas of set-membership estimation theory [68, 77], where for each instant of time a set of admissible values for the state vector is evaluated. The diameter of this set is proportional to the system uncertainty. Thus, the interval observers generate the estimate of the state and simultaneously evaluate the current error of this estimation.

The objective of this work is to propose an interval observer for estimation error of differentiators from [89, 115, 146], Super Twisting (ST), Homogeneous Differentiator (HOMD) and High Gain Differentiator (HGD) respectively. The coefficients of these nth order differentiators have to be tuned taking into account the maximum value of the $n+1$ derivative of the signal to be differentiated, which is a kind of uncertain signal in the differential equations of estimation error. Another source of uncertainty is the measurement noise, which is supposed to be almost bounded with a known upper and lower bound (*i.e.* bounded for all t for a set of zero Lebesgue measure). Taking all these constraints, the interval observer has to evaluate on-line the set of admissible

values for the error of differentiation.

To show the effectiveness of the proposed approach an on-line estimation of the extension velocity is carried out for the telescopic link of a hydraulic actuated industrial crane in which just the position can be measured. Such industrial equipment is widely used in forestry and the automation of tasks is the subject of many researches [112].

C.2 Preliminaries

Euclidean norm for a vector $x \in \mathbb{R}^n$ will be denoted as $|x|$, and for a measurable and locally essentially bounded input $u : \mathbb{R}_+ \to \mathbb{R}$ ($\mathbb{R}_+ = \{\tau \in \mathbb{R} : \tau \geq 0\}$) the symbol $||u||_{[t_0,t_1]}$ denotes its L_∞ norm:

$$||u||_{[t_0,t_1]} = ess\sup\{|u(t)|, t \in [t_0, t_1]\},$$

if $t_1 = +\infty$ then we will simply write $||u||$. We will denote as $\mathcal{L}_\infty$ the set of all inputs u with the property $||u|| < \infty$. Denote the sequence of integers $1, ..., k$ as $\overline{1,k}$. The symbols I_n, $E_{n\times m}$ and E_p denote the identity matrix with dimension $n \times n$, the matrix with all elements equal 1 with dimensions $n \times m$ and $p \times 1$ respectively. For a matrix $A \in \mathbb{R}^{n\times n}$ the vector of its eigenvalues is denoted as $\lambda(A)$.

For two vectors $x_1, x_2 \in \mathbb{R}^n$ or matrices $A_1, A_2 \in \mathbb{R}^{n\times n}$, the relations $x_1 \leq x_2$ and $A_1 \leq A_2$ are understood elementwise. The relation $P \prec 0$ ($P \succ 0$) means that the matrix $P \in \mathbb{R}^{n\times n}$ is negative (positive) definite. Given a matrix $A \in \mathbb{R}^{m\times n}$, define $A^+ = \max\{0, A\}$, $A^- = A^+ - A$ (similarly for vectors) and denote the matrix of absolute values of all elements by $|A| = A^+ + A^-$.

Lemma 9. [37] *Let $x \in \mathbb{R}^n$ be a vector variable, $\underline{x} \leq x \leq \overline{x}$ for some $\underline{x}, \overline{x} \in \mathbb{R}^n$.*

(1) *If $A \in \mathbb{R}^{m\times n}$ is a constant matrix, then*

$$A^+\underline{x} - A^-\overline{x} \leq Ax \leq A^+\overline{x} - A^-\underline{x}. \tag{C.1}$$

(2) *If $A \in \mathbb{R}^{m\times n}$ is a matrix variable and $\underline{A} \leq A \leq \overline{A}$ for some $\underline{A}, \overline{A} \in \mathbb{R}^{m\times n}$, then*

$$\begin{aligned} \underline{A}^+\underline{x}^+ - \overline{A}^+\underline{x}^- - \underline{A}^-\overline{x}^+ + \overline{A}^-\overline{x}^- \leq Ax \\ \leq \overline{A}^+\overline{x}^+ - \underline{A}^+\overline{x}^- - \overline{A}^-\underline{x}^+ + \underline{A}^-\underline{x}^-. \end{aligned} \tag{C.2}$$

A matrix $A \in \mathbb{R}^{n\times n}$ is called Hurwitz if all its eigenvalues have negative real parts, it is called Metzler if all its elements outside the main diagonal are nonnegative. Any solution of linear system

$$\begin{aligned} \dot{x} = Ax + B\omega(t),\ \omega : \mathbb{R}_+ \to \mathbb{R}^q_+, \\ y = Cx + D\omega(t), \end{aligned} \tag{C.3}$$

with $x \in \mathbb{R}^n$, $y \in \mathbb{R}^p$ and a Metzler matrix $A \in \mathbb{R}^{n\times n}$, is elementwise nonnegative for all $t \geq 0$ provided that $x(0) \geq 0$ and $B \in \mathbb{R}^{n\times q}_+$ [40, 131]. The output solution $y(t)$ is nonnegative if $C \in \mathbb{R}^{p\times n}_+$ and $D \in \mathbb{R}^{p\times q}_+$. Such dynamical systems are called cooperative (monotone) or nonnegative if only initial conditions in $\mathbb{R}^n_+$ are considered [40, 131].

The L_1 and L_∞ gains for nonnegative systems (C.3) have been studied in [16, 34], for this kind of systems these gains are interrelated.

Lemma 10. [16, 34] *Let the system (C.3) be nonnegative (i.e. A is Metzler, $B \geq 0$, $C \geq 0$ and $D \geq 0$), then it is asymptotically stable if and only if there exist $\lambda \in \mathbb{R}^n_+ \setminus \{0\}$ and a scalar $\gamma > 0$ such that the following Linear Programming (LP) problem is feasible:*

$$\begin{bmatrix} A\lambda + BE_q \\ C\lambda - \gamma E_p + DE_q \end{bmatrix} < 0.$$

Moreover, in this case the L_∞ gain of the operator $\omega \to y$ is lower than γ.

The conventional results and definitions on L_2/L_∞ stability for linear systems can be found in [74].

C.3 Interval differentiator

The differentiators from [89, 115, 146] can be presented in the following generalized form:

$$\begin{aligned} \dot{x}_i(t) &= -\chi_i[t, x_1(t) - y(t)] + x_{i+1}(t),\ i = \overline{1,n}; \\ \dot{x}_{n+1}(t) &= -\chi_{n+1}[t, x_1(t) - y(t)], \\ y(t) &= f(t) + v(t),\ t \geq 0, \\ x_1(0) &= y(0),\ x_k(0) = 0,\ k = \overline{2,n+1}, \end{aligned} \tag{C.4}$$

where $x(t) = [x_1(t), \ldots, x_{n+1}(t)] \in \mathbb{R}^{n+1}$ is the differentiator state; $y(t) \in \mathbb{R}$ is the signal available for measurements, $f(t) \in \mathbb{R}$ is the signal to be differentiated n times and it is supposed that it has $n+1$ derivatives; $v(t) \in \mathbb{R}$ is the measurement noise, $v \in_\infty$; the locally bounded functions $\chi_i : \mathbb{R}^2 \to \mathbb{R}$ are varying depending on the differentiator. It is supposed that $x_i(t)$ corresponds to an estimate of $f^{(i-1)}(t)$ for $i = \overline{1,n+1}$, and also the following assumptions are adopted in this work. There is a known $V > 0$ such that $|v(t)| \leq V$ for almost all $t \geq 0$.

There are known functions $\underline{f}^{(j)}, \overline{f}^{(j)} \in_\infty$, $j = \overline{0,n}$ such that for almost all $t \geq 0$

$$\begin{aligned} \underline{f}^{(j)}(0) \leq f^{(j)}(0) \leq \overline{f}^{(j)}(0). \\ \underline{f}^{(n+1)}(t) \leq f^{(n+1)}(t) \leq \overline{f}^{(n+1)}(t). \end{aligned}$$

Under these assumptions we are going to design an interval observer for differentiation errors

$$e_i(t) = x_i(t) - f^{(i-1)}(t),\ i = \overline{1,n+1},$$

first for a generic order n, and next this solution will be detailed for $n = 1$. Define $e = [e_1, \ldots, e_{n+1}]$.

C.3.1 High order case

The dynamics of differentiation errors can be presented as follows:

$$\begin{aligned} \dot{e}_i(t) &= -\chi_i[t, e_1(t) + v(t)] + e_{i+1}(t),\ i = \overline{1,n}; \\ \dot{e}_{n+1}(t) &= -\chi_{n+1}[t, e_1(t) + v(t)] - f^{(n+1)}(t), \\ \underline{e}_0 &\leq e(0) \leq \overline{e}_0, \\ \underline{e}_0 &= [-V, -\overline{f}^{(1)}(0) \ldots, -\overline{f}^{(n)}(0)], \\ \overline{e}_0 &= [V, -\underline{f}^{(1)}(0) \ldots, -\underline{f}^{(n)}(0)], \end{aligned}$$

where the signal $\psi(t) = e_1(t) + v(t)$ is available for measurements, or equivalently

$$\dot{e}_i(t) = \rho_i[t, \psi(t)] - a_i e_1(t) + a_i v(t) + e_{i+1}(t),\ i = \overline{1,n};$$
$$\dot{e}_{n+1}(t) = \rho_{n+1}[t, \psi(t)] - a_{n+1} e_1(t) + a_{n+1} v(t) - f^{(n+1)}(t),$$

where $\rho_i[t, \psi(t)] = a_i \psi(t) - \chi_i[t, \psi(t)]$ for $i = \overline{1, n+1}$ and the coefficients $a = [a_1, \ldots, a_{n+1}]$ satisfy the following requirement. The matrix

$$A = \begin{bmatrix} -a_1 & 1 & 0 \ldots 0 & 0 \\ \vdots & \vdots & \ddots & \vdots \\ -a_n & 0 & 0 \ldots 0 & 1 \\ -a_{n+1} & 0 & 0 \ldots 0 & 0 \end{bmatrix}$$

is Hurwitz and there exists a nonsingular matrix $S \in \mathbb{R}^{(n+1)\times(n+1)}$ such that the matrix $R = S^{-1}AS$ is Metzler. The conditions of existence of such a S for a Hurwitz matrix A are studied in [117], a time-varying similarity transformation $S(t)$ is proposed in [100]. In the vector representation $e = [e_1, \ldots, e_{n+1}]$ we obtain

$$\dot{e}(t) = Ae(t) + \rho[t, \psi(t)] + av(t) + bf^{(n+1)}(t), \tag{C.5}$$

where $\rho(t, \psi) = [\rho_1(t, \psi), \ldots, \rho_{n+1}(t, \psi)]$ and $b = [0, 0, \ldots, 0, -1]$. To design an interval observer for (C.5) we need to transform this system to its positive counterpart [117], for this purpose introduce new coordinates $\epsilon = S^{-1}e$, then

$$\dot{\epsilon}(t) = R\epsilon(t) + \eta[t, \psi(t)] + \alpha v(t) + \beta f^{(n+1)}(t), \tag{C.6}$$

where $\eta[t, \psi(t)] = S^{-1}\rho[t, \psi(t)]$, $\alpha = S^{-1}a$ and $\beta = S^{-1}b$. Using (C.1) we obtain:

$$\underline{\beta f}^{(n+1)}(t) \le \beta f^{(n+1)}(t) \le \overline{\beta f}^{(n+1)}(t),$$
$$\underline{\beta f}^{(n+1)}(t) = \beta^+ \underline{f}^{(n+1)}(t) - \beta^- \overline{f}^{(n+1)}(t),$$
$$\overline{\beta f}^{(n+1)}(t) = \beta^+ \overline{f}^{(n+1)}(t) - \beta^- \underline{f}^{(n+1)}(t),$$
$$-|\alpha| V \le \alpha v(t) \le |\alpha| V.$$

Then an interval observer for (C.6) takes the form:

$$\dot{\underline{\epsilon}}(t) = R\underline{\epsilon}(t) + \eta[t, \psi(t)] - |\alpha| V + \underline{\beta f}^{(n+1)}(t), \tag{C.7}$$
$$\dot{\overline{\epsilon}}(t) = R\overline{\epsilon}(t) + \eta[t, \psi(t)] + |\alpha| V + \overline{\beta f}^{(n+1)}(t),$$
$$\underline{\epsilon}(0) = [S^{-1}]^+ \underline{e}_0 - [S^{-1}]^- \overline{e}_0,$$
$$\overline{\epsilon}(0) = [S^{-1}]^+ \overline{e}_0 - [S^{-1}]^- \underline{e}_0,$$

where $\underline{\epsilon}(t)$ and $\overline{\epsilon}(t)$ are lower and upper estimates for the vector $\epsilon(t)$, and

$$\underline{e}(t) = S^+ \underline{\epsilon}(t) - S^- \overline{\epsilon}(t), \tag{C.8}$$
$$\overline{e}(t) = S^+ \overline{\epsilon}(t) - S^- \underline{\epsilon}(t).$$

Theorem 14. *Let assumptions C.3–C.3.1 be satisfied. Then in the differentiator (C.4) the differentiation errors $e_i(t)$, $i = \overline{1, n+1}$ satisfy the inequalities:*

$$\underline{e}(t) \le e(t) \le \overline{e}(t) \quad \forall t \ge 0 \tag{C.9}$$

and $\underline{\epsilon}, \overline{\epsilon}, \underline{e}, \overline{e} \in \in_\infty^n$ in (C.7), (C.8) provided that $e_1 \in \in_\infty$.

Proof. The interval estimation can be easily substantiated for $\epsilon(t)$ by introducing the errors $\underline{\varepsilon}(t) = \epsilon(t) - \underline{\epsilon}(t)$ and $\overline{\varepsilon}(t) = \overline{\epsilon}(t) - \epsilon(t)$:

$$\begin{aligned} \dot{\underline{\varepsilon}}(t) &= R\underline{\varepsilon}(t) + \alpha v(t) + |\alpha|V + \beta f^{(n+1)}(t) - \underline{\beta f}^{(n+1)}(t), \\ \dot{\overline{\varepsilon}}(t) &= R\overline{\varepsilon}(t) + |\alpha|V - \alpha v(t) + \overline{\beta f}^{(n+1)}(t) - \beta f^{(n+1)}(t). \end{aligned} \tag{C.10}$$

According to assumptions C.3 and C.3, $\alpha v(t) + |\alpha|V \geq 0$, $|\alpha|V - \alpha v(t) \geq 0$, $\beta f^{(n+1)}(t) - \underline{\beta f}^{(n+1)}(t) \geq 0$ and $\overline{\beta f}^{(n+1)}(t) - \beta f^{(n+1)}(t) \geq 0$ for all $t \geq 0$, $\underline{\varepsilon}(0) \geq 0$ and $\overline{\varepsilon}(0) \geq 0$ by construction, and the matrix R is Metzler from Assumption C.3.1, then $\underline{\varepsilon}(t) \geq 0$ and $\overline{\varepsilon}(t) \geq 0$ for all $t \geq 0$ that implies the estimates:

$$\underline{\epsilon}(t) \leq \epsilon(t) \leq \overline{\epsilon}(t) \quad \forall t \geq 0.$$

Then from (C.1) the expressions (C.8) implies (C.9). Boundedness of all variables follows from boundedness of $v(t)$, $e_1(t)$ and derivative $f^{n+1}(t)$ claimed in assumptions C.3 and C.3. □

In general just boundedness of estimates is not enough, and some optimality in (C.9) should be obtained using, for example, result of Lemma 10. However, it is easy to see that the solving problem is highly nonlinear, and to propose some LMIs for its solutions some constraint have to be imposed or some variables have to be fixed, as in the following result.

Property 1. *Giving a Metzler matrix $R \in \mathbb{R}^{(n+1)\times(n+1)}$, let there exist $\lambda \in \mathbb{R}^{n+1}_{+}\backslash\{0\}$ and a scalar $\gamma > 0$ such that the following LP problem is feasible:*

$$\begin{gathered} \begin{bmatrix} R\lambda + Xb \\ \lambda - \gamma E_{n+1} \end{bmatrix} < 0, \; Xb \geq 0, \\ RX = XA_0 - wc, \; c = [1, 0, \ldots, 0], \\ A_0 = \begin{bmatrix} 0 & 1 & 0 \ldots 0 & 0 \\ \vdots & \vdots & \ddots & \vdots \\ 0 & 0 & 0 \ldots 0 & 1 \\ 0 & 0 & 0 \ldots 0 & 0 \end{bmatrix}, \end{gathered}$$

where $X \in \mathbb{R}^{(n+1)\times(n+1)}$ is a nonsingular matrix and $w \in \mathbb{R}^{n+1}$, then $S = X^{-1}$ and $a = X^{-1}w$ satisfy Assumption C.3.1. In addition, the L_∞ gain of the operator $f^{(n+1)} \to \epsilon$ is lower than γ in (C.6).

Proof. The proof follows Lemma 10 by a direct substitution ($A = A_0 - ac$). □

Note that $\beta = S^{-1}b \geq 0$ under conditions of Proposition 1, then $\underline{\beta f}^{(n+1)}(t) = \beta \underline{f}^{(n+1)}(t)$ and $\overline{\beta f}^{(n+1)}(t) = \beta \overline{f}^{(n+1)}(t)$, therefore the L_∞ gains of operators $\underline{f}^{(n+1)}(t) \to \underline{\epsilon}$, $\overline{f}^{(n+1)}(t) \to \overline{\epsilon}$, $f^{(n+1)} - \underline{f}^{(n+1)} \to \underline{\varepsilon}$ and $\overline{f}^{(n+1)} - f^{(n+1)} \to \overline{\varepsilon}$ are optimized and lower than γ in (C.7) and (C.10), which improves accuracy of the interval estimation by (C.7), (C.8).

C.3.2 First order derivative estimation

Let us consider with more details the case of the first derivative estimation, then

$$\begin{aligned} \dot{x}_1(t) &= -\chi_1[t, x_1(t) - y(t)] + x_2(t), \\ \dot{x}_2(t) &= -\chi_2[t, x_1(t) - y(t)], \\ y(t) &= f(t) + v(t),\ t \geq 0, \\ x_1(0) &= y(0),\ x_2(0) = 0, \end{aligned} \tag{C.11}$$

and let assumptions C.3 and C.3 be satisfied. To check Assumption C.3.1 note that

$$A = \begin{bmatrix} -a_1 & 1 \\ -a_2 & 0 \end{bmatrix}$$

and for any $a_1 > 0$ and $a_2 > 0$ it is Hurwitz and has eigenvalues

$$\lambda(A) = \frac{1}{2} \begin{bmatrix} -a_1 + \sqrt{a_1^2 - 4a_2} \\ -a_1 - \sqrt{a_1^2 - 4a_2} \end{bmatrix},$$

which are real and distinct for $a_1 \geq 2\sqrt{a_2}$. The corresponding eigenvectors form the matrix for given $r_1 > 0,\ r_2 > 0$,

$$S = \begin{bmatrix} \frac{a_1 + \sqrt{a_1^2 - 4a_2}}{2r_1 a_2} & \frac{\sqrt{a_1^2 - 4a_2} - a_1}{2r_2 a_2} \\ r_1^{-1} & -r_2^{-1} \end{bmatrix},$$

which admits the conditions of Assumptions C.3.1:

$$S^{-1}AS = R = \frac{1}{2} \begin{bmatrix} -a_1 - \sqrt{a_1^2 - 4a_2} & 0 \\ 0 & -a_1 + \sqrt{a_1^2 - 4a_2} \end{bmatrix}.$$

Since

$$S^{-1} = \begin{bmatrix} \frac{a_2 r_1}{\sqrt{a_1^2 - 4a_2}} & \frac{r_1}{2}\left(1 - \frac{a_1}{\sqrt{a_1^2 - 4a_2}}\right) \\ \frac{a_2 r_2}{\sqrt{a_1^2 - 4a_2}} & -\frac{r_2}{2}\left(1 + \frac{a_1}{\sqrt{a_1^2 - 4a_2}}\right) \end{bmatrix},$$

then

$$\beta = S^{-1}b = \begin{bmatrix} \frac{r_1}{2}\left(\frac{a_1}{\sqrt{a_1^2 - 4a_2}} - 1\right) \\ \frac{r_2}{2}\left(1 + \frac{a_1}{\sqrt{a_1^2 - 4a_2}}\right) \end{bmatrix} \geq 0$$

and the pair (R, β) forms a nonnegative system. According to Lemma 10, this system has L_∞ gain of the transfer function $f^{(n+1)} \to \epsilon$ less than $\gamma > 0$ if for some $\lambda \in \mathbb{R}^2$, $\lambda > 0$ we have

$$\begin{bmatrix} R\lambda + \beta \\ \lambda - \gamma E_p \end{bmatrix} < 0,$$

but this LP problem has always a solution if the following restrictions on r_1 and r_2 are satisfied:

$$\begin{aligned} r_1 &< \sqrt{a_1^2 - 4a_2}\frac{a_1 + \sqrt{a_1^2 - 4a_2}}{a_1 - \sqrt{a_1^2 - 4a_2}}\gamma, \\ r_2 &< \sqrt{a_1^2 - 4a_2}\frac{a_1 - \sqrt{a_1^2 - 4a_2}}{a_1 + \sqrt{a_1^2 - 4a_2}}\gamma \end{aligned}$$

for a given $\gamma > 0$.

From (C.8), it is necessary to minimize L_∞ norms of S^+ and S^- to ensure a good L_∞ gain for the transfer $[\underline{f}^{(n+1)}\ \overline{f}^{(n+1)}] \to [\underline{e}\ \overline{e}]$. For this purpose, define

$$r_1 = \varsigma_1 \sqrt{a_1^2 - 4a_2}\, \frac{a_1 + \sqrt{a_1^2 - 4a_2}}{a_1 - \sqrt{a_1^2 - 4a_2}} \gamma,$$
$$r_2 = \varsigma_2 \sqrt{a_1^2 - 4a_2}\, \frac{a_1 - \sqrt{a_1^2 - 4a_2}}{a_1 + \sqrt{a_1^2 - 4a_2}} \gamma$$

for some $\varsigma_1, \varsigma_2 \in (0, 1)$, then

$$S^+ = \frac{a_1 - \sqrt{a_1^2 - 4a_2}}{\gamma \varsigma_1 \sqrt{a_1^2 - 4a_2}} \begin{bmatrix} \frac{1}{2a_2} & 0 \\ \frac{1}{a_1 + \sqrt{a_1^2 - 4a_2}} & 0 \end{bmatrix},$$
$$S^- = \frac{a_1 + \sqrt{a_1^2 - 4a_2}}{\gamma \varsigma_2 \sqrt{a_1^2 - 4a_2}} \begin{bmatrix} 0 & \frac{1}{2a_2} \\ 0 & \frac{1}{a_1 - \sqrt{a_1^2 - 4a_2}} \end{bmatrix}$$

and

$$||S^+||_\infty = \frac{a_1 - \sqrt{a_1^2 - 4a_2}}{\gamma \varsigma_1 \sqrt{a_1^2 - 4a_2}} \max \left\{ \frac{1}{2a_2}, \frac{1}{a_1 + \sqrt{a_1^2 - 4a_2}} \right\},$$
$$||S^-||_\infty = \frac{a_1 + \sqrt{a_1^2 - 4a_2}}{\gamma \varsigma_2 \sqrt{a_1^2 - 4a_2}} \max \left\{ \frac{1}{2a_2}, \frac{1}{a_1 - \sqrt{a_1^2 - 4a_2}} \right\}.$$

In order to minimize these norms it is necessary to take $\varsigma_1 = \varsigma_2 \simeq 1$ and since for $\varsigma_1 = \varsigma_2$

$$||S^-||_\infty > ||S^+||_\infty,$$

then the problem of minimization of the function

$$\varpi(a_1, a_2) = \max \{\varpi_1(a_1, a_2), \varpi_2(a_1, a_2)\}$$
$$\varpi_1(a_1, a_2) = \frac{1}{a_2} \frac{a_1 + \sqrt{a_1^2 - 4a_2}}{2\sqrt{a_1^2 - 4a_2}},$$
$$\varpi_2(a_1, a_2) = \frac{2}{a_1 - \sqrt{a_1^2 - 4a_2}} \frac{a_1 + \sqrt{a_1^2 - 4a_2}}{2\sqrt{a_1^2 - 4a_2}}$$

can be posed. Computing the partial derivatives of ϖ_i, $i = 1, 2$ we obtain that $\frac{\partial \varpi_1}{\partial a_1}$ and $\frac{\partial \varpi_2}{\partial a_1}$ are always negative and $\frac{\partial \varpi_1}{\partial a_2} = 0$ for

$$a_2 = \frac{3}{16} a_1^2,$$

$\frac{\partial \varpi_2}{\partial a_2} = 0$ for

$$a_2 = \frac{1 + \sqrt{2}}{6 + 4\sqrt{2}} a_1^2.$$

Both these solutions correspond to minimums of ϖ_i, $i = 1, 2$. After substitution of this optimal selection of a_2 in ϖ_i we obtain

$$\varpi(a_1) = a^{-1} \max \left\{ \frac{5\sqrt{2} + 7}{\sqrt{2\sqrt{2} + 3}}, 8a_1^{-1} \right\},$$

then

$$a_2 = a_1^2 \begin{cases} \frac{3}{16} & \text{if } a_1 \leq 8\frac{\sqrt{2}+1}{5\sqrt{2}+7}, \\ \frac{1+\sqrt{2}}{6+4\sqrt{2}} & \text{otherwise.} \end{cases} \tag{C.12}$$

Therefore, increasing the value of a_1 and taking a_2 from (C.12) minimize the L_∞ gain for the transfer $[\underline{f}^{(n+1)}\ \overline{f}^{(n+1)}] \to [\underline{e}\ \overline{e}]$, but increasing a_1 and a_2 augments the same gain with respect to the noise $v(t)$. To evaluate the gain with respect to noise, note that

$$\alpha = S^{-1}a = \gamma\frac{a_2}{2}\begin{bmatrix} \varsigma_1\frac{\left(a_1+\sqrt{a_1^2-4a_2}\right)^2}{a_1-\sqrt{a_1^2-4a_2}} \\ \varsigma_2\frac{\left(a_1-\sqrt{a_1^2-4a_2}\right)^2}{a_1+\sqrt{a_1^2-4a_2}} \end{bmatrix}$$

is a nonnegative vector, thus L_∞ gain $\gamma_v > 0$ of the transfer $v \to \epsilon$ can be evaluated using Lemma 10 as follows:

$$\begin{bmatrix} R\lambda + \alpha \\ \lambda - \gamma_v E_p \end{bmatrix} < 0,\ \lambda > 0,$$

where $\lambda \in \mathbb{R}^2$. This LP problem has a solution if

$$\gamma a_2\varsigma_1\frac{a_1+\sqrt{a_1^2-4a_2}}{a_1-\sqrt{a_1^2-4a_2}} < \lambda_1 < \gamma_v,$$
$$\gamma a_2\varsigma_2\frac{a_1-\sqrt{a_1^2-4a_2}}{a_1+\sqrt{a_1^2-4a_2}} < \lambda_2 < \gamma_v$$

that implies

$$\gamma_v = \gamma a_2\frac{a_1+\sqrt{a_1^2-4a_2}}{a_1-\sqrt{a_1^2-4a_2}}.$$

Thus, L_∞ gain of the error $\epsilon(t)$ with respect to the noise $v(t)$ is higher (worse) than that with respect to $f^{(n+1)}(t)$. Substituting (C.12) we obtain

$$\gamma_v = \gamma a_1^2 \begin{cases} \frac{9}{16} & \text{if } a_1 \leq 8\frac{\sqrt{2}+1}{5\sqrt{2}+7}, \\ 0.5 & \text{otherwise.} \end{cases}$$

Normally in applications $||v|| \ll ||f^{(n+1)}||$, thus it is reasonable to limit the value of a_1 using the last expression assuming that the influence of the noise $v(t)$ on the errors should not exceed the influence of $f^{(n+1)}(t)$, *i.e.* $0.5\gamma a_1^2 V \leq \gamma||f^{(n+1)}||$, then

$$a_1 \leq \sqrt{2\frac{||f^{(n+1)}||}{V}}. \tag{C.13}$$

Let us check the performance of the proposed interval differentiator in numerical experiments.

C.4 Forestry-Standard Mobile-Hydraulic crane

The on-line velocity estimation problem is an important issue in mobile hydraulics where instrumentation is limited. It follows the construction of a first order interval differentiator that can be applied for this purpose. The system under study is the telescopic

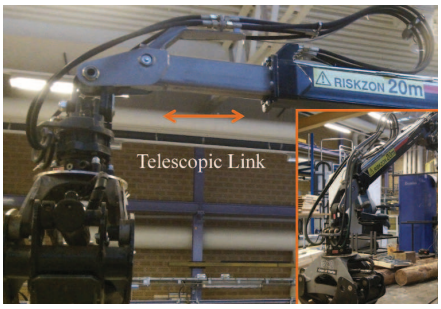

Figure C.1: Hydraulic Forestry Crane.

link of an industrial hydraulic forestry crane. Such industrial equipment is widely used in forestry and the automation is a subject of many researches, see [112].

The method is applied to the telescopic link of the crane, see Fig. C.1, however similar results can be easily obtained for different joints. The telescopic link consists of a double-acting single-side hydraulic cylinder and a solid load which is attached to a piston of the cylinder. Position of the link x varies from 0 to 1.55m; positive velocity $\dot{x}$ corresponds to extraction of the cylinder. This link can be described as a 1-DOF mechanical system actuated by a hydraulic force, and the equation of the motion is

$$m\ddot{x} = f_h - f_g - f_{fric}, \tag{C.14}$$

where m is the mass, f_h is the generated hydraulic force, f_g is the gravity force and f_{fric} is the friction force. The friction is modeled as a Coulomb friction plus a viscous friction: $f_{fric} = f_c \operatorname{sign}(\dot{x}) + f_v\,\dot{x}$. The force generated by the hydraulics is presented below:

$$f_h = P_a A_a - P_b A_b, \tag{C.15}$$

where the piston areas A_a and A_b are known geometric parameters, P_a and P_b are the measured pressures in chambers A and B of the cylinder. The dynamics of the pressures is given, see [102, Sec. 3.8], by

$$\dot{P}_a = \tfrac{\beta}{V_a(x)}\left(-\dot{x}A_a + q_a\right), \quad \dot{P}_b = \tfrac{\beta}{V_b(x)}\left(\dot{x}A_b - q_b\right), \tag{C.16}$$

where $V_a(x) = V_{a0} + x\,A_a$and $V_b(x) = V_{b0} - x\,A_b$ are volumes of the chambers A and B at the given piston position x, V_{a0} and V_{b0} are known geometric constants, β is a known bulk modulus, q_a and q_b are flows to the chamber A and from the chamber B.

C.4.1 Bounds of $\ddot{x}$

Differentiating (C.15) and substituting (C.16) leads to

$$\dot{x} = \eta_0(x, q_a, q_b) - \eta_1(x)\,\dot{f}_h,$$

where

$$\eta_0(x, q_a, q_b) = \frac{A_a\, V_b(x)\, q_a + A_b\, V_a(x)\, q_b}{A_a^2\, V_b(x) + A_b^2\, V_a(x)},$$
$$\eta_1(x) = \frac{V_a(x)\, V_b(x)\, \beta^{-1}}{A_a^2\, V_b(x) + A_b^2\, V_a(x)}.$$

Note that since x is bounded, η_0 and η_1 are bounded. Substituting the equation above, $\dot{x}$, in (C.14) it follows

$$\ddot{x} = -c_0(x, \dot{x}, q_a, q_b) + c_1 f_h + c_2(x)\, \dot{f}_h - f_g, \tag{C.17}$$

with $c_0(\cdot) = \frac{f_c}{m}\text{sign}\dot{x} + \frac{f_v}{m}\eta_0$, $c_1 = \frac{1}{m}$, $c_2(\cdot) = -\frac{f_v}{m}\eta_1$. The pressures are measured with installed pressure transducers that allow the hydraulic force to be estimated, equation (C.15), and precisely this measurement in conjunction with equation (C.17) provides the lower and upper bounds for the second derivative as follows:

$$-L(t) \leq \ddot{x} \leq L(t)$$

where $L(t)$ is a continuous positive function

$$L(t) = \gamma_0 + \gamma_1 |f_h| + \gamma_2 \zeta(f_h),$$

where parameters γ_0, γ_1 and γ_2 are positive constants; the rate of variation of f_h, is given by $\zeta(f_h)$, which is a positive function that depends on the available pressure measurements. One option is:

$$\zeta(f_h) = \frac{|f_h(t - \tau_1) - f_h(t - \tau_2)|}{\tau_2 - \tau_1},$$

with $\tau_2 > \tau_1 > 0$. The values of physical parameters for the considered crane are given in Table I.

Table I: Physical parameters of the link

$A_a,\ \text{m}^2$	$A_b,\ \text{m}^2$	$V_{a0},\ \text{m}^3$	$V_{b0},\ \text{m}^3$
$1.26 \cdot 10^{-3}$	$0.76 \cdot 10^{-3}$	$0.012 \cdot 10^{-3}$	$1.19 \cdot 10^{-3}$
P_t, Pa	P_s, Pa	$\bar{q}$, l/min	β, Pa
$5 \cdot 10^5$	$180 \cdot 10^5$	90	$17 \cdot 10^8$
m, kg	$\bar{f}_h$, N	f_c, N	f_v, N·s/m
200	8000	750	6500

Both pressures P_a and P_b are bounded by the tank pressure P_t and the supply pressure P_s. However it is not a realistic practical situation when both pressures have extreme contrary values simultaneously. Due to internal restrictions the practical bound is $|f_h| \leq \bar{f}_h$. Both flows q_a and q_b are bounded by a factory-set level of a maximum flow through a valve, $|q_{a,b}| \leq \bar{q}$. Moreover, the flows cannot go in the same direction simultaneously, *i.e.* they always are of the same sign. A practical bound of the velocity is $|\dot{x}| \leq 1.1\text{m/s}$, obtained by experiments. From measurements an off-line estimation of $\ddot{x}$ is obtained (black in Fig. C.2), and $L(t)$ is computed as shown in red in Fig. 2 that indeed overcomes $\ddot{x}$.

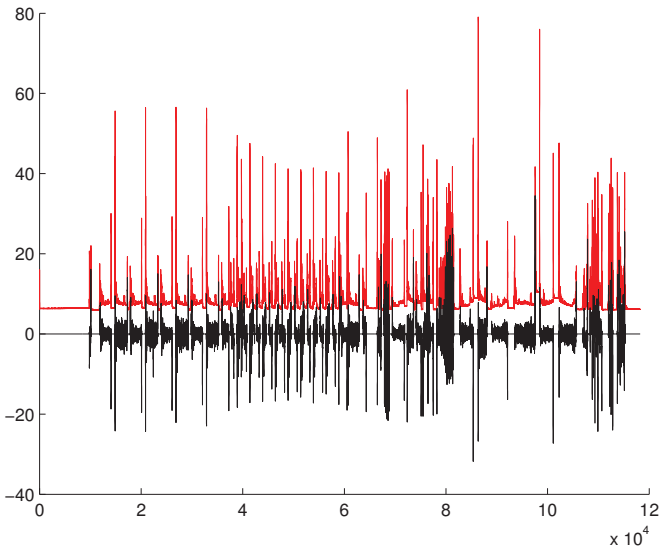

Figure C.2: An estimation of the $L(t)$ function in red with $\gamma_0 = 5$ $\gamma_1 = 0.0011$ $\gamma_2 = 0.0035$

C.4.2 Simulations and Experimental results

The proposed interval observer (C.7) has been tested for three differentiators, The first one proposed in [88] by Levant (ST),

$$\begin{aligned} \dot{\zeta}_1(t) &= -1.5L(t)|e(t)|^{0.5}(e(t)) + \zeta_2(t) \\ \dot{\zeta}_2(t) &= -1.1L(t)(e(t)) \end{aligned}, \tag{C.18}$$

the second one proposed by Vázquez *et al.* [147] (HGD),

$$\begin{aligned} \dot{\zeta}_1(t) &= -\bar{\alpha_1}e(t) + \zeta_2(t) \\ \dot{\zeta}_2(t) &= -\bar{\alpha}_2 e(t) - 1.1L(t)(e(t)) \end{aligned}, \tag{C.19}$$

the last one presented in [115] by Perruquetti *et al.* (HOMD) has the form

$$\begin{aligned} \dot{\zeta}_1(t) &= -\underline{\alpha}_1|e(t)|^{0.75}(e(t)) + \zeta_2(t) \\ \dot{\zeta}_2(t) &= -\underline{\alpha}_2|e(t)|^{0.5}(e(t)) \end{aligned}. \tag{C.20}$$

The differentiators have clearly the structure presented in (C.4), in each of them $e(t) = \zeta_1(t) - y(t)$; they should process position data from the robotic platform Forestry-Standard Mobile-Hydraulic crane. The position of the telescopic link is measured with a wire-actuated encoder. The encoder provides 2381 counts for the range from 0 to 1.55m; the quantization interval is $Q = 0.651\text{mm}$. The measured signal x represents the position signal with an additive uniform noise with a variance $\frac{Q^2}{12}$. Such a signal is smoothed by spline method then differentiated *off-line* to obtain an idea of the velocity profile (Fig. C.3); it is worth to remark that the proposed method works *on-line* and the differentiation by spline is just a priori step which allows to characterize the variables $V = 0.0005$ and $|\ddot{x}| \leq 104$ adopted in the experiments.

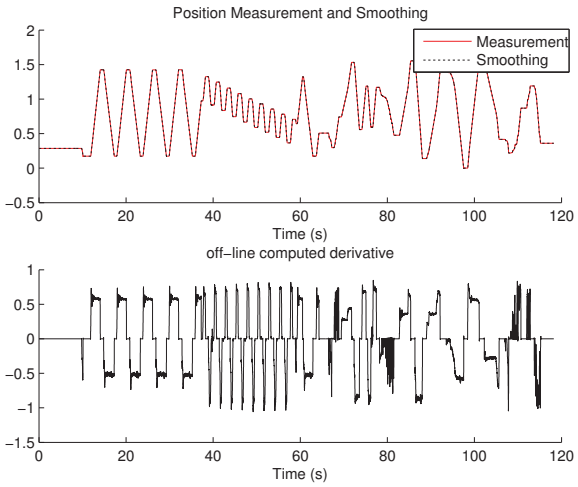

Figure C.3: Measured and smoothed position / off-line derivative.

	$\mu_{\Gamma-}$	$\sigma_{\Gamma-}$	$\mu_{\Gamma+}$	$\sigma_{\Gamma+}$
Levant [88]	0.1776	0.1193	0.0229	0.0937
Vázquez [147]	0.1776	0.1193	0.0099	0.0761
Perruquetti [115]	0.1776	0.1193	0.0235	0.0893

Table C.1: Comparison between the three Interval Observer performances

Then, a_1 and a_2 are chosen following (C.12) and (C.13), for this particular set of experiments $a_1 = 150$. It is worth to remark that the coefficients for the three differentiators must be chosen to achieve the best performances from the differentiators themselves. In the experiments the coefficients are $\bar{\alpha}_1 = 165$, $\bar{\alpha}_2 = 5638$, $\underline{\alpha}_1 = 45$ and $\underline{\alpha}_2 = 12\underline{\alpha}_1$. In Fig. C.4 the behavior of the three differentiators are presented in black and the performances of the interval differentiator are shown for each of them for the entire length of the dataset that is $120s$ ($\bar{e}(t)$ in red and $\underline{e}(t)$ in blue (C.8)) . Two different zooming options are shown in Fig. C.5 for particular parts of the dataset in which the change of velocity is abrupt, it can be clearly seen that the interval observer gives the upper and lower bound to the estimation following the velocity profile keeping the actual estimation in between as desired.

To quantify the performances of the interval observer let us introduce two variables $\Gamma^-(t) = |\bar{\epsilon}(t) - \underline{\epsilon}(t)|/2$ and $\Gamma^+(t) = |\bar{\epsilon}(t) + \underline{\epsilon}(t)|/2$, with the respective means and standard deviations whose values are shown in Table C.1. The variable Γ^- reveals that the proposed Interval Observer is independent from the differentiator used as soon it has the form specified in (C.4), indeed the values for $\mu_{\Gamma-}$ and $\sigma_{\Gamma-}$ are equals for the three different techniques. Moreover, Γ^+ gives information about the quality of the interval observer: the lower $\mu_{\Gamma+}$the better the overall differentiator quality, the lower $\sigma_{\Gamma+}$ the better is the behavior with respect to the oscillation.

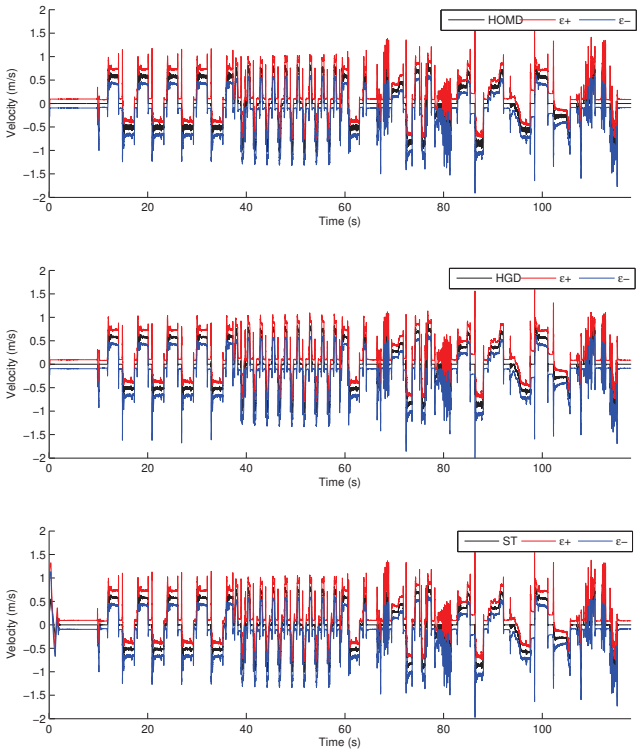

Figure C.4: Interval differentiators performances for Homogeneus Differentiator (HOMD), High Gain Differentaitor (HGD) and Super Twisting (ST)

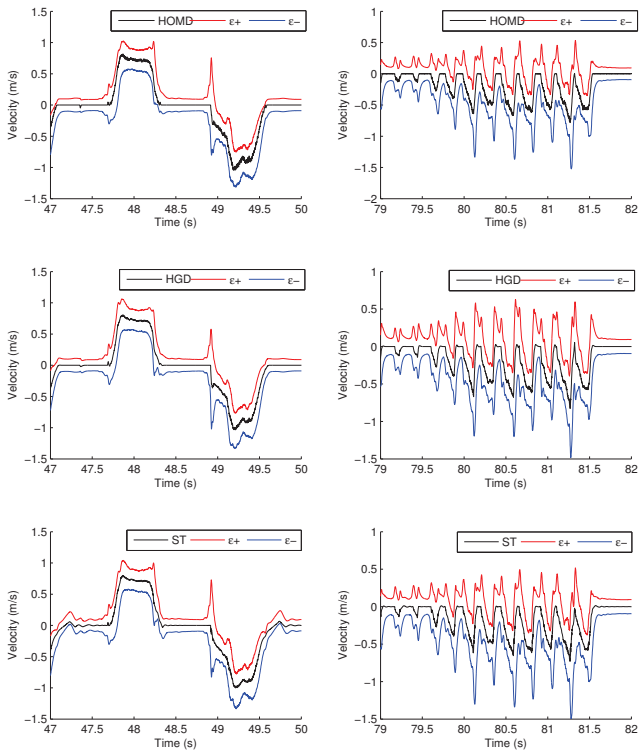

Figure C.5: Interval differentiators performances (zooming)

C.5 Conclusion

This work presents the construction of an interval observer for the estimation error for differentiation techniques. The main results are presented for the high order case whereas, for the application and experiments, a first order derivative estimation is carried out considering three different techniques.

The method has been applied on the velocity estimation on the telescopic link of a hydraulic actuated robotic crane used in forestry. The results obtained show the efficiency of the proposed method which bounds the error of estimation and it is shown to be independent with respect to the differentiation method chosen.

Appendix D

Lie Algebra

Given a scalar function $h(x)$ and a vector field $f(x)$ one can define a new scalar function $\mathcal{L}_f h$ called *Lie derivative* of h with respect to f

Definition 20. *Let $h : \mathbf{R}^n \longrightarrow \mathbf{R}$ be a smooth scalar function and $f : \mathbf{R}^n \longrightarrow \mathbf{R}^n$ a smooth vector field on $\mathbf{R}^n$, then the* Lie Derivative *of h with respect to f is a scalar function defined by*

$$\mathcal{L}_f h = \nabla h f \tag{D.1}$$

Definition 21. *Let f and g be two vector fields on $\mathbf{R}^n$. The* Lie Bracket *of f and g is a third vector defined by:*

$$[f, g] = \nabla g f - \nabla f g$$

The *Lie Bracket* have the following properties:

- bilinearity:

$$[\alpha_1 f_1 + \alpha_2 f_2, g] = \alpha_1 [f_1, g] + \alpha_2 [f_2, g] \tag{D.2}$$
$$[f, \alpha_1 g_1 + \alpha_2 g_2] = \alpha_1 [f, g_1] + \alpha_2 [f, g_2] \tag{D.3}$$

  where f, g, f_1, f_2, g_1 and g_2 are smooth vector fields and α_1 and α_2 are constant scalars;

- skew-commutativity:

$$[f, g] = -[g, f]$$

- Jacobi identity:

$$\mathcal{L}_{[f,g]} h = \mathcal{L}_f \mathcal{L}_g h - \mathcal{L}_g \mathcal{L}_f h$$

  where $h(x)$ is a smooth scalar function of x

Definition 22. *A function $\phi : \mathbb{R}^n \longrightarrow \mathbb{R}^n$, defined in a region Ω, is called a* diffeomorphism *if it is smooth, and if its inverse exists and is smooth.*

If the region Ω in the whole space $\mathbb{R}^n$, then $\phi(x)$ is called a global diffeomorphism.

Lemma 11. *Let $\phi(x)$ be a smooth function defined in a region $\Omega \in \mathbb{R}^n$. If the Jacobian matrix $\nabla\phi$ is non-singular at a point $x = x_0$ of Ω, then $\phi(x)$ defines a local diffeomorphism in a subregion of Ω.*

A diffeomorphism can be used to transform a nonlinear system into another nonlinear system in terms of a new set of states, similarly to what is commonly done in the analysis of linear systems.

Definition 23. *A linearly independent set of vector fields $\{f_1, f_2, ldots, f_m\}$ on $\mathbb{R}^n$ is said to be* completely integrable *if, and only if, there exist $n|m$ scalar functions $(h_i(x), h_2(x), \ldots, h_{n-m}x)$ satisfying the system of partial differential equations:*

$$\nabla h_i f_j = 0 \tag{D.4}$$

where $1 < n|m$, $1 < j < m$, and the gradients ∇h_i are linearly independent.

Note that with the number of vectors being m and the dimension of the associated space being n, the number of unknown scalar functions h_i involved is $(n-m)$ and the number of partial differential equations is $m(n-m)$.

Definition 24. *A linearly independent set of vector fields $\{f_1, f_2, \ldots, f_m\}$ is said to be* involutive *if, and only if, there are scalar functions $a_{ijk} : \mathbb{R}^n \longrightarrow \mathbb{R}$ such that*

$$[f_i, f_j](x) = \sum_{k=1}^{m} a_{ijl}(x) f_k(x) \forall i, j \tag{D.5}$$

Involutivity means that if one forms the Lie bracket of any pairs of vector fields from the set $\{f_1, f2, ..., fm\}$, then the resulting vector field can be expressed as a linear combination of the original set of vector fields. Note that

- Constant vector fields are always involutive. Indeed, the Lie bracket of two constant vectors is simply the zero vector, which can be trivially expressed as linear combination of the vector fields.
- A set composed of a single vector f is involutive. Indeed, $[f, f] = \nabla_f f - \nabla_f f = O$.
- Checking whether a set of vector fields $\{f_1, f2, ..., fm\}$ is involutive amounts to checking whether

  $$\text{rank}\,(f_1(x) \ldots f_m(x)) = \text{rank}\,(f_1(x) \ldots f_m(x))\,[f_i, f_j](x)$$

  for all x and all i, j.

Theorem 15. Frobenius Theorem*: Let $\{f_1, f2, ..., fm\}$ be a set of linearly independent vector fields. The set is completely integrable if, and only if, it is involutive.*

D.1 Frobenius applied to distributions

Let M be an m-dimensional manifold, TpM the tangent space to $p \in M$, and TM the tangent bundle of M.

Definition 25. *A k-dimensional (tangent) distribution on M is a choice of k-dimensional linear subspace $Dp \subset TpM$ at each point $p \in M$.*

Definition 26. *An immersed submanifold S is an* integral manifold *of the distribution D if $TsS = Ds$ for all $s \in S$, and D is integrable if each point of M is contained in an integral manifold of D.*

Lemma 12. Frobenius *: If D is an integrable distribution, then D is necessarily involutive.*

Bibliography

[1] A. Ailon, A. Cosic, I. Zohar, and A. Rodic, "Control for teams of kinematic unicycle-like and skid-steering mobile robots with restricted inputs: Analysis and applications", *2011 15th International Conference on Advanced Robotics (ICAR)*, June 2011, no. 1, pp. 371–376.

[2] D. Angeli and D. Efimov, "On Input-to-State Stability with respect to decomposable invariant sets", *Proc. 52nd IEEE Conference on Decision and Control*, Florence, 2013.

[3] S. Aranovskiy, "Modeling and Identification of Spool Dynamics in an Industrial Electro-Hydraulic Valve", *21st Mediterranean Conference on Control and Automation*, 2013, pp. 82–87.

[4] A. Astolfi, "Exponential stabilization of a wheeled mobile robot via discontinuous control", *Journal of dynamic systems, measurement, and control*, 1999, vol. 121, no. 1, pp. 121–126.

[5] F. Aurenhammer, "Voronoi Diagrams&Mdash;a Survey of a Fundamental Geometric Data Structure", *ACM Comput. Surv.* 1991, vol. 23, no. 3, pp. 345–405.

[6] A Bacciotti and L Rosier, *Lyapunov Functions and Stability in Control Theory*, ed. by B. Springer, 2nd, Springer, 2005.

[7] J Back and H Shim, "Adding robustness to nominal output feedback controllers for uncertain nonlinear systems: a nonlinear version of disturbance observer", *Automatica*, 208, vol. 44, no. 9, pp. 2528–2537.

[8] T. Balch and R. Arkin, "Behavior-based formation control for multirobot teams", *Robotics and Automation, IEEE Transactions on*, 1998, vol. 14, no. 6, pp. 926–939.

[9] T. Balch and M. Hybinette, "Behavior-based coordination of large-scale robot formations", *MultiAgent Systems, 2000. Proceedings. Fourth International Conference on*, 2000, pp. 363–364.

[10] R. Beard, J. Lawton, and F. Hadaegh, "A coordination architecture for spacecraft formation control", *Control Systems Technology, IEEE Transactions on*, 2001, vol. 9, no. 6, pp. 777–790.

[11] E Bernuau, A Polyakov, D Efimov, and W Perruquetti, "Verification of {ISS}, i{ISS} and {IOSS} properties applying weighted homogeneity", *Systems & Control Letters*, 2013, vol. 62, no. 12, pp. 1159–1167.

[12] G Besanon, ed., *Nonlinear Observers and Applications*, vol. 363, Lecture Notes in Control and Information Sciences, Springer, 2007.

[13] S. P. Bhat and D. S. Bernstein, "Geometric homogeneity with applications to finite-time stability", *Mathematics of Control, Signals and Systems*, 2005, vol. 17, pp. 101–127.

[14] N. P. Bhatia and G. P. Szegö, *Stability Theory of Dynamical Systems*, Berlin: Springer-Verlag, 1970.

[15] J Borenstein and Y Koren, "The vector field histogram-fast obstacle avoidance for mobile robots", *Robotics and Automation, IEEE Transactions on*, June 1991, vol. 7, no. 3, pp. 278–288, ISSN: 1042-296X, DOI: 10.1109/70.88137.

[16] C Briat, "Robust stability analysis of uncertain Linear Positive Systems via Integral Linear Constraints: L1- and Linfty-gain characterizations", *Proc. 50th IEEE CDC and ECC*, Orlando, 2011, pp. 6337–6342.

[17] O. Brock and O. Khatib, "High-speed navigation using the global dynamic window approach", *Robotics and Automation, 1999. Proceedings. 1999 IEEE International Conference on*, vol. 1, 1999, pp. 341–346.

[18] R. W. Brockett, "Asymptotic Stability and Feedback Stabilization", *Differential Geometric Control Theory*, ed. by R. S. M. R. W. Brockett and H. J. Sussmann, Boston: Birkhauser, 1983, pp. 181–191.

[19] G. Campion, B. George, and B. D'Andréa-Novel, "Structural Properties and Classification of Kinematic and Dynamic Models Of Wheeled Mobile Robots", *Structural Properties and Classification of and Dynamic Models Of Wheeled Mobile Robots*, 1996, pp. 47–62.

[20] Y. Cao, W. Ren, and Z. Meng, "Decentralized finite-time sliding mode estimators and their applications in decentralized finite-time formation tracking", *Systems & Control Letters*, 2010, vol. 59, no. 9, pp. 522–529.

[21] C.-Y. Chang and H Wijaya Lie, "Real-Time Visual Tracking and Measurement to Control Fast Dynamics of Overhead Cranes", *Industrial Electronics, IEEE Transactions on*, Mar. 2012, vol. 59, no. 3, pp. 1640–1649.

[22] H. M. Choset, *Principles of robot motion: theory, algorithms, and implementation*, MIT press, 2005.

[23] C Combastel, "Stable Interval Observers in C for Linear Systems with Time-Varying Input Bounds", *Automatic Control, IEEE Transactions on*, 2013, vol. PP, no. 99, pp. 1–6, ISSN: 0018-9286, DOI: 10.1109/TAC.2012.2208291.

[24] C. I. Connolly, J. B. Burns, and R. Weiss, "Path planning using Laplace's equation", *Robotics and Automation, 1990. Proceedings., 1990 IEEE International Conference on*, May 1990, 2102–2106 vol.3, DOI: 10.1109/ROBOT.1990.126315.

[25] B. D'Andréa-Novel, G. Campion, and G. Bastin, "Control of Nonholonomic Wheeled Mobile Robots by State Feedback Linearization", *The International Journal of Robotics Research*, 1995, vol. 14, pp. 543–559.

[26] B. D'andréa-novel, G. Campion, and G. Bastin, "Control of wheeled mobile robots not satisfying ideal velocity constraints: A singular perturbation approach", *International Journal of Robust and Nonlinear Control*, 1995, vol. 5, no. 4, pp. 243–267.

[27] W. Danwei and B. L. Chang, "Modeling and Analysis of Skidding and Slipping in Wheeled Mobile Robots: Control Design Perspective", *Robotics, IEEE Transactions on*, 2008, vol. 24, no. 3, pp. 676–687.

[28] S. N. Dashkovskiy, D. V. Efimov, and E. D. Sontag, *Automation and Remote Control*, no. 8, pp. 1579–1614.

[29] C. De Wit and O. Sordalen, "Exponential stabilization of mobile robots with nonholonomic constraints", *Automatic Control, IEEE Transactions on*, 1992, vol. 37, no. 11, pp. 1791–1797.

[30] M. Defoort, T. Floquet, A. Kokosy, and W. Perruquetti, "Sliding-Mode Formation Control for Cooperative Autonomous Mobile Robots", *Industrial Electronics, IEEE Transactions on*, 2008, vol. 55, no. 11, pp. 3944–3953.

[31] E. W. Dijkstra, "A note on two problems in connexion with graphs", *Numerische mathematik*, 1959, vol. 1, no. 1, pp. 269–271.

[32] W. E. Dixon, D. M. Dawson, E. Zergeroglu, and A. Behal, *Nonlinear Control of Wheeled Mobile Robots*, Secaucus, NJ, USA: Springer-Verlag New York, Inc., 2001, ISBN: 1852334142.

[33] D. D. Dudenhoeffer and M. Jones, "A formation behavior for large-scale microrobot force deployment", *Simulation Conference, 2000. Proceedings. Winter*, vol. 1, 2000, 972–982 vol.1.

[34] Y. Ebihara, D. Peaucelle, and D. Arzelier, "L1 Gain Analysis of Linear Positive Systems and Its Application", *Proc. 50th IEEE CDC and ECC*, Orlando, 2011, pp. 4029–4035.

[35] D. Efimov, A. Loria, and E. Panteley, "Multigoal output regulation via supervisory control: Application to stabilization of a unicycle", *American Control Conference, 2009. ACC '09 St Louis, MO, USA*. 2009, pp. 4340–4345.

[36] D Efimov, T Ra\"issi, and A Zolghadri, "Control of nonlinear and LPV systems: interval observer-based framework", *IEEE Trans. Automatic Control*, 2013, vol. 58, no. 3, pp. 773–782.

[37] D Efimov, L. M. Fridman, T Ra\"issi, A Zolghadri, and R Seydou, "Interval Estimation for {LPV} Systems Applying High Order Sliding Mode Techniques", *Automatica*, 2012, vol. 48, pp. 2365–2371, DOI: 10.1016/j.automatica.2012.06.073.

[38] D Efimov, T Ra\"issi, S Chebotarev, and A Zolghadri, "Interval State Observer for Nonlinear Time Varying Systems", *Automatica*, 2013, vol. 49, no. 1, pp. 200–205.

[39] O. ernard and J. L. Gouzé, "Closed loop observers bundle for uncertain biotechnological models", *Journal of Process Control*, 2004, vol. 14, no. 7, pp. 765–774, ISSN: 0959-1524.

[40] L Farina and S Rinaldi, *Positive Linear Systems: Theory and Applications*, New York: Wiley, 2000.

[41] A Ferreira, F. J. Bejarano, and L. M. Fridman, "Robust Control With Exact Uncertainties Compensation: With or Without Chattering?", *Control Systems Technology, IEEE Transactions on*, 2011, vol. 19, no. 5, pp. 969–975, ISSN: 1063-6536, DOI: 10.1109/TCST.2010.2064168.

[42] M. Fliess, C. Join, and H. Sira-Ramirez, "Nonlinear estimation is easy", *Int. J. Modelling, Identification and Control*, 2008, vol. 4, no. 1, pp. 12–27.

[43] T. Floquet, J. P. Barbot, and W. Perruquetti, "Higher-Order Sliding Mode Stabilization for a Class of Nonholonomic Perturbed Systems", *Automatica*, 2003, vol. 39, no. 6, pp. 1077–1083.

[44] T. I. Fossen and H. Nijmeijer, *New Directions in Nonlinear Observer Design*, Springer, 1999.

[45] D Fox, W Burgard, and S Thrun, "The dynamic window approach to collision avoidance", *Robotics Automation Magazine, IEEE*, Mar. 1997, vol. 4, no. 1, pp. 23–33, ISSN: 1070-9932, DOI: 10.1109/100.580977.

[46] L. B. Freidovich and H. K. Khalil, "Performance recovery of feedbacklinearization-based designs", *IEEE Transactions on Automatic Control*, 2008, vol. 53, no. 10, pp. 2324–2334.

[47] G. Gamage, G. Mann, and R. Gosine, "Discrete event systems based formation control framework to coordinate multiple nonholonomic mobile robots", *Intelligent Robots and Systems, 2009. IROS 2009. IEEE/RSJ International Conference on, St. Louis, MO, USA*, 2009, pp. 4831–4836.

[48] S. S. Ge and Y. J. Cui, "New potential functions for mobile robot path planning", *Robotics and Automation, IEEE Transactions on*, Oct. 2000, vol. 16, no. 5, pp. 615–620, ISSN: 1042-296X, DOI: 10.1109/70.880813.

[49] J. Ghommam, H. Mehrjerdi, and M. Saad, "Robust formation control without velocity measurement of the leader robot", *Control Engineering Practice*, 2013, vol. 21, no. 8, pp. 1143–1156.

[50] J. L. Gouzé, A Rapaport, and M. Z. Hadj-Sadok, "Interval observers for uncertain biological systems", *Ecological Modelling*, 2000, vol. 133, pp. 46–56.

[51] A. Griewank, *Evaluating Derivatives: Principles and Techniques of Algorithmic Differentiation*, Philadelphia, PA: SIAM, 2000.

[52] J Guckenheimer and P Holmes, "Structurally stable heteroclinic cycles", *Math. Proc. Camb. Phil. Soc.* 1988, vol. 103, pp. 189–192.

[53] M. Guerra, D. Efimov, G. Zheng, and W. Perruquetti, "Finite-Time Supervisory Stabilization for a Class of Nonholonomic Mobile Robots Under Input Disturbances", *19th IFAC World Congress, Cape Town, South Africa*, Aug. 2014, pp. 4867–4872.

[54] J. Guldner and V. Utkin, "Stabilization of non-holonomic mobile robots using Lyapunov functions for navigation and sliding mode control", *Decision and Control, 1994., Proceedings of the 33rd IEEE Conference on, Lake Buena Vista, FL, USA*, vol. 3, 1994, 2967–2972 vol.3.

[55] J Guldner, V. I. Utkin, H Hashimoto, and F Harashima, "Tracking gradients of artificial potential fields with non-holonomic mobile robots", *American Control Conference, Proceedings of the 1995*, vol. 4, June 1995, 2803–2804 vol.4.

[56] L Guo and S Cao, "Anti-disturbance control theory for systems with multiple disturbances: A survey", *ISA Transactions*, 2014, vol. 53, pp. 846–849.

[57] J Han, "A class of extended state observers for uncertain systems", *Control and Decision*, 1995, vol. 10, no. 1, pp. 85–88.

[58] J. Han, "From PID to Active Disturbance Rejection Control", *Industrial Electronics, IEEE Transactions on*, Mar. 2009, vol. 56, no. 3, pp. 900–906.

[59] G. Harrar, *Radical Robots: Can You Be Replaced*, Aladdin Paperbacks, 1990.

[60] P. E. Hart, N. J. Nilsson, and B. Raphael, "A formal basis for the heuristic determination of minimum cost paths", *Systems Science and Cybernetics, IEEE Transactions on*, 1968, vol. 4, no. 2, pp. 100–107.

[61] J. a. P. Hespanha, D. Liberzon, and A. Morse, "Hysteresis-based switching algorithms for supervisory control of uncertain systems", *Automatica*, Feb. 2003, vol. 39, no. 2, pp. 263–272, ISSN: 00051098, DOI: 10.1016/S0005-1098(02)00241-8, URL: http://linkinghub.elsevier.com/retrieve/pii/S0005109802002418.

[62] Y Huang and W Xue, "Active disturbance rejection control: Methodology and theoretical analysis", *ISA Transactions*, 2014, vol. 53(4), pp. 963–976.

[63] Y. K. Hwang and N. Ahuja, "Gross Motion Planning - A Survey", *ACM Computing Surveys*, 1992, vol. 24, no. 3, pp. 219–291.

[64] IEEE Spectrum, *Can Japan Send In Robots To Fix Troubled Nuclear Reactors?*, 2011, URL: http://spectrum.ieee.org/automaton/robotics/industrial-robots/japan-robots-to-fix-troubled-nuclear-reactors (visited on 09/01/2015).

[65] International Federation Of Robotics, *Executive Summary - World Robotics 2014 - Industrial Robotics*, 2015, URL: http://www.ifr.org/industrial-robots/ (visited on 08/28/2015).

[66] International Federation Of Robotics, *Executive Summary - World Robotics 2014 -Service Robotics*, 2015, URL: http://www.ifr.org/service-robots/ (visited on 08/28/2015).

[67] A. Isidori, *Nonlinear Control Systems*, ed. by M. Thoma, E. D. Sontag, B. W. Dickinson, A. Fettweis, J. L. Massey, and J. W. Modestino, 3rd, Secaucus, NJ, USA: Springer-Verlag New York, Inc., 1995, ISBN: 3540199160.

[68] L. Jaulin, "Nonlinear bounded-error state estimation of continuous time systems", *Automatica*, 2002, vol. 38, no. 2, pp. 1079–1082.

[69] M. Jin, J. Lee, P. H. Chang, and C. Choi, "Practical Nonsingular Terminal Sliding-Mode Control of Robot Manipulators for High-Accuracy Tracking Control", *Industrial Electronics, IEEE Transactions on*, Sept. 2009, vol. 56, no. 9, pp. 3593–3601.

[70] I. Kamon, E. Rivlin, and E. Rimon, "A new range-sensor based globally convergent navigation algorithm for mobile robots", *Robotics and Automation, 1996. Proceedings., 1996 IEEE International Conference on*, vol. 1, 1996, 429–435 vol.1.

[71] E. Kaplan, *Understanding GPS - Principles and applications*, 2nd edition, Artech House, 2005.

[72] H. Khalil, "Universal integral controllers for minimum-phase nonlinear systems", *IEEE Transactions on Automatic Control*, 2000, vol. 45, no. 3, pp. 490–494, ISSN: 0018-9286, DOI: 10.1109/9.847730.

[73] H. K. Khalil, *Nonlinear Systems*, Macmillan, 1992.

[74] H. K. Khalil, *Nonlinear Systems*, {NJ} 07458, Upper Saddle River: Prentice-Hall, 1996.

[75] . Khatib and R Chatila, "An extended potential field approach for mobile robot sensor motions", *Proceedings of the Intelligent Autonomous Systems IAS-4, IOS Press, Karlsruhe, Germany*, 1995, pp. 490–496.

[76] O Khatib, "Real-Time Obstacle Avoidance for Manipulators and Mobile Robots", *IEEE International Conference on Robotics and Automation*, St. Louis, Missouri, 1985, pp. 500–505.

[77] M Kieffer and E Walter, "Guaranteed nonlinear state estimator for cooperative systems", *Numerical Algorithms*, 2004, vol. 37, pp. 187–198.

[78] S. Koenig and M. Likhachev, "Fast replanning for navigation in unknown terrain", *Robotics, IEEE Transactions on*, 2005, vol. 21, no. 3, pp. 354–363.

[79] Y Koren and J Borenstein, "Potential field methods and their inherent limitations for mobile robot navigation", *Proc. IEEE Conf. Robotics and Automation*, Sacramento, CA, 1991, pp. 1398–1404.

[80] J.-W. Kwon and D. Chwa, "Hierarchical Formation Control Based on a Vector Field Method for Wheeled Mobile Robots", *Robotics, IEEE Transactions on*, 2012, vol. 28, no. 6, pp. 1335–1345.

[81] J.-C. Latombe, *Robot Motion Planning*, Norwell, MA, USA: Kluwer Academic Publishers, 1991, ISBN: 079239206X.

[82] S. M. LaValle and J. J. Kuffner Jr, "Rapidly-exploring random trees: Progress and prospects", 2000.

[83] S. M. LaValle, "Rapidly-Exploring Random Trees A ew Tool for Path Planning", 1998.

[84] L.-H. Lee, C.-H. Huang, S.-C. Ku, Z.-H. Yang, and C.-Y. Chang, "Efficient Visual Feedback Method to Control a Three-Dimensional Overhead Crane", *Industrial Electronics, IEEE Transactions on*, Aug. 2014, vol. 61, no. 8, pp. 4073–4083.

[85] R. Lenain, B. Thuilot, C. Cariou, and P. Martinet, "Adaptive control for car like vehicles guidance relying on RTK GPS: rejection of sliding effects in agricultural applications", *Robotics and Automation, 2003. Proceedings. ICRA '03. IEEE International Conference on*, vol. 1, 2003, pp. 115–120.

[86] R. Lenain, B. Thuilot, C. Cariou, and P. Martinet, "High accuracy path tracking for vehicles in presence of sliding: Application to farm vehicle automatic guidance for agricultural tasks", *Autonomous Robots*, 2006, vol. 21, no. 1, pp. 79–97.

[87] N. Leonard and E. Fiorelli, "Virtual leaders, artificial potentials and coordinated control of groups", *Decision and Control, 2001. Proceedings of the 40th IEEE Conference on*, vol. 3, 2001, 2968–2973 vol.3.

[88] A Levant, "Exact Differentiation of Signals with Unbounded Higher Derivatives", *IEEE Transactions on Automatic Control*, 2012, vol. 57, no. 4, pp. 1076–1080.

[89] A Levant, "Robust exact differentiation via sliding mode technique", *Automatica*, 1998, vol. 34, no. 3, pp. 379–384.

[90] A. Levant, "Universal SISO Sliding-Mode Controllers with Finite-Time Convergence", *IEEE Trans. Automat. Contr.* 2001, vol. 46, no. 9, pp. 1447–1451.

[91] F. L. Lewis, H Zhang, K Hengster-Movric, and A Das, *Cooperative Control of Multi-Agent Systems*, Communications and Control Engineering, Springer, 2014.

[92] M. A. Lewis and K.-H. Tan, "High Precision Formation Control of Mobile Robots Using Virtual Structures", *Auton. Robots*, Oct. 1997, vol. 4, no. 4, pp. 387–403, ISSN: 0929-5593.

[93] D. Liberzon, *Switching in systems and control*, Boston, Massachusetts: Birkhauser, 2003.

[94] M. Likhachev, D. Ferguson, G. Gordon, A. T. Stentz, and S. Thrun, "Anytime Dynamic A*: An Anytime, Replanning Algorithm", *Proceedings of the International Conference on Automated Planning and Scheduling (ICAPS)*, 2005.

[95] T. Lozano-Pérez and M. A. Wesley, "An algorithm for planning collision-free paths among polyhedral obstacles", *Communications of the ACM*, 1979, vol. 22, no. 10, pp. 560–570.

[96] V. Lumesky and A. Stepanov, "Path-Planning Strategies for a Point Mobile Automaton Moving Amidst Unknown Obstacles of Arbitrary Shape", *Algorithmica*, 1987, pp. 403–430.

[97] E. Masehian and D. Sedighizadeh, "Classic and Heuristic Approaches in Robot Motion Planning A Chronological Review", *Proceedings World Academy of Science Engineering and Technology*, 2007, pp. 101–106.

[98] A. A. Masoud, "A harmonic potential field approach for navigating a rigid, nonholonomic robot in a cluttered environment", *Robotics and Automation, 2009. ICRA '09. IEEE International Conference on*, May 2009, pp. 3993–3999.

[99] I. Matsune, T. Kobayashi, and J. Imae, "Towards Exponential Stabilization of Nonholonomic Systems via a Hybrid Control Method", *2006 6th World Congress on Intelligent Control and Automation*, 2006, no. 3, pp. 2344–2348.

[100] F Mazenc and O Bernard, "Interval observers for linear time-invariant systems with disturbances", *Automatica*, 2011, vol. 47, no. 1, pp. 140–147.

[101] H. Mehrjerdi, J. Ghommam, and M. Saad, "Nonlinear coordination control for a group of mobile robots using a virtual structure", *Mechatronics*, 2011, vol. 21, no. 7, pp. 1147–1155.

[102] H. E. Merrit, *Hydraulic Control Systems*, Wiley, 1967.

[103] T Meurer, K Graichen, and E.-D. Gilles, eds., *Control and Observer Design for Nonlinear Finite and Infinite Dimensional Systems*, vol. 322, Lecture Notes in Control and Information Sciences, Springer, 2005.

[104] M Moisan, O Bernard, and J. L. Gouzé, "Near optimal interval observers bundle for uncertain bio-reactors", *Automatica*, 2009, vol. 45, no. 1, pp. 291–295.

[105] H. Moravec and A. Elfes, "High resolution maps from wide angle sonar", *Robotics and Automation. Proceedings. 1985 IEEE International Conference on*, vol. 2, 1985, pp. 116–121, DOI: 10.1109/ROBOT.1985.1087316.

[106] E Moulay and W Perruquetti, "Finite Time Stability of Non Linear Systems", {*IEEE*} *Conference on Decision and Control*, Hawaii, USA, 2003, pp. 3641–3646.

[107] P. F. Muir and C. P. Neuman, "Kinematic modeling of wheeled mobile robots", *Journal of robotic systems*, 1987, vol. 4, no. 2, pp. 281–340.

[108] N Niksefat and N Sepehri, "Designing Robust Force Control of Hydraulic Actuators Despite System and Enviromental Uncertainties", *IEEE Control Systems Magazine*, 2001, vol. 21, no. 2, pp. 66–77.

[109] Z Nitecki and M Shub, "Filtrations, Decompositions, and Explosions", *American Journal of Mathematics*, 1975, vol. 97, no. 4, pp. 1029–1047.

[110] G. Oriolo, a. De Luca, and M. Vendittelli, "WMR control via dynamic feedback linearization: design, implementation, and experimental validation", *IEEE Transactions on Control Systems Technology*, Nov. 2002, vol. 10, no. 6, pp. 835–852, ISSN: 1063-6536, DOI: 10.1109/TCST.2002.804116, URL: http://ieeexplore.ieee.org/lpdocs/epic03/wrapper.htm?arnumber=1058053.

[111] D Panagou, H. G. Tanner, and K. J. Kyriakopoulos, "Control of nonholonomic systems using reference vector fields", *Decision and Control and European Control Conference (CDC-ECC), 2011 50th IEEE Conference on*, Dec. 2011, pp. 2831–2836.

[112] E Papadopoulos, B. Mu, and R Frenette, "On modeling, identification, and control of a heavy-duty electrohydraulic harvester manipulator", *Mechatronics, IEEE/ASME Transactions on*, 2003, vol. 8, no. 2, pp. 178–187.

[113] M. G. Park and M. C. Lee, "Real-time path planning in unknown environment and a virtual hill concept to escape local minima", *Industrial Electronics Society, 2004. IECON 2004. 30th Annual Conference of IEEE*, vol. 3, Nov. 2004, 2223–2228 Vol. 3.

[114] K Pathak and S. K. Agrawal, "An integrated path-planning and control approach for nonholonomic unicycles using switched local potentials", *Robotics, IEEE Transactions on*, Dec. 2005, vol. 21, no. 6, pp. 1201–1208.

[115] W Perruquetti, T Floquet, and E Moulay, "Finite-Time Observers: Application to Secure Communication", *Automatic Control, IEEE Transactions on*, 2008, vol. 53, no. 1, pp. 356–360, ISSN: 0018-9286, DOI: 10.1109/TAC.2007.914264.

[116] J Preminger and J Rootenberg, "Some considerations relating to control systems employing the invariance principle", *IEEE Transactions on Automatic Control*, 1964, vol. 9, no. 3, pp. 209–215.

[117] T Ra\"issi, D Efimov, and A Zolghadri, "Interval state estimation for a class of nonlinear systems", *IEEE Trans. Automatic Control*, 2012, vol. 57, no. 1, pp. 260–265.

[118] W. Ren and R. Beard, "Formation feedback control for multiple spacecraft via virtual structures", *Control Theory and Applications, IEE Proceedings*, 2004, vol. 151, no. 3, pp. 357–368.

[119] C. W. Reynolds, "Flocks, Herds and Schools: A Distributed Behavioral Model", *SIGGRAPH Comput. Graph.* Aug. 1987, vol. 21, no. 4, pp. 25–34.

[120] H. Rezaee and F. Abdollahi, "A decentralized cooperative control scheme with obstacle avoidance for a team of mobile robots", *Industrial Electronics, IEEE Transactions on*, 2014, vol. 61, no. 1, pp. 347–354.

[121] E Rimon and D. E. Koditschek, "Exact robot navigation using artificial potential functions", *Robotics and Automation, IEEE Transactions on*, Oct. 1992, vol. 8, no. 5, pp. 501–518, ISSN: 1042-296X.

[122] L Rosier, "Homogeneous {L}yapunov Function for Homogeneous Continuous Vector Field", *Systems Control Lett.* 1992, vol. 19, pp. 467–473.

[123] M. Rubagotti, A. Estrada, F. Castanos, A. Ferrara, and L. Fridman, "Integral Sliding Mode Control for Nonlinear Systems With Matched and Unmatched Perturbations", *Automatic Control, IEEE Transactions on*, 2011, vol. 56, no. 11, pp. 2699–2704.

[124] C Samson, "Commande de v{é}hicules non-holonomes pour le suivi de trajectoire et la stabilisation vers une posture d{é}sir{é}e", *Colloque Automatique pour les V{é}hicules Terrestres*, 1993.

[125] R. G. Sanfelice and C. Prieur, "Uniting Two Output-Feedback Controllers with Different Objectives", *American Control Conference*, 2010, pp. 910–915, ISBN: 9781424474271.

[126] K. Sato, "Deadlock-free motion planning using the Laplace potential field", *Advanced Robotics*, 1992, vol. 7, no. 5, pp. 449–461, DOI: 10.1163/156855393X00285, URL: http://dx.doi.org/10.1163/156855393X00285.

[127] G Schipanov, "Theory and methods of designing automatic regulators", *Automatika in Telemekhanika*, 1939, vol. 4, no. 1, pp. 49–66.

[128] B. Siciliano, L. Sciavicco, L. Villani, and G. Oriolo, *Robotics: modelling, planning and control*, Springer Science & Business Media, 2009.

[129] R. Siegwart and I. R. Nourbakhsh, *Introduction to Autonomous Mobile Robots*, Bradford Company, 2004.

[130] R. Simmons, "The curvature-velocity method for local obstacle avoidance", *Robotics and Automation, 1996. Proceedings., 1996 IEEE International Conference on*, vol. 4, 1996, 3375–3382 vol.4.

[131] H. L. Smith, *Monotone Dynamical Systems: An Introduction to the Theory of Competitive and Cooperative Systems*, vol. 41, Surveys and Monographs, Providence: AMS, 1995.

[132] J. Solomon and M. J. Z. Hartmann, "Extracting object contours with the sweep of a robotic whisker using torque information", *The International Journal of Robotics Research*, 2010, vol. 29, no. 9, 1233–1245.

[133] E. D. Sontag and Y. Wang, "Notions of input to output stability", *Systems & Control Letters*, 1999, vol. 38, no. 4–5, pp. 235–248, ISSN: 0167-6911, DOI: http://dx.doi.org/10.1016/S0167-6911(99)00070-5, URL: http://www.sciencedirect.com/science/article/pii/S0167691199000705.

[134] E. D. Sontag and Y. Wang, "Notions of input to output stability", *Systems & Control Letters*, Dec. 1999, vol. 38, no. 4-5, pp. 235–248, ISSN: 01676911, DOI: 10.1016/S0167-6911(99)00070-5, URL: http://linkinghub.elsevier.com/retrieve/pii/S0167691199000705.

[135] O. Souissi, R. Benatitallah, D. Duvivier, A. Artiba, N. Belanger, and P. Feyzeau, "Path planning: A 2013 survey", *Industrial Engineering and Systems Management (IESM), Proceedings of 2013 International Conference on*, Oct. 2013, pp. 1–8.

[136] Y. X. Su, C. H. Zheng, D. Sun, and B. Y. Duan, "A Simple Nonlinear Velocity Estimator for High-Performance Motion Control", *Industrial Electronics, IEEE Transactions on*, Aug. 2005, vol. 52, no. 4, pp. 1161–1169.

[137] H. Tanner, A. Jadbabaie, and G. Pappas, "Stable flocking of mobile agents, part I: fixed topology", *Decision and Control, 2003. Proceedings. 42nd IEEE Conference on*, vol. 2, 2003, 2010–2015 Vol.2.

[138] H. Tanner, A. Jadbabaie, and G. Pappas, "Stable flocking of mobile agents part II: dynamic topology", *Decision and Control, 2003. Proceedings. 42nd IEEE Conference on*, vol. 2, 2003, 2016–2021 Vol.2.

[139] H. Tanner, S. Loizou, and K. Kyriakopoulos, "Nonholonomic stabilization with collision avoidance for mobile robots", *Proceedings 2001 IEEE/RSJ International Conference on Intelligent Robots and Systems.* 2001, vol. 3, pp. 1220–1225, DOI: 10.1109/IROS.2001.977149, URL: http://ieeexplore.ieee.org/lpdocs/epic03/wrapper.htm?arnumber=977149.

[140] H. Tanner, G. Pappas, and V. Kumar, "Leader-to-formation stability", *Robotics and Automation, IEEE Transactions on*, 2004, vol. 20, no. 3, pp. 443–455.

[141] G Tao and P. V. Kokotović, "Adaptive Control of Plants with Unknown DEad-Zones", *IEEE Transactions on Automatic Control*, 1996, vol. 39, no. 1, pp. 59–68.

[142] A. Tayebi and A. Rachid, "Adaptive controller for non-holonomic mobile robots with matched uncertainties", *Advanced Robotics*, 2000, vol. 14, no. 2, pp. 105–118.

[143] G. Tian and Z. Gao, "From Poncelet's invariance principle to Active Disturbance Rejection", *American Control Conference, 2009. ACC '09.* 2009, pp. 2451–2457, DOI: 10.1109/ACC.2009.5160285.

[144] I Ulrich and J Borenstein, "VFH*: local obstacle avoidance with look-ahead verification", *Robotics and Automation, 2000. Proceedings. ICRA '00. IEEE International Conference on*, vol. 3, 2000, 2505–2511 vol.3, DOI: 10.1109/ROBOT.2000.846405.

[145] I. Ulrich and J. Borenstein, "VFH+: reliable obstacle avoidance for fast mobile robots", *Proc. IEEE Int. Conf. on Robotics and Automation*, 1998, pp. 1572–1577.

[146] L. K. Vasiljevic and H. K. Khalil, "Error bounds in differentiation of noisy signals by high-gain observers", *Syst. Contr. Lett.* 2008, vol. 57, no. 10, pp. 856–862.

[147] C Vázquez, S Aranovskiy, and L Freidovich, "Time Varying Gain Second Order Sliding Mode Differentiator", *19th IFAC World Cogress*, pp. 1374–1379.

[148] P. Veelaert and W. Bogaerts, "Ultrasonic potential field sensor for obstacle avoidance", *IEEE transactions on Robotics and Automation*, 1999, vol. 15, no. 4, pp. 774–779.

[149] T. Vicsek, A. Czirok, E. Ben-Jacob, I. Cohen, and O. Shochet, "Novel Type of Phase Transition in a System of Self-Driven Particles", *Phys. Rev. Lett.* 1995, vol. 75, pp. 1226–1229.

[150] R. Volpe and P. Khosla, "Manipulator Control with Superquadric Artificial Potential Functions: Theory and Experiments", *IEEE Transactions on Systems, Man, and Cybernetics*, 1990, vol. 20, pp. 1423–1436.

[151] D. Wang and C. B. Low, "An Analysis of Wheeled Mobile Robots in the Presence of skidding and slipping: Control Design Perspective", *Robotics and Automation, 2007 IEEE International Conference on*, 2007, pp. 2379–2384.

[152] D. Xu, B. Jiang, and P. Shi, "A Novel Model-Free Adaptive Control Design for Multivariable Industrial Processes", *Industrial Electronics, IEEE Transactions on*, Nov. 2014, vol. 61, no. 11, pp. 6391–6398.

[153] T. Yamamoto and K. Watanabe, "A Switching Control Method for Stabilizing a Nonholonomic Mobile Robot Using Invariant Manifold Method", *SICE annual conference*, vol. 1, 1, 2010, pp. 3278–3284.

[154] J. Yao, Z. Jiao, and D. Ma, "Extended-State-Observer-Based Output Feedback Nonlinear Robust Control of Hydraulic Systems With Backstepping", *Industrial Electronics, IEEE Transactions on*, Nov. 2014, vol. 61, no. 11, pp. 6285–6293.

[155] K Youcef-Toumi and S.-T. Wu, "Input/output linearization using Time Delay Control", *ASME Journal of Dynamic Systems Measurement and Control*, 1992, vol. 114, pp. 10–19.

Titre: **Le Déploiement et l'Évitement d'Obstacles en Temps Fini pour Robots Mobiles à Roues**

Résumé:Ce travail traite de l'évitement d'obstacles pour les robots mobiles à roues. D'abord, deux solutions sont proposées dans le cas d'un seul robot autonome. La première est une amélioration de la technique des champs de potentiel afin de contraster l'apparition de minima locaux. Le résultat se base sur l'application de la définition de l' Input-to-State Stability pour des ensembles décomposables. Chaque fois que le robot mobile approche un minimum local l'introduction d'un contrôle dédié lui permet de l'éviter et de terminer la tâche. La deuxième solution se base sur l'utilisation de la technique du Supervisory Control qui permet de diviser la tâche principale en deux sous tâches : un algorithme de supervision gère deux signaux de commande, le premier en charge de faire atteindre la destination, le deuxième d'éviter les obstacles. Les deux signaux de commande permettent de compléter la mission en temps fini en assurant la robustesse par rapport aux perturbations représentant certaines dynamiques négligées. Les deux solutions ont été mises en service sur un robot mobile Turtlebot 2. Pour contrôler une formation de type leader-follower qui puisse éviter collisions et obstacles, une modification de l'algorithme de supervision précédent a été proposée ; elle divise la tâche principale en trois sous-problèmes gérés par trois lois de commande. Le rôle du leader est adapté pour être la référence du groupe avec un rôle actif : ralentir la formation en cas de manœuvre d'évitement pour certains robots. La méthode proposée permet au groupe de se déplacer et à chaque agent d'éviter les obstacles, ou les collisions, de manière décentralisée. Mot Clefs:Robotique, Evidement d'obstacle, Commande en temps fini, Supervisory Control, Leader-Follower formation, Champs de potentiel.

Title: **Finite Time Deployment and Collision Avoidance for Wheeled Mobile Robots**

Abstract: This dissertation work addresses the obstacle avoidance for wheeled mobile robots. The supervisory control framework coupled with the output regulation technique allowed to solve the obstacle avoidance problem and to formally prove the existence of an effective solution: two outputs for two objectives, reaching the goal and avoiding the obstacles. To have fast, reliable and robust results the designed control laws are finite-time, a particular class very appropriate to the purpose. The novelty of the approach lies in the easiness of the geometric approach to avoid the obstacle and on the formal proof provided under some assumptions. The solution have been thus extended to control a leader follower formation which, sustained from the previous result, uses two outputs but three controls to nail the problem. The Leader role is redesigned to be the reference of the group and not just the most advanced agent, moreover it has a active role slowing down the formation in case of collision avoidance manoeuvre for some robots. The proposed method, formally proven, makes the group move together and allow each agent to avoid obstacles or collision in a decentralized way. In addition, a further contribution of this dissertation, it is represented by a modification of the well known potential field method to avoid one of the common drawback of the method: the appearance of local minima. Control theory tools helps again to propose a solution that can be formally proven: the application of the definition of Input-to-State Stability (ISS) for decomposable sets allows to treat separate obstacles adding a perturbation which is able to move the trajectory away from a critic point.

Key-words: Robotics, Obstacle avoidance, Finite time control, Supervisory control, Leader Follower formation, Potential field.